EDITORIAL STAFF

R. M. Burns, *Chairman*
Cecil V. King, *Editor*
Norman Hackerman, *Technical Editor*
Ruth G. Sterns, *Managing Editor*
U. B. Thomas, *News Editor*
Natalie Michalski, *Assistant Editor*
Eleanor Blair, *Assistant Editor*

DIVISIONAL EDITORS

W. C. Vosburgh, *Battery*
J. V. Petrocelli, *Corrosion*
John J. Chapman, *Electric Insulation*
Abner Brenner, *Electrodeposition*
H. C. Froelich, *Electronics*
Sherlock Swann, Jr., *Electro-Organic*
Irvin R. Kramer, *Electrothermics and Metallurgy, I*
A. U. Seybolt, *Electrothermics and Metallurgy, II*
W. C. Gardiner, *Industrial Electrolytic*
C. W. Tobias, *Theoretical*

REGIONAL EDITORS

Howard T. Francis, *Chicago*
Joseph Schulein, *Pacific Northwest*
J. C. Schumacher, *Los Angeles*
G. W. Heise, *Cleveland*
Paul S. Brallier, *Niagara Falls*
Oliver Osborn, *Houston*
Earl A. Gulbransen, *Pittsburgh*
A. C. Holm, *Canada*
J. W. Cuthbertson, *Great Britain*
T. L. Rama Char, *India*

ADVERTISING OFFICE

Jack Bain
Advertising Manager
545 Fifth Avenue
New York 17, N. Y.
Phone—*Murray Hill 2-3345*

Journal of the
Electrochemical Society

SEPTEMBER 1955 VOL. 102 · NO. 9

CONTENTS

Editorial

Energy For The Future 209C

Technical Papers

Electrolytic Oxidation of Zinc in Alkaline Solutions. *Thedford P. Dirkse* 497
Anodic Polarization of Zirconium at Low Potentials; Formation Rates, Formation Field, Electrolytic Parameters, and Film Thicknesses of Very Thin Oxide Films. *George B. Adams, Jr., Mario Maraghini, and Pierre Van Rysselberghe* 502
Two Photoelectric Colorimeters for Television Picture Tubes. *Richard S. Hunter* 512
Oxidation States of Europium in the Alkaline Earth Oxide and Sulfide Phosphors. *P. M. Jaffe and E. Banks* 518
Preliminary Studies of the Perovskite-Type Ternary Oxides as Luminophors. *Salvador Terol and Roland Ward* 524
Infrared Quenching of Cadmium Sulfide. *S. H. Liebson* 529
Studies on Alternating-Current Electrolysis, III. Effects of Concentration on Polarization Capacity and Polarization Resistance. *A. Edward Remick and Herbert W. McCormick* 534
Potentiometric Titrations in Liquid Ammonia, VIII. Mercury-Saturated Mercury(II) Chloride Working Reference Electrode. *George W. Watt and Donald M. Sowards* 545

Technical Note

The Electrodeposition of Lead from Lead Phenol Sulfonate Solutions. *Harry C. Gatos and Frank C. Mathers* 554

Current Affairs

Complete Pittsburgh Meeting Program 211C
Hooker—ECS Sustaining Member 231C
Section News 233C
Personals 233C
Letter to the Editor 233C
Book Reviews 234C
News Items 236C
Recent Patents 237C
Literature from Industry
New Products

Published monthly by The Electrochemical Society, Inc., Mount Royal and Guilford Aves., Baltimore 2, Md., combining the JOURNAL and TRANSACTIONS OF THE ELECTROCHEMICAL SOCIETY. Editorial offices: 216 West 102nd Street, New York 25, N. Y. Statements and opinions given in articles and papers in the JOURNAL OF THE ELECTROCHEMICAL SOCIETY are those of the contributors, and The Electrochemical Society assumes no responsibility for them. Nondeductible subscription to members $5.00; subscription to nonmembers $15.00. Single copies $1.25 to members, $1.50 to nonmembers. Copyright 1955 by The Electrochemical Society, Inc. Entered as second-class matter November 15, 1947, at the Post Office at Baltimore, Md., under the act of August 24, 1912.

9 REASONS WHY "KARBATE" BRAND IMPERVIOUS GRAPHITE PROCESS EQUIPMENT DOES THE BEST JOB IN CORROSIVE PROCESSES

- Corrosion resistance
- Immunity to thermal shock
- No metallic contamination
- High thermal conductivity
- Low first cost and low maintenance
- Workability — readily fabricated and serviced in the field
- Sturdy, durable constructions
- Standard stock units
- Complete technical service

Manufactured only by NATIONAL CARBON COMPANY

■ Only the unique combination of properties provided by "Karbate" brand impervious graphite can virtually *eliminate* corrosion, contamination and thermal shock from your processes. You'll be pleased with the hidden economies you realize after replacing hitherto "satisfactory" process units with "Karbate" equipment.

Let us bring you up to date on the latest designs in this outstanding material. And remember — your operating-cost sheets don't have to be *bad* to be *bettered!*

WRITE FOR LITERATURE!

The term "Karbate" is a registered trade-mark of Union Carbide and Carbon Corporation

NATIONAL CARBON COMPANY

A Division of Union Carbide and Carbon Corporation, 30 East 42nd Street, New York 17, N. Y.

Sales Offices: Atlanta, Chicago, Dallas, Kansas City, Los Angeles, New York, Pittsburgh, San Francisco

IN CANADA: Union Carbide Canada Limited, Toronto

Pumps—
Catalog Section
S-7250

Pipe and Fittings—
Catalog Section
S-7000

Heat Exchangers—
Catalog Sections
S-6740 and S-6840

Cascade Coolers—
Catalog Section
S-8820

HCl Absorbers—
Catalog Section
S-7480

Improved Plating Techniques by Baker & Adamson

Vital Engine Parts Protected!

A harder coating, with better corrosion and wear resistance, is produced with a low tin-content B&A fluoborate bath for protecting bearings and other engine parts. Additional uses include depositing coatings on pistons and similar parts to provide marginal lubrication during break-in periods, electro-cladding wire and plating threaded parts for needed lubrication properties.

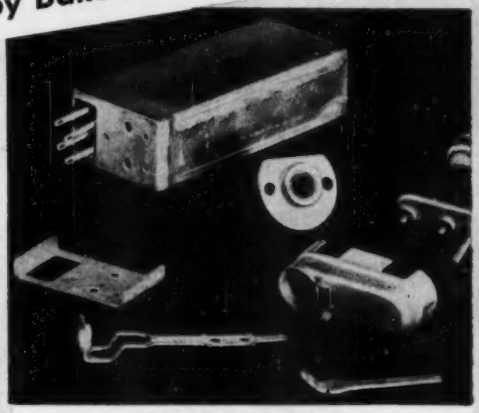

Soldering Made Easy!

A high-tin-content fluoborate bath produces coatings of excellent solderability on electronic or electrical parts where the use of a non-corrosive flux is desired. It also gives a uniform coating that expedites assembly, and where the parts can be fused, the B&A Fluoborate alloy bath can be used to deposit the solder, eliminating costly hand soldering.

NOW...You Can Plate CUSTOM-MADE Alloy Coatings with B&A Lead and Tin Fluoborates!

These are high-speed, low-cost operations . . . short-cuts to producing better, more economical products.

The plated coatings shown are actually tailor-made to specific requirements with Baker & Adamson Lead and Tin Fluoborate Solutions. When protective and lubricating coatings are required, as in bearings, lead-tin alloys of low tin content are readily plated. Where a deposit of good solderability is desired, as in electronic parts, alloys with 40-60% tin content can be produced. B&A Lead and Tin Fluoborate Solutions, combined in a bath using alloy anodes, produce dense, fine-grained, uniform deposits with pre-determined characteristics. Send the coupon for detailed technical bulletins.

B&A Fluoborate Plating Chemicals Include:

Lead • Tin • Iron • Copper • Nickel • Cadmium
Indium • Antimony* • Chromium* • Cobalt*
Fluoboric Acid

*Experimental quantities only

FINE CHEMICALS
B·A
REAGENTS

Clip to your letterhead and mail today!

BAKER & ADAMSON® PRODUCTS
GENERAL CHEMICAL DIVISION
ALLIED CHEMICAL & DYE CORPORATION
40 Rector Street, New York 6, N. Y.

Please send, without obligation:—

☐ Your Technical Bulletins No. TC38351, RA38351, and RB38351 on applications and techniques for plating lead and tin alloy coatings.

☐ Information on applications of other B&A Metal Fluoborates. Specify type_____

Name_____

Position_____

Company_____

City_____ Zone____ State_____

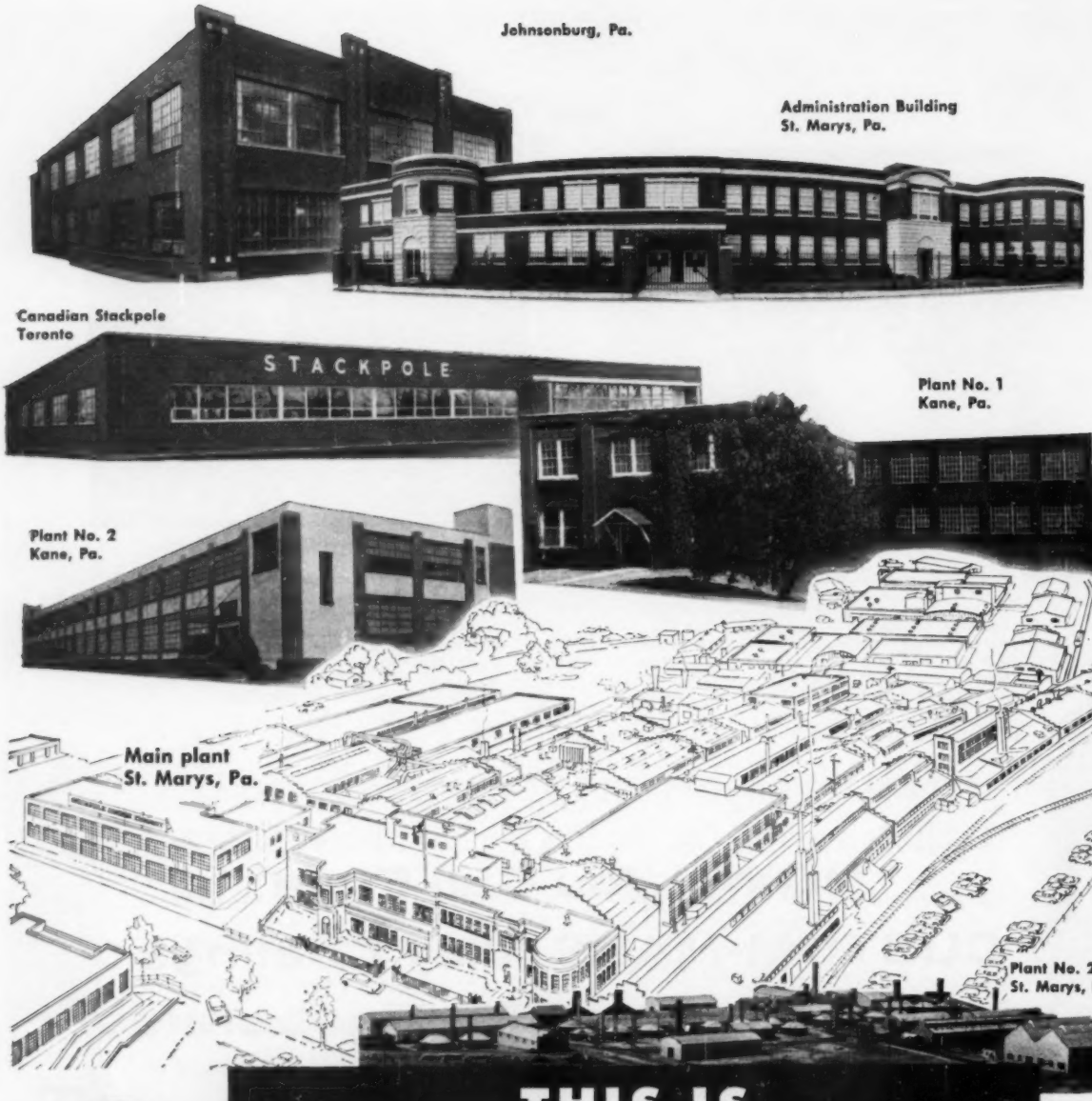

...THIS IS STACKPOLE

A dependable source for carbon, graphite, metal powder products

BRUSHES FOR ALL ROTATING ELECTRICAL EQUIPMENT
CARBON, GRAPHITE AND METAL POWDER CONTACTS
VOLTAGE REGULATOR DISCS • SEAL RINGS
POWER TUBE ANODES • CHEMICAL ANODES
PUMP VANES • FRICTION SEGMENTS • SPECTROGRAPHITE
CARBON RODS FOR SALT BATH RECTIFICATION
GROUND RODS • GRAPHITE NOZZLES
CARBON BEARINGS • CARBON MOLDS
WELDING AND BRAZING CARBONS . . . and specialties of all types.

Editorial

Energy for the Future

THE WORLD SYMPOSIUM on Applied Solar Energy to be held in Phoenix, Arizona, during the first five days of November will be concerned with the problem of man's future energy requirements. The astounding magnitude of these needs and their rate of growth lead to the conviction that practical means of direct utilization of the sun's energy must be found within the next century. The present per capita use of energy in this country is 150,000 kcal, or 50-fold that required to sustain the human machine. Moreover, this total energy figure will be doubled in the next 25 years. With the world population increasing by more than 25 million a year and in view of the growing industrialization of Asia and the accompanying trend toward a higher standard of living, it is apparent that fossil fuels face early exhaustion. Atomic fission can afford relief but will be hard pressed to supply the mounting energy needs for all mankind for a long period. At the present time the electrochemical industry alone consumes more than three times the total electric power that was generated in the United States forty years ago when many of the present leaders in this industry were graduating from college.

The chemical and metal industries are dependent upon electrolytic and electrothermal processes for such basic products as alkali, chlorine, calcium carbide, aluminum, magnesium, abrasives, and alloy steels. The vastly increasing tonnages of these materials that will be required in future years point up the importance of finding assured sources of adequate energy. Only the sun can provide the inexhaustible supply that will be needed by future generations.

The coming symposium on solar energy in bringing together the scientist, engineer, and businessman should make a real beginning by exploring the feasibility of reducing laboratory developments to practice. Every aspect of the subject from the findings of solid-state physics in the direct conversion of sunlight into electricity to the culture of low-order plants and animals designed to produce fuel and food will be discussed. The conference should determine the direction of greatest promise for providing the energy needs of the future. —RMB

After initial adjustments are made, as in photograph, "Mr. Meticulous" automatically performs critical operations in making junction tetrode transistors—tiny experimental devices which may find important uses in the telephone system.

The machine we call "Mr. Meticulous"

Bell Laboratories scientists, who invented the junction transistor, have now created an automatic device which performs the intricate operations required for the laboratory production of experimental model transistors.

It takes a bar of germanium little thicker than a hair and tests its electrical characteristics. Then, in steps of 1/20,000 of an inch, it automatically moves a fine wire along the bar in search of an invisible layer of positive germanium to which the wire must be connected. This layer may be as thin as 1/10,000 of an inch!

When the machine finds the layer, it orders a surge of current which bonds the wire to the bar. Then it welds the wire's other end to a binding post. Afterward, it flips the bar over and does the same job with another wire on the opposite side!

Once only the most skilled technicians could do this work, and even their practiced hands became fatigued. This development demonstrates again how Bell Telephone Laboratories scientists work in every area of telephony to make service better.

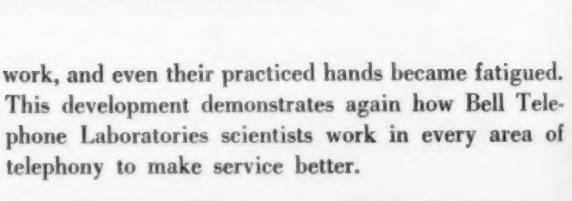

Transistor made by new machine is shown in sketch at left above, magnified 6 times. At right is sketch of area where wires are bonded. The wires are 2/1000 inch in diameter, with ends crimped to reduce thickness.

BELL TELEPHONE LABORATORIES

IMPROVING TELEPHONE SERVICE FOR AMERICA PROVIDES CAREERS FOR CREATIVE MEN IN MECHANICAL ENGINEERING

Pittsburgh Program

THE ELECTROCHEMICAL SOCIETY

One Hundred and Eighth Meeting

Sunday through Thursday

October 9, 10, 11, 12, and 13, 1955

CONDENSED TECHNICAL PROGRAM

Battery (Abs. 1–4)

(All sessions in Allegheny Room)

Monday, October 10—9:30 A.M.–11:30 A.M.
Monday, October 10—2:30 P.M.–5:00 P.M., Round-Table Discussion
Tuesday, October 11—9:00 A.M.–12:00 M., Round-Table Discussion
Tuesday, October 11—2:30 P.M.–4:00 P.M., Round-Table Discussion

Corrosion (Abs. 5–45)

(Monday, Tuesday, Wednesday in Urban Room; Thursday in Sky Room)

Monday, October 10—10:00 A.M.–12:00 M.
Monday, October 10—2:00 P.M.–5:00 P.M.
Tuesday, October 11—9:00 A.M.–12:00 M.
Tuesday, October 11—2:00 P.M.–4:00 P.M.
Wednesday, October 12—9:00 A.M.–11:30 A.M.
Wednesday, October 12—2:00 P.M.–5:00 P.M.
Thursday, October 13—9:30 A.M.–12:00 M.
Thursday, October 13—2:00 P.M.–3:30 P.M.

Electrodeposition (Abs. 46–58)

(All sessions in Allegheny Room)

Wednesday, October 12—9:00 A.M.–11:30 A.M.
Wednesday, October 12—2:30 P.M.–4:30 P.M. Round-Table Discussion
Thursday, October 13—9:00 A.M.–12:30 P.M.

Electronics-Semiconductors (No abstracts)

(All sessions in Monongahela Room)

Thursday, October 13—9:00 A.M.–12 M.
Thursday, October 13—2:00 P.M.–5:00 P.M.

Electro-Organic (Abs. 59–80)

(All sessions in Monongahela Room)

Monday, October 10—10:00 A.M.–11:30 A.M.
Monday, October 10—2:15 P.M.–5:15 P.M.
Tuesday, October 11—9:00 A.M.–11:30 A.M.
Tuesday, October 11—2:00 P.M.–3:30 P.M.
Wednesday, October 12—9:00 A.M.–11:30 A.M.
Wednesday, October 12—2:00 P.M.–5:00 P.M.

Electrothermics and Metallurgy (Abs. 81–101)

(All sessions in the Sky Room)

Monday, October 10—2:30 P.M.–4:30 P.M.
Tuesday, October 11—9:30 A.M.–12:00 M.
Tuesday, October 11—2:00 P.M.–4:00 P.M.
Wednesday, October 12—9:30 A.M.–11:30 A.M.
Wednesday, October 12—2:00 P.M.–4:00 P.M.

GENERAL INFORMATION

Convention headquarters will be at the Hotel William Penn, Grant Street, Pittsburgh, Pa.

Rates per day for rooms (with bath) will be: single-bed room (one person) $8.00, 8.50, 9.00, 9.50, 10.00, 10.50; double-bed room (two persons) $11.50, 12.00, 12.50, 13.00, 14.00; twin-bed room (2 persons) $11.50, 12.00, 13.00, 14.00, 15.00, 16.50; suites, parlor and twin-bed room, $25.00, 30.00, 35.00; parlor, two twin-bed rooms, $46.50, 50.00.

Requests for room reservations should be mailed to office of the General Manager, Hotel William Penn, Pittsburgh 30, Pa., with mention of The Electrochemical Society.

Technical sessions and registration will be on the 17th (Ballroom) floor, as will be the Secretary's Office (Parlor D) and Ladies' Headquarters (Parlor E).

Registration desk (17th floor) will be open during the following periods: Sunday, October 9, 5:00 P.M. to 8:00 P.M.; Monday, 8:00 A.M. to 5:00 P.M.; Tuesday and Wednesday, 8:30 A.M. to 5:00 P.M.; Thursday, 8:30 A.M. to 12:00 M.

Registration fees are:

Members	$7.00
Nonmembers	$13.00
Ladies	$3.00
Students	$2.00

ROUND TABLES AND SPECIAL SYMPOSIA

The Battery Division has scheduled three round-table discussions: 1. Methods of Dry-Charging Storage Batteries, Monday, October 10, at 2:00 P.M. in the Allegheny Room; 2. Processes Which Limit the Shelf-Life and Charge Retention of Batteries (Reactions at Negative Electrodes), Tuesday, October 11, at 9:00 A.M. in the Allegheny Room; 3. Processes Which Limit the Shelf-Life and Charge Retention of Batteries (Reactions at Positive Electrodes), Tuesday, October 11, at 2:30 P.M. in the Allegheny Room.

The Electrodeposition Division has scheduled a special symposium on Hydrogen Embrittlement, Wednesday, October 12, at 9:00 A.M., and a round-table discussion on Hydrogen Embrittlement, Wednesday, October 12, at 2:30 P.M. in the Allegheny Room.

The Electro-Organic Division has scheduled a round-table discussion on Mechanism of Reduction, Wednesday, October 12, at 2:00 P.M. in the Monongahela Room.

The Electrothermics and Metal-

lurgy Division has scheduled a special symposium on Fluidized Solid Techniques on Monday, October 10, at 2:30 P.M. in the Sky Room.

PALLADIUM MEDAL LECTURE

Dr. Ulick R. Evans, of Cambridge, England, will deliver the Palladium Medal Lecture at 4:00 P.M., Tuesday, October 11, in the Urban Room.

LUNCHEONS AND DINNERS

Monday Luncheon

The Society Luncheon will be held Monday, October 10, at 12:30 P.M. in the Monongahela Room. Speaker will be the Honorable John P. Robin, Secretary of Commerce, Commonwealth of Pennsylvania.

Monday Get-Acquainted Hour

On Monday, October 10, an informal get-acquainted hour will be held in the Fort Duquesne Room from 4:30 P.M.–8:00 P.M. Come and renew acquaintances. Information will be available on what to see and do in Pittsburgh. Refreshments will also be available.

Tuesday Palladium Medal Banquet

A reception and dinner in honor of the Palladium Medalist, Dr. U. R. Evans, will be held on Tuesday, October 11, in the Urban Room. Cocktails will be served at 6:30 P.M., dinner at 7:30 P.M.

Wednesday Theater Party

For those who enjoy the legitimate theater, Wednesday evening has been set aside for a theater party at the Pittsburgh Playhouse.

PLANT TRIPS

All trips are to leave the Hotel William Penn at 2:00 P.M. and leave plants at 5:00 P.M. for return to the hotel.

Monday, October 10

1. Irvin Works—U. S. Steel Corporation (Limit 45 persons. Persons who are not American citizens must make special arrangements at registration desk.)
2. The Pittsburgh Brewing Company—Iron City Brewery, 3340 Liberty Avenue (Limit 30 men)

Tuesday, October 11

3. The Pittsburgh Coke & Chemical Company, Neville Island (Limit 45 persons)

Wednesday, October 12

4. Elrama Power Station—Duquesne Light Company (Limit 45 persons. Persons who are not American citizens must make special arrangements at registration desk. A list of those attending, with company affiliations, must be furnished in advance.)
5. The Duquesne Brewing Company, S. 22nd St. (Limit 30 men)

LADIES' PROGRAM

Ladies' Headquarters will be in Parlor E on the Ballroom (17th) floor of the Hotel William Penn throughout the meeting. All ladies are requested to visit this headquarters and register for the program which has been arranged for their entertainment and information. The ladies' program has been arranged to cover interesting features of Pittsburgh and to provide for participation in entertainment features of the general convention, as well as to provide some free time for shopping and individual amusement.

Monday Morning—A get-acquainted meeting, with coffee and doughnuts, will be held at 9:30 A.M. in Parlor E. At this meeting discussion of arrangements for the features of the ladies' program will be held, as well as an opportunity for the ladies to get acquainted and express their wishes and desires in connection with the program. At 10:30 A.M. there will be a conducted tour of the new Alcoa Building.

Monday Noon—The ladies are invited to attend the Society Luncheon in the Monongahela Room at 12:30 P.M. (Price $3.50).

Monday Afternoon—Immediately following the luncheon, at 2:00 P.M. the ladies will board a bus to tour the Oakland Civic Center and the Nationality Rooms in the Cathedral of Learning at the University of Pittsburgh. They will return to the hotel about 4:30 P.M.

Monday Evening—The ladies are invited to attend the Get-Acquainted Hour in the Fort Duquesne Room from 4:30 P.M. to 8:00 P.M.

Tuesday Morning—Coffee will be served in the Ladies' Headquarters at 9:30 A.M. The rest of the morning is left open for shopping and individual tours of interest.

Tuesday Afternoon—At 12:30 P.M. buses will leave for a tour of the H. J. Heinz Co. Plant and a sight-seeing tour of the North Side, Block House, and Mt. Washington. Return about 4:30 P.M.

Tuesday Evening—Cocktails and dinner in honor of the Palladium Medalist, Dr. U. R. Evans, in the Urban Room at 6:30 P.M. ($10.50).

Wednesday Morning—Promptly at 9:30 A.M. a bus will leave for an all-day trip, via the Pennsylvania Turnpike, to Fort Ligonier. The return sight-seeing trip will be by Route 30. Return about 4:30 P.M. Tickets $3.00.

Wednesday Evening—Theater Party, stage play at the Pittsburgh Playhouse.

Thursday Morning—As usual, coffee will be served in the Ladies' Headquarters at 9:30 A.M. The remaining time is left open for shopping and individual entertainment. The Ladies' Committee will be glad to assist as guides or in just plain conversation. This is the time to satisfy individual desires, and the Ladies' Committee will be standing by to help in any way.

LUNCHEONS AND BUSINESS MEETINGS OF DIVISIONS

Battery Division will hold a luncheon and business meeting on Tuesday, October 11, at 12:30 P.M. in the Triangle Room (Club floor).

Corrosion Division will hold a luncheon and business meeting on Wednesday, October 12, at 12:30 P.M. in the Sky Room (17th floor).

Electrodeposition Division will hold a luncheon and business meeting on Wednesday, October 12, at 12:30 P.M. in the Fort Duquesne Room (17th floor).

Electro-Organic Division will hold a luncheon and business meeting on Wednesday, October 12, at 12:30 P.M. in Room 735 (7th floor).

Electrothermics and Metallurgy Division will hold a luncheon on Tuesday, October 11, at 12:30 P.M. in the Allegheny Room (17th floor).

BOARD AND COMMITTEE MEETINGS

(All meetings will be on the 17th floor.)

Sunday, October 9, 10:00 A.M.—Meeting of the Ways and Means Committee, Parlors B and C.

Sunday, October 9, 2:00 P.M.—Meeting of the Board of Directors, Parlors B and C.

Monday, October 10, 5:00 P.M.—

Meeting of the Editorial Staff, Parlor B.

Monday, October 10, 5:00 P.M.—Meeting of Council of Local Sections, Parlor C.

Wednesday, October 12, 5:00 P.M.—Meeting of Membership Committee, Parlor B.

Wednesday, October 12, 5:00 P.M.—Meeting of Sustaining Membership Committee, Parlor C.

COST OF VARIOUS FUNCTIONS

(other than registration)

Society Luncheon.....$3.50
Division Luncheons.....$3.50
Palladium Medal Reception and Banquet
(single).....$6.50
(couple).....$10.50
(including one free cocktail, additional cocktails $0.25 each)
Ladies' Scenic Drive and Luncheon $3.00
Plant Trips.....$1.25
(Gratuities and taxes included in above costs)

JOURNALS

Copies of the June, July, August, and September issues of the JOURNAL OF THE ELECTROCHEMICAL SOCIETY will be available at the registration desk. The price of single copies of the JOURNAL is $1.25 to members and $1.50 to nonmembers.

DISCUSSION

There will be no recordings made of oral discussions. Those contributing to the discussion of a paper and desiring their remarks published will be supplied by the symposium chairman with a printed form on which any discussion may be written. These forms should be given to the Secretary-Treasurer of the Division or to the Managing Editor of the JOURNAL after the session. The discussion will then be referred to the authors for reply. Written discussion should be submitted within two months following publication of any article in the JOURNAL.

A discussion section is published semiannually in the JOURNAL.

SLIDES AT TECHNICAL SESSIONS

The Board of Directors of the Society does not favor indiscriminate photographing of slides during technical sessions. It is requested that no such photographs be taken. Chairmen of technical sessions should administer this rule.

EMPLOYMENT POSTERS

Companies which desire to recruit employees at the Pittsburgh Meeting will have posters to this effect on a bulletin board near the registration desk.

TECHNICAL PROGRAM

Monday, October 10, 1955

9:00 A.M.—Formal Opening of the 108th Convention with Introduction by General Chairman J. P. Fugassi and response by President H. H. Uhlig (Urban Room).

Battery

Monday, October 10, 1955

Research Contributions

with N. C. Cahoon presiding

(ALLEGHENY ROOM)

9:30 A.M.—"Resistivity Studies of Various Leclanché Cathode Materials" by Richard Glicksman and C. K. Morehouse, RCA Labs., Radio Corp. of America, Princeton, N. J. (Abstract No. 1)

10:00 A.M.—"A Polarization Tech-

MEETING ROOM SCHEDULES

Meetings	Monday		Tuesday		Wednesday		Thursday	
	A.M.	P.M.	A.M.	P.M.	A.M.	P.M.	A.M.	P.M.
Battery	A	A	A	A				
Corrosion	U	U	U	U	U	U	S	S
Electrodeposition					A	A	A	
Electronics-Semiconductors							M	M
Electro-Organic	M	M	M	M	M	M		
Electrothermics and Metallurgy		S	S	S	S	S		

A—Meeting will be held in the Allegheny Room.
M—Meeting will be held in the Monongahela Room.
S—Meeting will be held in the Sky Room.
U—Meeting will be held in the Urban Room.

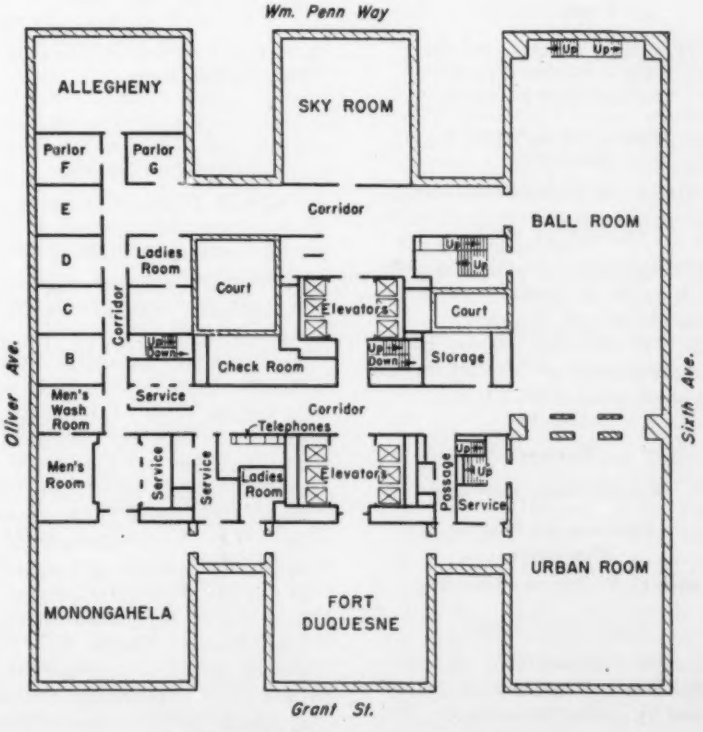

7th (ballroom) floor of the William Penn

nique for Evaluating Various Cathode Materials" by C. K. Morehouse and Richard Glicksman, RCA Labs., Radio Corp. of America, Princeton, N. J. (Abstract No. 2)

10:30 A.M.—"The Aluminum Dry Cell" by J. J. Stokes, Jr., Physical Chemistry Div., Aluminum Co. of America, New Kensington, Pa. (Abstract No. 3)

11:00 A. M.—"An Electron Diffraction Study of Lead Monoxides" by Jeanne Burbank, Electrochemistry Branch, Chemistry Div., Naval Research Lab., Washington, D. C. (Abstract No. 4)

12:30 P.M.—Society Luncheon in the Monongahela Room.

Battery

Round Table

Methods of Dry-Charging Storage Batteries

with Eugene Willihnganz presiding

(ALLEGHENY ROOM)

2:30 P.M.—Round-table discussion with panel of speakers, to be followed by general discussion.

Battery

Tuesday, October 11, 1955

Round Table

Processes Which Limit the Shelf-Life and Charge Retention of Batteries

(Reactions at Negative Electrodes)

with W. S. Herbert presiding

(ALLEGHENY ROOM)

9:00 A.M.—Round-table discussion with panel of speakers, to be followed by general discussion.

12:30 P.M.—Battery Division Luncheon and Business Meeting in the Triangle Room (Club floor).

Battery

Round Table (cont'd)

(Reactions at Positive Electrodes)

with U. B. Thomas presiding

(ALLEGHENY ROOM)

2:30 P.M.—Round-table discussion with panel of speakers, to be followed by general discussion.

* * *

4:00 P.M.—Palladium Medal Address by U. R. Evans, Cambridge, England, in the Urban Room.

Corrosion

Monday, October 10, 1955

Oxidation

with J. T. Waber presiding

(URBAN ROOM)

10:00 A.M.—"Oxidation of Oxygen-Free High Conductivity Copper, I. Oxidation of Copper to Cu_2O" by J. P. Baur, D. W. Bridges, and W. M. Fassell, Jr., Dept. of Metallurgy, University of Utah, Salt Lake City, Utah. (Abstract No. 5)

10:30 A.M.—"High Pressure Oxidation of Metals; Niobium in Oxygen" by D. W. Bridges and W. M. Fassell, Jr., Dept. of Metallurgy, University of Utah, Salt Lake City, Utah. (Abstract No. 6)

11:00 A.M.—"High Pressure Oxidation of Metals; Tungsten in Oxygen" by J. P. Baur, D. W. Bridges, and W. M. Fassell, Jr., Dept. of Metallurgy, University of Utah, Salt Lake City, Utah. (Abstract No. 7)

11:30 A.M.—"Oxidation of Tungsten" by W. W. Webb, J. T. Norton, and Carl Wagner, Dept. of Metallurgy, Massachusetts Institute of Technology, Cambridge, Mass. (Abstract No. 8)

12:30 P.M.—Society Luncheon in the Monongahela Room.

Corrosion

Oxidation (cont'd)

with J. T. Waber presiding

(URBAN ROOM)

2:00 P.M.—"Oxidation Studies in Metal-Carbon Systems" by W. W. Webb, J. T. Norton, and Carl Wagner, Dept. of Metallurgy, Massachusetts Institute of Technology, Cambridge, Mass. (Abstract No. 9)

2:25 P.M.—"Role of Dislocation in the Oxidation of Metals" by N. Cabrera, Dept. of Physics, University of Virginia, Charlottesville, Va. (Abstract No. 10)

2:50 P.M.—"Oxidation of Iron-Molybdenum and Nickel-Molybdenum Alloys" by S. S. Brenner, Research Lab., General Electric Co., Schenectady, N. Y. (Abstract No. 11)

3:15 P.M.—"Catastrophic Oxidation of Some Molybdenum-Containing Alloys" by S. S. Brenner, Research Lab., General Electric Co., Schenectady, N. Y. (Abstract No. 12)

3:40 P.M.—"A Spectrophotometric Study of the Oxidation of Uranium" by J. T. Waber and G. E. Sturdy, Los Alamos Scientific Lab., University of California, Los Alamos, N. Mex. (Abstract No. 13)

4:05 P.M.—"Oxidation of Iron-Nickel Alloys" by R. T. Foley, General Engineering Lab., General Electric Co., Schenectady, N. Y., and R. E. Fryxell and J. U. Druck, Transformer Labs. Dept., General Electric Co., Pittsfield, Mass. (Abstract No. 14)

4:30 P.M.—"Reaction of Hydrogen with Uranium" by W. M. Albrecht and M. W. Mallett, Battelle Memorial Institute, Columbus, Ohio. (Abstract No. 15)

Corrosion

Tuesday, October 11, 1955

Kinetics of Corrosion Reactions

with J. E. Draley presiding

(URBAN ROOM)

9:00 A.M.—"Formation of Porous Scale" by C. E. Birchenall, James Forrestal Research Center, Princeton University, Princeton, N. J. (Abstract No. 16)

9:30 A.M.—"Preliminary Results on the Kinetics of the Reaction of Metals with Water Vapor" by Paul Blackburn and E. A. Gulbransen, Westinghouse Research Labs., East Pittsburgh, Pa. (Abstract No. 17)

10:00 A.M.—"Oxidation Studies on Fe-Cr-Al Heater Alloys" by Kenneth Andrew and E. A. Gulbransen, Westinghouse Research Labs., East Pittsburgh, Pa. (Abstract No. 18)

10:30 A.M.—"Acceleration of the Dissolution of Iron in Sulfuric Acid by Ferric Ions" by H. C. Gatos, Engineering Dept., E. I. du Pont de Nemours & Co., Inc., Wilmington, Del. (Abstract No. 19)

11:00 A.M.—"Dissolution of Metals in Aqueous Acid Solutions, II. Kinetics for the Reactions of Steel" by N. M. Komodromos, A. C. Makrides, and Norman Hackerman, Dept. of Chemistry, University of Texas, Austin, Texas. (Abstract No. 20)

11:30 A.M.—"Effect of Alloying Elements in Iron on Hydrogen Overvoltage and Corrosion Rate in Acid Environments" by Milton Stern, Corrosion Lab., Massachusetts Institute of Technology, Cambridge, Mass. (Abstract No. 21)

Corrosion

Kinetics of Corrosion Reactions (cont'd)

with J. E. Draley presiding

(URBAN ROOM)

2:00 P.M.—"Dissolution of Cadmium in Chromic Chloride-Hydrochloric Acid Solutions" by C. V. King and Edward Hillner, Dept. of Chemistry, New York University, New York, N. Y. (Abstract No. 22)

2:30 A.M.—"Role of Hydrogen in Corrosion Reactions" by J. E. Draley and W. E. Ruther, Argonne National Lab., Lemont, Ill. (Abstract No. 23)

3:00 P.M.—"A Study of the Cathodic Reduction of Oxide Films on Iron, I. Reduction of Alpha-Fe_2O_3 Films" by H. G. Oswin and M. Cohen, Div. of Applied Chemistry, National Research Council, Ottawa, Ont., Canada. (Abstract No. 24)

3:30 P.M.—"Kinetics of Exchange Between Solid Copper and Silver Ions in Aqueous Solutions" by M. Simnad, A. Spilners, and Ling Yang, Metals Research Lab., Carnegie Institute of Technology, Pittsburgh, Pa. (Abstract No. 25)

* * *

4:00 P.M.—Palladium Medal Address by U. R. Evans, Cambridge, England, in Urban Room.

Corrosion

Wednesday, October 12, 1955

Role of Surface Films in Corrosion

with R. B. Hoxeng presiding

(URBAN ROOM)

9:00 P.M.—"A Study of the Effect of Chloride Ion on Films Formed on Iron in Sodium Nitrite Solutions" by G. W. Mellors, M. Cohen, and F. Beck, Div. of Applied Chemistry, National Research Council, Ottawa, Ont., Canada. (Abstract No. 26)

9:30 A.M.—"Mechanism of the Hydrogen Evolution Reaction on Silver and Tungsten Cathodes" by J. O'M. Bockris, Dept. of Chemistry, University of Pennsylvania, Philadelphia, Pa. (Abstract No. 27)

10:00 A.M.—"Oxygen Adsorption on Stainless Steel" by T. N. Rhodin, Jr., Engineering Dept., E. I. du Pont de Nemours & Co., Inc., Wilmington, Del. (Abstract No. 28)

10:30 A.M.—"Electrical Properties of the Oxide Film on Zirconium" by R. D. Misch, Argonne National Lab., Lemont, Ill. (Abstract No. 29)

11:00 A.M.—"Orthophosphates of Iron, Manganese, and Zinc" by Jeanne Burbank, Naval Research Lab., Washington, D. C. (Abstract No. 30)

12:30 P.M.—Corrosion Division Luncheon and Business Meeting in the Sky Room (17th floor).

Corrosion

Role of Surface Films in Corrosion (cont'd)

with R. B. Hoxeng presiding

(URBAN ROOM)

2:00 P.M.—"Influence of Specimen Area on the Pitting Probability of Aluminum" by P. M. Aziz and H. P. Godard, Aluminium Labs., Ltd., Kingston, Ont., Canada. (Abstract No. 31)

2:30 P.M.—"Pitting Corrosion of 18 Cr-8 Ni Stainless Steel, I. Development of Accelerated Electrolytic Pit Initiation Methods" by M. A. Streicher, E. I. du Pont de Nemours & Co., Inc., Wilmington, Del. (Abstract No. 32)

2:45 P.M.—"Pitting Corrosion of 18 Cr-8 Ni Stainless Steel, II. Investigation of Variables in the Metal and in the Electrolyte Which Control Pit Initiation" by M. A. Streicher, E. I. du Pont de Nemours & Co., Inc., Wilmington, Del. (Abstract No. 33)

3:00 P.M.—"Determination of Corrosion Rates in Aqueous Systems at Elevated Temperature and Pressure by a Hydrogen Effusion Method" by M. C. Bloom and M. Krulfeld, Naval Research Laboratory, Washington, D. C. (Abstract No. 34)

3:30 P.M.—"Galvanic Corrosion Characteristics of Aluminum Alloys" by M. J. Pryor and D. S. Keir, Dept. of Metallurgical Research, Kaiser Aluminum & Chemical Corp., Spokane, Wash. (Abstract No. 35)

4:00 P.M.—"Crystallization of Anodic Tantalum Oxide Films in the Presence of a Strong Electric Field" by D. A. Vermilyea, Research Lab., General Electric Co., Schenectady, N. Y. (Abstract No. 36)

4:30 P.M.—"Various Factors Affecting the Formation of Anodic Oxide Coatings in Sulfuric Acid Electrolytes" by R. B. Mason, Aluminum Research Labs., Aluminum Co. of America, New Kensington, Pa. (Abstract No. 37)

Corrosion

Thursday, October 13, 1955

with J. V. Petrocelli presiding

(SKY ROOM)

9:30 A.M.—"Electrochemical Studies of Aluminum Corrosion in Water" by Manuel Shaw and S. B. Twiss, Chrysler Corp., Detroit, Mich. (Abstract No. 38)

10:00 A.M.—"Anodic Polarization of Zirconium at Low Potentials: Formation Rates, Formation Field, Electrolytic Parameters, and Film Thicknesses of Very Thin Oxide Films" by G. B. Adams, Jr., and Pierre Van Rysselberghe, Dept. of Chemistry, University of Oregon, Eugene, Oreg., and Mario Maraghini, Institute of Applied Chemistry, University of Rome, Rome, Italy. (Abstract No. 39)

10:30 A.M.—"Electrochemical Thermodynamics of J. Willard Gibbs and the Stockholm Conventions; The Gibbs-Stockholm Electrode Potential" by A. J. de Béthune, Chemistry Dept., Boston College, Chestnut Hill, Mass. (Abstract No. 40)

11:00 A.M.—"Electrochemical Potentials of Grains and Grain Boundaries in Copper Solid Solutions" by R. Bakish and W. D. Robertson, Hammond Metallurgical Lab., Yale University, New Haven, Conn. (Abstract No. 41)

11:30 A.M.—"Effect of Fluorides and Other Addition Agents on the Cathodic Potential of Titanium in Hydrofluoric Acid" by M. E. Straumanis, S. T. Shih, and A. W. Schlechten, Dept. of Metallurgy, School of Mines and Metallurgy, University of Missouri, Rolla, Mo. (Abstract No. 42)

Corrosion

with T. P. May presiding

(SKY ROOM)

2:00 P.M.—"Natural and Thermally Formed Oxide Films on Aluminum" by M. S. Hunter and P. Fowle, Aluminum Research Labs., Aluminum Co. of America, New Kensington, Pa. (Abstract No. 43)

2:30 P.M.—"Some Observations Regarding Zinc Anode Corrosion Products" by J. Kruger, O. R. Gates, and M. C. Bloom, Naval Research Lab., Washington, D. C. (Abstract No. 44)

3:00 P.M.—"High Temperature Corrosion Rates of Several Metals with Nitric Oxide" by Milton Farber, A. J. Darnell, and D. M. Ehrenberg, Jet Propulsion Lab., California Institute of Technology, Pasadena, Calif. (Abstract No. 45)

Electrodeposition

Wednesday, October 12, 1955

Hydrogen Embrittlement

with C. A. Snavely presiding

(ALLEGHENY ROOM)

9:00 A.M.—"The Hydrogen Embrittlement Problem in High Strength Steels" by T. F. Kearns, Bureau of Aeronautics, Navy Dept., Washington, D. C. (Abstract No. 46)

9:30 A.M.—"Mechanism for Hydrogen Entry Into Metals During Chemical and Electrochemical Processing" by L. D. McGraw, Battelle Memorial Institute, Columbus, Ohio. (Abstract No. 47)

10:00 A.M.—"Absorption of Hydrogen by Austenite, Ferrite, and Martensite, and Associated Hydrogen Embrittlement" by W. D. Robertson, Hammond Metallurgical Lab., Yale University, New Haven, Conn. (Abstract No. 48)

10:30 A.M.—"Measurements Related to Hydrogen in Metals" by W. E. Ditmars, Jr., and C. B. Griffith, Battelle Memorial Institute, Columbus, Ohio. (Abstract No. 49)

11:00 A.M.—"Room Temperature Diffusion of Hydrogen in Annealed and Plastically Deformed Steel" by M. L. Hill and E. W. Johnson, Westinghouse Research Labs., East Pittsburgh, Pa. (Abstract No. 50)

11:30 A.M.—"Hydrogen in Titanium and Titanium Alloys" by G. A. Lenning and R. I. Jaffee, Battelle Memorial Institute, Columbus, Ohio. (Abstract No. 51)

12:30 P.M.—Electrodeposition Division Luncheon and Business Meeting in the Fort Duquesne Room (17th floor).

Electrodeposition

Round Table

(ALLEGHENY ROOM)

2:30 P.M.–4:30 P.M.—Round-table discussion on Hydrogen Embrittlement.

Electrodeposition

Thursday, October 13, 1955

with Sydney Barnartt presiding

(ALLEGHENY ROOM)

9:00 A.M.—"Effect of Thickness on Mechanical Processes of Electrodeposited Nickel" by H. J. Read and R. F. Higgs, Dept. of Metallurgy, Pennsylvania State University, University Park, Pa. (Abstract No. 52)

9:30 A.M.—"Direct Determination of the Adhesive Bond Strength of Chromium Electrodeposited on Steel" by W. H. Dancy, Jr., and A. R. Kuhlthau, Ordnance Research Lab., University of Virginia, Charlottesville, Va. (Abstract No. 53)

10:00 A.M.—"A Nucleation Mechanism for Cathodic Polarization at Metallic Electrodes" by T. R. Rubin, Dept. of Chemistry, Ohio State University, Columbus, Ohio. (Abstract No. 54)

10:30 A.M.—"Composite Coatings of Chromium and Nickel for the Protection of Molybdenum Against High Temperature Oxidation" by J. K. Taylor, Harold Shapiro, and Abner Brenner, Div. of Chemistry, National Bureau of Standards, Washington, D. C. (Abstract No. 55)

11:00 A.M.—"Metallographic Study of Electroplated Coatings of Chromium and Nickel on Molybdenum" by R. J. Runck, Battelle Memorial Institute, Columbus, Ohio. (Abstract No. 56)

11:30 A.M.—"Copper Deposit from Sulfate and Cyanide Plating Bath; Investigation by Electron Microscopy" by Shinzo Okada and Saburo Magari, Engineering Research Institute, Kyoto University, Kyoto, Japan. (Abstract No. 57)

12:00 M.—"Electron Microscope Studies on Copper Anodes in Sulfate and Cyanide Baths" by Shinzo Okada, Saburo Magari, and Kentaro Katsui, Engineering Research Institute, Kyoto University, Kyoto, Japan. (Abstract No. 58)

Electronics—Semiconductors

Thursday, October 13, 1955

(MONONGAHELA ROOM)

9:00 A.M.—Ten-minute papers of "late news" type. Program will be available at the registration desk. There will be no abstracts.

Electronics—Semiconductors

(MONONGAHELA ROOM)

2:00 P.M.—Ten-minute papers of "late news" type. Program will be available at the registration desk. There will be no abstracts.

Electro-Organic

Monday, October 10, 1955

with H. M. Scholberg presiding

(MONONGAHELA ROOM)

10:00 A.M.—"Anodic Reactions in the Electrolysis of Lead Formate" by A. N. Kappanna and A. S. Dewagan, College of Science, Nagpur, India. (Abstract No. 59)

10:30 A.M.—"Anodic Oxidation of Certain Carbohydrates" by J. V. Karabinos, Blockson Chemical Co., Joliet, Ill. (Abstract No. 60)

11:00 A.M.—"Electrolytic Reduction of Some Polynuclear Carbocyclic Aromatic Compounds" by G. B. Diamond, 60 Chapel St., Newark, N. J. (Abstract No. 61)

12:30 P.M.—Society Luncheon in the Monongahela Room.

Electro-Organic

with H. M. Scholberg presiding

(MONONGAHELA ROOM)

2:15 P.M.—"Electro-Organic Reduction of 4-Keto-Pimelic Acid to Pimelic Acid" by H. J. Read, Pennsylvania State University, University Park, Pa. (Abstract No. 62)

2:45 P.M.—"Electrolytic Reduction of Amides, II. *p*-Aminobenzanilide and Anisamide" by Sherlock Swann, Jr., J. C. Bresee, and R. A. Strehlow, Dept. of Chemistry and Chemical Engineering, University of Illinois, Urbana, Ill. (Abstract No. 63)

3:15 P.M.—"Electrolytic Reduction of Cyclic Acid Imides" by Buhei Sakurai, Shinshu University, Matsumoto, Japan. (Abstract No. 64)

3:45 P.M.—"An Improvement for the Electrolytic Preparation of Aminoguanidine" by Motoji Yamashita and Kiichiro Sugino, Tokyo Institute of Technology, Meguro-ku, Tokyo, Japan. (Abstract No. 65)

4:15 P.M.—"Electrolytic Reduction of Cyanamide" by Keijiro Odo and Kiichiro Sugino, Tokyo Institute of Technology, Meguro-ku, Tokyo, Japan. (Abstract No. 66)

4:45 P.M.—"Mechanism of Electrolytic Reduction of 2-Amino-4-Chloropyrimidines to 2-Aminopyrimidines, and of 2-Aminopyrimidine; An Example of Two Different Types of Electrolytic Reduction" by Kiichiro Sugino, Taro Sekine, and Kozo Shirai, Tokyo Institute of Technology, Meguro-ku, Tokyo, Japan. (Abstract No. 67)

Electro-Organic

Tuesday, October 11, 1955

with H. M. Scholberg presiding

(MONONGAHELA ROOM)

9:00 A.M.—"Radicals by Kolbe Electrolysis" by W. H. Urry, Dept. of Chemistry, University of Chicago, Chicago, Ill. (Abstract No. 68)

9:30 A.M.—"Kolbe Electrosynthesis: Effect of Alternating Current, I. Acetic Acid-Potassium Acetate" by C. L. Wilson and W. T. Lippincott, McPherson Chemical Lab., Ohio State University, Columbus, Ohio. (Abstract No. 69)

10:00 A.M.—"Use of a Rotating Cathode in Electrolytic Reduction" by C. L. Wilson and H. V. K. Udupa, McPherson Chemical Lab., Ohio State University, Columbus, Ohio. (Abstract No. 70)

10:30 A.M.—"Cathodic Reduction of *N*-Dimethylaminoethyl Tetrachlorophthalimide" by M. J. Allen and J. Ocampo, Research Dept., Ciba Pharmaceutical Products, Inc., Summit, N. J. (Abstract No. 71)

11:00 A.M.—"Aqueous Kolbe Electrolysis of Mesitoate Ion" by G. W. Thiessen, W. Farr, and B. T. Shawver, Monmouth College, Monmouth, Ill. (Abstract No. 72)

Electro-Organic

with H. M. Scholberg presiding

(MONONGAHELA ROOM)

2:00 P.M.—"Electrochemical Reduction of Nitroguanidine and Related Compounds, I. Behavior of Nitro and Nitrosoguanidine at the Dropping Mercury Electrode" by G. C. Whitnack and E. St. C. Gantz, Analytical Chemistry Branch, U. S. Naval Ordnance Test Station, China Lake, Calif. (Abstract No. 73)

2:30 P.M.—"Polarographic Studies in Acetonitrile and Dimethylformamide, III. Behavior of Quinones and Hydroquinones" by S. Wawzonek, R. Berkey, E. W. Blaha, and M. E. Runner, State University of Iowa, Iowa City, Iowa. (Abstract No. 74)

3:00 P.M.—"Polarographic Behavior of Nitrobenzene in the Solvent Acetonitrile" by M. E. Runner and G. Balog, Illinois Institute of Technology, Chicago, Ill. (Abstract No. 75)

* * *

4:00 P.M.—Palladium Medal Address by U. R. Evans, Cambridge, England, in Urban Room.

Electro-Organic

Wednesday, October 12, 1955

with H. M. Scholberg presiding

(MONONGAHELA ROOM)

9:00 A.M.—"Polarographic Reduction of *p*-Hydroxybenzaldehyde" by C. Wheeler, Dept. of Chemistry, University of New Hampshire, Durham, N. H. (Abstract No. 76)

9:30 A.M.—"Polarographic Studies of Some Carbonyl Compounds" by R. A. Day, Jr., Emory University, Emory, Ga. (Abstract No. 77)

10:00 A.M.—"Polarographic Study of Alpha-Keto Acids; Significance of the Wave Separation Resulting from Changes in the *p*H of the Buffer" by O. H. Müller and W. J. P. Neish, Dept. of Physiology, College of Medicine, State University of New York, Syracuse, N. Y. (Abstract No. 78)

10:30 A.M.—"Application of Nonaqueous Polarographic Techniques to the Study of the Kinetics of Peroxidic Reactions" by C. Ricciuti and C. L. Ogg, Eastern Regional Research Lab., Philadelphia, Pa. (Abstract No. 79)

11:00 A.M.—"Oxidation of the Leuco Base of Malachite Green" by M. J. Allen and V. J. Powell, Research Dept., Ciba Pharmaceutical Products, Inc., Summit, N. J. (Abstract No. 80)

12:30 P.M.—Electro-Organic Division Luncheon and Business Meeting in Room 735 (7th floor).

Electro-Organic

Round Table

Mechanism of Reduction

with Stanley Wawzonek presiding

(MONONGAHELA ROOM)

2:00 P.M.–5:00 P.M.—Round-table discussion on Mechanism of Reduction. Speakers: S. Swann, Jr., on "Influence of Cathode Materials on Electrolytic Reductions;" C. Wilson on "Mechanism of Reduction of Organic Compounds at a Mercury Cathode;" N. Hackerman on "Influence of Hydrogen Overvoltage on Electrolytic Reduction of Organic Compounds;" P. Elving on "Reduction of Organic Halogen Compounds;" and M. J. Allen on "Mechanism of Reduction of Aldehydes and Ketones to Their Respective Hydrols or Pinacols."

Electrothermics and Metallurgy

Monday, October 10, 1955

Fluidized Solid Techniques

with Robert Toomey presiding

(SKY ROOM)

2:30 P.M.—"Development of the Fluid-Solid Technique" by A. F. Kaulakis, Esso Research and Engineering Co., Linden, N. J. (Abstract No. 81)

3:00 P.M.—"Graphical Presentation of Fluids-Solids Dynamics; Fluidized Solids Handling in the Metallurgical Industry" by F. A. Zenz, M. W. Kellogg Co., Jersey City, N. J. (Abstract No. 82)

3:30 P.M.—"Chemical Reactions in Fluidized Beds" by F. M. Stephens, Jr., and L. W. Coffer, Battelle Memorial Institute, Columbus, Ohio. (Abstract No. 83)

4:00 P.M.—"Roasting Sulfides in a Fluidized Bed" by R. J. Priestley, Dorr-Oliver, Barry Place, Stamford, Conn. (Abstract No. 84)

Electrothermics and Metallurgy

Tuesday, October 11, 1955

Preparation, Analysis, and Properties of High-Purity Metals

with E. M. Sherwood presiding

(SKY ROOM)

9:30 A.M.—"Modern Technology and High-Purity Metals" by I. E. Campbell, Battelle Memorial Institute, Columbus, Ohio. (Abstract No. 85)

10:00 A.M.—"Fusion Electrolysis of Bismuth Trichloride" by Paul Gruzensky, Bureau of Mines, U. S. Dept. of the Interior, Albany, Oreg. (Abstract No. 86)

10:30 A.M.—"Preparation of Pure Nickel by Electrolysis of a Chloride

Solution" by W. A. Wesley, Research Lab., International Nickel Co., Bayonne, N. J. (Abstract No. 87)

11:00 A.M.—"Preparation of High-Purity Rhenium" by D. M. Rosenbaum, R. J. Runck, and I. E. Campbell, Battelle Memorial Institute, Columbus, Ohio. (Abstract No. 88)

11:30 A.M.—"Vacuum Melting and Casting of High-Purity Metals" by N. Darmara, Utica Tool and Drop Forge Co., Utica, N. Y. (Abstract No. 89)

12:30 P.M.—Electrothermics and Metallurgy Division Luncheon, in the Allegheny Room (17th floor).

Electrothermics and Metallurgy

Preparation, Analysis, and Properties of High-Purity Metals (cont'd)

with A. U. Seybolt presiding

(SKY ROOM)

2:00 P.M.—"Floating-Zone Purification of Zirconium" by G. D. Kneip, Jr., and J. O. Betterton, Jr., Union Carbide and Carbon Corp., Oak Ridge National Lab., Oak Ridge, Tenn. (Abstract No. 90)

2:25 P.M.—"Cage Zone Melting" by P. H. Brace and G. Comenetz, Westinghouse Research Labs., East Pittsburgh, Pa. (Abstract No. 91)

2:50 P.M.—"Quality-Control Techniques Employed in the Production of High-Purity Zirconium and Hafnium Metals" by H. L. Kall, Carborundum Metals Co., Inc., Akron, N. Y. (Abstract No. 92)

3:15 P.M.—"Determination of Trace Elements in Metals and Alloys by Radioactivation Analysis" by G. W. Leddicotte and W. A. Brooksbank, Jr., Union Carbide and Carbon Corp., Oak Ridge National Lab., Oak Ridge, Tenn. (Abstract No. 93)

* * *

4:00 P.M.—Palladium Medal Address by U. R. Evans, Cambridge, England, in the Urban Room.

Electrothermics and Metallurgy

Wednesday, October 12, 1955

Preparation, Analysis, and Properties of High-Purity Metals (cont'd)

with J. R. Musgrave presiding

(SKY ROOM)

9:30 A.M.—"A Study of Separations in the Analysis of High-Purity Metals" by O. R. Gates, Naval Research Lab., Washington, D. C. (Abstract No. 94)

10:00 A.M.—"Metallographic Techniques" by E. E. Thomas, Bell Telephone Labs., Murray Hill, N. J. (Abstract No. 95)

10:30 A.M.—"Special Techniques for Analyzing Semiconducting Materials" by J. M. Whelan, Bell Telephone Labs., Murray Hill, N. J. (Abstract No. 96)

11:00 A.M.—"Preparation and Analysis of High-Purity Tellurium" by S. E. Miller and H. L. Goering, Battelle Memorial Institute, Columbus, Ohio. (Abstract No. 97)

Electrothermics and Metallurgy

Preparation, Analysis, and Properties of High-Purity Metals (cont'd)

with B. W. Gonser presiding

(SKY ROOM)

2:00 P.M.—"Ductile Chromium" by W. H. Smith and A. U. Seybolt, Research Lab., General Electric Co., Schenectady, N. Y. (Abstract No. 98)

2:30 P.M.—"Effect of Impurities on the Hardness of Titanium" by T. D. McKinley, E. I. du Pont de Nemours & Co., Wilmington, Del. (Abstract No. 99)

3:30 P.M.—"Effect of Impurities on the Tensile Properties of Aluminum" by A. P. Young, Battelle Memorial Institute, Columbus, Ohio. (Abstract No. 100)

3:00 P.M.—"Addition of Controlled Amounts of Impurities to a Titanium-Molybdenum Alloy" by S. J. Noesen, General Electric Co., Schenectady, N. Y. (Abstract No. 101)

ABSTRACTS

BATTERY

Abstract No. 1

RESISTIVITY STUDIES OF VARIOUS LECLANCHÉ CATHODE MATERIALS

Richard Glicksman and
C. K. Morehouse

It has been suggested that there is a correlation between dry cell performance and the resistivity of various manganese dioxides. Resistivity data obtained on four types of manganese dioxides over a range of applied pressures up to 100,000 lb/in.^{2} show quite different resistivity vs. applied pressure relationships. These differences, however, are minimized by blending high-resistivity manganese dioxide with low-resistivity Shawinigan acetylene black and electrolyte, and it is concluded that no direct correlation between dry cell performance and resistivity of the manganese dioxide can be made.

Abstract No. 2

A POLARIZATION TECHNIQUE FOR EVALUATING VARIOUS CATHODE MATERIALS

C. K. Morehouse and
Richard Glicksman

A polarization apparatus and technique are described which enable a quick preliminary evaluation to be made of various manganese dioxides and other cathode materials in various electrolytes. Data are presented which show that the reaction of the manganese dioxide electrode during cell discharge is diffusion-controlled. It is also shown that the structure of the manganese dioxide material is an important property which determines the performance that is obtained when the electrode is discharged, not only in an NH_4Cl-$ZnCl_2$ type electrolyte, but also in a basic electrolyte.

Abstract No. 3

THE ALUMINUM DRY CELL

J. J. Stokes, Jr.

Aluminum dry cells of the familiar Leclanché type show much promise. Discharge characteristics are similar to those of zinc and magnesium cells. The electrolyte is aluminum or chromium chloride inhibited with ammonium or alkali chromates. Best results are obtained with alclad-type anodes which contain an aluminum-zinc alloy and cathodes of MnO_2 and acetylene black. Paper spacers are used instead of flour-starch gels. Storage tests at room temperature indicate shelf life at least comparable to the zinc cell.

Abstract No. 4

AN ELECTRON DIFFRACTION STUDY OF LEAD MONOXIDES

Jeanne Burbank

An electron diffraction study of the lead monoxides indicated the existence of a third form for this compound. A space lattice is suggested, followed by a discussion of its relation to the orthorhombic and tetragonal forms of PbO and to the lattice of pure lead.

CORROSION

Abstract No. 5

OXIDATION OF OXYGEN-FREE HIGH CONDUCTIVITY COPPER

I. Oxidation of Copper to Cu_2O

J. P. Baur, D. W. Bridges, and W. M. Fassell, Jr.

Effect of oxygen pressure on the oxidation behavior of copper was studied at 900° (5–10 mm-Hg), 950° (10–35 mm-Hg), and 1000° C (5–95 mm-Hg) under conditions involving the system $Cu/Cu_2O/O_2$. Weight increase per unit surface area was correlated with time decrement through use of two parallel reaction rates: (*a*) a diffusion-controlled step, and (*b*) a phase boundary reaction. Exception is taken with the unchecked increase of the parabolic rate constant with increased external oxygen pressure seemingly inferred in Wagner's equation, K_p = const. $(P_{O_2})^{1/n}$. Surface site saturation will lead to a cessation of the increase in the parabolic rate constant as the oxygen pressure increases to where the adsorption potential is sufficient to accommodate oxygen on all available surface sites. Photomicrographic study of the growth of CuO on Cu_2O is included.

Abstract No. 6

HIGH PRESSURE OXIDATION OF METALS

Niobium in Oxygen

D. W. Bridges and W. M. Fassell, Jr.

Niobium oxidized linearly in oxygen from 400° to 800°C at oxygen pressures ranging from 14.7 to 605 psia. Wide variations in oxidation rates were observed with variations in oxygen pressure. An equilibrium adsorption process occurs prior to the rate-determining step in the reaction. For niobium it was necessary to include an interaction energy term between the adsorbed oxygen molecules on the adsorption sites to interpret adequately results above 650°C. Orientation of the metal surface apparently influences the interaction energy. Enthalpy of activation was 9,000–10,000 cal/mole (500°–800°C). Enthalpy and entropy of adsorption were −48,550 cal/mole and −52.6 e.u. from 550°–650°C. The interaction energy, εV, varied from 8,300 cal/mole (500°C) to 11,900 cal/mole (800°C).

Abstract No. 7

HIGH PRESSURE OXIDATION OF METALS

Tungsten in Oxygen

J. P. Baur, D. W. Bridges, and W. M. Fassell, Jr.

Tungsten rod and sheet oxidized linearly in oxygen from 600° to 850°C at oxygen pressures ranging from 20 to 500 psia. Rate of oxidation increased with increased oxygen pressure at temperatures 750°–850°C. Theoretical considerations indicate that an equilibrium adsorption process occurs prior to the rate-determining step in the reaction. Assumption of a linear change of adsorption energy with increase of surface coverage allowed experimentally observed rates of oxidation to be corrected for pressure effect. The activation energy for the oxidation of tungsten (600°–850°C) is 84 kcal. Tungsten oxidation above 900°C was not reported as the metal oxide formed volatilizes. Tungsten sheet volatilization losses were appreciable above 800°C. Only rod data were free from volatilization losses at 850°C.

Abstract No. 8

OXIDATION OF TUNGSTEN

W. W. Webb,* J. T. Norton, and Carl Wagner

Two oxide layers form during the oxidation of tungsten between 700° and 1000°C. The outer layer is porous, powdery, yellow tungstic oxide WO_3 and the inner layer is a dense, thin, dark blue, tightly adherent oxide of uncertain composition. The oxidation reaction follows initially the parabolic rate law, but eventually there is a transition to the linear rate law. The rate of formation of the inner oxide is presumably inversely proportional to its thickness. The inner oxide seems to transform to the outer oxide at a constant rate. Upon combining the rate laws of the two individual processes, an over-all rate equation covering the whole range is obtained.

Abstract No. 9

OXIDATION STUDIES IN METAL-CARBON SYSTEMS

W. W. Webb,* J. T. Norton, and Carl Wagner

A general analysis of the characteristics of the oxidation of alloys containing carbon or carbides is given. Evolution of gaseous CO and CO_2 may rupture oxide films which, in the absence of carbon, are highly protective. On the other hand, if the base metal has a high affinity for oxygen, carbon may be retained in the alloy, or carbon may diffuse across the oxide layer. Experimental data are reported for the systems Ni-C, W-C, Mn-C, and Ti-C.

Abstract No. 10

ROLE OF DISLOCATION IN THE OXIDATION OF METALS

N. Cabrera

(No abstract received)

Abstract No. 11

OXIDATION OF IRON-MOLYBDENUM AND NICKEL-MOLYBDENUM ALLOYS

S. S. Brenner

Binary alloys of iron and molybdenum (up to 12.5 atomic % Mo) and nickel and molybdenum (up to 19.7 at. % Mo) do not exhibit "catastrophic oxidation" up to 1000°C either in stationary or in flowing atmospheres. In both systems, MoO_2 and iron molybdate or nickel molybdate are formed in addition to iron oxides or nickel oxide. Molybdenum significantly decreases the oxidation rate of iron by preventing formation of the cation deficient FeO normally formed on iron above 570°C. The oxidation rate of nickel, however, is affected only to a small extent. Up to 3 at. % molybdenum, the rate is slightly increased by formation of additional vacancies in the nickel oxide, while beyond 12 at. % the oxidation rate is again decreased owing to the densification of the MoO_2 subscale.

Abstract No. 12

CATASTROPHIC OXIDATION OF SOME MOLYBDENUM-CONTAINING ALLOYS

S. S. Brenner

When nickel or chromium is added to binary iron-molybdenum alloys, catastrophic oxidation occurs in certain concentration regions. Chromium is more effective than nickel in inducing this rapid type of oxidation. Catastrophic oxidation occurs because of the formation of liquid MoO_3 along the metal-oxide interface. This is preceded by the cracking of the chromium or

* Allegheny Ludlum Steel Co. Fellow 1953-1955; present address: Metals Research Labs., Union Carbide and Carbon Corp., Niagara Falls, N. Y.

nickel-containing oxide. Catastrophic oxidation does not occur with alloys containing large amounts of nickel.

Abstract No. 13

A SPECTROPHOTOMETRIC STUDY OF THE OXIDATION OF URANIUM

J. T. Waber and G. E. Sturdy

The spectrophotometric method has been used to study the initial stages of the oxidation of uranium. It was observed that corrosion behavior could be described adequately by a logarithmic growth law. The energy of activation for the logarithmic rate constant was found to be 4.5 kcal/g-mole. Also, the reflectivity of metallic uranium was measured.

Abstract No. 14

OXIDATION OF IRON-NICKEL ALLOYS

R. T. Foley, J. U. Druck, and R. E. Fryxell

The mechanism of the high temperature (600°–900°C) oxidation of an iron-nickel alloy containing 42% nickel was studied. Reaction products were examined by metallographic and electron diffraction techniques, as well as chemical analyses after stripping.

Temperature dependence of the parabolic oxidation rate constant follows the Arrhenius equation with parameters dependent on the method of surface preparation. The oxide film upon cooling possesses a two-phase structure with a nickel ferrite next to the alloy and Fe_2O_3. Differences in activation energies and oxidation rates are explained by diffusion through ferrite structures ranging from $NiFe_2O_4$ to Fe_3O_4.

Abstract No. 15

REACTION OF HYDROGEN WITH URANIUM

W. M. Albrecht and M. W. Mallett

Reaction rates of hydrogen with uranium follow the linear law in the temperature range 96°–400°C at pressure levels of $p - p_e$ equal to 430, 150, and 70 mm of mercury. Adsorption plays an important role in the over-all reaction mechanism of uranium with hydrogen. From 96° to about 250°C, adsorption is faster than the reaction to form hydride, but it is of the same order of magnitude. Therefore, formation of hydride is the rate-determining step. From about 250° to 400°C adsorption is probably the rate-controlling step, except for the initial parabolic reaction which would be diffusion controlled.

Abstract No. 16

FORMATION OF POROUS SCALES

C. E. Birchenall

(No abstract received)

Abstract No. 17

PRELIMINARY RESULTS ON THE KINETICS OF THE REACTION OF METALS WITH WATER VAPOR

Paul Blackburn and E. A. Gulbransen

(No abstract received)

Abstract No. 18

OXIDATION STUDIES ON Fe-Cr-Al HEATER ALLOYS

Kenneth Andrew and E. A. Gulbransen

Three studies were made of this alloy system. First, the oxidation of these alloys was studied under constant temperature conditions from 600° to 950°C with no strain present. Second, the oxidation at 900°C was studied before and after a 2% strain. This type of study gives information on the adhesion of the oxide as it affects the oxidation rate. Third, the composition and crystal structure of the oxide films formed during oxidation were studied by the high temperature electron diffraction method.

Results of these studies showed that the Fe-Cr-Al alloys oxidized faster than the Ni-Cr or Ni-Cr-Fe alloys. However, strain oxidation studies showed the Fe-Cr-Al alloys to be superior.

Abstract No. 19

ACCELERATION OF THE DISSOLUTION OF IRON IN SULFURIC ACID BY FERRIC IONS

H. C. Gatos

Dissolution of iron in H_2SO_4 was studied as a function of Fe^{+++} and H^+ concentration. For a given H_2SO_4 concentration the dissolution rate increases and the hydrogen evolution rate decreases with increasing Fe^{+++} concentration. On the other hand, for a given Fe^{+++} concentration the dissolution rate decreases and the hydrogen evolution rate increases with increasing H_2SO_4 concentration. The presence of Fe^{+++} shifts the electrode potential of iron in H_2SO_4 toward more noble values. An explanation of these phenomena is offered, based on the direct reduction of the Fe^{+++} at the local cathodes in competition with H^+.

Abstract No. 20

DISSOLUTION OF METALS IN AQUEOUS ACID SOLUTIONS

II. Kinetics for the Reactions of Steel

N. M. Komodromos,* A. C. Makrides,** and Norman Hackerman

Dissolution rates of mild steel in acid solutions containing ferric chloride, ceric sulfate, potassium dichromate, benzoquinone, tolu-*p*-quinone, and sodium anthraquinone sulfonate are reported. The effect of stirring velocity, surface roughness, and temperature is given. Results are consistent with the assumption that diffusion of depolarizer to the metal surface is rate limiting.

* Present address: E. I. du Pont de Nemours & Co., Flint, Mich.

** Present address: Institute for the Study of Metals, University of Chicago, Chicago, Ill.

Abstract No. 21

EFFECT OF ALLOYING ELEMENTS IN IRON ON HYDROGEN OVERVOLTAGE AND CORROSION RATE IN ACID ENVIRONMENTS

Milton Stern*

Alloying elements commonly found in steel were added to pure iron to establish their effect on hydrogen overvoltage and corrosion rate in 0.1*M* citric acid (*p*H 2.06), 0.1*M* malic acid (*p*H 2.24), and 4% sodium chloride at *p*H 1 and 2. Sulfur, phosphorus, and carbon proved detrimental to corrosion resistance. Copper and manganese were effective in decreasing the detrimental influence of sulfur. Hydrogen overvoltage data are used to explain the particular influences found for various addition elements.

* Present address: Metals Research Labs., Electro Metallurgical Co., Niagara Falls, N. Y.

Abstract No. 22

DISSOLUTION OF CADMIUM IN CHROMIC CHLORIDE-HYDROCHLORIC ACID SOLUTIONS

C. V. King and Edward Hillner

The dissolution rate of cadmium has been measured in chromic chloride solutions containing hydrochloric acid up to 4M, as a function of concentration, stirring speed, and temperature. In violet solutions, containing the hexaaquo ion, dissolution is slow and chemically controlled; in green solutions of the dichlorotetraaquo ion it is transport-controlled. Reaction with the green ion is rapid in spite of a driving force of only a few millivolts. The potential of the metal in these solutions is essentially that of the cadmium-cadmium ion couple, and there is little if any anodic polarization.

Abstract No. 23

ROLE OF HYDROGEN IN CORROSION REACTIONS

J. E. Draley and W. E. Ruther

Hydrogen produced during aqueous corrosion can influence the course of the reaction. Diffusion into the metal causes high stress concentrations, sometimes resulting in cracking or blistering. Formation of hydrogen gas beneath the protective barrier film can cause film rupture and accelerated corrosion. In the corrosion of certain hydride-forming metals, metal hydride is believed to form beneath the barrier film, destroying its adherence to the metal and reducing its protective properties. A number of unusual effects, such as anodic protection, are explainable in these terms.

Abstract No. 24

A STUDY OF THE CATHODIC REDUCTION OF OXIDE FILMS ON IRON

I. Reduction of Alpha-Fe_2O_3 Films

H. G. Oswin and M. Cohen

The apparatus and technique for the cathodic reduction of alpha-Fe_2O_3 films is described. Measurements of the efficiency of the reduction in buffered and unbuffered electrolytes are given. Effects of *p*H of the electrolyte, dissolved oxygen, current density, and film thickness are noted and discussed. Electrolytes containing "ferrous-complexing" ions have also been investigated. Methods of determining quantities of alpha-Fe_2O_3 in thin films are suggested and their limits of accuracy considered.

Abstract No. 25

KINETICS OF EXCHANGE BETWEEN SOLID COPPER AND SILVER IONS IN AQUEOUS SOLUTIONS

M. Simnad, A. Spilners, and Ling Yang

Rates of electrochemical exchange between solid copper specimens and silver ions in solutions have been studied. The effect of various factors, such as temperature, ionic concentration, and surface structure on the rate of exchange has been determined. Distribution of the exchanged ions on the metal surface is demonstrated by means of autoradiographs and by microscopic examination.

Abstract No. 26

A STUDY OF THE EFFECT OF CHLORIDE ION ON FILMS FORMED ON IRON IN SODIUM NITRITE SOLUTIONS

G. W. Mellors, M. Cohen, and F. Beck

The effect of chloride ion on the potential of iron in sodium nitrite solutions has been measured, and related to surface composition and topography by electron diffraction and electron microscopy. The effect of initial surface preparation has also been investigated. It was shown that in the absence of chloride ion the potential is noble and steady and that the surface remains practically unchanged. A film of γ-Fe_2O_3 is shown to be present by electron diffraction. When chloride ion was added to the system the potential became unsteady and less noble. Inclusions of a second phase grew in the oxide layer. This proved to be hydrated γ-Fe_2O_3 or lepidocrocite.

Abstract No. 27

MECHANISM OF THE HYDROGEN EVOLUTION REACTION ON SILVER AND TUNGSTEN CATHODES

J. O'M. Bockris

(No abstract received)

Abstract No. 28

OXYGEN ADSORPTION ON STAINLESS STEEL

T. N. Rhodin, Jr.

Chemisorption of oxygen occurs on deoxidized stainless steel at −195°C with very low energies of activation and high heats of adsorption. The amount and mechanism of adsorption show a unique dependence on the temperature from −195° to 100°C. The effectiveness of the original deoxidation treatment is critical.

Conversion of adsorbed layers to ultrathin oxide films occurs at temperatures from 0° to 30°C. Contrary to previous reports in the literature, chemisorption equivalent to a monolayer on a deoxidized surface or physical adsorption of 10 layers does not passivate the surface to 1*N* H_2SO_4 solution at 25°C.

Abstract No. 29

ELECTRICAL PROPERTIES OF THE OXIDE FILM ON ZIRCONIUM

R. D. Misch

A three-wire probe is employed to measure the electrical conductivity of thin oxide films on zirconium as a function of temperature. Anodic films from 1000 to 10,000 Å in thickness and natural corrosion films have been examined. Conduction begins at a well-defined temperature which depends on film thickness. Upon further slow heating, the current through the film rises rapidly and exponentially. Specimens can be cycled repeatedly into the conduction range, but often show permanent electrical breakdown. Curves of temperature of conduction vs. film thickness are a function of the base metal and the method of film preparation. The significance of these factors for gas-metal oxidation theory is discussed.

Abstract No. 30

ORTHOPHOSPHATES OF IRON, MANGANESE, AND ZINC

Jeanne Burbank

Iron, manganese, and zinc orthophosphates most likely to be encountered in phosphating processes and coatings were synthesized, and their x-ray diffraction patterns established. The solution rate of steel in phosphoric acid was determined as a function of time, temperature, and acid concentration.

Abstract No. 31

INFLUENCE OF SPECIMEN AREA ON THE PITTING PROBABILITY OF ALUMINUM

P. M. Aziz and H. P. Godard

The pitting probability of 2S aluminum was determined in Kingston tap

water as a function of area, for areas ranging in size from 0.06 cm² to 243 cm². The pitting probability was found to vary uniformly with area from 0.001 to 1 as the area increased from 0.06 cm² to 60 cm²; extrapolation indicated that the pitting probability becomes zero at an exposed area of about 0.055 cm². This work supports the contention that pitting sites in aluminum are not specific macrodefects in the metal surface, but rather arise in a random fashion through the interaction of myriads of anodic and cathodic elements on the metal surface.

Abstract No. 32

PITTING CORROSION OF 18 Cr-8 Ni STAINLESS STEEL

I. Development of Accelerated Electrolytic Pit Initiation Methods

M. A. Streicher

(No abstract received)

Abstract No. 33

PITTING CORROSION OF 18 Cr-8 Ni STAINLESS STEEL

II. Investigation of Variables in the Metal and in the Electrolyte Which Control Pit Initiation

M. A. Streicher

(No abstract received)

Abstract No. 34

DETERMINATION OF CORROSION RATES IN AQUEOUS SYSTEMS AT ELEVATED TEMPERATURE AND PRESSURE BY A HYDROGEN EFFUSION METHOD

M. C. Bloom and M. Krulfeld

A technique is described in which the corroding solution, sealed in a thin-walled capsule of the metal under test, is inserted in a glass system of known volume. After evacuation of the system, the capsule is dropped in a heated section and the hydrogen, generated by corrosion, permeates the capsule walls. Hydrogen collects in the glass system where its pressure is continuously recorded, giving a record of the corrosion reaction.

Abstract No. 35

GALVANIC CORROSION CHARACTERISTICS OF ALUMINUM ALLOYS

M. J. Pryor and D. S. Keir

Current flow and polarization data have been determined for aluminum-steel, zinc-steel, aluminum-copper, and aluminum-zinc couples in sodium chloride solutions. The effect of anode and cathode areas and the effect of stirring have been studied for the aluminum-steel and zinc-steel couples in similar solutions. Some of the factors controlling rates of galvanic corrosion are suggested.

Abstract No. 36

CRYSTALLIZATION OF ANODIC TANTALUM OXIDE FILMS IN THE PRESENCE OF A STRONG ELECTRIC FIELD

D. A. Vermilyea

Crystallization of amorphous anodic oxide films on tantalum may be accomplished by holding at temperatures in the neighborhood of room temperature, provided a strong electric field is present in the film. Such crystallization results in crystalline areas consisting of pie-shaped polycrystalline segments surrounded by coiled-up cylinders of the replaced amorphous phase. Factors affecting the nucleation and growth of these areas are discussed, and a mechanism of growth is proposed. Nucleation of the areas is not understood at present.

Abstract No. 37

VARIOUS FACTORS AFFECTING THE FORMATION OF ANODIC OXIDE COATINGS IN SULFURIC ACID ELECTROLYTES

R. B. Mason

Factors affecting the solubility of the coatings, such as had developed within the coating and time of immersion, have been investigated. Rapid changes in current and voltage, which occur in the first 15 sec after the current is turned on, give certain clues as to the possible mechanism of pore formation. The amount of sulfate found in anodic coatings formed on pure aluminum anodes in sulfuric acid electrolytes increased as the current density and concentration of acid increased, but decreased as the temperature was raised. Chemical analysis showed that the coatings consisted substantially of Al_2O_3 and SO_3 with practically no water.

Abstract No. 38

ELECTROCHEMICAL STUDIES OF ALUMINUM CORROSION IN WATER

Manuel Shaw and S. B. Twiss

A technique for measuring corrosion current is outlined, and its relationship to the effect of *p*H, chloride ion concentration, and additives on the corrosion or corrosion inhibition of aluminum is determined. Comparison of various natural waters indicates that large corrosion currents exist when the *p*H is greater than 10; below this value, corrosion of aluminum is determined primarily by chloride ion concentration. A large number of compounds are screened and classified according to current range as to their efficiency as inhibitors or stimulators of corrosion of alclad aluminum.

Abstract No. 39

ANODIC POLARIZATION OF ZIRCONIUM AT LOW POTENTIALS

Formation Rates, Formation Field, Electrolytic Parameters, and Film Thicknesses of Very Thin Oxide Films

G. B. Adams, Jr., Mario Maraghini, and Pierre Van Rysselberghe

Working below oxygen evolution potentials, the above quantities were evaluated from anodic potential-time measurements. Results obtained are shown to be internally consistent, and are in agreement with those found by others for anodic oxide films formed on zirconium in the high potential range.

Correlation is established between these results and the authors' previously reported work on the estimation of local currents from anodic potential-time measurements.

All results have been interpreted on the assumption of true oxide film growth below oxygen evolution potentials.

Abstract No. 40

ELECTROCHEMICAL THERMODYNAMICS OF J. WILLARD GIBBS AND THE STOCKHOLM CONVENTIONS

The Gibbs-Stockholm Electrode Potential

A. J. de Béthune

The electrode potential, defined by Gibbs' expression $V = V_m - V_e$ remains sign invariant upon the reversal of an infinitesimal current flow, while the half-cell emf E changes sign. For the potential of a metallic electrode, Gibbs writes $V_m - V_e = (RT/n_m\gamma) \ln \gamma/G$ where γ is the density of the metal ions in solution, and G is analogous to Nernst's "metal solution pressure." In

terms of the sign-invariant Gibbs-Stockholm electrode potential V, the free enthalpy is $F = +nV$ for anodic oxidations and $F = -n\gamma V$ for cathodic reductions. This makes V a measure of the oxidizing power of oxidizing agents. A positive V may be referred to as a galvanic "reduction" or "cathodic" potential, and as an electrolytic "oxidation" or "anodic" potential.

Abstract No. 41

ELECTROCHEMICAL POTENTIALS OF GRAINS AND GRAIN BOUNDARIES IN COPPER SOLID SOLUTIONS

R. Bakish and W. D. Robertson

Irreversible potentials of grains and grain boundaries were measured in pure copper, Cu_3Au, and in alpha brass; the three cases represent the structural grain boundary in a pure metal, an alloy in which only one component is oxidized, and an alloy in which both components are oxidized. Potentials were measured in ferric chloride and in aqueous ammonia, the former representing an electrolyte in which only Cu_3Au is susceptible to stress cracking, and the latter representing conditions in which brass is susceptible to stress cracking.

Abstract No. 42

EFFECT OF FLUORIDES AND OTHER ADDITION AGENTS ON THE CATHODIC POTENTIAL OF TITANIUM IN HYDROFLUORIC ACID

M. E. Straumanis, S. T. Shih, and A. W. Schlechten

Cathodic potentials of Ti in HF become more negative with the addition of alkali fluorides to the acid. The effect increases with the concentration of the salt and in the sequence $NH_4F \rightarrow KF \rightarrow NaF$, which is also the sequence of decreasing cationic radius. If the Ti cathode dissolves in the acid, the cathodic potential-current density relationship is linear; if the dissolution ceases (at higher concentrations of the added fluoride), Tafel's relationship is fulfilled. In between there is a mixed straight line and quasi logarithmic relationship, the latter occurring at higher current densities.

Abstract No. 43

NATURAL AND THERMALLY FORMED OXIDE FILMS ON ALUMINUM

M. S. Hunter and P. Fowle

Structure and rate of formation of natural and thermally formed oxide films on aluminum are discussed. It is shown that these films consist of a layer of barrier-type oxide, the thickness of which is primarily a function of temperature, and a porous layer, the thickness of which is determined by time and natural forces associated with the environment. Effects of temperature and environment on the formation rate and ultimate thickness of these layers are described.

Abstract No. 44

SOME OBSERVATIONS REGARDING ZINC ANODE CORROSION PRODUCTS

J. Kruger, O. R. Gates, and M. C. Bloom

Zinc as a galvanic anode in sea water has been plagued by the formation of insoluble products. Improved behavior has been demonstrated for low iron content (<0.0015%) anodes. Experiments are described pointing to the formation of adherent grain boundry material in the zincs of higher iron content as the offender. X-ray diffraction studies which give clues to the nature of this material are described.

Abstract No. 45

HIGH TEMPERATURE CORROSION RATES OF SEVERAL METALS WITH NITRIC OXIDE*

Milton Farber, A. J. Darnell, and D. M. Ehrenberg

An experimental study has been made of the high temperature corrosion rates of various metal filaments with nitric oxide. Corrosion rates have been determined for iron, tantalum, tungsten, molybdenum, nickel, copper, silver, and the alloys Inconel,** and stainless steel. Temperature range included temperatures from 800°–2000°K. Metals in order of decreasing corrosion resistance are Inconel, 25-20 stainless steel, molybdenum, nickel, tantalum, 18-8 stainless steel, tungsten, iron, and copper.

* This paper presents the results of one phase of research carried out at the Jet Propulsion Laboratory under Contract No. DA-04-495-Ord 18, sponsored by the Department of the Army, Ordnance Corps.

** Inconel is registered trade mark of the International Nickel Company.

ELECTRODEPOSITION

Abstract No. 46

THE HYDROGEN EMBRITTLEMENT PROBLEM IN HIGH STRENGTH STEELS

T. F. Kearns

The significance of the hydrogen embrittlement problem is developed on the basis of requirements primarily for aircraft for use of steels at very high strength levels. The pertinent fabrication processes and the sources of hydrogen are indicated and current methods of alleviating hydrogen damage are outlined. Data are presented on the relationship between stresses and hydrogen damage in steels at the 260 to 280,000 psi strength level. Fabrication processes which result in residual tensile stresses at the surface are serious complicating factors in hydrogen embrittlement of steels at this strength level in view of the low tempering temperatures required and the consequent inability to relieve residual stresses.

Abstract No. 47

MECHANISM FOR HYDROGEN ENTRY INTO METALS DURING CHEMICAL AND ELECTROCHEMICAL PROCESSING

L. D. McGraw

Proposed mechanisms for entry of hydrogen into metals are reviewed in terms of the experimental evidence supporting them. The possibilities that lattice defects, catalysis, hydride formation, and diffusion rate influence the permeability of metals to hydrogen are taken into consideration. The relation of hydrogen overvoltage phenomena to possible hydride formation, chemisorption of hydrogen, and rate of recombination of atomic hydrogen is discussed.

Abstract No. 48

ABSORPTION OF HYDROGEN BY AUSTENITE, FERRITE, AND MARTENSITE, AND ASSOCIATED HYDROGEN EMBRITTLEMENT

W. D. Robertson

The absorption and permeation rate of hydrogen in various steel structures has been determined. The delayed fracture of steel has been investigated as a function of measured hydrogen content, stress, time, and structure.

Abstract No. 49

MEASUREMENTS RELATED TO HYDROGEN IN METALS

W. E. Ditmars, Jr., and C. B. Griffith

Techniques used at present are briefly reviewed, including measurements on: (*a*) hydrogen entry; (*b*) hydrogen content of the metal; (*c*) form of hydrogen in the metal; and (*d*) hydrogen influenced changes in the properties of the metal. Iron and steels are emphasized. Measurements most satisfactory for studying particular types of problems are discussed. Problem areas where present techniques appear to give ambiguous answers are mentioned.

Abstract No. 50

ROOM TEMPERATURE DIFFUSION OF HYDROGEN IN ANNEALED AND PLASTICALLY DEFORMED STEEL

M. L. Hill and E. W. Johnson

The room temperature diffusivity, D, of hydrogen in annealed iron was determined from rates of hydrogen evolution from homogeneously charged cylinders. The result, 2.1×10^{-7} cm²/sec, is some 60 times a previous experimental value, but only 1% of other published values as obtained by extrapolation from above 350°C.

Plastic deformation greatly reduces the bulk diffusivity. Thus, hydrogen-charged, prestrained tensile test specimens retained their hydrogen, and hence their embrittlement, during aging sufficiently to eliminate the hydrogen from unstrained material. With heavier cold working diffusion apparently ceased altogether below 200°C.

Abstract No. 51

HYDROGEN IN TITANIUM AND TITANIUM ALLOYS

G. A. Lenning and R. I. Jaffee

An understanding of the effects of hydrogen in titanium and titanium alloys is important because of its embrittling action. Unalloyed titanium and titanium alloys containing alpha-stabilizing additions, such as aluminum, are most subject to hydrogen embrittlement at impact speeds in the presence of a notch. On the other hand, alpha-beta-type alloys containing beta-stabilizing elements, such as manganese, are most subject to embrittlement at slow test speeds.

Mechanical-property tests and failures in service have demonstrated the desirability of maintaining low hydrogen levels in titanium materials. To this end, sources of hydrogen contamination in extraction, melting, and processing of titanium materials have received intensive study recently.

Abstract No. 52

EFFECT OF THICKNESS ON MECHANICAL PROPERTIES OF ELECTRO DEPOSITED NICKEL

H. J. Read and R. F. Higgs

Tensile strengths and ductilities were determined by means of the hydraulic bulge test on nickel deposits ranging in thickness from 0.3 to 3 mils, prepared from Watts, nickel-chloride, and nickel-fluoborate baths. Thickness has very little effect on the tensile strength of the deposits, but the ductility as measured by significant strain at fracture decreases with decreasing thickness of nickel.

Abstract No. 53

DIRECT DETERMINATION OF THE ADHESIVE BOND STRENGTH OF CHROMIUM ELECTRODEPOSITED ON STEEL*

W. H. Dancy, Jr., and A. R. Kuhlthau

Small chromium plated rotors have been suspended in a magnetic field and accelerated until the centrifugal forces acting on the plate cause it to be torn from the hardened steel base metal. A knowledge of the size of the rotor, the thickness and density of the coating, and the speed of the rotor at failure allows one to compute directly the maximum stress imposed on the adhesive bond. Tests have been made to determine the effect of plate thickness on the bond strength and to determine the reduction in bond strength caused by various contaminants introduced on the surface of the base metal prior to plating.

* This work was supported by the U. S. Army Ordnance through the Watertown Arsenal Laboratories.

Abstract No. 54

A NUCLEATION MECHANISM FOR CATHODIC POLARIZATION AT METALLIC ELECTRODES

T. R. Rubin

An electrolysis mechanism for nickel and copper reduction based on nucleation of metal surfaces has been developed through a correlation of rate effects and potential current effects by means of the diffusion equation with drift. The process appears to cause a surface diffusion of charge originating from the point of nucleation. Charge effects appear to be localized within dimensions corresponding to the size of the water-ion coordination polyhedra found in the crystalline hydrates of copper sulfate pentahydrate and nickel sulfate hexahydrate. Nuclei appear to be composed of disordered atoms similar to that found in liquids. Intersurface tensions for the nuclei have been computed. Spontaneous spreading of nuclei over the metal surfaces occurs at higher potentials.

Abstract No. 55

COMPOSITE COATINGS OF CHROMIUM AND NICKEL FOR THE PROTECTION OF MOLYBDENUM AGAINST HIGH TEMPERATURE OXIDATION

J. K. Taylor, Harold Shapiro, and Abner Brenner

Techniques are described for obtaining adherent deposits of chromium and nickel on molybdenum. Data on the protective value of chromium-nickel composite coatings for the temperature range 1800°–2000°F are presented and evaluated. It appears that more than 0.002 in. thickness of nickel over 0.001 in. of chromium is required to offer significant periods of protection at temperatures of 1800°F and higher. On the other hand, 2200°F has been established as an upper limit of temperature beyond which no prolonged protection of molybdenum can be expected from chromium-nickel coatings about 0.01 in. thick.

Abstract No. 56

METALLOGRAPHIC STUDY OF ELECTROPLATED COATINGS OF CHROMIUM AND NICKEL ON MOLYBDENUM

R. J. Runck

Single-layer and multiple-layer coatings on molybdenum of electroplated nickel and chromium were studied metallographically to determine causes of failure of these coatings when heated in air. In single-layer coatings, chromium was found to be less subject to bonding failure than nickel and to afford better protection against oxidation. Cracking of chromium coatings was probably a major cause of failure, but good protection by chromium was

possible if a layer of chromium-molybdenum alloy was developed at the interface. Multiple-layer coatings of chromium and nickel in which chromium formed the initial layer may be superior to single-layer coatings, but the formation of blisters between the layers of chromium and nickel was a major cause of failure of this type of coating.

Abstract No. 57

COPPER DEPOSIT FROM SULFATE AND CYANIDE PLATING BATH

Investigation by Electron Microscopy

Shinzo Okada and Saburo Magari

The copper deposit from sulfate and cyanide bath at lower current densities is described. The unevenness of the deposit occurs on various kinds of copper electrodes at lower current densities. To clarify the unevenness of the deposit, several experiments were undertaken. From these experiments it was confirmed that the crystal structure of the base metal has a deep influence on the unevenness of the deposit. From precise observation it was found that the unevenness of the deposit goes on regularly. The deposit on one crystal has but one feature all over the crystal. This feature differs from the plating bath. That is, the planes which are parallel to (010) planes and (101) planes of the base crystal develop in sulfate copper plating bath, and the planes which are parallel to (130) planes of the base crystal develop in cyanide copper plating bath.

Abstract No. 58

ELECTRON MICROSCOPE STUDIES ON COPPER ANODES IN SULFATE AND CYANIDE BATHS

Suinzo Okada, Saburo Magari, and Kentaro Katsui

Copper anodes in sulfate and cyanide baths, at low current densities, dissolve regularly. The crystal structure of the base metal has a profound influence on the solution, which is characteristic for a given single crystal anode, and does not differ for the two different electrolytes. 012 planes of the base crystal develop in both copper plating baths and, in etching solutions for metallography, the same planes of the base crystal also develop.

ELECTRO-ORGANIC

Abstract No. 59

ANODIC REACTIONS IN THE ELECTROLYSIS OF LEAD FORMATE

A. N. Kappanna and A. S. Dewagan

The electrolysis of lead formate at platinum and gold anodes yields only lead dioxide when conducted below a limiting current density. Current yields and potentials are predictable within this range. Effects of additions of alkali formates and free formic acid are reported. New products appear at higher current densities.

Abstract No. 60

ANODIC OXIDATION OF CERTAIN CARBOHYDRATES

J. V. Karabinos

(No abstract received)

Abstract No. 61

ELECTROLYTIC REDUCTION OF SOME POLYNUCLEAR CARBOCYCLIC AROMATIC COMPOUNDS

G. B. Diamond

A new series of polynuclear carbocyclic aromatic compounds has been reduced electrolytically in high yield. In the case of the naphthyl ethers, the new series further demonstrates the efficacy of the method, and in the specific case of 1-methyl-2-methoxy naphthalene the enhanced selectivity of the electrolytic method as compared to the chemical method is strikingly illustrated. The feasibility of the method for the reduction of unsubstituted polynuclear carbocyclic aromatic compounds is demonstrated for the cases of naphthalene and phenanthrene.

Abstract No. 62

ELECTRO-ORGANIC REDUCTION OF 4-KETO-PIMELIC ACID TO PIMELIC ACID

H. J. Read

Electroreduction of 4-keto-pimelic acid to pimelic acid in aqueous sulfuric acid solutions at cadmium cathodes at 60°C gives yields of about 75% or higher with little undesirable by-product formation. Solubility data for reactants and products in water and in various concentrations of sulfuric acid were determined so that suitable conditions for continuous operation of the process could be predicted.

Abstract No. 63

ELECTROLYTIC REDUCTION OF AMIDES

II. *p*-Aminobenzanilide and Anisamide

Sherlock Swann, Jr., J. C. Bresee, and R. A. Strehlow

The electrolytic reduction of *p*-aminobenzanilide has been studied in sulfuric acid solutions at cathodes of zinc, cadmium, mercury, lead, aluminum, tin, bismuth, copper, iron, and cobalt. The starting material was not reduced at any cathode. A similar study was carried out of the electrolytic reduction of anisamide to *p*-methoxybenzylamine at the same metals as cathodes with the addition of nickel. Lead, cadmium, and zinc were active. The best and most consistent yields were obtained at lead.

Abstract No. 64

ELECTROLYTIC REDUCTION OF CYCLIC ACID IMIDES

Buhei Sakurai

One of the two carbonyl groups which are contained in the compounds belonging to this series was easily reducible to methylene electrolytically or purely chemically, but the other one could not be reduced to the same form. The author succeeded in achieving this object by using a zinc-amalgam electrode as cathode. The main compounds used for this purpose were phthalimide, naphthalimide, succinimide, glutarimide, camphoric acid imide, and their derivatives.

Abstract No. 65

AN IMPROVEMENT FOR THE ELECTROLYTIC PREPARATION OF AMINOGUANIDINE

Motoji Yamashita and Kiichiro Sugino

Nitroguanidine was reduced to aminoguanidine at lead and iron cathodes. By operating in an ammonium salt catholyte instead of one containing free sulfuric acid, yields of 80% of theoretical, and better, were obtained instead of the usual 50–60%. Increased stability of the intermediate nitrosoguanidine in the medium of higher *p*H is assumed to be the reason back of the improved yields.

Abstract No. 66

ELECTROLYTIC REDUCTION OF CYANAMIDE

Keijiro Odo and Kiichiro Sugino

Conversion of cyanamide to methylamine by cathodic reduction through hydrogen cyanide, previously recorded, could not be verified satisfactorily. However, cyanamide could be cathodically reduced to methylamine by way of formamidine in an ammonium sulfate-sulfuric acid catholyte.

Abstract No. 67

MECHANISM OF ELECTROLYTIC REDUCTION OF 2-AMINO-4-CHLOROPYRIMIDINES TO 2-AMINOPYRIMIDINES, AND OF 2-AMINOPYRIMIDINE

An Example of Two Different Types of Electrolytic Reduction

Kiichiro Sugino, Taro Sekine, and Kozo Shirai

By combining polarography with macro electrolysis and conventional identification of organic products, it was shown that certain halogenated derivatives of aminopyrimidine could have their halogens replaced by hydrogen, and that this could be followed by the electrolytic hydrogenation of the Kekule bonds within the nucleus.

Abstract No. 68

RADICALS BY KOLBE ELECTROLYSIS

W. H. Urry

(No abstract received)

Abstract No. 69

KOLBE ELECTROSYNTHESIS: EFFECT OF ALTERNATING CURRENT

I. Acetic Acid-Potassium Acetate

C. L. Wilson* and W. T. Lippincott

Kolbe electrosynthesis with acetate systems in aqueous and nonaqueous solvents was conducted with 60-cycle a.c. Products are similar to those from direct current, but yields are lower and the critical current density higher. Results of varying current density, temperature, and acetate concentration are reported, as are results of adding varying reagents. A practical ethane synthesis based on this procedure is offered.

* Present address: Hudson Foam Plastics Corp., Yonkers, N. Y.

Abstract No. 70

USE OF A ROTATING CATHODE IN ELECTROLYTIC REDUCTION

C. L. Wilson* and H. V. K. Udupa**

The effect of rotation of the cathode on the current efficiency of reduction on some unsaturated acids and carbonyl compounds was found to be favorable always. In some cases, the relative yield of bimolecular reduction compound to monomolecular was also increased. These results are explained on the assumption that diffusion to the electrode is a rate-determining step.

* Present address: Hudson Foam Plastics Corp., Yonkers, N. Y.

** Present address: Central Electrochemical Research Institute, Alagappa College, Karaikidi, India.

Abstract No. 71

CATHODIC REDUCTION OF *N*-DIMETHYLAMINOETHYL TETRACHLOROPHTHALIMIDE

M. J. Allen and J. Ocampo

It has been found that *N*-dimethylaminoethyl tetrachlorophthalimide can be reduced electrolytically to the respective isoindoline at high overpotential electrodes. Chemical methods, as well as previously described conditions used for the electrolytic reduction of other imides, were found unsatisfactory. Conditions used for the preparation of the isoindoline and results obtained at various electrodes studied using constant current density will be described. A comparison will be made between the efficiency obtained using constant current density and controlled potential electrolysis.

Abstract No. 72

AQUEOUS KOLBE ELECTROLYSIS OF MESITOATE ION

G. W. Thiessen, W. Farr, and B. T. Shawver

The well-known peculiarities of this acid, compared to benzoic acid, led to the prediction of possibility of its aqueous electrolysis and extensive discharge of its ion in competition with hydroxide. This prediction was fulfilled. The products are being studied. Insight has been gained into the nature of benzenoid inhibition.

Abstract No. 73

ELECTROCHEMICAL REDUCTION OF NITROGUANIDINE AND RELATED COMPOUNDS

I. Behavior of Nitro and Nitrosoguanidine at the Dropping Mercury Electrode

G. C. Whitnack and E. St. C. Gantz

Polarographic half-wave potentials and diffusion currents for both compounds were studied under various alkaline and acid conditions. Different mechanisms are postulated for basic and acid reductions. Optimum *p*H conditions are specified, with other details, both for determination of the nitroso compound in presence of the nitro compound, and for the reduction of the nitro compound to the nitroso one.

Abstract No. 74

POLAROGRAPHIC STUDIES IN ACETRONITRILE AND DIMETHYLFORMAMIDE

III. Behavior of Quinones and Hydroquinones

S. Wawzonek, R. Berkey, E. W. Blaha, M. E. Runner

Quinones in the above solvents are reduced stepwise to semiquinone anion and hydroquinone dianion. Addition of an appropriate proton source changes the reduction to a one-step process. Presence of the dianion was demonstrated for anthraquinone by macroelectrolysis. 2-Methyl-1,4-naphthohydroquinone resisted polarographic and chemical oxidation in the above anhydrous solvents, but yielded in the presence of water.

Abstract No. 75

POLAROGRAPHIC BEHAVIOR OF NITROBENZENE IN THE SOLVENT ACETONITRILE

M. E. Runner and G. Balog

Nitrobenzene, azobenzene, asoxybenzene, phenylhydroxylamine, and *o*-nitroaniline were polarographed in acetonitrile, at about millimolar concentrations, at 25°C, in presence of 0.1M tetrabutylammonium iodide. A mercury-pool anode was used. Double-wave polarograms always resulted. The second wave always equalled or exceeded the first, and was altered by addition of water. A one-electron initial reduction step is postulated, as for quinones. An interpretation is offered.

Abstract No. 76

POLAROGRAPHIC REDUCTION OF *p*-HYDROXYBENZALDEHYDE

C. Wheeler

Polarographic data for *p*-hydroxybenzaldehyde in well-buffered aqueous and 50% alcoholic solution are offered. One wave appears at low or high *p*H, but two for intermediate values. These *p*H's change with changing solvents, as does the half-wave potential. The mechanism postulated, like that for benzaldehyde, requires protonated aldehyde as an intermediate. The reaction proceeds through the dihydroxyhydrobenzoin to the hydroxybenzyl alcohol.

Abstract No. 77

POLAROGRAPHIC STUDIES OF SOME CARBONYL COMPOUNDS

R. A. Day, Jr.

Benzaldehydes and benzophenones with diverse substituents were polarographed in buffered water-ethanol solutions. These altered the normal carbonyl reduction characteristics in a manner consistent with assumption of metal ketyl intermediates. Phenyl-substituted acetones in dioxane-tetraalkylammonium systems were likewise studied. Varying behaviors were found and are explained on a steric basis.

Abstract No. 78

POLAROGRAPHIC STUDY OF ALPHA-KETO ACIDS; SIGNIFICANCE OF THE WAVE SEPARATION RESULTING FROM CHANGES IN THE *p*H OF THE BUFFER

O. H. Müller and W. J. P. Neish

Polarographic reduction of alpha-keto acids shows, in general, two waves of about equal total height, merging into one at sufficiently low *p*H. One theory explains this in terms of tautomerism, another in terms of differential reduction of the free acid and its anion. Neither theory is wholly consistent with all facts. A new explanation is offered, on the basis of a series of polarographic studies of alpha-keto acids and related compounds.

Abstract No. 79

APPLICATION OF NONAQUEOUS POLAROGRAPHIC TECHNIQUES TO THE STUDY OF THE KINETICS OF PEROXIDIC REACTIONS

C. Ricciuti and C. L. Ogg*

Peracid-unsaturated fatty acid ester reactions were polarographed in ammonium acetate-acetic acid, and hydroperoxide decompositions in lithium chloride-methanol-benzene. Peracid and hydroperoxide were estimated reliably and directly. Kinetic constants and rate orders were deduced, and correlated with locations of unsaturation.

* Eastern Regional Research Laboratory is part of the Eastern Utilization Research Branch, Agricultural Research Service, U. S. Dept. of Agriculture.

Abstract No. 80

OXIDATION OF THE LEUCO BASE OF MALACHITE GREEN

M. J. Allen and V. J. Powell

The oxidation of the leuco base of malachite green has been investigated polarographically at a rotating platinum electrode. It was found that in an acidic buffer medium the leuco base underwent a one-electron change to form a rather stable triphenylmethane-type free radical. There was no apparent shift in half-wave potential and a linear relationship was obtained between concentration and diffusion current in the range of concentrations studied.

ELECTROTHERMICS AND METALLURGY

Abstract No. 81

DEVELOPMENT OF THE FLUID-SOLID TECHNIQUE

A. F. Kaulakis

The fluid-solid technique is one of the most interesting chemical engineering developments of the past 20 years. The history behind its development is given. In addition, principles involved in applying the fluid-solid concept to industrial processes are reviewed. Fluid-bed density, entrainment, heat transfer, solids circulation, and recovery are discussed broadly and future possibilities are indicated.

Abstract No. 82

GRAPHICAL PRESENTATION OF FLUIDS-SOLIDS DYNAMICS

Fluidized Solids Handling in the Metallurgical Industry

F. A. Zenz

In this paper the author develops the construction of generalized fluids-solids flow diagram (phase diagram) in a qualitative manner without reference to any particular fluid-solid system. This development covers not only the region of fluidization in the strict sense, but also the regions of fluidized dilute- and dense-phase solids flow. Several examples are cited showing the phase diagram in relation to processes such as the roasting and calcination of ore concentrates, fluids-solids nuclear reactors, manufacture of activated carbon, reduction of iron ore, etc.

Abstract No. 83

CHEMICAL REACTIONS IN FLUIDIZED BEDS

F. M. Stephens, Jr., and L. W. Coffer

Increasingly important but less publicized than catalytic cracking are fluidized bed systems in which the solid phase takes part in or is the product of a chemical reaction. Metallurgical processes such as oxidation, sulfate roasting, calcination, vaporization of low boiling constituents in controlled atmospheres, chloridization, and reduction can be carried out efficiently in fluidized bed operations. The advantages and limitations of fluidized bed treatment as compared to more conventional methods for accomplishing chemical reactions will be discussed.

Abstract No. 84

ROASTING SULFIDES IN A FLUIDIZED BED

R. J. Priestley

The fluidized solids technique for roasting is a distinctive departure from conventional roasting practice. Many advantages, including high-strength gas flow, "temperature control," uniformity of product, ease of operation, and flexibility have made this system attractive to many companies.

Abstract No. 85

MODERN TECHNOLOGY AND HIGH-PURITY METALS

Ivor E. Campbell

The importance of high-purity metals in both research and industry is discussed and the wide variation in the degree of purity required in various fields of application is noted. Comparisons are made of the level of purity currently achieved for a number of metals. New techniques of preparation, fabrication, analysis, and evaluation required for high-purity metals are outlined.

Abstract No. 86

FUSION ELECTROLYSIS OF BISMUTH TRICHLORIDE

Paul Gruzensky

Bismuth has been deposited from a fused electrolyte containing 33 wt % bismuth trichloride in a lithium chloride-potassium chloride eutectic mixture as carrier salt at approximately 400°C. The electrolyte was maintained at the desired temperature by the electrolyzing current, requiring 1.2 kwhr of power per pound of bismuth deposited. Cathode current efficiency was nearly 100% and the average yield was 87.7%. The process readily lends itself to continuous operation.

Abstract No. 87

PREPARATION OF PURE NICKEL BY ELECTROLYSIS OF A CHLORIDE SOLUTION

W. A. Wesley

Pure nickel was prepared in the form of electrodeposits 3–5 mm thick from carefully purified nickel chloride-boric acid solution using iridium-platinum alloy anodes. The over-all reaction is

$$NiCl_2 = Ni_{(metal)} + Cl_{2(gas)}$$

As electrolysis proceeded, purified chloride solution was added automatically to maintain the metal content of the electrolyte. The gas content of the metal is not known, but the total of spectrographically detectable impurities is only 34 ppm. The metal is malleable and some data on mechanical and physical properties are included.

Abstract No. 88

PREPARATION OF HIGH-PURITY RHENIUM

D. M. Rosenbaum, R. J. Runck, and I. E. Campbell

Rhenium powder containing a maximum of 0.05% impurities has been prepared by hydrolysis of rhenium pentachloride and subsequent hydrogen reduction of the resultant hydrated rhenium dioxide. Particle size of the rhenium powder is such as to lead to easy densification by methods standard to powder metallurgy. Advantages of this method of preparation over previously employed methods will be given.

Abstract No. 89

VACUUM MELTING AND CASTING OF HIGH-PURITY METALS

N. Darmara

(No abstract received)

Abstract No. 90

FLOATING-ZONE PURIFICATION OF ZIRCONIUM

G. D. Kneip, Jr., and J. O. Betterton, Jr.

Certain impurities in iodide zirconium have been substantially reduced by a fractional crystallization process. The chemical reactivity of zirconium makes necessary the use of a molten zone suspended in the central part of a rod by surface tension. Successive passes of the liquid zone were made to achieve a high degree of purification. Neutron activation analyses and the temperature range over which the α/β transformation occurs for zirconium were used to establish the amount of purification.

Abstract No. 91

CAGE ZONE MELTING

P. H. Brace and G. Comenetz

A short induction coil is set about a long fluted metal rod which stands vertical. A short zone of the rod melts, all except the projecting edges. These remain as the bars of a "cage" that contains the melt. The rod is raised slowly, with the result that the molten zone travels down its length. The condition for zone refining, or for vaporization of volatile impurities or degassing, is thus provided without a crucible. Experiences with titanium, iron, silicon, and molybdenum will be recounted.

Abstract No. 92

QUALITY-CONTROL TECHNIQUES EMPLOYED IN THE PRODUCTION OF HIGH-PURITY ZIRCONIUM AND HAFNIUM METALS

H. L. Kall

To produce ductile zirconium metal and meet the specifications for this metal as established by the Atomic Energy Commission, it is necessary to control the levels of impurities in zirconium metal rigidly. The quality-control techniques employed by the Carborundum Metals Co. in the manufacture of reactor grade zirconium and hafnium metals will be discussed.

Abstract No. 93

DETERMINATION OF TRACE ELEMENTS IN METALS AND ALLOYS BY RADIOACTIVATION ANALYSIS

G. W. Leddicotte and W. A. Brooksbank, Jr.

Microgram and submicrogram concentrations of many elements appearing as impurities in various metals and alloys can be determined by radioactivation analysis, a specific and sensitive method of analysis in which contamination difficulties as experienced in conventional methods of analysis are negligible.

The method of radioactivation analysis in which neutrons are used as the bombarding particles can be applied to the determination of at least seventy of the elements. Analytical methods are available for the determination of many of these elements in such metals as aluminum, magnesium, titanium, beryllium, zirconium, hafnium, niobium, and their alloys. A general description of the method of radioactivation analysis, the manner in which samples are irradiated and processed, and some of the results obtained in specific analyses will be presented.

Abstract No. 94

A STUDY OF SEPARATIONS IN THE ANALYSIS OF HIGH-PURITY METALS

O. R. Gates

The application of colorimetric, spectrographic, or x-ray fluorescent techniques to the determination of trace impurities in high-purity metals is not usually possible without preliminary separation of the base metal or isolation of the desired impurity. Separations commonly used preparatory to instrumental analysis are mercury cathode electrolysis, organic solvent extraction, and precipitation with a collector.

A study has been made of these separations in the analysis of high-purity iron for impurities in the parts per million range. Techniques are evaluated in terms of applicability, effectiveness, and limitations, and details for the effective application of each are given.

Abstract No. 95

METALLOGRAPHIC TECHNIQUES

E. E. Thomas

The present emphasis on purity of metals and alloys, now including semi-

conductor materials, has resulted in heavier demands on metallographic techniques. Newer examination methods such as phase contrast are of great interest and will be briefly outlined.

Cleanliness requirements generally can be satisfied by electrolytic polishing, as in the case of aluminum. Where mechanical polishing must still be used, great care must be exercised to avoid abrasive contamination. Equally great care must also be exercised not only to avoid material flow but, often, to preserve intact physical configurations of major importance.

Abstract No. 96

SPECIAL TECHNIQUES FOR ANALYZING SEMICONDUCTING MATERIALS

J. M. Whelan

The resistivity, Hall effect, and lifetime of semiconducting materials are extremely sensitive to small concentrations of impurities. From low-temperature Hall-effect measurement, the major impurity in a semiconductor can be identified and its absolute concentration determined. This technique has been used to detect concentrations of impurities in silicon as low as one part in 10^{11}. The measured lifetime of excess current carriers depends on both the surface and volume properties of the semiconductor. This measurement can be used to estimate the maximum concentration of specific impurities in both germanium and silicon.

Abstract No. 97

PREPARATION AND ANALYSIS OF HIGH-PURITY TELLURIUM

S. E. Miller and H. L. Goering

The preparation of high-purity tellurium by sublimation methods is described. The analysis of tellurium is based on Hall effect and resistivity measurements. The efficiency of purification is represented by a plot of ionized impurities vs. the number of sublimations.

Abstract No. 98

DUCTILE CHROMIUM

W. H. Smith and A. U. Seybolt

Effects of certain impurities on the room temperature ductility of chromium have been investigated. Results indicate that nitrogen in amounts <0.01% raises the bend transition-temperature of annealed material above room temperature. No effect of oxygen on the ductility in amounts <0.3% was found. Sulfur in amounts as great as 0.1% does not appear to affect adversely the bend ductility of as-cast material, but carbon in amounts greater than 0.02% cannot be tolerated.

Preliminary work on the development of chromium-base alloys containing more than 90% chromium developed many unsolved problems.

Beneficial effects of adding rare earths to tie up harmful impurities in chromium are discussed. Results of mechanical tests on chromium-cerium alloys are presented.

Abstract No. 99

EFFECT OF IMPURITIES ON THE HARDNESS OF TITANIUM

T. D. McKinley

The object of this was to correlate the effect of varying amounts of impurities on the as-cast hardness of titanium buttons prepared under reproducible conditions. These correlations show the relative hardening effect of impurities and allow estimation of change in hardness with change in impurity level. Data to be presented also allow the estimation of the oxygen content of commercial-grade sponge from hardness measurement and conventional chemical analyses. Estimation of oxygen can be made in this manner with an expected error of 5–10% from values as determined by vacuum-fusion analysis.

Abstract No. 100

EFFECT OF IMPURITIES ON THE TENSILE PROPERTIES OF ALUMINUM

A. P. Young

Very considerable differences have been noted in the flow curves of aluminum single crystals of 99.99% and 99.95% purity. Also, differences in the slip-band structure have been observed. Some of these differences can be accounted for by the dislocation theory of deformation and the effect of impurity atoms on the motion of dislocation.

Abstract No. 101

ADDITION OF CONTROLLED AMOUNTS OF IMPURITIES TO A TITANIUM-MOLYBDENUM ALLOY

S. J. Noesen

A series of 1.25% titanium-molybdenum alloys was prepared by the cold-mold, inert-electrode, arc-melting process. Controlled amounts of the impurities carbon, oxygen, and nitrogen were added singly and in combination to enable the study of their effect on ingot soundness, microstructure, and physical properties.

This paper explains the logic behind the choice of the inert-electrode process to prepare these ingots and the selection and preparation of the raw materials. The melting procedure and data on compositional accuracy obtained are included. An analysis of the cast material is treated at some length.

SPRING MEETING
at the
MARK HOPKINS HOTEL
San Francisco, Calif.
April 29, 30, May 1, 2, and 3, 1956

Sessions probably will be scheduled on

Electric Insulation
Electronics: Instrumentation, Luminescence, Oxide-Cathodes, Phosphor Application, and Semiconductors
Electrothermics and Metallurgy
Industrial Electrolytic
Theoretical Electrochemistry

Abstracts for the Spring Meeting (*not exceeding 75 words in length*) must reach the Secretary's Office, 216 West 102nd Street, New York 25, N. Y. *not later than January 2, 1956* in order to be included in the program.

Indicate on abstract for which division the paper is to be scheduled.

INDEX TO AUTHORS

(Number in bracket following page number indicates column on page.)

Adams, G. B., Jr., 215C [3], 222C [3]
Albrecht, W. M., 214C [3], 220C [1]
Allen, M. J., 217C [1] [2], 226C [2], 227C [2]
Andrew, Kenneth, 214C [3], 220C [2]
Aziz, P. M., 215C [2], 221C [3]

Bakish, R., 215C [3], 223C [1]
Balog, G., 217C [2], 226C [3]
Baur, J. P., 214C [2], 219C [1] [2]
Beck, F., 215C [1], 221C [2]
Berkey, R., 217C [2], 226C [3]
Betterton, J. O., Jr., 218C [1], 228C [2]
Birchenall, C. E., 214C [3], 220C [2]
Blackburn, Paul, 214C [3], 220C [2]
Blaha, E. W., 217C [2], 226C [3]

Bloom, M. C., 215*C* [2] [3], 222*C* [1], 223*C* [2]
Bockris, J. O'M., 215*C* [1], 221*C* [2]
Brace, P. H., 218*C* [1], 228*C* [2]
Brenner, Abner, 216*C* [2], 224*C* [3]
Brenner, S. S., 214*C* [2], 219*C* [3]
Bresee, J. C., 216*C* [3], 225*C* [3]
Bridges, D. W., 214*C* [2], 219*C* [1] [2]
Brooksbank, W. A., Jr., 218*C* [1], 228*C* [3]
Burbank, Jeanne, 214*C* [1], 215*C* [2], 218*C* [3], 221*C* [3]

Cabrera, N., 214*C* [2], 219*C* [3]
Campbell, I. E., 217*C* [3], 218*C* [1], 227*C* [3], 228*C* [1]
Coffer, L. W., 217*C* [3], 227*C* [3]
Cohen, M., 215*C* [1], 221*C* [1] [2]
Comenetz, G., 218*C* [1], 228*C* [2]

Dancy, W. H., Jr., 216*C* [2], 224*C* [2]
Darmara, N., 218*C* [1], 228*C* [2]
Darnell, A. J., 216*C* [1], 223*C* [2]
Day, R. A., Jr., 217*C* [2], 227*C* [1]
de Béthune, A. J., 215*C* [3], 222*C* [3]
Dewagan, A. S., 216*C* [3], 225*C* [2]
Diamond, G. B., 216*C* [3], 225*C* [2]
Ditmars, W. E., Jr., 216*C* [1], 224*C* [1]
Draley, J. E., 215*C* [1], 221*C* [1]
Druck, J. U., 214*C* [3], 220*C* [1]

Ehrenberg, D. M., 216*C* [1], 223*C* [2]

Farber, Milton, 216*C* [1], 223*C* [2]
Farr, W., 217*C* [1], 226*C* [2]
Fassell, W. M., Jr., 214*C* [2], 219*C* [1] [2]
Foley, R. T., 214*C* [3], 220*C* [1]
Fowle, P., 215*C* [3], 223*C* [2]
Fryxell, R. E., 214*C* [3], 220*C* [1]

Gantz, E. St. C., 217*C* [1], 226*C* [3]
Gates, O. R., 215*C* [3], 218*C* [1], 223*C* [2], 228*C* [3]
Gatos, H. C., 214*C* [3], 220*C* [2]
Glicksman, Richard, 213*C* [3], 214*C* [1], 218*C* [2] [3]
Godard, H. P., 215*C* [2], 221*C* [3]
Goering, H. L., 218*C* [2], 229*C* [1]
Griffith, C. B., 216*C* [1], 224*C* [1]
Gruzensky, Paul, 217*C* [3], 228*C* [1]
Gulbransen, E. A., 214*C* [3], 220*C* [2]

Hackerman, Norman, 214*C* [3], 220*C* [3]
Higgs, R. F., 216*C* [2], 224*C* [2]
Hill, M. L., 216*C* [1], 224*C* [1]
Hillner, Edward, 215*C* [1], 221*C* [1]
Hunter, M. S., 215*C* [3], 223*C* [2]

Jaffee, R. I., 216*C* [1], 224*C* [1]
Johnson, E. W., 216*C* [1], 224*C* [1]

Kall, H. L., 218*C* [1], 228*C* [2]
Kappanna, A. N., 216*C* [3], 225*C* [2]
Karabinos, J. V., 216*C* [3], 225*C* [2]
Katsui, Kentaro, 216*C* [2], 225*C* [1]
Kaulakis, A. F., 217*C* [3], 227*C* [2]
Kearns, T. F., 216*C* [1], 223*C* [3]
Keir, D. S., 215*C* [2], 222*C* [1]
King, C. V., 215*C* [1], 221*C* [1]
Kneip, G. D., Jr., 218*C* [1], 228*C* [2]
Komodromos, N. M., 214*C* [3], 220*C* [3]
Kruger, J., 215*C* [3], 223*C* [2]
Krulfeld, M., 215*C* [2], 222*C* [1]
Kuhlthau, A. R., 216*C* [2], 224*C* [2]

Leddicotte, G. W., 218*C* [1], 228*C* [3]
Lenning, G. A., 216*C* [1], 224*C* [1]
Lippincott, W. T., 217*C* [1], 226*C* [1]

Magari, Saburo, 216*C* [2], 225*C* [1]
Makrides, A. C., 214*C* [3], 220*C* [3]
Mallett, M. W., 214*C* [3], 220*C* [1]
Maraghini, Mario, 215*C* [3], 222*C* [3]
Mason, R. B., 215*C* [2], 222*C* [2]
McGraw, L. D., 216*C* [1], 223*C* [3]
McKinley, T. D., 218*C* [2], 229*C* [2]
Mellors, G. W., 215*C* [1], 221*C* [2]
Miller, S. E., 218*C* [2], 229*C* [1]
Misch, R. D., 215*C* [2], 221*C* [3]
Morehouse, C. K., 213*C* [3], 214*C* [1], 218*C* [2] [3]
Müller, O. H., 217*C* [2], 227*C* [1]

Neish, W. J. P., 217*C* [2], 227*C* [1]
Noesen, S. J., 218*C* [2], 229*C* [2]
Norton, J. T., 214*C* [2], 219*C* [2]

Ocampo, J., 217*C* [1], 226*C* [2]
Odo, Keijiro, 216*C* [3], 226*C* [1]
Ogg, C. L., 217*C* [2], 227*C* [2]
Okada, Shinzo, 216*C* [2], 225*C* [1]
Oswin, H. G., 215*C* [1], 221*C* [1]

Powell, V. J., 217*C* [2], 227*C* [2]
Priestley, R. J., 217*C* [3], 227*C* [3]
Pryor, M. J., 215*C* [2], 222*C* [1]

Read, H. J., 216*C* [2] [3], 224*C* [2], 225*C* [2]
Rhodin, T. N., Jr., 215*C* [1], 221*C* [2]
Ricciuti, C., 217*C* [2], 227*C* [2]
Robertson, W. D., 215*C* [3], 216*C* [1], 223*C* [1] [3]
Rosenbaum, D. M., 218*C* [1], 228*C* [1]
Rubin, T. R., 216*C* [2], 224*C* [2]
Runck, R. J., 216*C* [2], 218*C* [1], 224*C* [3], 228*C* [1]
Runner, M. E., 217*C* [2], 226*C* [3]
Ruther, W. E., 215*C* [1], 221*C* [1]

Sakurai, Buhei, 216*C* [3], 225*C* [3]
Schlechten, A. W., 215*C* [3], 223*C* [1]
Sekine, Taro, 217*C* [1], 226*C* [1]
Seybolt, A. U., 218*C* [2], 229*C* [1]
Shapiro, Harold, 216*C* [2], 224*C* [3]
Shaw, Manuel, 215*C* [3], 222*C* [2]
Shawver, B. T., 217*C* [1], 226*C* [2]
Shih, S. T., 215*C* [3], 223*C* [1]
Shirai, Kozo, 217*C* [1], 226*C* [1]
Simnad, M., 215*C* [1], 221*C* [2]
Smith, W. H., 218*C* [2], 229*C* [1]
Spilners, A., 215*C* [1], 221*C* [2]
Stephens, F. M., Jr., 217*C* [3], 227*C* [3]
Stern, Milton, 214*C* [3], 220*C* [3]
Stokes, J. J., Jr., 214*C* [1], 218*C* [3]
Straumanis, M. E., 215*C* [3], 223*C* [1]
Strehlow, R. A., 216*C* [3], 225*C* [3]
Streicher, M. A., 215*C* [2], 222*C* [1]
Sturdy, G. E., 214*C* [3], 220*C* [1]
Sugino, Kiichiro, 216*C* [3], 217*C* [1], 225*C* [3], 226*C* [1]
Swann, Sherlock, Jr., 216*C* [3], 225*C* [3]

Taylor, J. K., 216*C* [2], 224*C* [3]
Thiessen, G. W., 217*C* [1], 226*C* [2]
Thomas, E. E., 218*C* [2], 228*C* [3]
Twiss, S. B., 215*C* [3], 222*C* [2]

Udupa, H. V. K., 217*C* [1], 226*C* [2]
Urry, W. H., 217*C* [1], 226*C* [1]

Van Rysselberghe, P., 215*C* [3], 222*C* [3]
Vermilyea, D. A., 215*C* [2], 222*C* [2]

Waber, J. T., 214*C* [3], 220*C* [1]
Wagner, Carl, 214*C* [2], 219*C* [2]
Wawzonek, S., 217*C* [2], 226*C* [3]
Webb, W. W., 214*C* [2], 219*C* [2]
Wesley, W. A., 218*C* [1], 228*C* [1]
Wheeler, C., 217*C* [2], 227*C* [1]
Whelan, J. M., 218*C* [2], 229*C* [1]
Whitnack, G. C., 217*C* [1], 226*C* [3]
Wilson, C. L., 217*C* [1], 226*C* [1] [2]

Yamashita, Motoji, 216*C* [3], 225*C* [3]
Yang, Ling, 215*C* [1], 221*C* [2]
Young, A. P., 218*C* [2], 229*C* [2]

Zenz, F. A., 217*C* [3], 227*C* [2]

Note

Hotel reservation cards for the Hotel William Penn will be mailed to members about September 1.

Separate program booklets will *not* be mailed to members. Reprints of the above program in booklet size will be available at the meeting.

Current Affairs

Hooker—ECS Sustaining Member

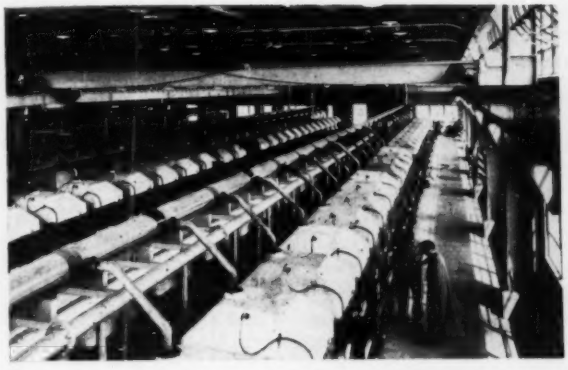

"The New"—Latest Type S-3A 25,000-amp cells installed at Hooker's $15 million plant at Montague, Mich., which began production in March 1954.

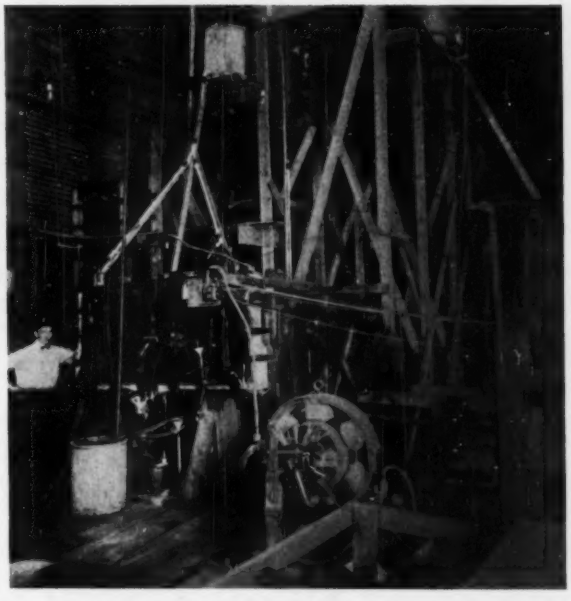

"The Old"—Experimental 1000-amp Townsend cell, housed in wing of Edison Power Station in Brooklyn, during 1904. H. Willard Hooker, at left, was one of several who helped conduct the tests. He later became plant superintendent, and, at the time of his death in 1937, was vice-president and treasurer.

"I take pleasure in advising you that the test of the Townsend cell has proven successful in all respects." These confident words of Elon Huntington Hooker were sent on August 26, 1904 to stockholders of the Development and Funding Co., predecessor of the Hooker Electrochemical Co. The Townsend process, one of the earliest developed (the first practical cell had been patented in 1886), had demonstrated itself an efficient, inexpensive means of manufacturing chlorine and caustic soda. Simple words and a calm statement of fact, but behind these words, as is often true, lay much past discouragement and many chastening events which might well have caused less stalwart men to give up.

The Development and Funding Co. had been founded by Elon Hooker early in 1903 to invest in promising businesses which needed capital. Altogether, the company had examined over 250 businesses before deciding to build a plant at Niagara Falls, N. Y., to utilize the Townsend cell, tested during 1904 in an experimental plant housed in a wing of the Edison Power Station in Brooklyn. Even as late as June 1904, Elon Hooker had dejectedly written, "We all recognize that the test has proven a failure and the process is not ready to form the basis of a business," but a circulating system which kept the brine constantly saturated proved to be the key to success.

The market for caustic soda, then used mostly in the textile, soap, and young petroleum industries, was strong. Almost 80% of the bleaching powder, made from chlorine, for bleaching pulp and textiles was imported and freight rates were high, so markets for both caustic soda and chlorine were ample. Hydrogen, the third product of the electrolytic cell, then had no commercial use.

On May 5, 1905 ground was broken for the first plant about three miles up the river from Niagara Falls, now one of the greatest electrochemical centers. Hooker quietly celebrated its fiftieth anniversary on May 5, 1955.

On January 9, 1906 there went into production sixty-eight 2000-amp Townsend cells, the original conception of Clinton P. Townsend, who remained a technical consultant to Hooker for many years, and of Elmer H. Sperry, electrical engineering genius, later to become famous for many inventions, the best known of which is the gyroscope. Dr. Leo H. Baekeland, inventor of the photographic paper, Velox, and later the phenolic plastic, Bakelite, had supervised the Brooklyn tests and was also a consultant during the company's early years.

Prime reasons for locating at Niagara were three: ample water from the world's largest fresh water supply, the Great Lakes system; inexpensive power from mighty Niagara; and salt from the largest salt mine in the western hemisphere, less than 60 miles away at Retsof, N. Y. Niagara Falls remains the site of the company's headquarters and largest plant.

The five-ton-a-day chlorine plant was unprofitably small and daily capacity was raised progressively to 42 tons of bleaching powder and 20 tons of caustic soda by 1910.

Meanwhile, in 1909 the Development and Funding Co. had set up its only subsidiary, the Hooker Electrochemical Co., and the Development Co. was later dissolved.

World War I saw Hooker begin its first product diversification and the Armistice in November 1918 found Hooker manufacturing 17 chemicals. The blockade of European organic chemicals and dyestuffs had pushed the young American industry into many chemical manufacturing fields new to this country. Hooker, launching into manufacture of its first organic product, monochlorobenzene, successfully operated the world's largest such plant, primarily to make picric acid for explosives.

A period of increasing plant efficiency and work on im-

proved cell design came in the 1920's. The deposited asbestos cell diaphragm (1925–1929) and the basic Type-S Cell design (1929–1934) were two of the most important developments in the history of the chlor-alkali industry. Installed in the Niagara Falls plant in 1934, the Type-S cell and later the larger capacity S-3 and S-3A designs were afterward licensed to others. Today, 28 companies in 36 locations all over the world are licensed to use such cells.

Another important development by Hooker in the twenties was the Northwest's first chlor-alkali plant, completed at Tacoma, Wash., in 1929. This plant was successful from the beginning, serving principally the pulp and paper, oil refining, soap, and other chemical processing industries. It has increased its capacity manyfold, diversifying recently with the Northwest's first manufacture of ammonia. Also, Hooker-Detrex, Inc., a jointly owned subsidiary, manufactures trichlorethylene at both Tacoma and Ashtabula, Ohio.

In 1932 came the formation of the Development Department, in the hands of R. Lindley Murray, now President. The success of that program accounts largely for the enormous strides made by Hooker in the last 15 years. A sustained research program resulted in diversification of Hooker's basic products along several lines: chlorine diversification, including chlorinated derivatives of toluene, benzene, pentane, and fatty acids; fluorine and fluorine derivatives; hydrogenated products; caustic soda derivatives, such as sodium sulfide and sodium sulfhydrate; and organic sulfur compounds.

During World War II, the Government installed Hooker cells at all four Chemical Warfare Service arsenals. Hooker received five Army-Navy E awards at Niagara, two at Tacoma, and made substantial contributions to the Manhattan Project.

The postwar period saw the greatest expansion program in Hooker's history. Investment in plant and equipment rose from less than $15 million in 1945 to nearly $45 million in early 1955 with about 25 new chemicals added to the list.

A major milestone in 1954 was the completion of a $15 million chlorine-caustic plant at Montague, Mich., the nearest such plant to the important Chicago and northern Midwest market.

An event of far-reaching importance to Hooker occurred on April 29 this year when Durez Plastics and Chemicals, Inc., a leading manufacturer of phenolic resins with three plants and assets of over $23 million, was merged into Hooker, whose assets were more than $63 million. This provides Hooker with an experienced basic position in the rapidly growing plastics industry.

On June 7 Hooker announced that it promptly will proceed to build the first chlorine-caustic soda plant on the Western Canadian seaboard at North Vancouver, B.C. To be completed by early 1957, the cost of the new plant is estimated to be in the neighborhood of $11 million.

Thus begins the second half century of Hooker activities. The manufacture of over 100 products for more than 30 basic industries is undoubtedly but a shadow of the things to come.

Ninth Annual Battery Conference

Reports on the development of practical batteries utilizing radioactive energy were presented at the Ninth Annual Battery Research and Development Conference held in Asbury Park, N. J., on May 18 and 19, under the sponsorship of the Power Sources Branch of the Signal Corps Engineering Laboratories. These conferences are sponsored each year in order to present to the battery industry the progress of the military battery research and development program and to encourage cooperative interchange of information on batteries with the aim of producing a more rapid advancement of knowledge in the battery art. Over 500 people representing government installations, the battery and allied industries, and universities were present at this two-day conference.

Papers on nuclear batteries were presented by J. H. Coleman, Radiation Research Corp., West Palm Beach, Fla.; Alexander Thomas, Tracerlab, Inc., Boston, Mass.; and P. E. Ohmart, Ohmart Corp., Cincinnati, Ohio. Coleman reported on an electrostatic type nuclear battery. One battery of this type was fabricated with polystyrene insulation and a 10 millicurie strontium 90 beta particle source. This battery, which had an output current of 50 $\mu\mu$a at zero voltage, was found to develop over 20,000 v. The total volume of this battery was only 1 in.^{3}, including the shielding which reduces the external radiation field to the acceptable AEC tolerance. Another group of batteries, using a tritium source, was fabricated. These battieries utilized the beta emission from solid tritiated-zirconium sources, carbon collectors, and vacuum insulation. The initial models of these batteries are being designed to yield 10^{-9} amp at potentials to 1000 v in a volume of 2 in.^{3}. Improved construction techniques may reduce the volume to nearer 1 in.^{3}.

Thomas reported on the development of a 60 v and a 300 v battery capable of delivering up to 10^{-9} amp and having a useful life of 15 years over a temperature range of from −65° to 165°F. These batteries develop their potential by the principle of radio-ionization of a gas located between dissimilar metallic electrodes. Ohmart stated that a similar battery has been developed as a source of constant current and constant voltage and is 1½ in. in diameter and 3 in. long. It generates currents of $\sigma \times 10^{-9}$ amp with an open circuit voltage in excess of 1 v when excited by 10 millicuries of strontium 90. Measurements have shown the output of these batteries to be constant over long periods of time. They have low temperature coefficients, will operate over wide range of temperature, are extremely rugged, and will withstand severe mistreatment without damage.

E. J. Linder, Radio Corp. of America, Princeton, N. J., spoke of his work on batteries which operate by converting radiant energy, such as beta rays or light, directly into electricity. In addition to the types discussed by the other speakers, the Radio Corp. of America has worked on semiconductor types. These consist of p-n junctions of materials, such as silicon or germanium, energized by radiation. By a simple internal process, the radiation energy is converted directly into electrical energy.

Diffused silicon p-n barrier energy converters for direct generation of electric power from solar radiation may eventually be an important source of primary power. However, the present high cost of purified silicon, and of the fabrication process, restricts the immediate application of low power experimental installations. K. D. Smith, Bell

Telephone Labs., Inc., Murray Hill, N. J., reported on the development program which has been initiated at Bell Labs. to study fabrication methods and improvement in performance of the cells. Energy conversion efficiency greater than 8% has been obtained for the better cells. Although tests of reliability are in an early stage, results obtained so far are encouraging. The principal factors affecting the economic feasibility of the silicon solar battery are: (*a*) the cost of usable silicon, (*b*) the fabrication process, (*c*) connections and mounting. The development of economic sources of suitable purified silicon is believed to be the dominant problem at the present time.

In addition to the papers presented on the nuclear batteries, electrochemical systems were discussed in great detail.

SECTION NEWS

India Section

The Fifth Annual Meeting of the India Section was held on June 28 at the Indian Institute of Science, Bangalore. The following officers were elected for the year 1955–1956:

Chairman—M. S. Thacker
Vice-Chairman—A. Joga Rao
Vice-Chairman—S. Ramaswamy
Secretary-Treasurer—S. Krishnamurthy, 543/1, 17th Cross, Malleswaram, Bangalore 3, India

S. Krishnamurthy,
Secretary-Treasurer

PERSONALS

Robert J. McKay, (Retired) Chemical Engineer, International Nickel Co., Inc., New York City, recently received from the American Society for Testing Materials an Award of Merit in recognition of intensive interest and contributions through Committee B-8 on Electrodeposited Metallic Coatings, of which he was a Charter Member and its second chairman, and for support of ASTM corrosion work.

M. Scott Hunter, in conjunction with William G. Fricke, Jr., has been presented with the Richard L. Templin Award of the American Society for Testing Materials for their paper "The Metallographic Aspects of Fatigue." The award was established in 1945 to stimulate research in the development of testing methods and apparatus. Mr Hunter is with the Aluminum Co. of America in New Kensington, Pa.

J. Balachandra, who came to the U.S.A. from India in September 1954, was at the University of Wisconsin, Madison, for nine months. He also visited several academic centers and industrial establishments. He is now at the U. S. Bureau of Mines, Albany, Oreg.

S. D. Gokhale has been awarded the Ph.D. degree by the University of Tubingen, W. Germany.

A. Joga Rao has returned to India from his trip in Europe. He attended the meetings of the International Committee of Electrochemical Kinetics and Thermodynamics, and the International Congress of Industrial Chemistry.

T. L. Rama Char, who has been in the U.S.A. since September 1954, was at the Illinois Institute of Technology, Chicago, for three months. Following this he visited several academic centers and industrial establishments in the field of corrosion and then joined the Corrosion Research Lab. of the University of Texas, Austin. He left Austin in July to visit important centers in the East, including the Massachusetts Institute of Technology. He shall return to India in September. Dr. Rama Char has been elected an Associate of the Institution of Metallurgists, London.

LETTER TO THE EDITOR

Transference Number Measurements in Solutions of Low Conductivity[1]

Dear Sir:

In the course of a study of the electrical properties of solutions of inorganic salts in organic solvents it became necessary to measure transference numbers in these solutions. This communication describes a simple apparatus for such measurements in systems of low conductance.

Because the organic solvents precluded the use of stopcocks or rubber connections in direct contact with the solvent, an all-glass system in the form of a W was tested.[2] It was found difficult to construct an apparatus of this form small enough to provide for a reasonably short period of electrolysis. The apparatus shown in Fig. 1 has the advantage of simple construction while providing a short electrical path between electrodes.

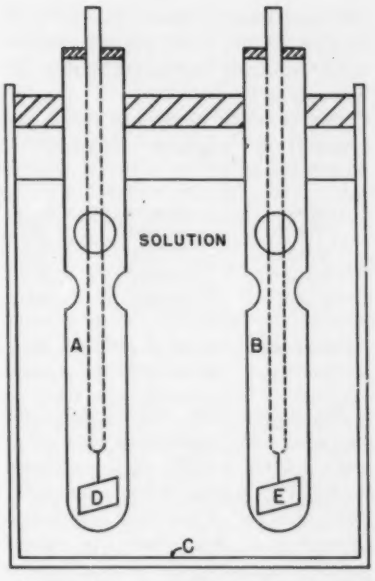

Fig. 1. Low resistance transference cell.

Apparatus.—Tubes A and B were of 12 mm OD Pyrex tubing sealed at one end and having a constriction near the upper end. A hole in each tube provided an electrical path through the solution. The tubes were fixed in position in the container C by the stopper through which they passed. To separate anolyte and catholyte it was only necessary to lift tubes A and B from the solution. Constriction in the tubes served to minimize mixing of the solutions when the tubes were removed.

Reagents and Methods.—Reagent grade silver nitrate was used without further purification. Acetone (bp 55.5–55.80) was redistilled after refluxing over calcium chloride. The anode in the transference number cell was a heavy platinum foil, D, upon which silver had been deposited, while the cathode, E, was bare platinum foil. A current of 10–15 ma was passed for about two hours through the cell and a conventional silver weight coulometer in series. Silver nitrate concentrations in the middle and anode compartments of the cell were determined by titration against standardized KCNS solution, using ferric ion as indicator. Within the limits

[1] From a portion of the M.S. thesis of E. A. Grimm.

[2] A. A. Noyes, *Z. physik. Chem.*, **36**, 63 (1901).

of experimental error the concentration of silver nitrate in the middle compartment remained unchanged during the electrolysis.

Results.—The table lists the cation transference numbers obtained at 25.00° ± 0.01°C.

Solvent	Molality	t_+
Water	0.0500	0.463
Water	0.0498	0.465
Water	0.0497	0.462
Water	0.0497	0.462
Acetone	8.57×10^{-3}	0.449
Acetone	8.57×10^{-3}	0.445

Discussion.—The average value for the silver ion transference number in water is 0.463 ± 0.003 (99% confidence limits). This average is not significantly different at the 10% level of significance ("Students *t*" test)[3] from the value,[4] 0.4664, obtained by the moving boundary method. The two results for dilute solutions of silver nitrate in acetone are included to show that the apparatus yields reasonably precise results for solutions of low conductivity.

Acknowledgment.—The support of this work by the Research Corporation of America through a Frederick Gardner Cottrell grant to the University of Idaho is gratefully acknowledged.

J. F. Murphy and E. A. Grimm
Div. of Metallurgical Research
Kaiser Aluminum and Chemical Corp.
Spokane, Wash.

[3] K. A. Brownlee, "Industrial Experimentation," p. 34, Chemical Publishing Co., Inc., Brooklyn (1949).

[4] D. A. MacInnes and L. G. Longworth, *Chem. Rev.*, **11**, 210 (1932).

BOOK REVIEWS

Precision Laboratory Standards of Mass and Laboratory Weights, NBS Circular 547, by T. W. Lashof and L. B. Macurdy. Published by National Bureau of Standards, U. S. Dept. of Commerce, Washington 25, D. C. 24 pages, 14 tables, 25¢.

As stated in both its announcement and its Foreword, the present circular modernizes part of Circular 3, which was published in 1918. The NBS specifications for precision in laboratory standards of weight, regulations governing submission of weights to the Bureau for tests, and the weight-calibration service of the Bureau have been presented. Reflecting the growth of microchemistry and its current use as a routine tool, a new class of weights has been introduced which has a tolerance of 3 micrograms for each weight. In addition, three other classes have been introduced at the macro level which satisfy the lower tolerances encountered in routine analyses, student use, and rough-way operations. As a result, the present standards now cover the entire spectrum of current needs. By its very nature this circular will be a necessary addition to the library of all users of laboratory balances, as well as to the manufacturers of the weights.

L. B. Rogers

A Short Textbook of Colloid Chemistry by B. Jirgensons and M. E. Straumanis. Published by John Wiley & Sons, Inc., New York, and Pergamon Press, Ltd., London, 1954. 420 pages, $8.00.

The authors state that this text is a completely revised version of their "Kurzes Lehrbuch der Kolloidchemie," published by Bergmann and Springer in 1949, and that it "is intended for students and research workers and for those interested in the branches of natural science which include medicine, pharmacy, and industrial applications, in all of which information about colloids is essential." It is the judgment of this reviewer that the authors have successfully presented the important phenomena and concepts of colloid chemistry in such a manner as to be of interest and value to those listed above.

The first three chapters of this book give the scope and basic terms of colloid chemistry and some simple experiments with colloids in brief form for those readers who wish only to obtain an acquaintance with the field. In the remaining sixteen chapters, the discussion is more thorough.

Among the chapter titles may be found the traditional topics of colloid chemistry including kinetic, optical, and electrical properties of colloids, preparation of colloidal solutions, lyophobic and lyophilic colloids, interfacial phenomena, gels, emulsions, foams, and aerosols. Individual chapters are devoted to the viscosity of colloidal solutions, the determination of particle size, the determination of particle shape, and to information on particle size, form, and structure obtainable by the use of x-rays and electrons.

Throughout the text the authors' statements are supported by many references to the periodical literature and to standard reference works. That a very large fraction of these are to publications of the past ten years is good evidence that the authors have kept up to date. The treatment of the results of recent studies on particle shape and size, including those based on light scattering phenomena, is particularly well done.

A simple, clear style of writing, excellent typography, and the liberal use of illustrations (a total of 179) have all contributed to the high quality of this text.

A. Witt Hutchison

MANUSCRIPTS AND ABSTRACTS FOR SPRING MEETING

Papers are now being solicited for the Spring Meeting of the Society, to be held at the Mark-Hopkins Hotel in San Francisco, April 29 and 30, and May 1, 2, and 3, 1956. Subjects to be covered at the technical sessions will be Electric Insulation, Electronics (including Luminescence, Oxide-Cathodes, Phosphor Application, Semiconductors, and Instrumentation), and Industrial Electrolytics, and probably Electrothermics and Metallurgy and Theoretical Electrochemistry.

To be considered for this meeting, triplicate copies of abstracts (not to exceed 75 words in length) must be received at Society headquarters, 216 West 102nd St., New York 25, N. Y., *not later than January 2, 1956.* Complete manuscripts should be sent in triplicate to the Managing Editor of the Journal at the same address.

* * *

The Fall 1956 Meeting will be held in Cleveland, Ohio, October 28, 29, 30, and 31, and November 1, at the Statler Hotel. Sessions will be announced in a later issue.

SONICS by Theodor F. Hueter and Richard H. Bolt. Published by John Wiley and Sons, Inc., New York, 1955. xi + 456 pages, $10.00.

In recent years many significant applications have been found for mechanical vibrations in analysis and testing, the study of molecular structure, and the processing of various types of materials. These applications are not limited by the frequency range of hearing of the human ear but extend from infrasonic through ultrasonic frequencies. The concepts and techniques associated with these applications are generally referred to by the term sonics and are the subject of the new book of this same title by Hueter and Bolt.

The fundamental aspects of mechanical waves and vibrations are presented in the first few chapters with just sufficient mathematics to provide for quantitative interpretations. The techniques for producing acoustical waves are discussed both on a general basis and in terms of specific applications. Devices and methods for the quantitative measurement of the amplitude of acoustical waves are also critically evaluated. One of the chapters of most interest to chemists is that concerned with the physical mechanisms involved in processing applications. A reasonably detailed description of sonically produced cavitation and the associated physical effects in liquids is presented. Reference is made to such applications as ultrasonic cleaning of metals, the effects of ultrasonic waves on electrodeposition, the production of colloidal suspensions, sonic precipitation of aerosols, and ultrasonic soldering, cutting, and drilling. The remainder of this book presents the principles and techniques involved in testing various materials and the study of the structure of matter. The discussion of acoustical relaxation mechanisms in fluids should help to demonstrate to the physical chemist the importance of ultrasonic velocity and absorption measurements in the study of molecular structure as well as the kinetics of chemical and physical processes with half lives even approaching 10^{-8} sec. These techniques are particularly significant in the investigation of various processes in electrolytic solutions, e.g., ion-pair formation, dissociation, ion-solvent interaction.

At the present time many chemists are interested in sonic techniques for fundamental research as well as for industrial testing and processing applications. This text is recommended to chemists with such interests since it should prove of considerable assistance in evaluating the possibilities which sonic techniques offer. The reader is assumed to have relatively little background information in physics and virtually none in acoustics. Throughout the text the authors make frequent use of electrical analogs for acoustical systems. Emphasis is placed on the common features of the applications for acoustical methods. This is particularly evident from the numerous well-organized tables in which various aspects of these applications are compared.

Heretofore, the chemist has made relatively limited use of acoustical methods. Hueter and Bolt's text, "Sonics," should help to remedy this situation.

ERNEST YEAGER

MOLECULAR VIBRATIONS: The Theory of Infrared and Raman Vibrational Spectra by E. B. Wilson, Jr., J. C. Decius, and P. C. Cross. Published by McGraw-Hill Book Co., Inc., New York, 1955. 388 pages, $8.50.

To the average chemist the literature of molecular spectra is apt to appear as a morass of difficult terminology, recondite mathematics, group theory, and awkward problems in geometry, all covered with a light quantum mechanical fog. "Molecular Vibrations" is a guide through this morass meant for the novice rather than the adept. It is concerned primarily with the methods of studying molecular vibrations rather than with the properties of any particular molecules.

After presenting the basic mechanical problem of finding the classical equations of motion of a polyatomic molecule and commenting upon some quantum mechanical properties of vibrating systems, the techniques of obtaining an appropriate set of coordinates are treated at length. The use of symmetry properties is explained very clearly. The potential and kinetic energy matrices are treated and an up-to-date discussion of methods of handling the secular determinant is given. Selection rules, vibration-rotation interactions, and a sample vibrational analysis are each given a chapter.

The audience to which this book is directed is presumably one which has as much acquaintance with classical mechanics and modern physics as might be expected of third or fourth year gradu-

KASIL POTASSIUM SILICATE BINDERS

Kasil #1 molecular ratio 1:3.9 (7.8% K_2O, 19.5% SiO_2); 28° Baume
Kasil #22 molecular ratio 1:3.45 (8.6% K_2O, 18.9% SiO_2); 28.6° Baume

These Kasil Potassium Silicates meet the high standards needed for TV tube production. Spectographic analyses indicate the high degree of purity—absence of copper, nickel and other elements which might cause contaminated screens.

Kasil's uniform quality is dependable—shipped in drums, tanktrucks and tankcars.

• *Ask for helpful publications: Potassium silicate binders for cathode ray tube formulas • Colloidal and surface phenomena in the preparation of cathode ray screens.*

PHILADELPHIA QUARTZ COMPANY
Established 1831

1156 Public Ledger Bldg.
Philadelphia 6, Pa.
Trademarks Reg. U. S. Pat. Off.

ate students. The presentation is excellent from a pedagogical point of view and is recommended to any student just entering the field.

BENSON R. SUNDHEIM

NEWS ITEMS

Science Grants and Awards

The National Science Foundation has announced a second program of postdoctoral fellowship awards for 1955–1956. These new awards, like those in the first program, are for advanced study and training in the natural and applied sciences. Those eligible to apply are postdoctoral students, staff members, holders of the M.D. degree who wish to pursue advanced training and research in one of the basic medical sciences, and terminal year graduate students who will receive the doctorate by February 1956. The National Academy of Sciences–National Research Council will again receive applications for the awards, evaluate them through its fellowship boards, and nominate candidates to the National Science Foundation.

For application write: The Fellowship Office, National Research Council, 2101 Constitution Ave., N.W., Washington 25, D. C. Applications must be in by September 12, 1955. Fellowships will be awarded on October 20.

The National Science Foundation has announced 297 grants totaling about $2,810,000 awarded during the quarter ending March 31, 1955, for the support of basic research in the natural sciences, for conferences and studies on science, scientific information exchange, for the scientific manpower register, and for attendance at scientific meetings.

The grants were made to institutions and scientists in the fields of astronomy, chemistry, developmental biology, earth sciences, engineering sciences, environmental biology, genetic biology, mathematical sciences, molecular biology, physics, psychobiology, regulatory biology, and systematic biology.

This is the third group of awards to be made during fiscal year 1955 by the Foundation for the support of basic research and related matters. Since the beginning of the program in 1951, over 1500 such awards have been made, totaling about $15,560,000.

An expanded program for Monsanto Chemical Co.'s financial aid to scientific education during the 1955–1956 school year was announced recently by Dr. Carroll A. Hochwalt, vice-president. A total of 53 American colleges and universities will benefit from 72 separate direct aid awards under the program.

The awards for the coming school year include 16 fellowships, 31 undergraduate scholarships, and 25 cash grants. The fellowships are established for graduate study with the larger part of their $3000 average value going to the fellow. The scholarships are intended to cover tuition costs with the administering schools awarding them on bases of both merit and need. The cash grants may be used at the schools' discretion to finance research, purchase equipment, or further any other scientific purpose.

In announcing the awards, Dr. Hochwalt called attention to the fact that the 1955–1956 program includes cash grants to five liberal arts colleges.

Nine Freshman Scholarships for the Missouri School of Mines and Metallurgy, Rolla, Mo., sponsored by the Alumni Association, have been announced by Dean Curtis L. Wilson, of that institution, and H. S. Pence, President of the Missouri School of Mines Alumni Association.

The scholarships carry a cash award of $500 for the freshman year and are based upon high school scholastic standing and leadership participation, and the comparative results of engineering aptitude tests. With the exception of one scholarship there are no geographic restrictions.

Applications must be on file prior to February 1 for entrance for the fall semester.

Bell Telephone Laboratories has announced the establishment of a fellowship program through which funds will be granted for students doing graduate study in electrical communications. To be known as the Bell Telephone Laboratories Fellowships, the awards are for study of one or two years, leading to a doctorate. Each fellowship carries a grant of $2000 to the fellow, and an additional $2000 to cover tuition, fees, and other costs to the institution at which he chooses to study.

Recipients of the fellowships will not be required to limit their study to electrical engineering, although the field of study and research must have a bearing on electrical communications. They may pursue various branches of mathematics, physics, chemistry, engineering mechanics, and mechanical engineering. Fellows may make their own choice of an academic institution within the United States.

The new awards continue a ten-year program of the Bell System in aiding graduate study. A program now being concluded involves the Frank B. Jewett Fellowships awarded since 1945 to postdoctoral students in the physical sciences.

The Dow Chemical Company has announced gifts totaling more than $300,000 for educational grants to colleges and universities for the advancement of science and engineering.

A major phase of the aid-to-education program is the authorization of $133,500 for distribution to 38 colleges and universities for the establishment of graduate fellowships and undergraduate scholarships and to two educational foundations for use in assisting deserving students. Another part consists of $167,500 allocated to 19 institutions, most of it earmarked for their unrestricted use in current expansion and operating programs. The bulk of these contributions goes to Case Institute of Technology, Cleveland, and to the Michigan College Foundation, with 14 liberal arts colleges participating.

Correction

In the paper by F. van der Maesen and J. A. Brenkman, "On the Behavior of Rapidly Diffusing Acceptors in Germanium," in the May issue of the JOURNAL, there are two errors with respect to the powers of the number e in equations (XII), (XIII), and (XIV).

$e - \tau_2^2$ and $e - \tau_1^2$ should be written $e^{-\tau_2^2}$ and $e^{-\tau_1^2}$.

Nonmember Journal Subscribers

Nonmember subscription rates to the JOURNAL in 1956 will be $18.00 instead of the $15.00 previously charged. Current subscribers will be mailed invoices for $18.00 late in September.

Mention the Journal

When making purchases from our advertisers, please be sure to mention that you saw the ad in the JOURNAL.

Over and above these grants, the company has allocated $140,000 for distribution to a number of schools for research on specific projects which supplement the company's own research in various fields.

The $133,500 in grants for fellowships and scholarships is distributed as follows: $110,500 is provided for 42 fellowships of $2500 each, two of $2000 each, and one of $1500. These will be used to aid outstanding graduate students who are for the most part in the last year of study for a doctor's degree in chemistry, physics, chemical engineering, or metallurgy.

Dow does not participate in any way in the selection of fellowship recipients. In all cases they are chosen by fellowship committees of the various schools receiving funds. A portion of each fellowship grant goes to the schools to cover tuition and other educational costs.

Engineering Foundation to Combat Corrosion

Metals engineers, metals scientists, chemists, and physicists are teaming up in the nation's first major assault upon one of the most costly and insidious enemies of American industry—metallic corrosion.

The Corrosion Research Council of the Engineering Foundation, formed with the aid of the American Institute of Mining and Metallurgical Engineers, the Intersociety Corrosion Committee, and The Electrochemical Society will make a determined effort to learn more about Industrial Enemy No. 1 which annually rolls up a staggering five billion or more in losses through failure and fatigue of metals in critical spots in industry.

Heading the organizing committee for the proposed Corrosion Research Council is H. H. Uhlig, chief of Massachusetts Institute of Technology's Corrosion Laboratory. Far too little is known about the basic problems of metallic corrosion, Dr. Uhlig states, because fewer than a handful of major U. S. universities are at present concerned with this study, and industry has met each specific problem as it arose, thus providing limited and sketchy knowledge for general use.

Two vital points back up the Committee's fight against the wasteful forces of corrosion. The current need is targeted on (*a*) increased fundamental scientific data and (*b*) close cooperation among scientists in electrochemistry, physical metallurgy, solid-state physics, nuclear physics, surface chemistry and physics, reaction, and others.

Establishment of a Corrosion Research Council with members chosen from American and Canadian technical societies, together with delegates from the sponsoring industries, would follow the expected financial backing by industry.

ECS members of the organizing committee, in addition to Dr. Uhlig, are F. L. LaQue, R. M. Burns, R. B. Mears, and R. M. Wick.

Direct contact may be made with The Engineering Foundation at 29 W. 39th St., New York 18, N. Y., or with any organizing committee member.

New Theoretical Division Editor

Dr. Carl Wagner, Dept. of Metallurgy, Massachusetts Institute of Technology, Cambridge, Mass., resigned as Theoretical Electrochemistry Division Editor of the JOURNAL on June 30. Dr. C. W. Tobias, Div. of Chemical Engineering, University of California, Berkeley, Calif., assumed Theoretical Division Editorship on July 1.

RECENT PATENTS

Selected from the Official Gazette by M. S. Wright, Librarian, National Carbon Research Laboratories, Cleveland, Ohio.

May 3, 1955

Conrad, M., 2,707,319, Semiconducting device

Lilliendahl, W. C., and Gregory, E., 2,707,679, Methods of producing zirconium and titanium

Lockwood, G. H., and Peterson, R. E., 2,707,687, Method of forming luminescent coating

Dorst, S. O., 2,707,703, Heat stable, insulated, electrical conductors and process for producing same

Leibowitz, J. R., 2,707,719, Apparatus for the vacuum melting of high purity materials

Anderson, W. M., and Ostlie, R. H., 2,707,721, Heat insulating jacket for storage batteries

May 10, 1955

Paoloni, C., 2,708,156, Electric furnace for the manufacture of carbon disulfide

Smith, E. M., 2,708,158, Production of titanium

Holmes, A. W., and Burns, R. H., 2,708,181, Electroplating process

Koren, H. W., and Baumstark, G., 2,708,211, Electric storage batteries and their production

Koren, H. W., and Baumstark, G., 2,708,212, Electric storage batteries

Koren, H. W., 2,708,213, Electric storage batteries

Galloway, H. R., 2,708,214, Battery cap

Ruben, S., 2,708,242, Radiation dosimeter

ANNOUNCEMENTS FROM PUBLISHERS

1954 SUPPLEMENTS TO BOOK OF ASTM STANDARDS. Published by the American Society for Testing Materials,

Physical Chemists, Electrochemists, or Chemical Engineers

Physical Chemists, Electrochemists, or Chemical Engineers with training in physical chemistry wanted for research and development. Work will involve laboratory studies of the fundamentals of corrosion chemistry, and analysis of practical corrosion problems that arise in all phases of the petroleum industry. Interest both in fundamentals and in engineering applications necessary. Corrosion experience and knowledge of statistics helpful but not required.

Address: **GULF RESEARCH & DEVELOPMENT COMPANY**
P. O. Drawer 2038
Pittsburgh 30, Pennsylvania

1916 Race St., Philadelphia 3, Pa. Heavy paper covers; 7 parts; $3.50 per part; $24.50 per set.

To keep up to date the triennially published Book of ASTM Standards, the American Society for Testing Materials, in the intervening years, issues Supplements to each part of the Book. The 1954 Supplements, issued in seven parts, give in their latest form 415 specifications, tests, and definitions which either were issued for the first time in 1954 or revised since their appearance in the 1952 Book or the 1953 Supplements.

Part 1. Ferrous Metals—608 pages. Includes 89 standards covering steel pipe (welded and seamless, high temperature service, stainless, etc.); steel tubes (boiler, superheater, heat exchanger, refinery service, general service, etc.); bolting materials; boiler and pressure vessel plate; structural and rivet steel; sheet and strip; billets, forgings, and axles; rails and accessories; railroad wheels and tires; concrete reinforcement; corrosion- and heat-resistant steels; metallic coated steel products; cast iron; and magnetic materials.

Part 2. Non-Ferrous Metals—444 pages. Includes 81 standards covering metallic electrical conductors; copper and copper-base alloys; aluminum and aluminum-base alloys; magnesium and magnesium-base alloys; electrical heating; resistance and related alloys for radio tubes, electronic devices, and lamps; metal powders; electrodeposited metallic coatings; corrosion tests and general methods of testing.

Part 3. Cement, Concrete, Ceramics, Thermal Insulation, Road Materials, Waterproofing, Soils—416 pages. Includes 77 standards covering cement (portland, portland-pozzolan, magnesium oxychloride, and magnesium oxysulfate); lime; gypsum; mortars (chemical resistant and masonry); masonry building units; pipe and drain tile; refractories; ceramic whiteware; porcelain enamel; glass and glass products; thermal insulating materials; mineral aggregates; concrete; highway materials (bituminous and nonbituminous); waterproofing and roofing materials; soils; and general testing methods.

Part 4. Paint, Naval Stores, Wood, Cellulose, Wax Polishes, Sandwich and Building Constructions, Fire Tests—160 pages. Includes 28 standards covering pigments; drying oils; paint driers and thinners; shellac and varnish; lacquer and lacquer materials; traffic paint (crushing resistance of glass spheres); printing inks (fineness of grind); general paint tests; paint weathering tests; naval stores; wood; wood preservatives; cellulose and cellulose derivatives; wax polishes; tests of building constructions; and fire tests.

Part 5. Fuels, Petroleum, Aromatic Hydrocarbons, Engine Antifreezes—308 pages. Includes 36 standards covering crude petroleum; butadiene; motor and aviation fuels; petroleum solvents and naphthas; kerosine and illuminating oils; lubricating, turbine, and electrical insulating oils; plant spray oils and petroleum sulfonates; lubricating greases; paraffin and hydrocarbon waxes, gaseous fuels; engine antifreezes; thermometers; hydrometers; and general testing methods.

Part 6. Rubber, Plastics, Electrical Insulation—532 pages. Includes 66 standards covering rubber products (chemical, physical, aging, and low temperature tests); automotive and aeronautical rubber; packing and gasket materials; hose; insulated wire and cable; latex foam, sponge, and expanded cellular rubber; rubber latex; electrical tests; plastics (specifications; strength, hardness, thermal, optical, and permanence properties; analytical methods, molds and molding processes, definitions and nomenclature); electrical insulating materials (shellac and varnish, mineral oils, fabrics, papers, mica); and electrical tests.

Part 7. Textiles, Soap, Water, Paper, Adhesives, Shipping Containers—296 pages. Includes 38 standards covering textile materials (terms and definitions, quantitative analysis, resistance to pests and microorganisms, fibers, yarns, fabrics); soaps and detergents; paper; adhesives; water (sampling and analytical methods); and methods of mechanical testing.

THE CHEMICAL INDUSTRY FACTS BOOK, 2nd edition. Published by the Manufacturing Chemists' Association, Inc., 1625 Eye St., N.W., Washington 6, D. C., 1955. 160 pages; $1.00, postage prepaid; discounts available on bulk quantities.

Included in this basic reference source on the chemical industry and its work in promoting better living in America are 15 chapters ranging from "What the Chemical Industry Makes" to such specifics as "Chemicals and Health" and "Chemicals in Defense." A teacher's guide, prepared by Dr. Walter S. Lapp, President, National Science Teachers Association, is available free to educators for use with the Facts Book.

ADVERTISERS' INDEX

Bell Telephone Laboratories, Inc. 210C
Enthone, Incorporated .... Cover 4
Baker & Adamson Products, General Chemical Division, Allied Chemical & Dye Corporation 207C
Great Lakes Carbon Corporation ..... Cover 2
National Carbon Company .. 206C
Philadelphia Quartz Company 235C
Stackpole Carbon Company .. 208C

STATISTICAL SUMMARY OF THE MINERAL INDUSTRY, Production, Exports, and Imports, 1948–1953. Prepared by the Mineral Resources Division, Colonial Geological Surveys. Published by Her Majesty's Stationery Office, Wembley, Middlesex, England. 356 pages; price, £1 7s. 6d. net (by post, £1 8s. Od.).

The Statistical Summary of the Mineral Industry is an annual volume of statistical tables which contains comprehensive details of the production, exports, and imports of all important commercial minerals and metals used throughout the world. The new edition covers the important period 1948 to 1953.

Volumes Wanted

Society Headquarters needs copies of Vol. 92 (1947), 93 (1948), and 95 (1949) of the TRANSACTIONS.

Will anyone who has a copy he no longer needs please so inform the Managing Editor, Journal of The Electrochemical Society, 216 W. 102nd St., New York 25, N. Y.

EMPLOYMENT SITUATION

Please address replies to box shown, c/o The Electrochemical Society, Inc., 216 W. 102nd St., New York 25, N. Y.

Position Wanted

CHEMIST, 36, 11 years' experience including batteries, electroplating, general physical and chemical commercial testing, seeks New Jersey, Philadelphia, New York City position. *Reply to Box 357.*

The Electrochemical Society

INSTRUCTIONS TO AUTHORS OF PAPERS

Address all correspondence to the Editor, JOURNAL OF THE ELECTROCHEMICAL SOCIETY, 216 W. 102nd St., New York 25, N. Y.

FORM

Manuscripts submitted for publication should be in triplicate to expedite review. They should be typewritten, double-spaced, with 2½–4 cm (1–1½ in.) margins.

Title should be brief, followed by the author's name and his business or university connection.

Abstract of about 100 words should state the scope of the paper and give a brief summary of results.

ILLUSTRATIONS

Drawings will be reduced to column width, 8 cm (3⅛ in.), and after reduction should have lettering at least 0.15 cm ($\frac{1}{16}$ in.) high. Original drawings in India ink on tracing cloth or white paper are preferred. Curves may be drawn on coordinate paper only if the paper is ruled in blue. All lettering must be of lettering-guide quality. See sample drawing on reverse page.

Photographs must be glossy prints and mounted flat.

Captions for all figures must be included on a separate sheet. Captions and figure numbers should not appear in the body of the figure.

General—Figures should be used only when necessary. Omit drawings or photographs of familiar equipment. Figures from other publications are to be used only when the publication is not readily available, and should always be accompanied with written permission for reprinting.

REFERENCES

Literature and patent references should be listed at the end of the paper on a separate sheet, in the order in which they are cited. They should be given in the style adopted by *Chemical Abstracts*. For example:

R. Freas, *Trans. Electrochem. Soc.*, **40,** 109 (1921).

H. T. S. Britton, "Hydrogen Ions," Vol. **1,** p. 309, D. Van Nostrand Co., New York (1943).

H. F. Weiss (To Wood Conversion Co.), U. S. Pat. 1,695,445, Dec. 18, 1928.

UNITS OF MEASUREMENT

Metric units should be used throughout but, where desirable, English units may be given in parentheses.

Corrosion rates in the metric system should preferably be expressed as milligrams per square decimeter per day (mdd), and in the English system as inches penetration per year (ipy).

As regards algebraic signs of potentials, the standard electrode potential for $Zn \rightarrow Zn^{++} + 2e$ is negative; for $Cu \rightarrow Cu^{++} + 2e$, positive.

ABBREVIATIONS

Abbreviations should conform with the American Standards Association's list of "Abbreviations for Scientific and Engineering Terms."

GENERAL

Authors should be as brief as is consistent with clarity, and must omit all material which can be regarded as familiar to specialists in the particular field.

The use of proprietary names, trade-marks, and trade names should be avoided if possible. If used, these should be capitalized so that the owner's legal rights are not jeopardized.

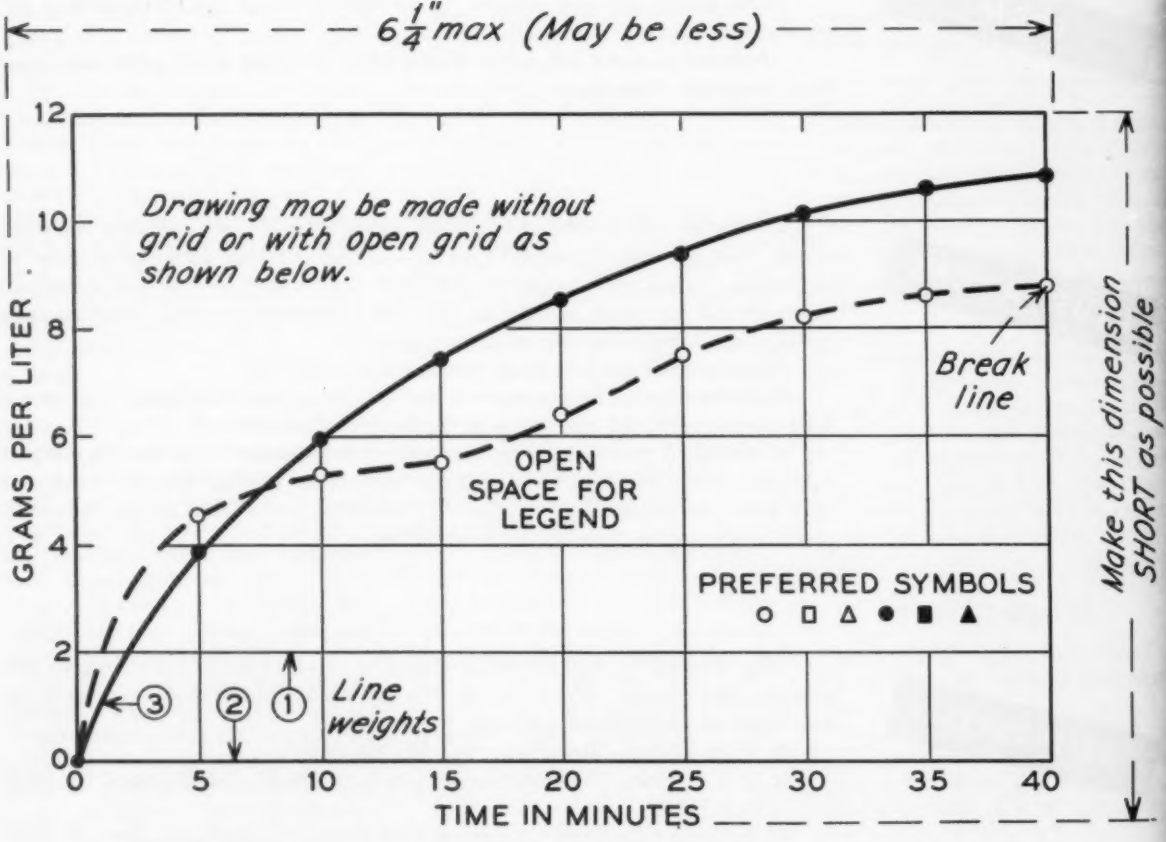

Remarks: Line weight ② is used for borders and zero lines. When several curves are shown, each may be numbered and described in the caption. Lettering is approx. 1/8".

SAMPLE CURVE DRAWING FOR REDUCTION TO $\frac{1}{2}$ SIZE

n's list

all ma-

voided
hts are

Electrolytic Oxidation of Zinc in Alkaline Solutions[1]

THEDFORD P. DIRKSE

Calvin College, Grand Rapids, Michigan

ABSTRACT

A study has been made of the mechanism of the reaction taking place when zinc is anodically treated in potassium hydroxide solutions. The zinc-containing ion present in solution as a result of the anodic treatment is $Zn(OH)_4^{--}$. However, zinc oxide or hydroxide is an intermediate leading to the formation of $Zn(OH)_4^{--}$. This latter ion then decomposes slowly to form zinc oxide.

INTRODUCTION

Although the electrolytic oxidation of zinc in aqueous alkaline solutions is an industrial reaction of some importance, comparatively little has been written or reported on the mechanism of this reaction which occurs during the discharge of alkaline batteries having zinc negative plates. It may also be the anodic reaction in alkaline zinc plating baths.

RESULTS AND DISCUSSION

When zinc is anodically treated in potassium hydroxide solutions, a white turbidity eventually appears in the electrolyte. This has been observed at temperatures of 0°–45°C, and in solutions of 10–40% potassium hydroxide. Many samples of this white substance have been collected and analyzed. Results indicate that it is zinc oxide. It has also been observed that, during the anodic oxidation of zinc in alkaline media, zinc gradually becomes covered with a dark colored substance. In some instances this material could be scraped off the electrode. Chemical analysis showed it to be zinc oxide. In other cases where this covering could not be scraped off, it was subjected to x-ray analysis and again found to be practically pure zinc oxide. It is possible that small amounts of finely divided zinc were also present. Thus it appears that the end product of this electrode reaction is zinc oxide which may be produced as a white substance eventually precipitating from the electrolyte, or as a dark colored substance adhering to the electrode.

Although on anodic oxidation of zinc in alkaline solutions zinc oxide ultimately precipitates from the solution, the appearance of this zinc oxide is not a simple solubility or supersaturation phenomenon. This was shown by using solutions of potassium hydroxide saturated with zinc oxide and then filtered. This clear filtrate was used as the medium for the anodic oxidation of zinc. In some cases the solution remained clear during several days of anodic oxidation of zinc. Yet analysis showed that the zinc content of the solution was gradually increasing (see Fig. 1). Eventually a white precipitate did appear and, when such solutions were allowed to stand, zinc oxide gradually precipitated out and the composition of the solution approached that of a potassium hydroxide solution saturated with zinc oxide. In some instances, over a year was necessary at room temperature for the solution to approach this composition. It appears then that at least two reactions are involved: (*a*) a reaction whereby zinc is introduced into solution; and (*b*) a reaction whereby this dissolved zinc species decomposes to zinc oxide.

There is other evidence for such an interpretation. Cells containing zinc negative plates, nickel oxide positives, and potassium hydroxide solutions as electrolyte were discharged at a low rate. A magnetic stirring device was used to agitate the electrolyte and provision was made for inserting a dip type conductivity cell into the electrolyte. The resistance, or conductance, of the electrolyte was followed during the course of the discharge. The specific conductance of the electrolyte decreased as the discharge proceeded until the turbidity appeared in the solution. After this, as the zinc oxide continued to precipitate out, the conductance increased slowly (Fig. 2). The rate at which the conductance recovers depends on the discharge current, which governs the dissolution rate of the zinc, and the rate at which the zinc oxide precipitates out. The fact that the conductance varies with time up to the appearance of a precipitate indicates that excess zinc is dissolved in the electrolyte and is not present in a colloidal form. Other physical properties such as density and viscosity also vary with excess zinc concentration.

To study this mechanism further it is obvious that some information is needed with respect to the zinc-containing species in solution. This is the substance that decomposes to form the zinc oxide and it is also the substance produced by the electrode reaction. The composition of this zinc-containing ion was

[1] Manuscript received January 3, 1955. This paper was prepared for presentation before the Boston Meeting, October 3 to 7, 1954.

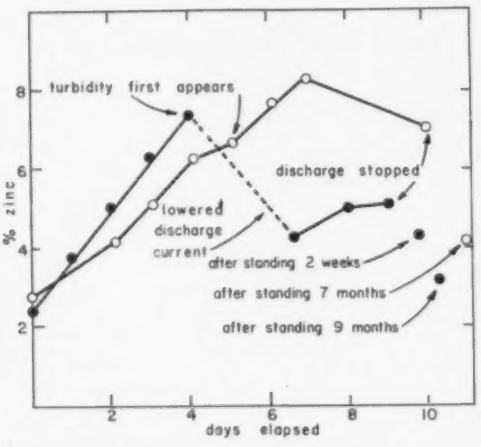

FIG. 1. Zinc content of electrolyte during discharge: ○—47% KOH saturated with ZnO; ●—25% KOH saturated with ZnO; current density, 0.005 amp/in.^{2}.

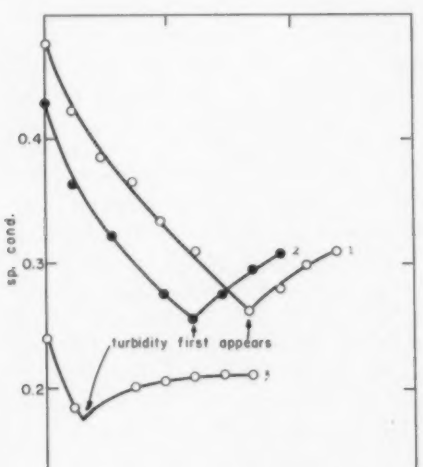

FIG. 2. Specific conductance of electrolyte during discharge: curve 1, 15% KOH; curve 2, 12% KOH; curve 3, 8% KOH; current density, 0.015 amp/in.^{2}.

determined by using galvanic cells (1). Certain potassium hydroxide solutions were used as the electrolyte in cells containing zinc negative and nickel oxide positive plates. As the cell was discharged, samples of the electrolyte were withdrawn at intervals. The potential of a zinc electrode in such a solution was then determined immediately and the solution was later analyzed for its zinc content.

Using the method previously described (1), a plot was made of (E_{Zn} − 0.118 log a_{H_2O}) vs. log a_{OH^-}. A straight line having a slope of 0.120 was obtained, showing that $Zn(OH)_4^{--}$ is the zinc-containing ion produced in solution by the anodic oxidation of zinc under such conditions.

From this it may tentatively be concluded that the mechanism of the reaction taking place is

$$Zn + 4\ OH^- = Zn(OH)_4^{--} \qquad (I)$$

followed by

$$Zn(OH)_4^{--} = ZnO + H_2O + 2\ OH^- \qquad (II)$$

Reaction (II) is obviously a slow reaction. These two reactions will now be considered separately.

Reaction (I).—It has been suggested by ohters (2, 3) that the electrode reaction produces a zinc oxide or hydroxide. This substance is then dissolved by the electrolyte. When the solvent action of the electrolyte is reduced to such an extent that the oxide layer can be built up on the electrode surface, then the electrode becomes passive. An intensive study was made of the electrode reaction and the evidence obtained is consistent with this interpretation.

Using the method described by Huber (2), the limiting current density at which the zinc electrode becomes passive was determined under a variety of conditions. Zinc electrodes were coated with polystyrene, leaving an exposed area of definite dimensions. These were used as anodes, while larger zinc electrodes served as cathodes. The electrolyte was aqueous potassium hydroxide. As the current applied to the cell was increased the potential between the anode and an auxiliary zinc electrode was measured. Curves of the type given by Huber (2) were obtained. The limiting current density varied with the time required for making the measurements. Consequently, values obtained are relative, not absolute. However, several runs were made under each set of conditions and results given here represent the average of all such runs.

Several factors affect the ability of potassium hydroxide solutions to dissolve the zinc oxide or hydroxide produced on the electrode surface. Some of these factors are: amount of electrolyte, rate of stirring, concentration of electrolyte, and temperature. In the first set of experiments the amount of electrolyte and rate of stirring were held constant. The effects of varying the temperature and electrolyte concentration are shown on Fig. 3 and 4. The variation with temperature is what would be expected. As the temperature increases the zinc oxide or hydroxide becomes more soluble in the electrolyte. As a result, with increasing temperature a higher limiting current density is obtained since the film formed on the electrode is removed more readily.

The variation of limiting current density with electrolyte concentration (Fig. 4) shows a maximum at about 20–30% potassium hydroxide, the exact value depending on the temperature. The decrease in the limiting current density at the higher concentrations is undoubtedly related to the high viscosity of such solutions. This decreases the mobility

of the ions and, thus, hydroxyl ions are not able to reach the electrode surface as readily. The hydroxyl ions used in the electrode process to produce the zinc oxide are not replaced rapidly enough by other hydroxyl ions which are necessary to dissolve the film that was formed.

In another set of experiments the zinc anode was allowed to operate at a given current density for five minutes before the current density was changed. The current density was increased by definite increments until the electrode became passive. In these runs the speed of stirring was changed, as was the amount of electrolyte. However, no great changes were noted by either of these variables. At the higher concentrations of electrolyte, increasing the speed of mechanical stirring did bring about a slight, but definite, increase in limiting current density. Apparently the increased stirring rate aided the mobility of the ions in solution. The fact, however, that this effect was slight, indicates that the mobility of the ions in solution is determined primarily by the potential gradient in the solution and the physical characteristics of the electrolyte.

In all these experiments relatively large amounts of electrolyte were used compared to the electrode surface area exposed. This ratio of electrolyte to surface area was much larger than used in batteries. Consequently, increasing the amount of electrolyte had no effect on the limiting current density since the limitation was due to the mobility of the ions, not to a lack of them.

There is still another factor that may have a bearing on the limiting current density, and that is the presence of dissolved zinc in the electrolyte. If, as the anodic process continues, the film produced is dissolved by the electrolyte, the concentration of zinc in the electrolyte increases. As this increases, the electrolyte becomes less able to dissolve more zinc oxide, and the limiting current density should be less. This effect was observed as shown in Fig. 5. At low concentrations of potassium hydroxide, addition of zinc oxide to the electrolyte had no effect on the limiting current density because such solutions do not contain much zinc. However, as the concentration of potassium hydroxide is increased, more zinc oxide can be dissolved. Thus, higher concentrations of potassium hydroxide, when saturated with zinc oxide, show increasingly lowered values of limiting current density.

These results are consistent with the idea that the electrode product is a very soluble form of zinc oxide or hydroxide which is removed by further reaction with the electrolyte.

$$Zn + 2\,OH^- \rightarrow Zn(OH)_2 + 2e \qquad \text{(III)}$$

$$Zn(OH)_2 + 2\,OH^- \rightarrow Zn(OH)_4^{--} \qquad \text{(IV)}$$

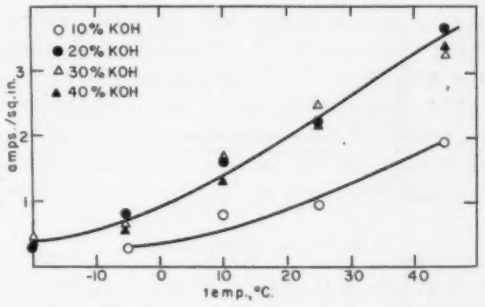

FIG. 3. Limiting current density as a function of temperature.

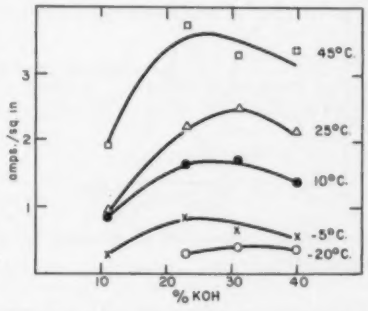

FIG. 4. Limiting current density as a function of electrolyte concentration.

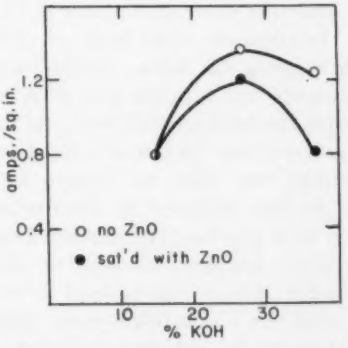

FIG. 5. Effect of dissolved zinc on limiting current density.

There is other evidence that supports this contention. It was observed in studying the conductance of cell electrolytes on discharge that the conductance of such electrolytes decreased even when the current was interrupted. An illustration of this is shown on Fig. 6. A likely interpretation of this phenomenon is that the anodic oxidation of zinc results in the formation of zinc oxide or hydroxide. A part of this, at least, is then dissolved slowly by the alkali. Thus, the zinc content, and, hence, the resistance of the electrolyte, increases when the discharge is discontinued.

Furthermore, it was also observed in studying the limiting current density at which the zinc electrode becomes passive that, after an electrode had become

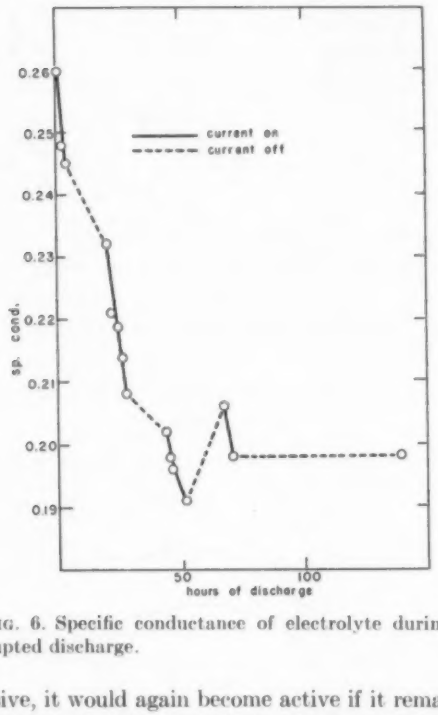

FIG. 6. Specific conductance of electrolyte during interrupted discharge.

passive, it would again become active if it remained in contact with the electrolyte with no current flowing. In some cases, standing only a minute was sufficient to allow the electrode to carry current again. At times the electrode could be made active again merely by reducing the current density. Apparently in such cases the rate of production of the zinc oxide film was then slowed down sufficiently so that it was again dissolved at least as fast as it was formed.

No attempt was made to identify further the nature of the film produced by the electrode reaction. However, it was observed that in all cases when an electrode was examined immediately after it had become passive that it was covered with a silver-like film. This film had a bright luster and may be that produced by electropolishing of zinc. In those cases where an electrode was allowed to remain in the electrolyte for some time after it had become passive, the exposed electrode area had a grayish cast, quite unlike the film on a passive surface. It was remarked earlier that the zinc electrode frequently became covered with a black or dark-colored film which is zinc oxide. This black film, while common, was not found on any passive surface. Hence, it is not responsible for the passivation of the electrode. When electrodes were oxidized at a low current density, the zinc electrode became covered with this black film soon after oxidation had begun. This film remained on the electrode until oxidation was complete, i.e., until the exposed zinc had been completely eaten away.

Reaction (II).—Since it has been shown that the main zinc-containing ion in solution is $Zn(OH)_4^{--}$, concentration of free hydroxyl ions in solution can be determined by analysis. A given solution can be treated with a known excess of acid and back titrated with a base. From the total alkalinity so determined the number of hydroxyl ions bound up in the zinc complex ion can be subtracted. This difference then gives the concentration of the free hydroxyl ions.

Three different electrolytes, 10, 20, and 30% potassium hydroxide, were used in cells containing nickel oxide positive and zinc negative plates. These cells were discharged until the electrolyte became turbid. The electrolyte was then withdrawn, filtered, kept at 25°C, and stirred magnetically from time to time. Samples were withdrawn from this electrolyte, filtered, and analyzed over a period of up to a week. The ratio of increase of free hydroxyl ion to decrease of zinc in solution was thus determined. Ratios obtained ranged from 1.4 to 2.6. Considering the limitations of the method, it seems reasonable to assume that this ratio is two, in agreement with equation (II). Using these same data and plotting log M_{Zn} vs. time, a straight line is obtained, confirming the assumption that the reaction is a first order one with respect to zinc ion.

CONCLUSIONS

The fact that, during the electrolytic oxidation of zinc in alkaline solutions, two reactions [equations (I) and (II)] occur is not as unlikely as it may at first appear. A similar phenomenon has been noted with zinc oxide in potassium hydroxide solutions. Solutions of potassium hydroxide ranging from 15% to 32% were kept at 25°C. Then an excess of zinc oxide was added and the solutions were stirred thoroughly. Samples were taken at intervals, filtered, and analyzed. In each case the zinc content of the solution increased and reached a constant value in about three hours. After two weeks samples were again taken and in each case the zinc content was found to have decreased beyond experimental error. The extent of decrease was greater in more concentrated potassium hydroxide solutions. This, too, can be accounted for by a two-step process, the first being rapid and the second slow. The fact that in this case

$$ZnO(A) + 2\,OH^- + H_2O \rightarrow Zn(OH)_4^{--} \quad (V)$$

$$Zn(OH)_4^{--} \rightarrow ZnO(B) + 2\,OH^- + H_2O \quad (VI)$$

the solutions reached equilibrium sooner than do cell electrolytes is probably due to the difference in the kind of zinc oxide which first dissolved in the potassium hydroxide solutions. If equations (V) and (VI) represent reactions taking place in the solution, then

it is likely that the zinc oxide referred to in each equation is physically different from the other, i.e., has a different free energy content.

Samples of hyperfine zinc oxide produced by Merck and Company were made available and, when this oxide was used in such solubility experiments, the decrease of zinc content in the solution on standing was still greater. The hyperfine zinc oxide is undoubtedly more soluble than the ordinarily available zinc oxide, due to its particle size. Because of this greater solubility, reaction (V) can proceed to a greater extent before reaction (VI) becomes of significance. Consequently, the zinc content of the solution can exceed the normal equilibrium value by a greater amount. On standing, then, the decrease of zinc content in solution will be greater.

It appears that the zinc oxide which precipitates from, and is in equilibrium with, potassium hydroxide solutions has a particular physical structure, different from other forms of zinc oxide which are available. For that reason a long time is necessary to establish equilibrium in potassium hydroxide solutions saturated with zinc oxide. For that reason, too, values reported for the zinc content of such solutions have varied (4). In many cases equlibrium had not been reached before the analyses were made.

It is very likely that the type of zinc oxide or hydroxide which is produced by the anodic treatment of zinc in alkaline solutions is a very soluble form. For this reason, and the fact that reaction (VI) is slow, the electrolyte in alkaline cells having zinc negative plates may be clear and yet have a zinc content higher than that of a saturated solution.

Acknowledgment

Thanks are due to Merck and Company, and the New Jersey Zinc Sales Company for supplying some of the materials used in this project. It is a pleasure to express thanks also to the Office of Naval Research under whose sponsorship this work was carried out.

Any discussion of this paper will appear in a Discussion Section to be published in the June 1956 JOURNAL.

REFERENCES

1. T. P. DIRKSE, *This Journal*, **101**, 328, 638 (1954).
2. K. HUBER, *Z. Elektrochem.*, **48**, 26 (1942); *Helv. Chim. Acta*, **26**, 1037 (1943); *This Journal*, **100**, 376 (1953).
3. Z. A. IOFA, S. YA. MIRLINA, AND N. B. MOISEEVA, *Zhur. Priklad. Khim.*, **22**, 983 (1949).
4. G. F. HÜTTIG AND B. STEINER, *Z. anorg. u. allgem. Chem.*, **199**, 149 (1931).

Anodic Polarization of Zirconium at Low Potentials

Formation Rates, Formation Field, Electrolytic Parameters, and Film Thicknesses of Very Thin Oxide Films[1]

GEORGE B. ADAMS, JR., AND PIERRE VAN RYSSELBERGHE

Department of Chemistry, University of Oregon, Eugene, Oregon

AND

MARIO MARAGHINI

Institute of Applied Chemistry, University of Rome, Rome, Italy

ABSTRACT

Methods are described for making quantitative studies on the growth of very thin oxide films on zirconium, and for estimating the film thickness as this growth progresses. These methods have been shown to be internally consistent and have been correlated with Mott's theory of metal oxidation. Experimental results so obtained are in agreement with previous work.

These methods should be readily adaptable to studies on the effect of temperature, ultraviolet radiation, electrolyte, and metal composition and physical properties, on the ionic current causing oxide film growth.

INTRODUCTION

A recent publication (1)[2] described the potential-time curve obtained when zirconium was anodized at constant current strength in certain aqueous electrolytes. This curve can be divided into three branches (Fig. 1). With a freshly abraded specimen there is initially a rapid rise in potential with a rate of change which decreases until a constant value is reached (branch AB).[3] This constant rate is maintained until the potential has risen sufficiently for oxygen evolution to occur. Then the rate drops abruptly to a very low value, which gradually increases over a long time interval (branch BC). During this period, visible localized gas evolution takes place. Finally, after a time interval dependent on the current being passed, the potential rises at an accelerated rate which quickly attains a constant value, lower than that of branch AB; this rate is maintained as the potential climbs steadily to 100 v or more (branch CD). The maximum voltage then attainable is limited only by the breakdown potential of the film.

With varying current density the potential-time curves change as shown in Fig. 1; with very high current densities the flat branch is undetectable by instruments used in this study, and with very low current densities the upper branch is not reached. The length of the branch BC and the slope of the branch CD are both highly dependent on oxygen concentration in the solution. Increasing concentrations of oxygen in the electrolyte shorten the flat branch and increase the slope of the upper branch, but do not affect the slope of the lower branch. A change in electrolyte does not affect the qualitative pattern of the curves, but may change certain parameters which can be derived quantitatively from them. An important exception is that of electrolytes containing halide ions in concentration of 0.001M or greater; in this case a stable horizontal branch occurs at a potential below that of the branch BC.

Properties of the oxide film formed along this second steep branch of the curve have been studied most recently by Charlesby (2) who showed that the anodic film growth follows the empirical law

$$I_+^0 = A_+ \exp(B_+F) \qquad (I)$$

between the true ionic current density I_+ and the electrostatic field F across the film. He re-evaluated the electrolytic parameters A_+ and B_+, and the field F, using a better value for the dielectric constant of the oxide than that employed by Günther-schulze and Betz (3).

Mott (4) also obtained an equation of the form of (I). He assumes that at high fields equilibrium is not

[1] Manuscript received December 27, 1954. This paper was prepared for delivery before the Pittsburgh Meeting, October 9 to 13, 1955.

[2] The caption of Fig. 8, in "Studies on the Anodic Polarization of Zirconium and Zirconium Alloys," by M. Maraghini, G. B. Adams, Jr., and P. Van Rysselberghe [*This Journal*, **101**, 404 (1954)] should read: "Logarithm of the rate of increase of potential vs. potential in aerated 1.5*M* HCl."

[3] The initial curvature in branch AB is apparent only at current densities of about 10 μa/cm^2 or less. Its significance has been explained previously (1).

established for the movement of metal ions across the barrier, and the derivation is carried out on the premise that the oxide film is so thin that the effect of any space charge built up by metal ions dissolving in the film in the course of its formation is negligible, with the consequence that the movements of ions and of electrons can be considered independently. On this basis, parameters A_+ and B_+ can be evaluated in terms of the barrier height, the barrier half-width, and certain physical properties of the metal. This film-building mechanism should be valid for the growth of thin oxide films formed by anodization as well as for the growth of oxide films on metals in air, caused by the electrostatic field set up across the oxide film when a contact potential difference is established between metal and adsorbed oxygen. Below a certain critical temperature, oxidation of metal in air or in aqueous electrolyte solution, due to this intrinsic field, will proceed only until a limiting oxide film thickness, generally of less than 100 Å, has been built up; it will stop effectively when this field has been decreased sufficiently by the growth of oxide film to reduce greatly further passage of metal ions across the metal-oxide interface.

It would thus seem that, in order to evaluate properly the electrolytic parameters A_+ and B_+ and their variation with temperature in studying the early stages of the oxidation process, it would be preferable to work with oxide films less than 100 Å in thickness, since the Mott equation was derived for oxide films so thin that the effect of space charge on the formation field is negligible.[4] Indeed, as Cabrera and Mott (7) point out, recent experimental work would indicate that, at sufficiently low temperatures, it is probable that the initial stages of the growth of oxide films on all readily oxidizable metals is governed by this same barrier mechanism. Oxidation of aluminum, chromium, titanium, tungsten, zinc, zirconium, and many other metals follows this type of law at room temperature; barium, copper, iron, and other metals show the same behavior at liquid air temperatures. Oxidation is very rapid at first, then drops to low or negligible values with the formation of a stable oxide film 20–100 Å thick.

Films thicker than 200 Å can be studied accurately by capacitance measurements, but for the thin films produced in the narrow range of potentials along the branch AB of the potential-time curve this method cannot be employed with certainty (8). These very thin films can be studied easily by following the change in the potential of the electrode surface with time, and the aim of the present research was to study the growth of these thin films over a potential range in which they exist, i.e., in the lower branch of the potential-time curve. Interpretation of results is greatly simplified by the fact that, for zirconium, the current efficiency of the film-building process is unity below oxygen evolution potentials. The principal uncertainty in quantitative interpretation along the lines of the Mott theory lies in the assumption that the density of these very thin films is that of the oxide in bulk.

In what follows, methods which have been used in the high potential range are adapted and extended for use in obtaining the parameters A_+ and B_+ from potential-time measurements taken in the low-potential range. Two equations are derived from (I) and two sets of experiments were carried out to test their validity. A third relationship derivable from (I) is shown to hold experimentally in the low potential range.

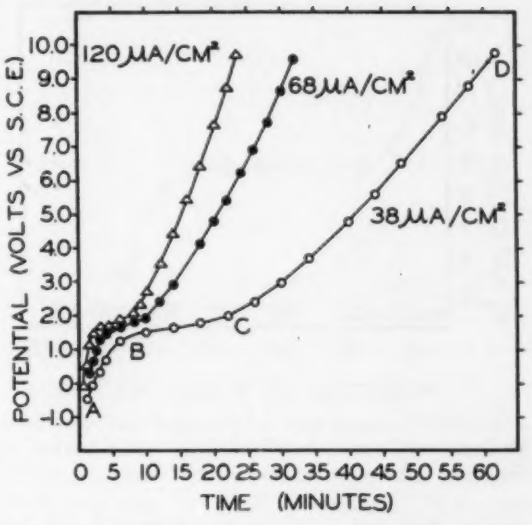

FIG. 1. Potential time curves for zirconium in air-saturated ammonium borate solution at 20.0°C.

RATE OF CHANGE OF POTENTIAL AT CONSTANT CURRENT

Introducing the apparent ionic current density, calculated from the projected area of the electrode, $I_+ = \sigma I_+^0$ (μa/cm²) where σ is the roughness factor for the electrode surface, and identifying the ionic

[4] Since this paper was submitted for publication, Dewald (5) has interpreted some of Vermilyea's results on the anodic oxidation of Ta (6) in terms of a theory which takes into account the action of space charge formation on the average formation field in the oxide film. He thus explains the observed temperature independence of the Tafel slope for films some thousands of Angströms in thickness, whereas the Mott theory for thin films requires a Tafel slope proportional to the absolute temperature.

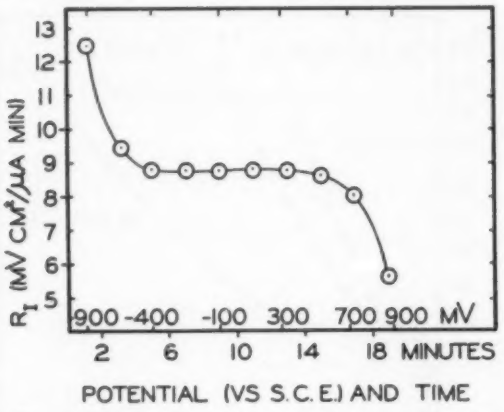

FIG. 2. Formation rate vs. potential and time for a single run at 12 μa/cm². 1.0M Na_2CO_3, air saturated, at 25.0°C.

current with the total anodic current I (in the absence of electron current), (I) becomes:

$$I = \sigma A_+ \exp(B_+ F) \qquad \text{(II)}$$

If X_o is the oxide film thickness on the electrode before anodization is begun; r, the volume of oxide formed/μa min (3.36×10^{-9} cc/μa min), assuming, with Charlesby (2), that the oxide formed has a density of 5.7; X, the film thickness at time t built up by anodization, with $X = X_o + r \int_0^t I/\sigma \, dt$; and E, the potential drop across the film at time t (mv), then

$$F = E/X = (1/B_+) \ln (I/\sigma A_+) \qquad \text{(III)}$$

When an external anodic current flows in the polarizing circuit between the zirconium anode and an auxiliary cathode, the potential measured in the potentiometric cell, zirconium-saturated calomel electrode (S.C.E.), will be

$$E' = E + K$$

where K is the constant sum of all potential differences in the chain other than that across the oxide film.

Substituting in (III),

$$E' = (r/B_+)\left[\int_0^t (I/\sigma)\, dt\right] \ln (I/\sigma A_+) + (X_o/B_+) \ln (I/\sigma A_+) + K \qquad \text{(IV)}$$

For I and σ constant in time,

$$\left(\frac{\partial E'}{\partial t}\right)_{I,\sigma} = \left(\frac{\partial E}{\partial t}\right)_{I,\sigma} = (rI/\sigma B_+) \ln (I/\sigma A_+) \qquad \text{(V)}$$

Designating the formation rate at apparent current density I, by R_I, where

$$R_I = 1/I \, (\partial E/\partial t)_{I,\sigma}$$

then

$$R_I = (r/\sigma B_+) \ln I + (r/\sigma B_+) \ln (1/\sigma A_+) = rF/\sigma \qquad \text{(VI)}$$

Potential-time measurements can be obtained for the film-building process at constant polarizing current after the local anodic current has decayed to a negligible value, i.e., along the linear portion of branch AB, Fig. 1. If $(\partial E/\partial t)_{I,\sigma}$ remains constant in time, it can be assumed that σ is also constant in time. If this is true, if equation (I) is valid for thin films, and if σ is independent of I, a plot of the formation rate vs. ln I should give a straight line. From the slope S of this line (mv cm²/μa min), and its intercept H (mv cm²/μa min),

$$B_+ = r/S\sigma \qquad \text{(VII)}$$

$$\ln (1/\sigma A_+) = H/S \qquad \text{(VIII)}$$

EXPERIMENTS AT CONSTANT CURRENT

Equation (VI) has been tested experimentally for zirconium in ammonium borate and sodium carbonate solutions, and it was found that $(\partial E/\partial t)_I$ becomes constant with time and that R_I is linear with ln I.

In Fig. 2 a sample run is shown, where a plot of R_I vs. time and vs. potential indicates the constancy of the formation rate after the local anodic current has become negligible.[5] In Fig. 3 the linearity of the plots of R_I vs. ln I is evident. Each point is the mean value of five determinations, and vertical bars mark off the probable errors. The lines were drawn on the basis of the method of least squares. The mean values of the constant rates for a given current density for borate and carbonate solutions are reported in Table I, together with the values of σA_+, σB_+, and F/σ derived therefrom.

Comparison with Previous Work

Results obtained in borate solution at 20.0°C may be compared directly with those of Charlesby (2), which were obtained from measurements taken on much thicker films over a potential range of 10–100 v and higher. His work was done at 18°C.

Line (A) of Fig. 3 has a slope of 1.69 and an intercept of 7.68.

[5] The first descending branch of the curve in Fig. 2 indicates that, in addition to the effect of the constant external anodic current, there is additional oxide film building due to the direct chemical action of the freshly abraded Zr surface with the solution. This action can be expressed in terms of a local anodic current (1) which decays with increasing film thickness. When the local current has become negligible compared to the constant value of the impressed anodic current, the formation rate becomes constant for a given value of the impressed current.

TABLE I. *Variation of formation rate with apparent current density*

Solution	I μa/cm²	Log (I/1 μa cm⁻²)	R_I mv cm²/μa min	σB_+ cm/mv	σA_+ μa/cm²	F/σ mv/cm at 100 μa/cm²
Ammonium borate, 20.0°C	1.22	0.085	7.84 ± 0.09			
	3.85	0.585	8.63 ± 0.03			
	12.2	1.085	9.52 ± 0.04	4.6×10^{-9}	2.9×10^{-5}	3.3×10^{9}
	38.5	1.585	10.4 ± 0.10			
	122.0	2.085	11.2 ± 0.06			
Sodium carbonate, 25.0°C	1.22	0.085	7.43 ± 0.08			
	3.85	0.585	7.99 ± 0.02			
	12.0	1.078	8.70 ± 0.04	6.0×10^{-9}	0.20×10^{-5}	2.9×10^{9}
	37.5	1.575	9.33 ± 0.07			
	118.0	2.074	9.94 ± 0.10			

From (III), (VII), and (VIII):

$$\sigma B_+ = 4.6 \times 10^{-9} \text{ cm/mv}$$
$$\sigma A_+ = 2.9 \times 10^{-5} \text{ μa/cm}^2$$
$$F/\sigma = 3.29 \times 10^{9} \text{ mv/cm at } 100 \text{ μa/cm}^2$$

Charlesby reports a B_+ value of 3.4×10^{-9}, an A_+ value of 1.6×10^{-5}, and an average value for F of 4.5×10^{9} at 100 μa/cm². These values include a roughness factor, which Charlesby takes as essentially unity.

If this evaluation is correct, then designating Charlesby's values by the subscript Ch:

$$\frac{\sigma B_+}{(B_+)_{Ch}} = 4.6/3.4 = 1.35; \quad \frac{\sigma A_+}{(A_+)_{Ch}} = 2.9/1.6 = 1.8;$$

$$\frac{F_{Ch}}{F/\sigma} = 4.5/3.3 = 1.35,$$

and, for agreement a roughness factor of about 1.4 must be assumed for the surface of the abraded specimens after the formation rate has decreased to its limiting value. The third ratio is independent of the other two because F_{Ch} was determined from capacitance measurements, which were not directly related to A_+ and B_+. The second check does not carry the same weight as the others because of the large uncertainty involved in evaluating A_+, due to its exponential relationship to the field.

The value of 1.4 thus deduced for the roughness factor of the surfaces of the abraded specimens after anodization to negligible local current has been substantiated further. The roughness factor for the freshly abraded specimens, prior to immersion, was found to be 2.1 ± 0.2, using a small-volume gas adsorption apparatus with krypton gas as adsorbate.[6] This value of the roughness factor must be considered as an upper limit. The actual electrochemical roughness factor should lie between this value and unity. This has been shown by comparing formation rates for highly polished electrode surfaces with those for abraded surfaces. The average formation rate for a highly polished zirconium electrode surface is approximately 40% higher than the formation rate for an abraded surface, which again would indicate that, if the roughness factor for the polished electrode surfaces were very nearly unity, as Young claims for Ta (6), the roughness factor for the abraded surfaces after anodization to a constant rate would then be about 1.4.

A final check with Charlesby's results can be made independently of an assumed roughness factor. The product B_+F is dimensionless. For a current density of 100 μa/cm² this product is $4.6/\sigma \times 3.3\ \sigma = 15$, from the present measurements. If F is extrapolated to 1000 μa/cm², using (II), this product becomes 17.6. Charlesby gives a value of 17 for this product, but does not state the corresponding current density. Much of his work, however, was done at current densities in the range 500–1000

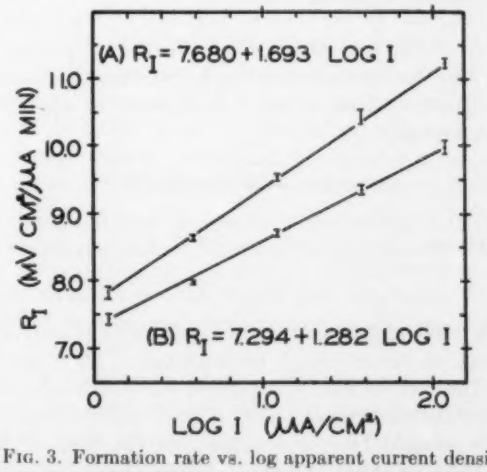

FIG. 3. Formation rate vs. log apparent current density for air-saturated solutions; (A) ammonium borate, 20.0°C; (B) sodium carbonate, 25.0°C.

[6] Determinations of roughness factors were made for the authors by Ralph J. Brodd through the courtesy of Professor Norman Hackerman, University of Texas, Austin, Texas.

TABLE II. *Comparison of formation rates as calculated from equation (VI) or from equation (IX). Ammonium borate, 20.0°C*

I μa/cm²	$1/I\left(\frac{\partial E}{\partial t}\right)$ mv cm²/μa min, I, Equation (VI)	$1/I\left(\frac{\partial E}{\partial t}\right)$ mv cm²/μa min, I, Equation (IX)	% Difference
0.1	5.99*	6.64*	10.8
1	7.68	7.76	1.04
10	9.37	9.30	0.74
50	10.6	10.5	0.94
100	11.1	11.1	0.00
1000	15.7*	13.3*	15.3

* By extrapolation. Equation (VI) assumed valid.

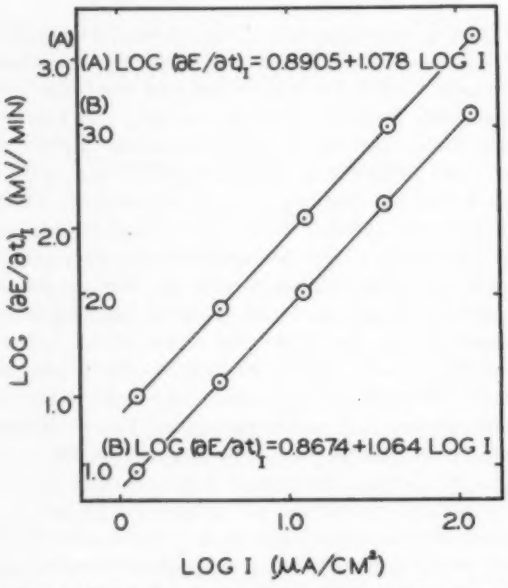

FIG. 4. Log rate vs. log apparent current density for air-saturated solutions: (A) ammonium borate, 20.0°C; (B) sodium carbonate, 25.0°C.

μa/cm². The agreement seems satisfactory, inasmuch as the comparison was made between zirconium specimens which differed somewhat in chemical composition.

Correlation with Previous Work

The empirical relation between rate of change of potential and current reported previously, namely,

$$(\partial E/\partial t)_I = AI^B \qquad \text{(IX)}$$

is a good approximation to equation (VI) over the range of current densities employed. This is shown in Table II. In Fig. 4, data used in constructing Fig. 3 are shown as log-log plots of the variables in (IX). The straight lines were drawn on the basis of the method of least squares. From these lines the empirical constants A and B have been evaluated. A values of 7.77 and 7.37 mv/min and B values of 1.08 and 1.06 are obtained for ammonium borate and sodium carbonate solutions, respectively.

Equation (IX) is of a form which is directly applicable to the estimation of local currents from potential-time measurements in the manner outlined previously (1).

Change in Potential with Change in Current at Constant Film Thickness

Validity of the relationship expressed in (I) can be tested by another approach. Equation (III) may be written:

$$E' = X/B_+ \ln I + (X/B_+) \ln (1/\sigma A_+) + K \qquad \text{(X)}$$

For an experiment carried out at constant film thickness, a plot of the measured potential vs. the logarithm of the apparent current density should give a straight line. This experimental work was done, and the linearity of the plot of these variables is indicated by the straight lines of Fig. 5. Points such as those shown were obtained as follows.

After the freshly abraded zirconium electrode had been polarized at constant current density I_1 to give a value of $(\partial E/\partial t)_I$ which was constant with time, the current density was increased abruptly to another value I_2 by short circuiting a resistor in the polarizing circuit. The potential rose rapidly and passed through a maximum then a minimum value before settling down to another fixed rate of change with time. This behavior is shown in Fig. 6, where E_1' is the value of the potential at time t_0 when the current density I_1 is suddenly increased to a value I_2. E_2' is the value of the potential as it passes through its minimum before attaining a new steady

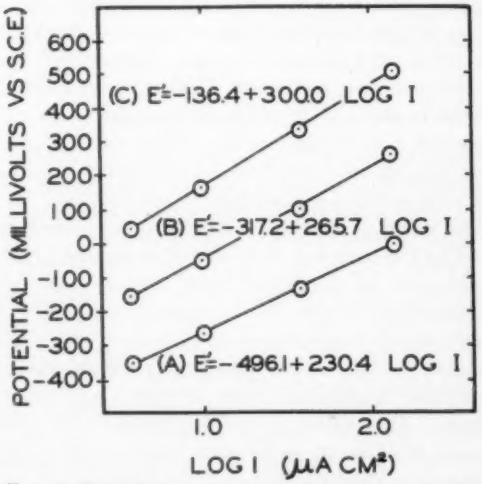

FIG. 5. Potential vs. log apparent current density at constant film thickness. Air-saturated ammonium borate solution, 20.0°C. (A) σX_a = 46 Å; (B) σX_b = 53 Å; (C) σX_c = 59 Å.

rate. (If I_2 is large enough, the maximum and minimum merge to give only a momentary stop before the rate reaches its new value.) E'_1 corresponds to the potential drop across the film of thickness X_1 at current I_1, and E'_2 corresponds to the potential drop across the same film of thickness X_1 at current I_2 (neglecting the small increase in film thickness occurring between the change in current and the new potential readings). Another run was begun with a freshly abraded electrode surface at a constant polarizing current density of value I_2, and the potential was followed until it reached the value E'_2. At that time the film again had reached the thickness X_1; the current density was increased abruptly to a new value I_3 with a potential value E'_3 which corresponded to the potential drop across the film necessary to pass current I_3 through the thickness X_1. Again, starting with current density I_3, and E'_3 being reached, the current was increased to I_4 and a value of E'_4 was determined, etc. When the above values of E'_1, E'_2 . . . are plotted against those of ln I_1, ln I_2 . . . , a straight line should be obtained if (II) is correct.

This method has been tested experimentally in ammonium borate at 20.0°C and the results are shown in Fig. 5. Table III contains the data from which lines (A), (B), and (C), respectively, were constructed. Duplicate runs were generally found to be sufficient because of the good reproducibility.

The linearity indicated in (X) is thus experimentally established, giving further evidence for the validity of (I). Since the linearity indicated in (I) has already been verified by experiment, the linearity of the curves in Fig. 5 can be considered as a check on the experimental procedure just outlined, and it may be concluded that this procedure does, in fact, give potential increments corresponding to current increments at constant film thickness.

The most important conclusion from (X) is that the oxide film thickness should be given by

$$X = L(B_+) \qquad \text{(XI)}$$

where L is the slope of the line. From Fig. 5a an apparent film thickness σX_a of 45.7 Å is obtained. Referring to Table III, it is seen that this apparent oxide film thickness is that formed on a freshly abraded electrode anodized at 3.85 μa/cm² to a potential of −358 mv vs. the saturated calomel electrode. Similarly, from the slope of line (B) an apparent oxide film thickness of 52.7 Å is obtained, and it is seen that this apparent thickness is attained by anodizing a freshly abraded electrode to a potential of −159 mv at 3.85 μa/cm². The slope of line (C) gives an apparent thickness of 59.5 Å obtained by anodizing a freshly abraded electrode at 3.85 μa/cm² to a potential of 41 mv.

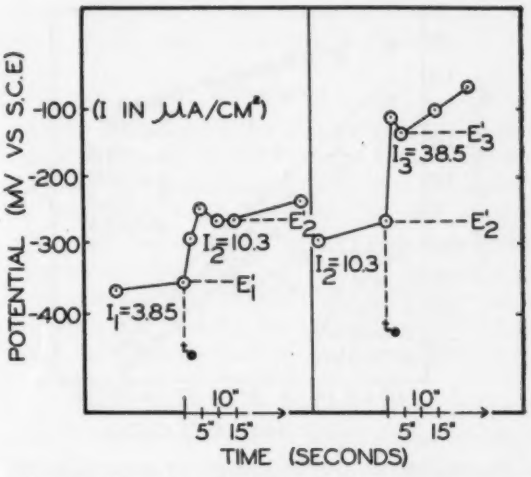

FIG. 6. Change in potential with change in current at constant film thickness. Air-saturated ammonium borate solution, 20.0°C.

TABLE III. *Variation of potential with apparent current density at constant film thickness. Ammonium borate, 20.0°C*

σX_a = 46 Å		σX_b = 53 Å		σX_c = 59 Å	
Log I/ 1μa/cm²	E' mv vs. S.C.E.	Log I/ 1μa/cm²	E' mv vs. S.C.E.	Log I/ 1μa/cm²	E' mv vs. S.C.E.
0.585	−358	0.585	−159	0.585	41.0
1.015	−265	1.002	−52.5	1.002	164.0
1.585	−135	1.585	99	1.585	334.5
2.139	0	2.129	252	2.129	505.5

Thus, an increment in potential of 200 mv at 3.85 μa/cm² represents an increase of about 7 Å in apparent film thickness.

This increase in apparent thickness can be checked quantitatively. At 3.85 μa/cm² the unitary rate is 8.63 mv cm²/μa min (Table I); the time required for the potential to increase by 200 mv at this current density is 200/(3.85 × 8.63) = 6.02 min, or 23.2 μa min. This is equivalent to 23.2 × 3.36 × 10^{-9} cm or 7.7 Å in apparent thickness. This check is independent of the actual value of the roughness factor; the actual thickness is given by the ratio of the apparent thickness to the roughness factor.

It should be pointed out that each of the lines (A), (B), (C) of Fig. 5 is actually an anodic polarization curve at constant oxide film thickness. It is evident that the lines become steeper with increased film growth.

It is interesting to note that the ratio of the formation rates at two different current densities, I_1 and I_2, is, from (I):

$$R_2/R_1 = \frac{r/\sigma B_+ \ln (I_2/\sigma A_+)}{r/\sigma B_+ \ln (I_1/\sigma A_+)} = \frac{\ln (I_2/\sigma A_+)}{\ln (I_1/\sigma A_+)}$$

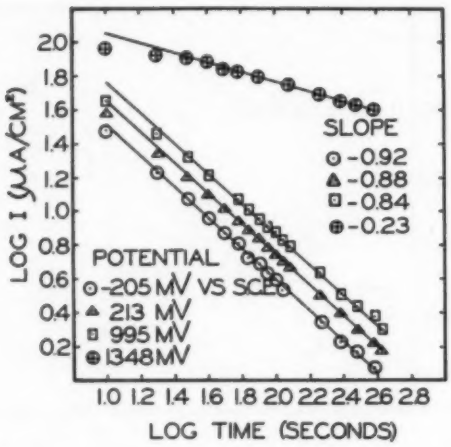

FIG. 7. Current decay at constant formation potential. Air-saturated ammonium borate solution, 20.0°C.

TABLE IV. *Current decay at constant formation potential: slopes of the decay curves*

E' mv vs. S.C.E.	$-d \log I/d \log t$	E' mv vs. S.C.E.	$-d \log I/d \log t$
−367	0.93	35	0.83
−320	0.86	120	0.87
−277	0.89	176	0.89
−264	0.92	213	0.88
−220	0.89	251	0.84
−220	0.83	313	0.89
−205	0.92	380	0.86
−204	0.89		
−172	0.90		
−20	0.90		

The ratio of the ordinates of lines (B) and (A) in Fig. 5 at the same current densities I_1 and I_2 is:

$$\frac{E_2'^b - E_2'^a}{E_1'^b - E_1'^a} = \frac{X_b - X_a}{X_b - X_a} \frac{1/B_+ \ln (I_2/\sigma A_+)}{1/B_+ \ln (I_1/\sigma A_+)}$$

$$= \frac{\ln (I_2/\sigma A_+)}{\ln (I_1/\sigma A_+)} = R_2/R_1$$

Thus, an experimental verification of the equality of the first and last ratios should provide a check on the internal consistency of the two methods.

From line (A), Fig. 5

$$\frac{R_{\log I=0.5}}{R_{\log I=1.5}} = 0.834; \frac{R_{\log I=1.0}}{R_{\log I=1.5}} = 0.916; \frac{R_{\log I=2.0}}{R_{\log I=2.5}} = 1.083$$

and from the three lines in Fig. 5, taking the average value of the vertical distance between lines, (since $X_b - X_a \cong X_c - X_b$)

$$\frac{\Delta(E')_{\log I=0.5}}{\Delta(E')_{\log I=1.5}} = 0.834; \frac{\Delta(E')_{\log I=1.0}}{\Delta(E'_0)_{\log I=1.5}} = 0.925;$$

$$\frac{\Delta(E')_{\log I=2.0}}{\Delta(E')_{\log I=1.5}} = 1.075$$

The difference is within 1–2% error in the determination of formation rates.

This agreement serves as a check on the validity of the experimental procedure used in constructing Fig. 5, especially in the selection of the minimal values of the increased potential resulting from abrupt increases in polarizing current (E_2', E_3' as sketched in Fig. 6).

Current Decay at Constant Formation Potential

A third test of equation (I) can be obtained from current decay measurements at constant formation potential in the low potential range.

Charlesby (2) has shown that, for an ion current decaying through a growing oxide film at constant formation potential according to the Mott relationship, (I), a plot of the logarithm of the current density vs. the logarithm of the time should be linear, with a slope determined by the value of the B_+F product for the film formation process. He gives values of −0.87 and −0.90 for this theoretical slope for B_+F ranges of 10–15, and 15–20, respectively.

A B_+F value of 15 was obtained for abraded zirconium specimens in the low potential range from the work reported above on formation rates at constant current. This value is for an apparent current density of 100 μa/cm² in dilute ammonium borate solution at 20.0°C.

In Fig. 7 typical curves of current decay at constant formation potential are shown. These were obtained using abraded zirconium in dilute ammonium borate solution at 20.0°C. The curves shown are for a single specimen electrode for which four consecutive current decay experiments were carried out at constant formation potentials. These formation potentials became progressively more positive from one run to another as the oxide film thickness increased.

It was noted that for each series of runs like that shown in Fig. 7 a definite trend of decreasing slope with increasing formation potential usually occurred. In Table IV the values of the slope obtained from 17 individual curves are tabulated with the value of the corresponding formation potential. Only runs with formation potentials definitely below that for oxygen evolution (600 mv vs. S.C.E.) have been included. The mean value of the slopes obtained for all 17 runs over the formation potential range −367 to 380 mv vs. S.C.E. is −0.88 ± 0.01. For proper comparison with the B_+F value obtained from formation rates at constant current, only those slopes obtained from runs with formation potentials near −200 mv vs. S.C.E. should be taken, since all

formation rates were tabulated at this potential. The mean value of the slopes for the 7 runs over the formation potential range −277 to −172 mv vs. S.C.E. is −0.89 ± 0.01. This value of $d \log I/d \log t$ corresponds to a theoretical B_+F value of 15. This checks with the value of 15 determined from the formation rate experiments at constant current, and again confirms the validity of equation (I) in the low potential range.

Current Efficiency of Oxide Formation in the Low Potential Range

The agreement with Charlesby's work is based entirely on the assumption of unit current efficiency for oxide formation below the potentials for oxygen evolution. The fact that agreement was obtained is a point in favor of this assumption; another is the fact that the only reaction thermodynamically possible below the reversible potential for oxygen evolution is the oxidation of zirconium. Also, when the potential-time measurements are being taken, the constant rate drops abruptly soon after the reversible potential for oxygen evolution is reached, indicating that a second reaction is then starting (Fig. 2). Further evidence for unit efficiency in the low potential range accrues from formation rate measurements which have been obtained for the steep branch of the potential-time curve above 2 v, where oxide film formation and oxygen evolution occur simultaneously. It has been found that the concentration of oxygen in the solution affects the formation rate very noticeably. Thus, in borate solution at 20.0°C, increasing the oxygen concentration from its value in a nitrogen-saturated solution to that in an oxygen-saturated solution causes an increase in the formation rate of some 20%. This is in the direction to be expected for an oxygen electrode. However, when the same experiment was repeated in the low potential range, no difference in rate was observed between a nitrogen-saturated and an oxygen-saturated solution. This result would be expected if the current efficiency for oxide formation were, in fact, unity in the low potential range.

The agreement obtained in the work on current decay at constant formation potential reported above provides strong support for the assumption of unit current efficiency in the low potential range. An electron current which decayed at the same rate as the ion current would not manifest itself in a decreased value of $d \log I/d \log t$, but it is evident from Fig. 7 that the electron current involved in the oxygen evolution process decays much more slowly than the ion current. Thus, the assumption of unit current efficiency in the region of −200 mv vs. S.C.E. would seem to be fully substantiated.

Discussion

From Fig. 1 and Table I it is evident that the values of A_+, B_+, and F for ammonium borate are significantly different from the corresponding values for sodium carbonate solution. The inequality is larger than can be accounted for by the five degree temperature difference between the two sets of measurements. This inequality must be due mainly to specific effects of the electrolytes themselves. Any such effect should manifest itself at the oxide-solution interphase.

A tentative explanation might lie in the ability of small pores, located in the thin oxide film, to reduce the effective electrostatic field across the film. It is known that the concentration and size of such pores depend on the type of electrolyte in which the oxide film is formed (9).

Alteration of the field in this way would result in different values of A_+ and B_+. Since A_+ is related exponentially to the field, a small change in F would cause an order-of-magnitude change in A_+.

It should be mentioned that this experimental work has been interpreted on the assumption that the increase in potential of the electrode from initial immersion to the oxygen evolution potential results from the growth of a true oxide film. The agreement obtained with the work on visible oxide films, carried out in the high potential range, would support this view.

Experimental

Polarizing circuit and cell.—This apparatus has been described previously (1).

Preparation of metal electrodes.—Coupons were cut from 0.070-in. zirconium sheet in the shape of square electrodes with extensions for electrical connections. These were completely covered with an impervious baked coating of enamel. The enamel was then ground away from one face of the electrode to leave a projected area of 2.6 cm^2. Prior to each run the exposed face of the electrode was abraded with 0, 2/0, and 3/0 emery cloth, using a standardized procedure.

Analysis of electrode specimens.—This work was done on a sample of hafnium-free zirconium prepared by the Kroll process, designated by the code number WA-3983. It was 10–20% cold worked with a Rockwell B hardness of 68–81. It had the following analysis (in ppm):[7]

[7] The authors appreciate the cooperation of Dr. Earl T. Hayes, Chief, Physical Metallurgy Branch, Bureau of Mines, Albany, Oregon, in supplying them with this analysis.

Al	20	Cu	50	Ni	20	V	50
B	0.3	Fe	600*	O_2	1650*	Zn	< 50
C	370*	Mg	10	Pb	30	Hf (estimated)	< 300
Cd	0.5	Mn	10	Si	100		
Co	< 10	Mo	10	Sn	500*		
Cr	< 5	N_2	70*	Ti	50		

* Values marked with an asterisk were determined chemically; the others were determined spectroscopically.

Solutions.—All solutions were made up from A.R. salts and distilled water. The ammonium borate solution was prepared by saturating distilled water with boric acid at 20.0°C. Ammonia gas was bubbled through the solution until the *p*H reached a value of 8.0.

All results reported here were obtained with air-saturated solutions, unless otherwise stated.

Potential-time measurements at constant current.—Runs always were begun within 3 min after completion of the abrasion operation. All potentials were measured against the saturated calomel electrode. Polarizing current was maintained constant by manual control. Measurements of current, potential, and time, as well as current control, were all carried out with an accuracy of 1% or better. The range of current densities employed was from 1 to 100 $\mu a/cm^2$, and the potential ranged from -1200 to $+600$ mv.

During anodization, potentials were recorded at given time intervals and the formation rates calculated. Results for a single run are shown in Fig. 2, where it is seen that, after a period of decreasing rate corresponding to the decreasing local current, there is a constant rate period which terminates when potentials are reached for which a second reaction, the oxidation of hydroxide ion, is possible. The rate then decreases because the current efficiency for the film-building process is no longer unity. In order to avoid including portions of the first and last branch of this curve in the constant rate, the two values nearest -200 mv were averaged to give the formation rate to be used in equation (VI). The scatter in the five individual runs taken at each current density is higher than would be expected from the accuracy in the basic measurements. This scatter is probably due to differences which exist in the abraded electrode surfaces in one run compared to another.[8] However, with five individual runs taken per point the probable error is reduced to a value of 1–2%.

[8] Recent experiments have been carried out which indicate that increased precision can be obtained by pre-anodizing specimen electrodes at a current density of 0.1 $\mu a/cm^2$ for about 12 hr, until each specimen has attained the same starting potential before a run is begun.

Potential Measurements at Constant Film Thickness

The general procedure has been discussed above. It should be added, however, that large current increments at constant film thickness give potentials which fall low, compared to those obtained with smaller increments. Thus, it was found that, for a current range of 10–316 μa, steps of 10–31.6, 31.6–100, and 100–316 μa gave points which fell on the same straight line. When this current range was divided into four, five, or six increments, the resulting points all fell on the same straight line as that obtained with three increments. However, if this range was divided into one or only two steps, the resulting points fell low. A safe change of current density was found to be one for which $\Delta \log I \cong 0.5$.

Current Decay Measurements at Constant Formation Potential

Zirconium electrode specimens were freshly abraded, and the 2.6 cm^2 exposed surface was masked down to a circular area of 1.0 cm^2 by partially covering the surface with a beeswax-rosin mixture.

Direct current was obtained from a battery-operated, low-power voltage regulator. Formation potentials were maintained constant to within ± 10 mv by the voltage regulator as the anodic current decayed from 100 through 1 μa. By manually controlling the grid potential of the voltage regulating tube, these formation potentials were maintained constant to within ± 3 mv.

Current was measured with a Weston milliammeter Model 622, over a range of 1–100 μa. The potential was measured vs. S.C.E. with a Beckman Model M *p*H meter in series with a student potentiometer. The temperature of the electrolyte was maintained constant at 20.0° ± 0.1°C with a constant temperature bath.

Current decay runs were made by immersing the freshly abraded and masked electrode specimen in the dilute ammonium borate solution contained in the polarization cell. The polarization circuit was then closed, and the potential was increased until a current somewhat larger than 100 μa registered on the milliammeter. The potential was maintained constant by one operator while a second observer recorded the current. Zero time was taken as the instant the current decayed through 100 μa. After the current had decayed through 1 μa, a second run was begun by again increasing the potential until a current somewhat larger than 100 μa was obtained; the formation potential was then maintained constant at the new value as the second set of current decay measurements was taken.

Summary

On the assumption that the time-linear potential increase observed when an abraded zirconium electrode is anodically polarized to oxygen evolution results from the growth of an oxide film, it is shown experimentally that in the range of low formation potentials ion current through the film varies exponentially with the formation field, $I_+ = A_+ \exp(B_+F)$. This well-established relationship for describing growth of anodic oxide films in the range of high formation potentials has now been extended to the low formation potential range.

From anodic potential-time measurements, taken below oxygen evolution potentials, formation rates at constant current, formation field, electrolytic parameters, A_+ and B_+, and thicknesses of very thin anodic oxide films have been evaluated.

Results so obtained are compared with those of other work for thicker oxide films formed in the high potential range and are found to be in agreement. Correlation is established between these results and previously reported work on estimation of local currents from anodic polarization measurements.

Experimental verification of the relationship between ion current and formation field in the potential range below oxygen evolution was carried out along three lines: (*a*) evaluation of formation rates from potential-time measurements at constant current; (*b*) measurement of the change of formation potential with change of current at constant film thickness; (*c*) measurement of the decay of ion current at constant formation potential.

Results obtained in these experiments were shown to be internally consistent.

Evidence is presented to substantiate the working assumption of unit current efficiency for the oxide-film-building process below oxygen evolution potentials.

Acknowledgment

The work reported in the present paper is part of a research program carried out at the University of Oregon under a contract with the U. S. Atomic Energy Commission.

Any discussion of this paper will appear in a Discussion Section to be published in the June 1956 Journal.

REFERENCES

1. M. Maraghini, G. B. Adams, Jr., and P. Van Rysselberghe, *This Journal*, **101**, 400 (1954); Technical Report to the U. S. Atomic Energy Commission AECU-2797, September, 1953.
2. A. Charlesby, *Acta Met.*, **1**, 340 (1953); Atomic Energy Research Establishment, Harwell, Report M/R-1014, September, 1952.
3. A. Güntherschulze and H. Betz, *Z. Elektrochem.*, **37**, 726 (1931).
4. N. F. Mott, *Trans. Faraday Soc.*, **43**, 429 (1947).
5. J. F. Dewald, *This Journal*, **102**, 1 (1955).
6. D. A. Vermilyea, *Acta Met.*, **1**, 282 (1952).
7. N. Cabrera and N. F. Mott, *Repts. Prog. Phys.*, **12**, 163 (1948–49).
8. L. Young, *Trans. Faraday Soc.*, **50**, 153 (1954).
9. F. Keller, M. S. Hunter, and D. L. Robinson, *This Journal*, **100**, 411 (1953).

Two Photoelectric Colorimeters for Television Picture Tubes[1, 2]

RICHARD S. HUNTER

Hunter Associates Laboratory, Falls Church, Virginia

ABSTRACT

Two photoelectric tristimulus instruments for the colors of television picture tubes, fluorescent lamps, and the phosphors used in them are described. One uses a single photocell and three filters on a disk. The photocell currents corresponding to each of the three filters are converted by equations or nomographs to values of color. The second makes use of three photocells, each with different filters. The currents from these photocells are measured with a special current-balancing bridge which gives direct readings of luminance and chromaticity. A new reversed-signal circuit has been devised for improved sensitivity and precision.

INTRODUCTION

Television picture tubes fall in the category of extended-area light sources, the colors of which are specified by luminance and chromaticity. Luminance is luminous (visual) intensity, or projected light flux per unit of projected area; for television picture tubes it is commonly expressed in footlamberts. Chromaticity is a two-dimensional measure of the nonintensity attributes of color. Its customary dimensions, x and y, are the respective fractions of two of the tristimulus values in the total of three X, Y, and Z, which may be derived by integration from the spectral distribution of any specimen (1).

Fig. 1 is an x, y diagram on which the chromaticities of all colors may be located within the roughly triangular locus of spectrum colors. As is well known, near whites plot in the central area of this diagram, while saturated colors plot near the spectrum locus, each in a direction from the center corresponding to that of the wave length which it most resembles.

The instruments described are intended primarily for monochrome picture tubes. However, there appears to be no reason why they cannot also be used to measure the colors of color-television picture tubes and the phosphors used in them. A color-standard box with incandescent lamp, diffusing screen, and slot for color filters has been built to facilitate color measurements. This box is shown in Fig. 2.

Fig. 3 and 4 are diagrams of the two colorimeters. Fig. 5 is a photograph of the instrument diagrammed in Fig. 4. The exposure unit which receives the signal consists in each case of a stand supporting photocell or cells and filters and an aluminum housing 10 x 10 x 15 in. long. In the front of this box is a 12 cm round window where the television tube or other specimen is presented for measurement. Dotted lines in Fig. 4 show the positions of reflecting or transmitting specimens and the sealed-beam, reflector-type lamps which may be used to illuminate them. Also shown in dotted lines is the position of a daylight filter, D, which may be used to convert the incandescent-illuminant colors of objects to their daylight colors.

PHOTOELECTRIC TRISTIMULUS COLORIMETRY

The use of filters with barrier-layer photocells for photoelectric tristimulus measurements of color has been developed by Barnes (2), Hunter (3), and others. Filters are designed for barrier-layer photocells that will give these cells spectral relative responses nearly duplicating those of the CIE standard observer for colorimetry (1). The four tristimulus filters used in the present instruments are like those described by Barnes (2) and were designed by the Corning Glass Works.

In Fig. 6, the CIE $\bar{x}$, $\bar{y}$, and $\bar{z}$ distribution functions are compared with spectral responses of the filter-photocell combinations used in the present apparatus. The filter-photocell curves have been adjusted so that the areas under them are the same as those under the corresponding CIE functions. The $\bar{z}$-blue filter consists of three components: the usual blue and Noviol components, and a third blue-green element to absorb the far red. The other three filters consist of two components each, one absorbing the short-wave side, and one the long-wave side of the

[1] Manuscript received December 18, 1954. This paper was prepared for delivery before the Chicago Meeting, May 2 to 6, 1954.

[2] These instruments were developed at the suggestion of the Joint Electron Tube Engineering Council Subcommittee 6.3.

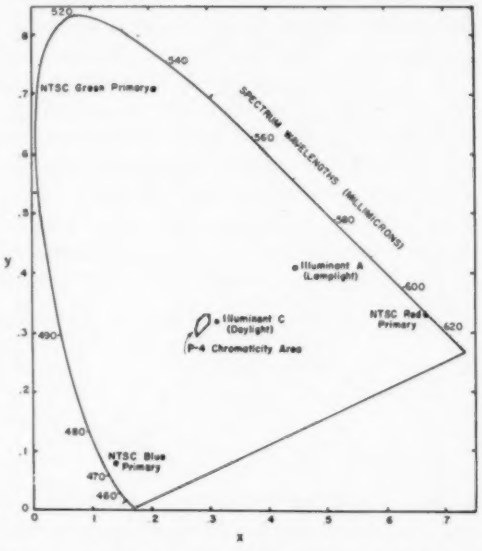

FIG. 1. CIE x, y chromaticity diagram with boundary of spectrum colors, standard illuminants C (daylight) and A (lamplight), area recommended by JETEC for P4 television picture tubes, and the NTSC red, green, and blue primaries.

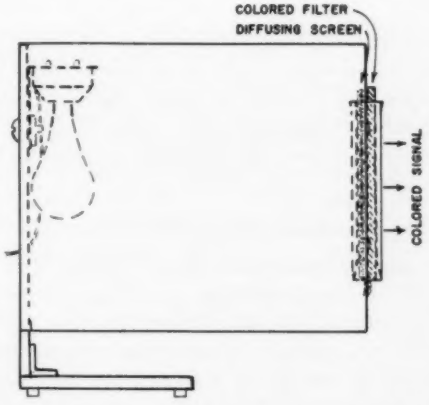

FIG. 2. Diagram of color-standard box with incandescent lamp, diffusing screen, and colored filter in slot.

spectral band passed by the filter. As will be shown below, the fourth $\bar{x}$-blue filter is used for only one of the two models of the new apparatus; thus there are two blue ends of the $\bar{x}$-filter-photocell function in Fig. 6, one for the four-filter set and the other for the three-filter set which used the $\bar{z}$-blue filter for the blue hump of the $\bar{x}$ curve as well as for the $\bar{z}$ curve.

Successful photoelectric tristimulus colorimetry requires standards similar to the specimens to be measured in both color and spectral distribution of energy. Hunter (3) showed that, on the average, a series of values of chromaticity measured by a

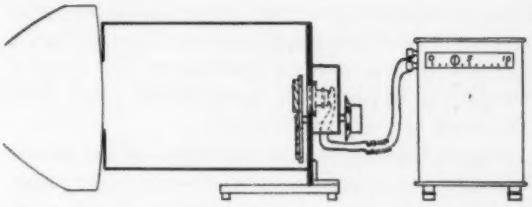

FIG. 3. Diagram of one-photocell, filter-disk colorimeter for television picture tubes.

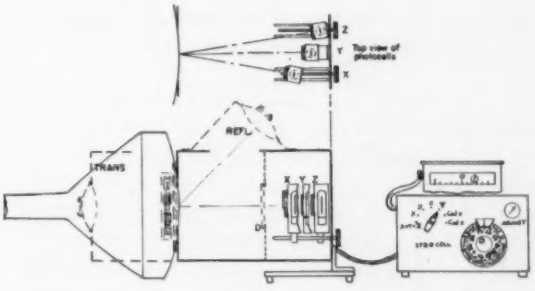

FIG. 4. Diagram of three-photocell, direct-reading colorimeter for television picture tubes, fluorescent lamps, and nonluminous objects. In dotted lines are shown the positions of reflecting and transmitting specimens, the sealed-beam lamps which may be used to illuminate them, and a daylight filter (D) which may be used to convert the incandescent-illuminant colors of objects to their daylight colors.

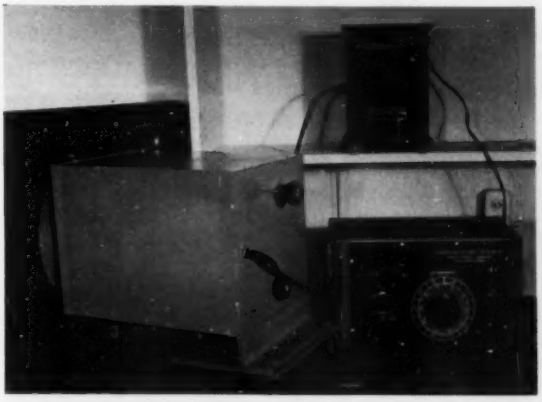

FIG. 5. Photograph of three-photocell, direct-reading colorimeter with exposure unit facing television tube at left, measurement unit at right, and galvanometer on shelf above.

photoelectric tristimulus instrument contains errors which are roughly 10% of the chromaticity differences between the specimens and the standard used. The source of this error is the failure of the source-filter-photocell combinations to duplicate spectrally the CIE functions (see Fig. 6). Fig. 7 shows examples of these errors by the present instru-

ment by illustrating the shifts from standard values (computed from spectrophotometric data) to values observed with the three-cell instrument. For color by reflection in daylight, the lamp (REFL.) and filter (D) shown in Fig. 4 were used.

Because these errors are spectral in origin, standards used for photoelectric tristimulus colorimetry must be similar in spectral distribution as well as in color to the specimens to be measured. In Fig. 8, the spectral distribution of a typical P4 phosphor is compared with that of the Illuminant C lamp and filter combination frequently used as standard. It was shown in Fig. 1 that these two are close in

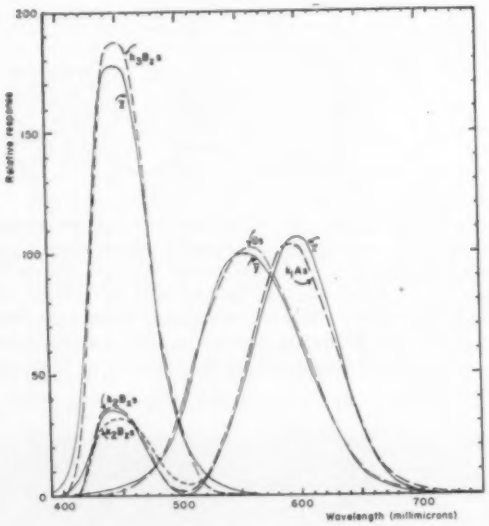

FIG. 6. Intercomparison of CIE $\bar{x}$, $\bar{y}$, and $\bar{z}$ (solid lines) and the filter-photocell combinations designed to duplicate them (dashed lines). The dotted line, k_2B_2s shows the inferior duplication of the blue end of the $\bar{x}$ curve obtained when the z-blue filter is used instead of the 4th x-blue filter.

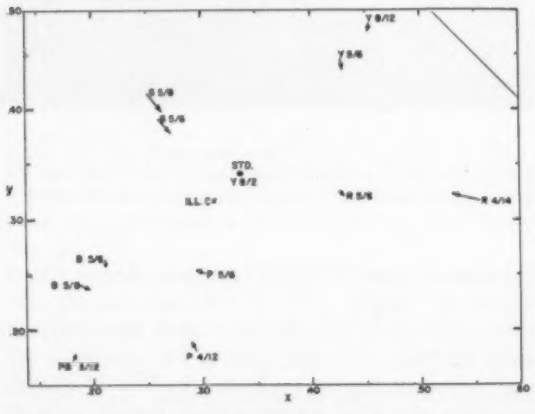

FIG. 7. Errors in measurements of Munsell colors for daylight. Munsell paper Y 8/2 was used as standard.

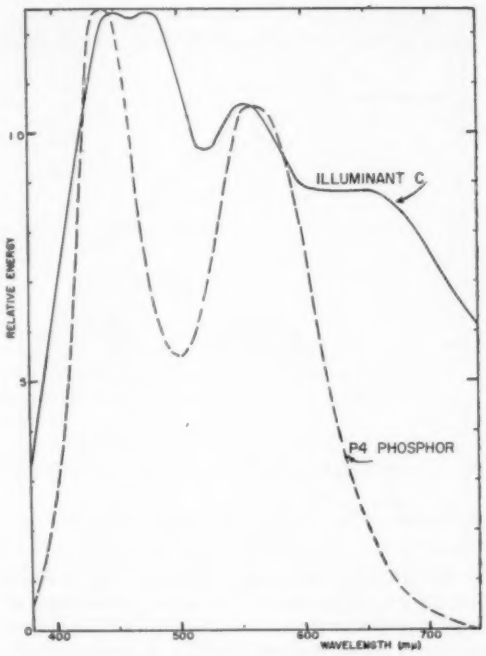

FIG. 8. Spectral distributions of CIE illuminant C and P4 phosphor which were shown in Fig. 1 to have nearly the same chromaticity.

chromaticity, but Fig. 8 shows them to be different spectrally. Because most monochrome phosphors differ spectrally from the standards regularly used for colorimetry, arrangements have been made for the calibration of monochrome television picture tubes as standards.[3]

FILTER-DISK MODEL

The simpler instrument shown in Fig. 3 is like one used by Martin, Noland, and Vogel (4), except that addition of the sheet-metal housing permits operation in a partially lighted room and readings of luminance as well as x and y. The hermetically sealed photocell (5), which has a sensitive area 2 in. in diameter, is behind a disk on which the filters are mounted. Signals from this photocell are measured by deflections of a spotlight galvanometer. There are four positions on the filter disk. One blocks all light from the photocell so that the galvanometer scale can be adjusted for zero deflection. The other three carry green, amber, and blue filters, respectively.

Measurements are made of a picture tube operating from a stabilized power supply at full-size raster with no picture information. The 12 cm window of

[3] The Joint Electron Tube Engineering Council Cathode Ray Tube Committee (JTC-6) has arranged for this to be done by the RCA Industry Service Laboratories, Newark, N. J.

the photoelectric instrument is centered against the face of the picture tube. Its luminance is brought to at least 20 footlamberts as indicated by the green-filter deflection of the galvanometer.

After a suitable warm-up, deflections are read with each of the three filters. Luminance and chromaticity are derived by the use of four constants whose values are found by a calibrating procedure described in the following paragraphs. If G, A, and B are the deflections with the green, amber, and blue filters, respectively, then one may write:

$$\text{Luminance} = k_L G$$

$$x = \frac{k_1 A + k_2 B}{k_1 A + G + (k_2 + k_3) B}$$

$$y = \frac{G}{k_1 A + G + (k_2 + k_3) B}$$

The constants k_1, k_2, k_3 are required to adjust the filter-photocell responses A and B to the right magnitudes for combining with the response G in the computation of chromaticity. The adjusted X-response has the component $k_1 A$ corresponding to the long-wave-length portion of the $\bar{x}$ curve in Fig. 6, and the component $k_2 B$ corresponding to the short wave-length portion. The Z-response is represented by $k_3 B$.

To calibrate a filter-disk instrument and find its values of k for a given type of specimen, one requires a standard spectrally similar to the specimens with known values of luminance (Y) and chromaticity (x, y, z). If, as before, G, A, and B are galvanometer deflections with the green, amber, and blue filters, respectively, this time for the standard, the k_1 for luminance and the k_3 constant to convert blue-filter signal are computed simply:

$$k_L = \frac{\text{Lum}}{G}$$

$$k_3 = \frac{G}{y} \cdot \frac{z}{B}$$

The selection of constants for x is complicated by the fact that the $\bar{x}$ function consists of blue and amber components, which are not reported as separate values in the calibration of the standard. Two methods are available for obtaining values of k_1 and k_2 for the amber and blue components, respectively. The simpler one makes use of the fact that the area under the blue hump of the $\bar{x}$ curve in Fig. 1 is 0.167 of the area under the $\bar{z}$ curve. From this fact, one may divide the x value of the standard into two parts:

$$x_b = 0.167z$$
$$x_a = x - 0.167z$$

It is a simple matter to compute from the foregoing and the galvanometer deflections, G, A, and B of the standard

$$k_1 = \frac{G}{y} \cdot \frac{x_a}{A}$$

$$k_2 = 0.167\, k_3$$

The second method of computing these two constants requires two calibrated standards different in color to provide, in effect, simultaneous equations to solve for the two unknowns k_1 and k_2.

$$k_1 = \frac{x_1 f_1 B_2 - x_2 f_2 B_1}{A_1 B_2 - A_2 B_1}$$

$$k_2 = \frac{x_2 f_2 A_1 - x_1 f_1 A_2}{A_1 B_2 - A_2 B_1}$$

where f is the fraction G/y, and subscripts 1 and 2 refer to standard tubes 1 and 2, respectively.

The two methods of computing these two constants do not in general give the same values. Thus, in one experiment using two standardized P4 television picture tubes (Nos. 1 and 4), the two methods gave:

		k_1	k_2	k_3
By direct method	Std. 1	1.151	0.297	1.78
	Std. 4	1.191	0.307	1.83
Average		1.171	0.302	1.805
By simultaneous equations		1.009	0.433	—

Fig. 9 shows the effect of these differences on actual computed values of chromaticity. Even though tubes 1 and 4 were used as standards for the simultaneous-equation values of k_1 and k_2, the observed values of chromaticity for these two tubes do not accord with those assigned because k_3 differed from one standard to the other and the average was used for k_3.

Fig. 9 presents evidence of the accuracy of the filter-disk colorimeter used on television picture tubes. Assuming one of the standards had been used for the color measurement of the other, the chromaticity error would have been approximately the sum of the two distances between standard and measured values shown on the graph. This sum is roughly 0.007 for the separate-constants values and 0.005 for the equations-constants values. This suggests that the latter may be superior. The direct reading colorimeter gave an error of 0.005 when used to measure one of these standards after adjustment with the other.

Unfortunately, the filters used in these colorimeters when the foregoing values were obtained are not the best ones which are represented by filter-photocell curves in Fig. 6. The anticipated improvement in accuracy is less than a factor of two. Thus the better filters will not eliminate susceptibility of the instrument to appreciable errors when standards and specimens are spectrally different. Some further improvement may be possible by selecting photocells, but for substantial improvement in accuracy,

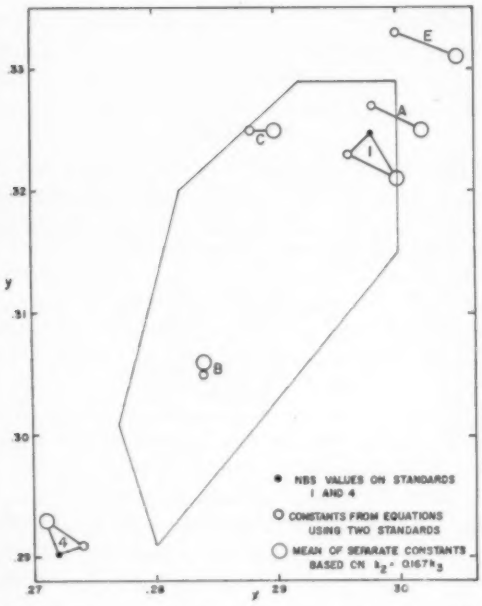

FIG. 9. Enlargement of the P4 area of the chromaticity diagram with values computed from readings with the filter-disk model using separate sets of the constants K_1 and K_2.

additional or improved filter components will have to be developed.

THREE-CELL MODEL

The second instrument, shown by diagram in Fig. 4 and photograph in Fig. 5, is similar to the device described by Barnes (6). It uses a separate photocell for each of the three tristimulus functions. In the new device, the distances from the X and Z photocells to the viewing window are adjustable by screws through the back so that in calibrating the instrument these signals may be made proportional to the actual color values of the standard; thus, the k's used with the first model are mechanically adjusted to unity in the second one. Color values for the specimens may then be read directly from the instrument scale. It should be noted that the filter over the X photocell has two parts, one blue and one amber. The areas of each are approximately proportional to the blue and amber components of the $\bar{x}$ distribution function in Fig. 6.

As shown in Fig. 4 and 5, color values from this second instrument are read from the dial of a ten-turn potentiometer. This potentiometer adjusts the current from a 1.5-v No. 6 dry cell to that required to balance each photocell current subject to measurement. Condition of balance is indicated by zero deflection of a galvanometer or other suitable null indicator. The current-balancing circuit provides ideal "zero potential" conditions for operation of the photocells, yet a sensitive high-resistance galvanometer or null indicator may be used.

In operating this instrument, all settings are made by placing the galvanometer spot at zero. At Y switch position, luminance (brightness) is read (standard cell maintains calibration); at $X + Y + Z$ switch position, the adjusting knob is turned for balance; then at x, y, and z switch positions, chromaticity is read directly from the dial.

The reversed-signal measuring circuit used to give values of chromaticity is more elaborate than the Barnes circuit previously used for the purpose. Instead of adjusting $X + Y + Z$ to 1.00 then measuring the separate X, Y, and Z currents one at a time, as with the Barnes circuit, the new instrument adjusts $X + Y + Z$ to 0.5 scale units, then for each component reverses the polarities of the other two components and reads the increment in scale units from the middle of the scale. Quantities actually measured by the new instrument are:

$$x = \tfrac{1}{2}\left[1 - \frac{-X + Y + Z}{X + Y + Z}\right]$$

$$y = \tfrac{1}{2}\left[1 - \frac{X - Y + Z}{X + Y + Z}\right]$$

$$z = \tfrac{1}{2}\left[1 - \frac{X + Y - Z}{X + Y + Z}\right]$$

Advantages of this reversed-current technique are:

1. The signal change obtained by reversing each component in the total signal is double that of the component itself; thus, sensitivity to interval differences is doubled.

2. Because differences between the chromaticity components are being measured, rather than the components themselves, fluctuations in total intensity to factors like voltage fluctuation in television tube power supply are minimized in the resultant observations.

The photocells are the hermetically sealed version of the very stable and widely used General Electric rectangular cell (5). Each filter is mounted on an aluminum coil can which is placed over the tubular glass photocell after a window of the proper size is cut in it. Because the three photocells lie in different directions from the specimen, it is important that light being measured be well diffused about the axis of the instrument, or nonuniform light distribution will be erroneously measured as color.

The problem of k_1 and k_2 constants is less serious with the three-cell model because it uses a separate blue filter designed specifically to fit the blue hump of the $\bar{x}$ function. The relative magnitudes of these constants are in effect adjusted during assembly of the instrument by the setting of relative areas of amber and blue filters over the x photocell. Settings

on yellow and blue standards of known x value are used to make this adjustment.

Because all three signals are present during reversed-signal readings of x, y, and z, it is necessary to provide separate switch contacts for adjustments of the individual x, y, and z signals. The Cal X and Cal Z positions on the scale-selector switch shown in Fig. 4 are used only for calibration. At these positions, the X and Z signals are presented individually, and positions of the corresponding photocells are adjusted to standard, using screws that project through the back of the instrument. Where values of x and z alone are available for a standard, X and Z are computed:

$$\frac{X}{x} = \frac{Z}{z} = \frac{Y(\text{Lum})}{y}$$

Summary

Compared with other instruments used for the same purpose, those described in the foregoing article have a number of advantages:

1. They are rapid and precise. During observation of seven picture tubes, the average difference between pairs of readings of chromaticity of the same tube was 0.001 with both models.
2. A separate meter is not required to read luminance.
3. A dark room is not required.
4. The instruments employ hermetically sealed photocells which are not subject to the changes in response with humidity that are characteristic of other barrier-layer photocells.
5. Both instruments may be used to measure the colors of reflecting surfaces and transmitting films and volumes as well as illuminant colors.

In addition to the foregoing advantages of both instruments, several noteworthy features of the three-cell, reversed-signal model may be noted:

1. Values of chromaticity and luminance are read directly.
2. Errors from instability in television tube power supply are halved, the signal increment available for measurement is doubled by the reversed-signal technique.
3. The instrument uses a current-balancing circuit which gives high signal sensitivity, and, at the same time, the highly desirable condition of zero effective external resistance for the photocells.
4. With a frequency-insensitive electronic null indicator, the reversed-signal model may be operated in areas of severe vibration where conventional galvanometers will not work.

The major weakness of the new instruments is common to all photoelectric tristimulus colorimeters. Failure of the filter-photocell combinations spectrally to duplicate the functions of the CIE standard observer for colorimetry limits accurate color measurements to intercomparisons of samples and standards that are spectrally similar.

Any discussion of this paper will appear in a Discussion Section to be published in the June 1956 Journal.

References

1. Nat. Bur. Stds. Circular C 478, *Colorimetry* (1950); "The Science of Color," Optical Soc. of America, Crowell, New York (1953).
2. B. T. Barnes. *J. Opt. Soc. Amer.*, **29,** 440 (1939).
3. R. S. Hunter. Nat. Bur. Stds. Circular C429 (1942); *J. Opt. Soc. Amer.*, **32,** 509 (1942).
4. A. E. Martin, J. A. Noland, and R. Q. Vogel, *ibid.*, **43,** 335 (1953).
5. General Electric Co. Catalog GEC-690, Photovoltaic Cell Types PV-1, PV-2, PV-10 (1950).
6. B. T. Barnes, *Rev. Sci. Instr.*, **16,** 337 (1945).

Oxidation States of Europium in the Alkaline Earth Oxide and Sulfide Phosphors[1]

P. M. Jaffe[2] and E. Banks

Department of Chemistry, Polytechnic Institute of Brooklyn, Brooklyn, New York

ABSTRACT

Emission and absorption spectra of the alkaline earth sulfides activated with europium and fired in a neutral atmosphere have been re-investigated. The emission and absorption spectra of the alkaline earth oxides, also activated with Eu, and fired in a neutral or a reducing atmosphere have been obtained. The sulfides show both band emission and band absorption, as does SrO fired in hydrogen. The other hydrogen-fired oxides have band absorption, except for MgO, and give either mixed band and line emission or only line emission. The nitrogen-fired oxides, except MgO, give line emission and little, if any, selective absorption. MgO emits a broad line spectrum for both the nitrogen- and hydrogen-fired samples and shows no absorption peaks. Emission and absorption spectra have been correlated with the oxidation state of the activator in the several phosphors, the line emissions being associated with the presence of Eu^{+3} and the band emissions with Eu^{+2}.

Introduction

It is well known that alkaline earth sulfide phosphors containing europium as the activator show band emission (1–7). It is also known that europium-activated alkaline earth oxides show line emission (5, 6, 8, 9). This difference in emission character has been ascribed to a difference in the oxidation state of europium, which is divalent in the sulfides (10) and trivalent in the oxides. From a comparison of the energy required for inclusion of Eu^{+3} and the formation of lattice defects with the energy required for the reduction of Eu^{+3} to Eu^{+2} and its substitution for the cation in an alkaline earth oxide or sulfide, Brauer (5) concluded that Eu must be divalent in the sulfides and trivalent in the oxides. He verified this by comparing the band spectra of europium-activated sulfides with the line spectra in the corresponding oxides. The present work is an attempt to verify Brauer's observations and to demonstrate that divalent europium may be introduced into certain oxides under chemically reducing conditions.

Preparation of Materials

Sulfides.—Magnesium sulfide was prepared from magnesium ammonium chloride, according to the method of Russo (11). Calcium, strontium, and barium sulfides were prepared by reduction of the respective sulfates by firing in hydrogen at 1050°C. Sulfates were prepared according to the method of Ward (12, 13) except for barium sulfate, which was Mallinckrodt's Ultra-Pure grade.

Oxides.—Magnesium oxide was prepared from Mallinckrodt's Ultra-Pure magnesium carbonate by thermal decomposition at 1050°C. Calcium and strontium carbonates, which were prepared according to Ward (14), were similarly converted. Barium oxide was prepared from Mallinckrodt's S.L. barium carbonate by heating at 1050°C for 4 hr in vacuo.

Chlorides.—Magnesium chloride was prepared from magnesium ammonium chloride by heating at 600°C in an atmosphere of nitrogen and hydrogen chloride. Calcium, strontium, and barium chlorides were prepared by dissolving the respective carbonates in freshly prepared HCl and evaporating to dryness.

Fluxes.—Due to the nature of the base materials, the flux and the activator had to be added in the dry form. This was accomplished by incorporating the activator into the flux, which in all cases was the chloride of the metallic constituent of the matrix. The desired amount of activator was added to the matrix by weighing out the proper quantity of activated flux and then adding the necessary amount of unactivated flux to give a total flux concentration of 5 wt %.

Except in the case of magnesium oxide, activated mixtures were molded into cylindrical pellets $\frac{7}{8}$ in. in diameter and approximately 1 in. long in a stainless steel mold under 20,000 psi. After firing, the pellet was cleaved perpendicular to its cylindrical axis. This was done so that a fresh uncontaminated surface would be available for measurements. Although the mechanical stress involved in cleaving the

[1] Manuscript received March 15, 1954. This paper was prepared for delivery before the New York Meeting, April 12 to 16, 1953, and was submitted to the Polytechnic Institute of Brooklyn, Brooklyn, N. Y., in partial fulfillment of the requirements for the M.S. degree in Chemistry.

[2] Present address: Research Department, Westinghouse Electric Corporation, Bloomfield, N. J.

specimens may have reduced the luminescence efficiency, it was not expected to shift the emission or absorption bands since, to the authors' knowledge, no such effect has been observed in the alkaline earth sulfides. Magnesium oxide samples were prepared by pressing the powder into a cell built up on a microscope slide.

All firing was carried out in a silica tube 20 in. long and 1⅞ in. ID, closed at one end. The open end was closed with a rubber stopper having a long silica tube as a gas inlet and a short tube for the outlet. All samples were fired for 1 hr at 1050°C.

Method of Measurement

Emission spectra were obtained with the aid of a Schmidt-Haensch double Rutherford glass prism spectrograph. Eastman Kodak super-pan press plates, type C, which are sensitive in the range 3900–6700 Å, were used. The positions of the lines were obtained with a Gaertner comparator. Band spectra were recorded by taking a profile of the spectrograms with a recording densitometer. The profile was corrected for plate sensitivity by using a sensitivity curve supplied by the manufacturer. Absorption spectra were obtained with a Beckman Model DU spectrophotometer with a diffuse reflectance attachment. In order to show positive peaks for absorption bands, the measured per cent reflectance was subtracted from 100 and reported as "per cent absorption." The absorption below 400 mμ was not investigated because of the lack of a suitable source at the time the work was done.

It should be noted that the use of the reflectance attachment (without filters) in the region where excitation may take place will lead to spurious results, particularly high apparent reflectance in these regions. It is, therefore, likely that the sharp dips in per cent absorption around 400 mμ in Fig. 2, 4, 6, and 8 are incorrect. Since these dips are not essential to an argument based on the broad band character of these absorptions, no corrected absorption spectra were prepared. It is believed, however, that less pronounced dips than those shown are actually present for most of these phosphors, since they are not very efficient, and the emission is only a small fraction of the incident energy.

Results

Sulfide phosphors containing 200 ppm europium and 5 wt % of the corresponding alkaline earth chloride as flux were prepared by firing in nitrogen. All the samples showed reflection colors: MgS—yellow orange, CaS—pink, SrS—orange, BaS—yellow. Emission spectra are given in Fig. 1. The position of the calcium sulfide peak is somewhat in doubt since it occurs near the region of plate cut-off. However, it is in good agreement with previous work done in this laboratory (7). It will be noticed that the position of the peak depends on the matrix and shifts to shorter wave lengths on going from CaS to SrS to BaS. MgS is anomalous in that its emission falls between that of BaS and SrS. These findings agree with those of Brauer (6). Absorption bands are similar to each other and show a shift similar to, although not as great as, the shift in the emission spectra (Fig. 2).

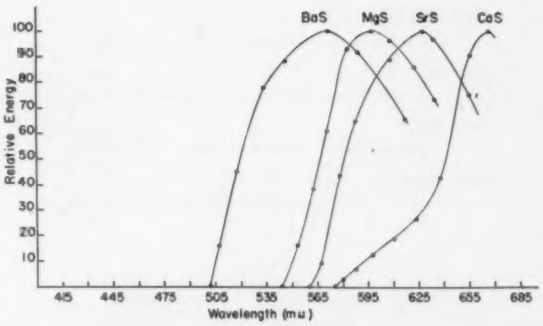

Fig. 1. Emission spectra of alkaline earth sulfides (MCl_2 flux – Eu 220 ppm).

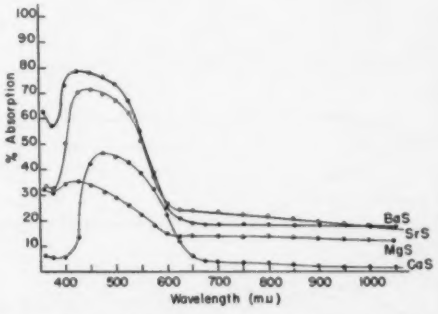

Fig. 2. Absorption spectra of europium-activated alkaline earth sulfides.

Oxide Phosphors

Magnesium oxide.—Two samples containing 500 ppm Eu and 5 wt % $MgCl_2$ were prepared as powders, one in hydrogen, the other in nitrogen. Both samples were white. Excitation by 2537 Å gave a red emission for both samples, while under 3650 Å they were nonluminescent. Emission spectra appeared to consist of three overlapping broad lines. However, due to the poor resolution of the densitometer, the lines were not resolved. The apparent positions of these lines are given in Fig. 3.

Calcium oxide.—Two samples containing 150 ppm Eu and 5 wt % $CaCl_2$ were prepared as pellets, one in hydrogen, the other in nitrogen.

The nitrogen-fired samples were white under reflected light (Fig. 4). Excitation by 2537 Å or 3650

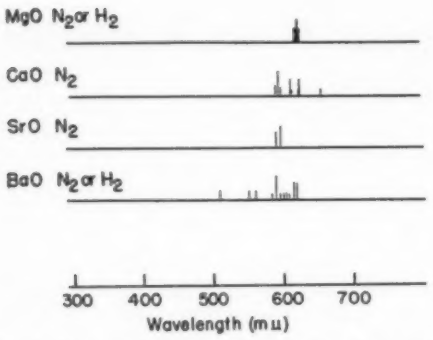

FIG. 3. Line emission spectra of europium-activated alkaline earth oxides.

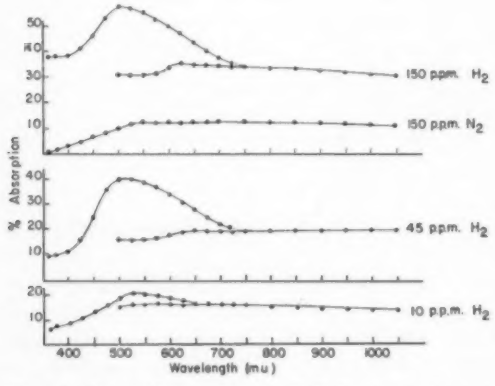

FIG. 4. Absorption spectra of CaO:Eu for various concentrations and firing atmospheres.

Å gave a pink emission which consisted of a series of lines (Fig. 3).

Hydrogen-fired samples appeared lavender. The absorption spectra of this sample and the next two samples discussed (Fig. 4) show two branches in the region of overlapping sensitivities of the two phototubes in the Beckman spectrophotometer. The reason for this effect is discussed below.

Excitation by 3650 Å gave a weak purple emission, while the emission under 2537 Å was much stronger. A spectrogram taken with the sample excited by 2537 Å showed a band in the blue, several lines, and a band in the red (Fig. 5). The positions of the lines are the same as those of the nitrogen-fired sample. To see what effect a low europium concentration would have, a sample containing 10 ppm Eu was prepared. This sample was light lavender and had a blue emission under both 2537 Å and 3650 Å. A spectrogram showed only a band in the blue and a very faint line (Fig. 5). After a 48-hr exposure to air, another spectrogram was taken. The line was just visible on the plate, whereas before it could be detected only by the densitometer. In order to see if the band in the red was due to trivalent Eu alone or to the presence of both Eu^{+2} and Eu^{+3}, a 45 ppm Eu sample was prepared. A spectrogram showed the band in the blue and the lines and the band in the red (Fig. 5). Since neither the nitrogen-fired sample nor the hydrogen-fired 10 ppm sample showed the red band, it is suggested that the red band is due neither to Eu^{+2} nor to Eu^{+3} alone, but to the presence of both. The red band may originate from Eu^{+2}, as does the blue band, but may be shifted to longer wave lengths due to the presence of Eu^{+3} or associated cation vacancies. For example, the presence of a vacant cation site close to some of the Eu^{++} ions might be responsible for a local distortion of the conduction band, with a consequent shift of the Eu^{++} band to longer wave lengths. Such an interpretation would assume that europium emission is due to a transition from the conduction band to an Eu^{++} center. This would be an untenable interpretation if photoconductivity were absent. Since no photoconductivity data are available, this suggestion cannot be very strongly supported. However, since europium-activated strontium sulfide and selenide do show photoconductivity under ultraviolet excitation (15), it seems plausible to suppose that it may also occur in europium-activated oxides.

In measuring the absorption of the "reduced" CaO (Fig. 4) and comparing readings of the blue-sensitive and the red-sensitive photocells in the region of overlap (500–720 mm) it was found they did not agree. This difference increased with increasing Eu and was larger at the long wave-length end. Apparently, excitation in the region of strong absorption gave rise to an emission in the red, which was not picked up by the blue-sensitive photocell. The "secondary" emission could be filtered out by insertion of a Corning No. 9780 filter in front of the phototube housing.

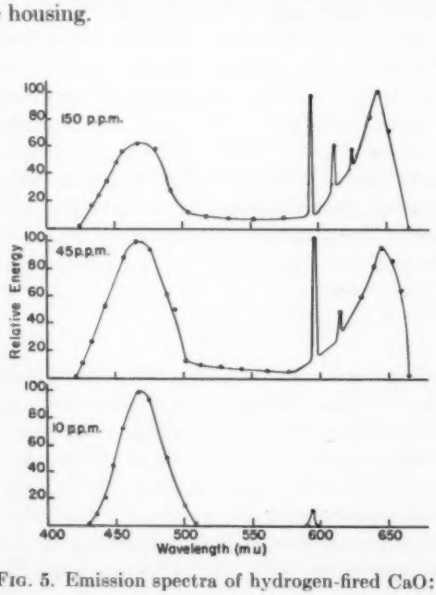

FIG. 5. Emission spectra of hydrogen-fired CaO:Eu

Attempts to photograph the secondary emission by excitation with either the Hg 436 mμ line or the Hg 546 mμ line were unsuccessful. Since the photographic plate cuts off at 6700 Å, the emission seemed to be located beyond this limit. This is also suggested by the following facts: (*a*) the No. 9780 filter does not transmit in the region 680–1250 mμ so the emission must be in this range; and (*b*) no secondary emission is picked up by the blue-sensitive photocell. The latter is shown by the fact that the absorption measured by the red-sensitive phototube with the filter is the same as that measured with the blue-sensitive phototube. However, considering the uncertainty of locating the emission peaks by photographic methods, this secondary emission may actually be the red band shown in Fig. 5. If the true position of the peak is at longer wave lengths, the blue-sensitive photocell or the filter-photocell combination might not detect it. Failure to detect it photographically under excitation by 436 mμ and 546 mμ may be due to a low sensitivity to these wave lengths. Since the excitation spectra are not known, no estimate can be made of the significance of the nonappearance of the red band on the plate. Hence, the emission cannot be definitely attributed to the 6500 Å band or to another band at longer wave lengths.

Strontium oxide.—Two pellets containing 100 ppm Eu and 5 wt % $SrCl_2$ were prepared, one in nitrogen, the other in hydrogen.

The nitrogen-fired sample was white (Fig. 6). The sample had a pink-orange emission under 2537 Å. Spectroscopically, two lines were found as shown in Fig. 3.

The hydrogen-fired sample was lavender (Fig. 6). Excitation by 2537 Å gave a weak red band emission, which was much stronger under 3650 Å (Fig. 7). No secondary emission was found. After this sample was exposed to air for 24 hr, another spectrogram showed both line and band emission. The position of the lines was the same as that found with the nitrogen-fired sample.

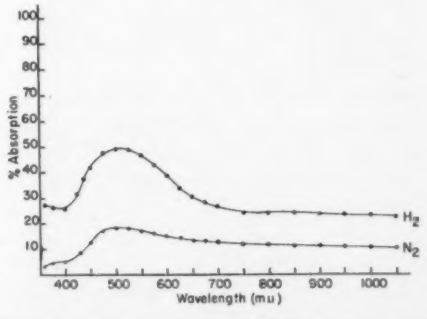

FIG. 6. Absorption spectra of SrO:Eu fired in H_2 and in N_2.

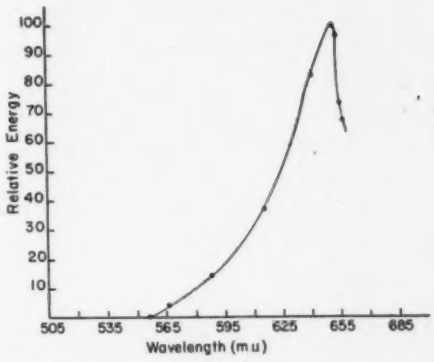

FIG. 7. Emission spectrum of H_2-fired SrO:Eu

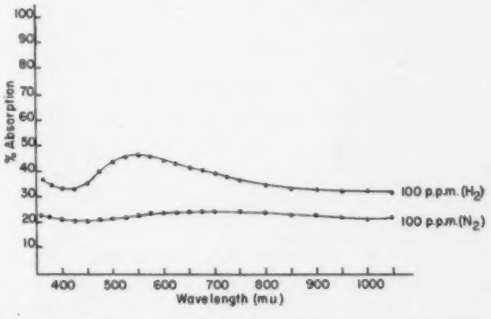

FIG. 8. Absorption spectra of BaO:Eu, fired in H_2 and in N_2.

Barium oxide.—Two samples containing 100 ppm Eu and 5 wt % $BaCl_2$ were prepared, one in nitrogen, the other in hydrogen.

The nitrogen-fired sample was white (Fig. 8). Both 2537 Å and 3650 Å excited a pink-orange emission which was found to consist of a series of lines (Fig. 3).

The hydrogen-fired sample was light lavender (Fig. 8). Refiring for one hour in hydrogen did not deepen the color. A 200 ppm sample was prepared which was slightly, if at all, darker than the one containing 100 ppm. Under 2537 Å, a weak pink-orange emission was found. Emission under 3650 Å was very weak. Even after a 50-hr exposure only line emission was found, as in the nitrogen-fired sample. If there is band emission, it is beyond the 6700 Å plate cut-off and so could not be found.

DISCUSSION

The most usual oxidation state of the rare earths is +3. Europium, however, can easily be reduced to the divalent condition by heating in a reducing atmosphere, while most of the other rare earths give the free metal (8, 16–19). All attempts to prepare EuO and Eu_2S_3 have been unsuccessful, and only Eu_2O_3 and EuS are known (17–19). On inclusion of

$EuCl_3$ into an alkaline earth oxide or sulfide, the following reactions may occur:
For the sulfide:

$$2EuCl_3 + 3MS \rightleftharpoons 3MCl_2 + Eu_2S_3$$
$$Eu_2S_3 \rightleftharpoons 2EuS + S$$

For the oxide:

$$2EuCl_3 + 3MO \rightleftharpoons 3MCl_2 + Eu_2O_3$$
$$Eu_2O_3 \rightleftharpoons 2EuO + \tfrac{1}{2}O_2$$

where M is an alkaline-earth metal. That the conversion of Eu_2S_3 to EuS occurs has been shown by Prener (20) who heated coprecipitated $SrSO_4$ and $EuSO_4$ in hydrogen and obtained a phosphor very similar to one prepared by heating SrS + $EuCl_3$ in nitrogen. Heating the oxides in hydrogen reduces Eu^{+3} to Eu^{+2} and, unless Eu^{+2} can be stabilized, it will revert to Eu^{+3} as discussed below.

Samarium, which is one atomic number lower than europium, gives a line emission in both the alkaline earth oxide and sulfide phosphors (21, 22). Chemically, Sm is more difficult to reduce than Eu, so that it can be assumed Sm is in all cases trivalent. Eu^{+3} in pure europium(III) compounds has line emission similar to that of Eu incorporated into the "normal" oxide phosphors (6). Recently, it has been shown that divalent Eu salts have band emission (23, 24). Thus it appears that line emission is characteristic of Eu^{+3} and band emission of Eu^{+2}. The fact that oxides prepared in a reducing atmosphere show band spectra indicates that Eu in oxide phosphors can be present in two different oxidation states.

Consideration of the electronic configuration of Eu indicates the type of emission that should be exhibited by Eu^{+2} and Eu^{+3}. Line emission is associated with electronic transitions occurring within inner shielded electronic shells so that there is little, if any, influence by the surroundings. Band emission occurs when there are electronic interactions with the surrounding lattice. The ground state of Eu is, neglecting inner filled orbits, $4f^6\ 5s^2\ 5p^6\ 5d\ 6s^2$ (8, 25). Loss of the two 6*s* electrons to give Eu^{+2} leaves the 5*d* electron exposed and free to interact with the surroundings so that band emission is to be expected. Loss of the $6s^2$ and $5d^1$ electrons to give Eu^{+3} leaves, as the outer shell, the stable $5s^2\ 5p^6$ shells, so electronic transitions are now limited to the 4*f* shell. Since transitions are between discrete levels and not strongly influenced by the surroundings, line emission results. There is some influence by the surroundings, as shown by variation in the number and position of the lines of Eu^{+3} in different host lattices (Fig. 3).

If Eu is trivalent when dissolved in the oxides, as normally prepared, it would seem that heating in a hydrogen atmosphere produces divalent Eu. However, europium in MgO and BaO phosphors is not reduced, as evidenced by the presence of line emission only. Comparison of the absorption curves for the hydrogen-fired oxides of Mg, Ca, Sr, and Ba shows that the last three are similar, whereas absorption in hydrogen-fired MgO is very similar to that in nitrogen-fired oxide samples. Even though only line emission was found for the hydrogen-fired BaO, it is very possible that there is band emission located in the infrared. This seems plausible, since band emission in CaO and SrO containing divalent Eu is accompanied by band absorption, and the emission shifts from blue to red in going from "reduced" CaO to SrO and may be expected to shift in the same way on going from SrO to BaO. This shift is the reverse of the shift in the sulfides.

TABLE I

	Å		Å
Eu^{+2}	1.12	Ca^{+2}	0.98
Eu^{+3}	0.97	Sr^{+2}	1.15
Mg^{+2}	0.71	Ba^{+2}	1.31

The presence of strong line emission in reduced CaO (10 ppm Eu) and the nonreduction of Eu in MgO can be partially explained by consideration of the size of the ions concerned. These are listed in Table I.

There is a 58% difference in size between Eu^{+2} and Mg^{+2}. As seen, EuO is not stable and so must be stabilized after formation by incorporation into a stabilizing crystal structure. Because of the large size difference between Eu^{+2} and Mg^{+2}, stabilization of EuO by incorporation into the MgO lattice is not possible. This concept of the stabilization of Eu^{+2} is supported by consideration of hydrogen-fired CaO. Reduced high activator CaO gives both line and band emission, whereas low activator CaO shows relatively strong band emission and faint line emission. This indicates that Eu^{+3} is being reduced, but only a limited amount of Eu^{+2} can be incorporated into the CaO lattice and so stabilized, while the excess reverts back to Eu^{+3}. The net result is the presence of both divalent and trivalent europium, each having its own emission spectra. It appears that a size difference of 14% between Ca^{+2} and Eu^{+2} allows only a limited solubility. Ba^{+2} differs from Eu^{+2} by 13%, which would, by comparison with Ca^{+2}, indicate that there should also be a limited solubility of Eu^{+2} in BaO. This must be the case since reduced BaO has an absorption spectrum similar to that of the other reduced oxides and also has line emission indicative of Eu^{+3}. Strontium oxide is the ideal case in that there is only a 3% difference in size between Sr^{+2} and Eu^{+2}, and there appears to be complete

solubility in concentrations up to 150 ppm, since no line emission is found.

Hydrogen-fired SrO showed the reappearance of line emission after long exposure to air. This indicates that some divalent Eu has been oxidized to the +3 condition and both oxidation states are emitting their characteristic type of spectrum. The spectrogram of 10 ppm CaO showed the presence of one extremely faint line whose intensity increased on standing in air. This indicates that initially there was a small amount of Eu^{+3}. Due to oxidation by oxygen or water vapor in the air, the concentration of Eu^{+3} has been increased, resulting in a more intense line spectrum.

Conclusion

Europium is divalent in the sulfides and trivalent in the oxides when they are prepared in inert atmospheres. Use of a reducing atmosphere in preparing oxide phosphors also gives divalent Eu, at least for CaO, SrO, and possibly BaO. As in the sulfides, the peak emission of the reduced oxides is dependent on the matrix, while the lines of the normal oxides show less dependence on the nature of the host crystal.

Acknowledgments

The authors wish to thank Professor H. W. Schleuning, of the Polytechnic Institute of Brooklyn, for his advice and aid in obtaining the emission spectra, and Professor T. I. Taylor, of Columbia University, for the use of the recording densitometer.

Any discussion of this paper will appear in a Discussion Section to be published in the June 1956 Journal.

References

1. K. Przibram, *Nature*, **163**, 989 (1949).
2. F. Urbach, D. Pearlman, and H. Hemmendinger, *J. Opt. Soc. Amer.*, **36**, 372 (1946).
3. P. Brauer, *Z. Naturforsch.*, **1**, 70 (1946).
4. E. Nichols and H. L. Howe, *J. Opt. Soc. Amer.*, **13**, 573 (1926).
5. P. Brauer, *Z. Naturforsch.*, **6A**, 255 (1951).
6. P. Brauer, *ibid*, **6A**, 561 (1951).
7. Report on Preparation of Infrared Phosphors, p. 63, Contract No. OEMsr 982, Polytechnic Institute of Brooklyn, September 1, 1945.
8. W. Hanle and A. Schmillen in "FIAT Review of German Science," Part 3, Vol. 2, Wiesbaden, Germany (1948).
9. F. H. Spedding, *Trans. Faraday Soc.*, **35**, 67 (1939).
10. R. Ward in "Preparation and Characteristics of Solid Luminescent Materials," p. 299, Cornell Symposium of American Phys. Soc., John Wiley & Sons, Inc., New York (1948).
11. E. Banks, V. J. Russo, and R. Ward, *J. Am. Chem. Soc.*, **72**, 3173 (1950).
12. R. Ward, R. K. Osterheld, and R. D. Rosenstein in "Inorganic Synthesis," Vol. 3, p. 11, (L. F. Audrieth, Editor), McGraw-Hill Book Co., New York (1950).
13. R. Ward in "Preparation and Characteristics of Solid Luminescent Materials," Cornell Symposium of American Phys. Soc., Paper No. 2, p. 22, John Wiley & Sons, Inc., New York (1948).
14. W. Primak, Dissertation, Polytechnic Institute of Brooklyn (1946).
15. J. J. Dropkin, Thesis, Polytechnic Institute of Brooklyn (1947); Dissertation, Polytechnic Institute of Brooklyn (1948).
16. D. Yost, H. Russell, and C. Garner, "The Rare-Earth Elements and Their Compounds," p. 10, John Wiley & Sons, Inc., New York (1947).
17. G. Beck and W. Nowacki, *Naturwiss.*, **26**, 495 (1938).
18. W. Klemm and H. Senff, *Z. anorg. u. allgem. Chem.*, **241**, 259 (1939).
19. G. Beck and W. Nowacki, *Z. Krist.*, **99**, 339 (1938).
20. J. Prener, Dissertation, Polytechnic Institute of Brooklyn (1949).
21. G. Cohen, Master's Thesis, Polytechnic Institute of Brooklyn (1947).
22. R. Tomaschek, *Physik Z.*, **33**, 878 (1932).
23. K. Przibram, *Z. Physik.*, **107**, 709 (1937).
24. S. Freed and S. Katcoff, U. S. Atomic Energy Commission Report, MDDC 1228 (1947).
25. H. Emeleus and J. Anderson, "Modern Aspects of Inorganic Chemistry," p. 11, Table 4, D. Van Nostrand Co., Inc., New York (1948).

Preliminary Studies of the Perovskite-Type Ternary Oxides as Luminophors[1]

SALVADOR TEROL[2] AND ROLAND WARD

Department of Chemistry, University of Connecticut, Storrs, Connecticut

ABSTRACT

The properties of lanthanum aluminum oxide as a phosphor base material have been studied. The purest available lanthanum oxide samples gave products which were weakly cathodoluminescent because of the presence of praesodymium or samarium as impurities. The rare earth ions Pr^{+3}, Sm^{+3}, and Eu^{+3} were the only activators which were effective. Emission spectra of these phosphors are given. Other common activators were ineffective. The presence of rare earth impurities causes a pronounced body color to develop in the lanthanum aluminum oxide when the samples are ignited in air. This proves to be a more sensitive means of detection of impurities than spectrographic analysis.

INTRODUCTION

The perovskite structure is common among compounds of the type ABX_3 where A represents a large cation capable of 12-fold coordination with the anion X, B a smaller cation suitable for sixfold coordination with X, while X is nearly always the fluoride ion or the oxide ion. The ideal perovskite structure is cubic with the B cation at the corners of the unit cell, the A cation at the center, and the anion at the midpoint of the edges.

With a few notable exceptions, compounds of this type are stoichiometric. When X is the fluoride ion, the choice of cations represented by A and B is quite restricted, A usually being one of the larger alkali metal cations and B a divalent cation such as magnesium or zinc. It has been shown by Smith (1) that compounds such as $KMgF_3$ and $KZnF_3$ activated with manganese have an orange emission when excited by cathode rays. The divalent manganese would be expected to have sixfold coordination in these crystals. On the other hand, the cathodoluminescence of manganese-activated calcium fluoride, in which the manganese is presumably in eightfold coordination, is green.

With X representing the oxide ion, a greater variety of cations is possible since the sum of the positive valences is six. Many representatives of the types of $A^{I}B^{V}O_3$, $A^{II}B^{IV}O_3$, and $A^{III}B^{III}O_3$ are known. Moreover, it has been shown that the oxidation state of the B cation may be adjusted by valence compensation. The valence of manganese in the perovskite phase $(La_{1-x}Sr_x)(Mn^{III}_{1-x}Mn^{IV}_x)O_3$, for example, is a function of the strontium content (2).

It, therefore, occurred to the authors that a colorless ternary oxide of the perovskite type would offer very interesting possibilities as a base material for phosphors. A list of such compounds is given in Table I. There is but little information on the luminescent characteristics of these compounds. Kröger (3) reports some luminescence for $BaZrO_3$, $SrZrO_3$, $CaSnO_3$, and $CdSnO_3$. In seeking base materials for the activator titanium, Kröger also tried $LaAlO_3$, but did not observe any luminescence.

The fact that Al_2O_3:Cr has well-known luminescent characteristics was encouraging. In this luminophor, chromium is probably in sixfold coordination with oxide ions in the corundum lattice. The environment of chromium dissolved in the perovskite lattice of $LaAlO_3$ should be similar, and it was hoped to find a phosphor resembling artificial ruby. No such phosphor was obtained, but some luminescent materials were discovered which showed some interesting properties. This paper describes the preparation and properties of these phosphors.

EXPERIMENTAL

Purification of materials.—A solution of $Al(NO_3)_3 \cdot 9H_2O$ in distilled water was treated with H_2S at a *p*H near 6 and the mixture boiled and filtered. Aluminum nitrate, recrystallized from the filtrate, was treated by three different methods for the removal of iron: (*a*) by means of cupferron, (*b*) by acetylacetone, and (*c*) by boiling with excess potassium hydroxide and precipitating the alumina from the alkaline solution. Each of these procedures gave comparable products in which no trace of heavy metals was found by spectroanalysis.

Three samples of lanthanum oxide were used. A commercial sample (Fairmount Chemical Company) was dissolved as the nitrate, and recrystallized six times after treatment with hydrogen sulfide. The

[1] Manuscript received December 27, 1954. This paper was prepared for delivery before the Cincinnati Meeting, May 1 to 5, 1955.

[2] Present address: Optical Institute and Naval Research Laboratory, Madrid, Spain.

TABLE I. *Colorless compounds with perovskite structure**

Substance	a_o	Substance	a_o
$BaZrO_3$	4.17	$LaGaO_3$	3.89
$SrZrO_3$	4.08	$NaTaO_3$	3.88
$CaZrO_3$	3.99	$NaNbO_3$	3.88
$KTaO_3$	3.98	$CaTiO_3$	3.84
$BaTiO_3$	3.97	$CdSnO_3$	3.80
$CaSnO_3$	3.92	$LaAlO_3$	3.78
$SrTiO_3$	3.89	$YAlO_3$	3.67
$PbTiO_3$	3.89		

* Wyckoff, Interscience Publishers Inc., New York (1948).

second sample, originating in Luigi Rolla's laboratory in Rome, Italy, had been purified by classical procedures. The third sample, obtained from the Atomic Energy Commission, had presumably been purified by use of ion exchange resins. The last two samples showed no trace of heavy metal impurities upon spectrographic examination.

Lanthanum aluminum oxide was prepared by heating stoichiometric mixtures of the two oxides at 1150°C for about 12 hr. The most convenient method of obtaining the oxide mixture was by coprecipitating the hydroxides from a solution of the nitrates using ammonium hydroxide. This procedure was especially useful when activators were being introduced. The products gave only the x-ray diffraction pattern of the cubic perovskite structure (a_o = 3.79 Å). None of the lines of the reactants was discernible in the pattern. It was found, however, that a rather rapid hydrolysis of the lanthanum aluminum oxide occurred on exposure to moist air. The stronger lines of $La(OH)_3$ appeared in the pattern of the products which had been allowed to stand in the open for as short a period as two hours. It was necessary, therefore, to keep all samples in a good desiccator.

Solid solutions of lanthanum aluminum oxide with calcium titanium oxide and strontium titanium oxides were prepared over a wide range of composition. The composition-lattice constant relationship was found to obey Vegard's law within experimental error. With barium titanium oxide, on the contrary, no solid solution was detected by x-ray analysis.

Products which had been prepared by heating in a hydrogen atmosphere were invariably white, but those prepared by ignition in air showed a pronounced body color. The commercial sample of lanthanum oxide and the sample from the A.E.C. gave a pink colored product, while that from Rolla's laboratory gave a tan coloration. Use of different reaction vessels (zircon, alundum, silica, and platinum were tried) did not eliminate or change this body color. Hence, it was concluded that it must be due to the presence in the lanthanum oxide of an oxidizable impurity, presumably one of the lanthanide elements. Analysis using a 21-ft grating spectrograph did not reveal the presence of any rare earth impurity, in the lanthanum oxide from Fairmount or from the A.E.C., but a trace of samarium was found in Rolla's preparation. All samples of lanthanum oxide, however, remained white upon ignition in air.

Luminescent Properties

Although some of the samples were found to luminesce weakly under 2537 Å radiation, cathode ray excitation was apparently more efficient. Most of the authors' attention was given to the latter.

Cathodoluminescence was found for all samples prepared without the intentional addition of impurities. A fairly strong orange emission was obtained from the samples prepared with Rolla's lanthanum oxide, and a weak yellowish-green emission from the others.

The addition of several rare earth ions to lanthanum aluminum oxide gave the results listed in Table II. These samples were all prepared using the lanthanum oxide from the A.E.C. It was observed that the addition of praeseodymium up to 10^{-3} gram atoms per mole of $LaAlO_3$ increased the in-

TABLE II. *Lanthanides as activators in the cathodoluminescence of lanthanum aluminum oxide*

Addition in atom/mole	Body-color firing in		Cathodoluminescence	
	Air	H_2	Color	Intensity
10^{-4} Ce	PT	—	GY	4
10^{-4} Ce	—	W	G	4
10^{-3} Ce	FT	—	GY	4
10^{-3} Ce	—	W	G	4
10^{-2} Ce	T	—	GY	5
10^{-2} Ce	—	YW		
10^{-4} Pr	P	—	YG	2
10^{-4} Pr	—	W	GY	2
10^{-3} Pr	P	—	GY	1
10^{-3} Pr	—	W	GY	1
10^{-2} Pr	P	—	GY	1
10^{-2} Pr	—	W	GY	1
5.10^{-2} Pr	PT	—	G	3
5.10^{-2} Pr	—	W	G	3
10^{-3} Nd	FT	—	Y	4
10^{-3} Nd	—	W	YG	3
10^{-2} Nd	T	—	Y	5
10^{-2} Nd	—	W	GY	3
10^{-4} Sm	FT	—	Y	1
10^{-4} Sm	—	W	Y	1
10^{-3} Sm	FT	—	Y	1
10^{-3} Sm	—	W	Y	1
10^{-4} Eu	FT	—	RO	3
10^{-4} Eu	—	W	RO	3
10^{-3} Eu	T	—	RO	3
10^{-3} Eu	—	W	RO	3
10^{-3} Gd	W	—	YO	2
10^{-3} Gd	—	W	YO	2

KEY: T = tan colored, F = faint, P = pink, W = white, G = green, Y = yellow, R = red, O = orange. 1 = Very strong, 2 = strong, 3 = medium, 4 = weak, 5 = very weak.

tensity of yellowish green emission, while the addition of samarium caused a strong yellow emission. Addition of cerium and neodymium, on the other hand, did not increase the brightness of the emission and, in some cases, appeared to diminish the luminescence. Addition of europium and gadolinium gave materials with medium to strong cathodoluminescence. From these results it seemed most probable that the impurity which caused the orange cathodoluminescence in $LaAlO_3$ prepared from Rolla's lanthanum oxide was samarium, while that giving rise to the greenish-yellow luminescence was praeseodymium. Somewhat similar results have been reported with lanthanum oxychloride phosphors (4) prepared from lanthanum oxide from the Lindsay Light Chemical Company.

The emission spectra of some of the products are given in Fig. 1 to 5. With the exception of Fig. 2, all of these refer to preparations from lanthanum oxide obtained from the A.E.C. In Fig. 1 the emission curve for the "unactivated" phosphor is compared to a phosphor activated with 10^{-3} mole of praeseodymium. The major emission peaks at 510, 630, and 660–670 mμ, obtained by this addition, are noticeable in the spectrum of the "unactivated" lanthanum aluminum oxide. A comparison is also given in Fig. 1 of the emission spectra of the phosphors prepared in oxidizing and reducing atmospheres. The lesser peaks at 490 and 550 mμ appear to be slightly increased while those at 630 and 670 mμ are somewhat diminished in the product prepared in hydrogen. The band width in these spectra was dependent on the slit width of the spectroradiometer used. Fig. 2 gives a comparison of the emission spectrum of $LaAlO_3$:Pr obtained under 2537 Å excitation with the emission under cathode ray excitation. This

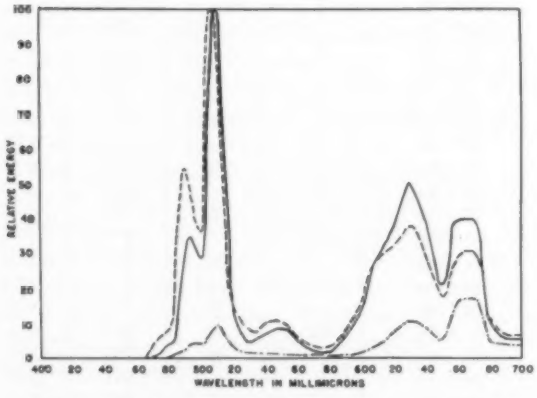

FIG. 1. Emission spectra under cathode ray excitation of lanthanum aluminum oxide prepared using lanthanum oxide from A.E.C. -·-·- $LaAlO_3$ fired in air with no intentional addition of activator; ——— $LaAlO_3$: 10^{-3} Pr fired in air; - - - - $LaAlO_3$: 10^{-3} Pr fired in hydrogen.

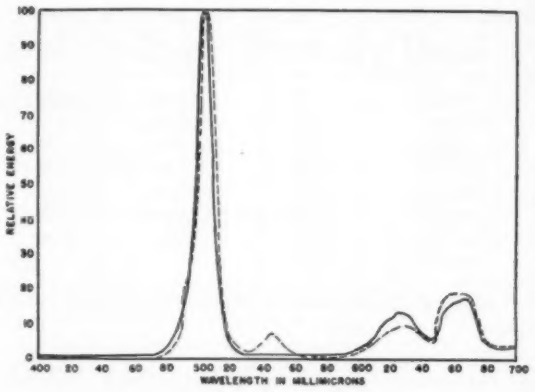

FIG. 2. Emission spectra of $LaAlO_3$ 10^{-3} Pr prepared using lanthanum oxide from The Fairmount Company. ——— excitation by 2537 Å radiation; - - - - excitation by cathode rays.

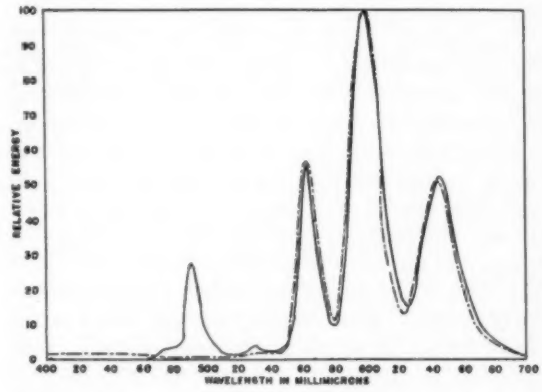

FIG. 3. Emission spectra under cathode ray excitation of $LaAlO_3$ containing samarium as activator. These samples were prepared using lanthanum oxide from the A.E.C. - - - - $LaAlO_3$:10^{-4} Sm; ——— $LaAlO_3$:10^{-3} Pr + 10^{-4} Sm.

phosphor was fired in a hydrogen atmosphere and was prepared from lanthanum oxide from the Fairmount Chemical Company. The spectra are essentially the same except for the absence of the minor peak at 490 mμ in the emission under ultraviolet excitation.

The addition of 10^{-4} mole of samarium gives a phosphor with three strong emission peaks at about 565, 600, and 645 mμ as shown in Fig. 3. When 10^{-3} mole of praeseodymium is added to this phosphor, the only praeseodymium band which appears in the spectrum is at 490 mμ while the samarium spectrum is substantially unaltered.

The emission curve for lanthanum aluminum oxide containing europium, shown in Fig. 4, consists of two sharp peaks at 590 and 620 mμ. The same emission is obtained whether the phosphor is prepared in an oxidizing or a reducing atmosphere. The emission is

apparently due to trivalent europium, stabilized in this oxidation state in the lattice of the matrix.

With gadolinium, the same emission curve was obtained as with samarium. On account of the high sensitivity of samarium as an activator, this response is likely to be due to the presence of samarium as an impurity in the gadolinium.

Use of strontium or barium as charge compensators in the preparation of the praeseodymium phosphor was apparently without effect. Substitution of one-third of the aluminum with gallium in preparations activated with samarium or praeseodymium did not lead to any noticeable difference in the emission characteristics. Lanthanum oxide activated with praeseodymium or with samarium gives essentially the same cathodoluminesence as is obtained with these activators in lanthanum aluminum oxide,

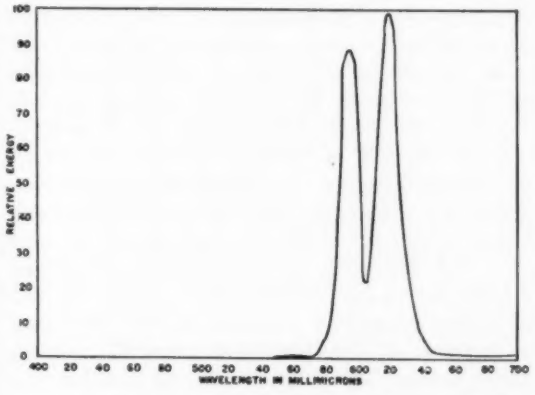

FIG. 4. Emission spectrum under cathode ray excitation of $LaAlO_3$: 10^{-3} Eu. This sample was prepared using lanthanum oxide from the A.E.C.

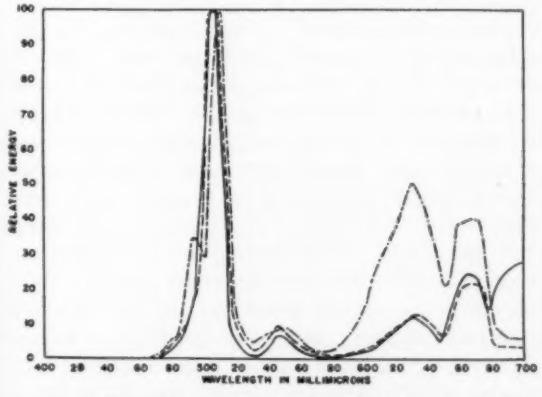

FIG. 5. Emission spectra under cathode ray excitation of $LaA10_3$:Pr containing additional activators. These samples were prepared using lanthanum oxide from the A.E.C. All samples were fired in hydrogen.– – – $LaAlO_3$: 10^{-3} Pr; ——— $LaAlO_3$: Pr + 2% V_2O_5; – – – $LaAlO_3$ Pr + 4×10^{-3} Cr.

but the emission appears to be somewhat stronger with the latter as host crystal.

Several other elements which commonly act as activators were tested by themselves. Among these were chromium, vanadium, manganese, copper, bismuth, and antimony. No striking change in emission characteristics was noticed with any of them. Fig. 5 shows the emission curves obtained with the first two of these in comparison with the emission of the praeseodymium phosphor. The effect of their presence is the suppression of the smaller praeseodymium peaks at 490, 630, and 660–670 mμ. A similar effect is obtained upon increasing the concentration of the praeseodymium to 10^{-2}. A broad weak band in the neighborhood of 700 mμ is present in the vanadium-activated sample.

Addition of increasing quantities of manganese to $LaAlO_3$:Pr causes progressive lowering of the intensity of emission. The body color of these samples fired in air becomes less marked with increasing manganese concentration and the samples containing 2×10^{-3} Mn are white. No emission curves of these samples were obtained.

Discussion of Results

The results of these experiments indicate that lanthanum aluminum oxide resembles lanthanum oxide as a host crystal rather than aluminum oxide.

The unavoidable presence of rare earth impurities in all of the products vitiates to some extent the original purpose of this investigation. There seems to be little reason to doubt that the transition metal activators which were used would enter the perovskite structure in the positions of sixfold coordination. The energy absorbed by the lattice, however, is not transferred to these impurities. Some of the energy is dissipated by emission from the rare earth impurity. It is possible that energy transfer to the transition metal impurity might occur in the complete absence of praeseodymium or samarium. The emission curve of the vanadium-activated sample suggests this possibility.

Production of the distinctive body colors on ignition of the lanthanum aluminum oxide in air and the fact that cathodoluminescence is readily observed in the samples prepared without activation from the spectroscopically pure materials suggest that these phenomena might be useful in following the purification of lanthanum compounds.

Acknowledgments

The authors are greatly indebted to Dr. Frank J. Studer of the General Electric Research Laboratories for his kindness in determining the emission curves,

to Dr. A. Camunas (Institute de Optica, Madrid) for his assistance to one of the authors in the use of the grating spectrograph, and to Dr. Edmond Botti for samples of pure rare earth oxides. They would also like to express their gratitude to the Consejo Superior Investigaciones Cientificas of Spain for sponsoring the stay of one of the authors in the U.S.A. during the period of this research.

Any discussion of this paper will appear in a Discussion Section to be published in the June 1956 JOURNAL.

REFERENCES

1. A. L. SMITH, *This Journal*, **101**, 189 (1954).
2. G. H. JONKER AND J. H. VAN SANTEN, *Physica*, **16**, 337 (1950).
3. F. A. KRÖGER, "Some Aspects of the Luminescence of Solids," Elsevier Press, Houston (1948).
4. F. E. SWINDELLS, *This Journal*, **101**, 415 (1954).

Infrared Quenching of Cadmium Sulfide[1]

S. H. Liebson

United States Naval Research Laboratory, Washington, D.C.

ABSTRACT

Infrared quenching of CdS has been investigated as a function of applied voltage and both infrared and exciting light intensities. Infrared quenching of photoconductivity due to light of wave lengths shorter than that corresponding to the absorption edge increases as the voltage is increased. The quenching spectrum is found to shift with temperature in approximately the same amount as the corresponding shift of the absorption edge. An explanation of infrared quenching is offered based on infrared freed holes recombining with trapped electrons within the crystal.

Introduction

Luminescence and electrical properties of the hexagonal form of both cadmium and zinc sulfide crystals are affected by exposure to infrared radiation. As examples, infrared causes a decrease in the photoconductivity of CdS (1), a stimulation of phosphorescence in CdS-ZnS phosphors (2), an increase in the photovoltaic effect with CdS (3), stimulation of photocurrent in ZnCdS (4), and quenching of luminescence in a ZnS phosphor (5). Since these are closely related materials, it is reasonable to expect that, for those phenomena which respond to infrared peaking at 0.9 and 1.5 ev for CdS (6) and at about 0.95 and 1.8 ev for ZnS (7), absorption occurs in similar centers for both compounds. Different manifestations of response to infrared may be understood on the basis of double activation where, as an example, stimulation of phosphorescence originates with infrared absorption in one activation center and ends with emission in another (7).

Frerichs (8) has proposed a mechanism for quenching of photoconductivity wherein infrared empties electrons from traps located along conduction paths within the crystal, the emptied traps serving to inhibit the further passage of current. With the additional observation that an increase in current is observed prior to quenching action when infrared is first made incident on a photoconducting crystal, Rose (9) postulated that infrared frees holes which contribute to the current before combining with electrons from the conduction band. Taft and Hebb (10) favored this hypothesis and, based on the observed symmetrical quenching spectrum, suggested that infrared excited trapped holes to higher energy states which were then thermally freed to the valence band. From observations of a rectifying contact to CdS, Liebson (3) has also proposed that holes were freed by infrared.

In the case of phosphors, Fonda (2) observed that the stimulation spectrum was independent of the activator for ZnS:Pb and ZnS:Mn and suggested stimulation to be related to a displacement of Zn atoms from their normal positions by the activator atoms. Pearlman, Nail, and Urbach (7) measured stimulation as a function of activator concentration and concluded that copper was responsible for infrared stimulation. Froelich (11), based on careful preparation of ZnS:Cu phosphors, also concluded that infrared stimulability was related to the presence of copper in the crystal. In this connection, Klasens (12) suggested that Cu produced hole traps which could be excited to the valence band. For the phosphor ZnS:Cu:In, as an example, Klasens proposed that under infrared stimulation holes were freed from Cu centers, migrating through the valence band to recombine with indium traps, giving the characteristic indium emission. Klasens also showed how this mechanism was capable of explaining some temperature effects in these phosphors.

This investigation was undertaken to supply additional information relating to infrared quenching of photoconductivity in CdS crystals.

Description of Crystals

Crystals of CdS were prepared by M. E. Bishop by a modification of Frerichs' method (13). Except where noted, crystals were chosen which showed no increased sensitivity at the indium electrodes, in an attempt to minimize the possibility of electrode barrier effects obscuring the measurements. The relative sensitivity of regions of the crystals was determined by scanning with a beam of blue light 0.001 in. in diameter, obtained by directing suitably filtered light through the eyepiece of a microscope and on to the crystal under the microscope objective. In general it was found that the photosensitive

[1] Manuscript received December 20, 1954. This paper was prepared for delivery before the Cincinnati Meeting, May 1 to 5, 1955.

region was also most affected by infrared. Crystals were examined for luminescence at the focus of a 100 watt mercury arc with an ultraviolet filter whose transmission centered around 3660 Å. Crystals were mounted with indium electrodes applied within a day of growth to insure ohmic contact. The first two digits of a crystal identifying number refers to a particular crystal batch.

Crystal 57-1 was a hexagonal needle about 0.1 in. long and about 0.03 in. wide after contacts were placed on it, and showed several sensitive regions under the light probe. It exhibited almost no ultraviolet luminescence. Its photoconductive spectrum peaked sharply at 5200 Å.

Crystal 57-4 was 0.1 in. long and about 0.02 in. wide, hexagonal in cross section, and exhibited a sensitive region as determined with the light probe, located 0.025 in. from one contact. This region showed both photoconductive and infrared quenching characteristics. The remainder of the crystal did not respond to photoconductive light to the limit of sensitivity of the apparatus, about two orders of magnitude less than the photoconductive peak reading. No observable photoconductive response was found at either electrode, making it likely that rectifying contacts did not affect current measurements, although the crystal did show internal rectification. The crystal was red luminescent under ultraviolet excitation.

Crystal 73-1 was about 0.002 in. thick and 0.16 in. long. No peaks were detected with the light probe, the crystal apparently having a sensitivity varying by less than two over its length. Reversal of polarity indicated little or no apparent polarization or rectification. This was the only crystal in several hundred examined that satisfied these conditions. The crystal was weakly red luminescent.

Crystal 73-2 was 0.3 in. long and 0.01 in. wide. Under probe by a beam of light, it showed a sensitive region internal to the crystal which determined its photoconductive behavior. This region seemed to be associated with a grain boundary when viewed under a microscope. This crystal exhibited a greater infrared sensivitity than any of the others tested, and was red luminescent.

Batches 57 and 73 were spectroscopically analyzed for metallic impurities. Both contained about 0.1% silicon with smaller amounts of magnesium, iron, silver, and copper. Batch 57 contained of the order of 0.0001% copper and batch 73 contained about 0.01% copper. Except for 57-1, as noted above, all crystals had a photoconductive spectrum peaking near 5150 Å, falling off sharply at longer wave lengths and more gradually toward shorter wave lengths.

Experimental

The infrared source consisted of a 100 watt tungsten lamp in conjunction with a Polaroid Company Type XR7X filter, having a short wave length cut-off at about 8000 Å. Infrared and visible light intensities were varied by means of gray filters whose transmissions were determined at 5000 Å and at 14,000 Å. A Gaertner quartz monochromator was used for all spectral determinations.

Crystals were mounted by means of their electrodes to terminals on glass insulators and inserted into a brass cylindrical container which was evacuated to about 10^{-6} mm Hg. The crystal could be heated or cooled by means of temperature baths mounted external to the container, thermal conductivity being obtained by means of a few microns pressure of helium which could be admitted to the container. The crystal was connected in series with a potentiometer across a battery supply. Light was admitted to the container through a quartz window.

The time constant for current equilibrium was of the order of ½ hr for all crystals so that measurements, to insure reproducibility, were made after intervals of time approaching an hour. Measurements of current change due to infrared, at the higher values of photoconductive current, suffer from appreciable error due to the fact that the change in current due to infrared was of the order of magnitude of fluctuations in the crystal and current measuring system. This accounts in large measure for the relatively poor fit at larger photo-illumination readings in Fig. 1.

Voltage Dependence of Infrared Quenching

The voltage dependence of infrared quenching was determined for constant intensities of both photoconductive and quenching irradiation. Most crystals showed a behavior indicating polarization. This was evidenced for crystals whose current had come to equilibrium at a fixed voltage and photoconductive light intensity. Upon increasing the applied voltage, the current immediately increased approximately in proportion and then decreased slowly for several minutes, the final equilibrium values being those shown in Fig. 2 and 3. Fig. 2 shows the equilibrium current through crystal 57-4 as a function of applied voltage. These results are typical of those for all crystals at high voltages in that the proportional decrease in current due to infrared increased as the voltage was increased across the crystal. Crystal 73-1 was the only one in more than 100 tested which showed a comparative uniformity of response when scanned with a fine beam of light. This crystal was also the only one observed which had linear resistance characteristics with

photoconductive light, as shown in Fig. 3, and was the least sensitive in response to infrared, requiring approximately 300 times the infrared intensity used to obtain the data in Fig. 2. Crystal 73-1 was atypical in that infrared quenching decreased at high voltages for photo-excitation at 5200 Å, outside the absorption band.

The current through crystal 57-4 at low light intensities varied as the 0.7 power of the light intensity with 1 v across the crystal and as the 0.8 power of the intensity with 100 v across the crystal. Crystal 73-1 showed a linear variation of current vs. intensity at 10 v and 100 v. Crystal 57-1 current varied as 0.8 power of light intensity at 1 v and 0.95 power at 100 v.

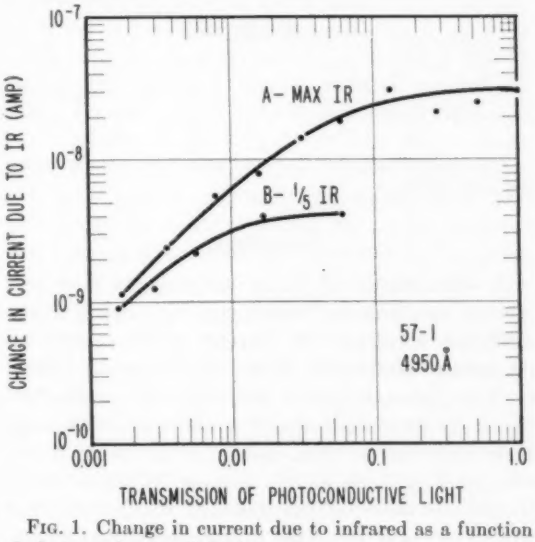

FIG. 1. Change in current due to infrared as a function of photoconductive light intensity.

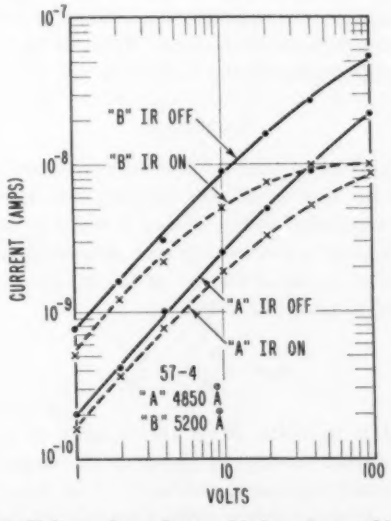

FIG. 2. Voltage dependence of infrared quenching for a typical CdS crystal.

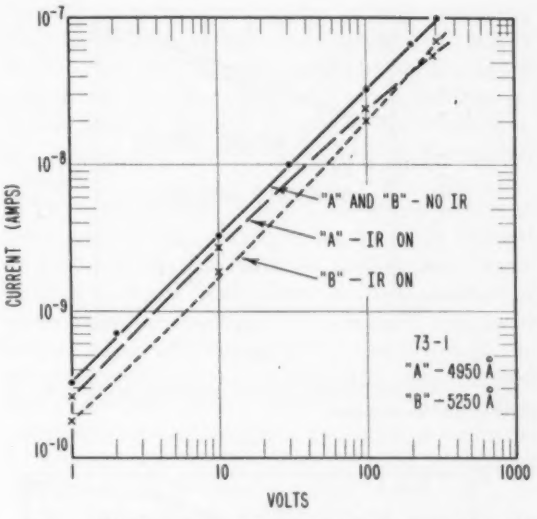

FIG. 3. Voltage dependence of infrared quenching for ohmic photoconducting crystal.

For crystal 57-4 shown in Fig. 2 with the applied voltage in the low impedance direction, two sets of data are given, one with excitation at 4850 Å and the other at 5200 Å. The crystal exhibited a photoconductive peak at 5150 Å, the wave lengths used for the measurements in Fig. 2 lying on either side of both the photoconductive peak and the absorption edge. The effect of infrared was more pronounced at 5200 Å despite the fact that the current produced at this wave length was greater than that produced by the 4850 Å light.

Fig. 4 shows the proportional change in current with constant photoconductive and quenching light intensities as a function of voltage applied in the low and high impedance directions. In the high impedance direction the proportional quenching first decreased as the voltage was increased. The low impedance characteristic is typical of most crystals.

Quenching Linearity

Typical measurements of quenching action are shown in Fig. 1 for variable photoconductive light and in Fig. 5 for variable infrared intensity. The current change due to infrared, shown in Fig. 1, approached a constant value at high photoconductive light intensities. The scatter in experimental points is due to the fact that, as the photoconductive intensity is increased, the proportional change in current with infrared diminishes, making errors due to system fluctuations of increasing importance.

Curves A and B of Fig. 5 show the increased quenching action at higher voltages, tending to "saturate" sooner at lower values of infrared inten-

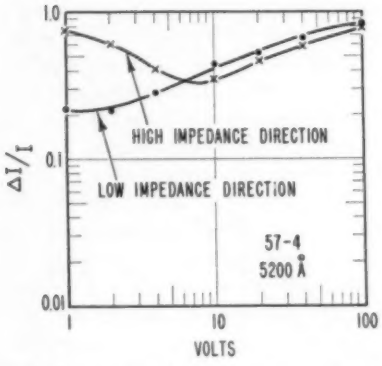

FIG. 4. Voltage dependence of proportional change in current due to infrared.

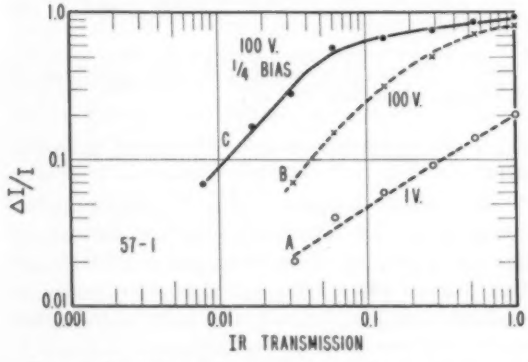

FIG. 5. Variation of proportional change in current with infrared intensity.

sity. In curve C, taken at reduced photoconductive light intensity, the quenching action for lower values of infrared intensity (at 100 v) increases to approximately the extent by which the photoconductive light is decreased.

Infrared Quenching Spectrum

The infrared quenching spectrum was first measured by Frerichs (8) and redetermined by Taft and Hebb (10) at room temperature and shown to consist of two broad bands peaking at 1.5 and 0.9 ev. For the purpose of measurement at low temperature a crystal (73-2) was chosen with a sensitive region approximately midway along the crystal. As observed by Taft and Hebb, there was a marked decrease in infrared quenching at low temperatures. For this crystal at −175°C a change in peak location was observed corresponding to an increase of approximately 0.13 ev of both peaks. This is approximately equal to the temperature shift measured by Kröger (14) of the absorption edge. The relative insensitivity of these crystals at low temperatures made it difficult to get a meaningful band shape.

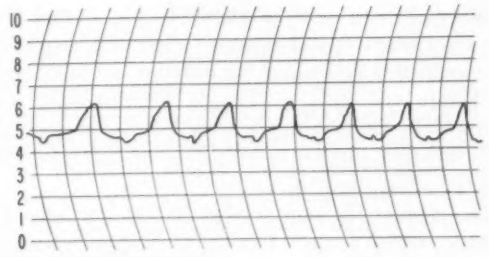

FIG. 6. Oscillations due to infrared incident on a rectifying contact.

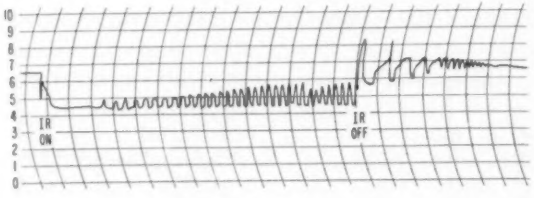

FIG. 7. Build up and decay of oscillations under infrared irradiation.

Oscillations

In the course of these investigations several crystals were prepared with rectifying contacts which exhibited variations in current of the nature of relaxation oscillations under conditions of simultaneous photoconductive and infrared irradiation. Fig. 6 shows a chart record of the current through such a crystal at chart speeds of one division per minute. Fig. 7 shows the manner in which these oscillations build up and diminish when infrared is turned on and off. The frequency of oscillations increases with voltage and is eliminated at either very high or very low infrared intensities, approaching a maximum amplitude somewhere in between. These oscillations have been observed only with crystals having rectifying contacts.

DISCUSSION

The increase of photovoltaic effects at contacts to CdS under irradiation by infrared has been previously attributed to the freeing of holes by infrared (3). This may be more easily seen by considering the potential of a planar barrier at the crystal contact, expressed in practical units

$$\phi = \frac{Me^2l^2}{2K} = \frac{\sigma el}{2K}$$

where ϕ is in volts, M is the density of positive centers within the barrier region of thickness l, K is the dielectric constant, and σ is the surface charge density. At a rectifying contact made with conducting electrodes, σ might be expected to show little change. As a consequence if M is reduced by the

action of infrared, l must increase, giving the new photovoltage as

$$\phi + \Delta\phi = \frac{\sigma e(l + \Delta l)}{2K}$$

The effect of infrared is to increase the generated photovoltage to $\phi + \Delta\phi$ and to increase the thickness of the barrier to $l + \Delta l$. The increase of barrier thickness may then result in a more effective utilization of the incident photoconductive light to provide an increase of generated current, in accord with observation. Oscillations shown in Fig. 6 and 7 are probably related to the ability of infrared to change the height of the barrier, although insufficient information is available to give a satisfactory explanation.

The curves presented in Fig. 1, 3, and 5 show a strong field dependence of infrared quenching. These crystals appeared to have internal regions of high impedance. In Fig. 2, for a crystal with no apparent internal barriers, comparatively little infrared quenching is observed. The results show that strong fields enhance infrared quenching. Klasens (15) has suggested that the increased field may increase the range of travel of holes to recombination regions resulting in greater quenching action. Another possible explanation is that the increased fields increase the internal space charge or polarization. For either case the following explanation is offered for infrared quenching. Referring to Fig. 8, infrared frees holes (step 1), perhaps with the aid of thermal ionization (10) (step 2), the holes are swept by the field to the potential barrier due to trapped electrons (step 3) when recombination takes place with the trapped electron (step 4). The empty trap is now available for removing electrons from the conduction band, resulting in quenching.

The decrease and subsequent increase in proportional infrared quenching in the high impedance direction shown in Fig. 3 for crystal 57-4 has two possible explanations. At low voltage, quenching may be determined by a residual internal barrier which is diminished by the applied potential and is supplanted at high voltages by other barriers, or, on the basis of Klasens' suggestion, the recombination region may change depending on the applied voltage.

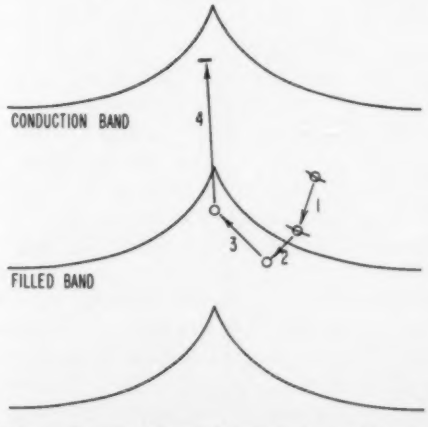

FIG. 8. Proposed recombination due to infrared

The characteristics of Fig. 4 and 5 may be understood in terms of the relative amounts of infrared and photoconductive light. At high relative photocurrent, infrared may effect a fixed amount of recombination, resulting in a constant change in current independent of the total current through the crystal. At relatively low photocurrents the infrared is not effectively useful for quenching due to either an insufficient number of trapped holes or electrons, so that the diminution in current due to infrared increases as the photocurrent is increased.

The shift with temperature of the peaks of the infrared quenching spectrum of cadmium sulfide, of the same amount as the change in forbidden band width, implies that either the bottom of the conduction band or the top of the valence band moves with respect to the infrared absorption centers. If the nature of change in forbidden band width with temperature were known, it could help to decisively determine whether infrared frees electrons or holes.

ACKNOWLEDGMENTS

The author is indebted to Mr. M. E. Bishop who grew the crystals used, to Mr. S. Cress for the spectroscopic analysis, to Dr. R. E. Kagarise for calibration of the gray filters at 1.4, and to Dr. H. A. Klasens of the Philips Gloeilampenfabrieken, Eindhoven, for his helpful suggestions.

Any discussion of this paper will appear in a Discussion Section to be published in the June 1956 JOURNAL.

REFERENCES

1. A. E. HARDY, *Trans. Electrochem. Soc.*, **87**, 355 (1945).
2. G. R. FONDA, *J. Opt. Soc. Amer.*, **36**, 382 (1946).
3. S. H. LIEBSON, *This Journal*, **101**, 359 (1954).
4. H. KALLMAN, Prog. Rpt. 4, Fluorescence and Conduction Phenomena, NYU, May 1954.
5. N. T. MELAMED, *This Journal*, **97**, 33 (1950).
6. R. FRERICHS, *Phys. Rev.*, **76**, 1869 (1949).
7. D. PEARLMAN, N. R. NAIL, AND F. URBACH, "Preparation and Characteristics of Solid Luminescent Materials," John Wiley & Sons, Inc., New York (1948).
8. R. FRERICHS, *Phys. Rev.*, **72**, 594 (1947).
9. A. ROSE, *RCA Rev.*, **12**, 362 (1951).
10. E. A. TAFT AND M. H. HEBB, *J. Opt. Soc. Amer.*, **42**, 249 (1952).
11. H. C. FROELICH, *This Journal*, **100**, 280 (1953).
12. H. A. KLASENS, *ibid.*, **100**, 72 (1953).
13. M. E. BISHOP AND S. H. LIEBSON, *J. Appl. Phys.*, **24**, 660, 963 (1950).
14. F. A. KRÖGER, *Physica*, **7**, 1 (1940).
15. H. A. KLASENS, Private communication.

Studies on Alternating-Current Electrolysis

III. Effects of Concentration on Polarization Capacity and Polarization Resistance[1]

A. Edward Remick and Herbert W. McCormick

Department of Chemistry, Wayne University, Detroit, Michigan

ABSTRACT

The main purpose of this work was to study the influence of electrolytic concentration on the equivalent series capacitance (C_S) and resistance (R_S) of an a-c cell and to analyze these three variables into their components. The cell electrolytes were aqueous solutions containing equimolar concentrations of potassium ferrocyanide and ferricyanide together with potassium sulfate or sodium benzene sulfonate as supporting electrolytes. Platinum electrodes were used and the interelectrode distance was variable. A suitable cleaning method for platinum was discovered which gave reproducible electrodes.

Studies at low current densities resulted in the discovery of a component of the resistance which has its seat at the electrode surface and is frequency-independent. Adding this circuit element (R_L) to Grahame's equivalent circuit and using his mathematical theory of the faradaic admittance together with the authors' bridge data made it possible to calculate the equivalent series capacitance (C_S^*) and resistance (R_S^*) of the faradaic branch of the circuit. The variations of C_S^*, R_S^*, and R_L with depolarizer concentration, ionic strength, and frequency were studied. It was found that the variations of C_S^* and R_S^* with frequency and depolarizer concentration accorded well with the quantitative requirements of Grahame's theory only if the speed of electron transfer were considered to be much faster (i.e., Grahame's θ to be much smaller) than had hitherto been suspected. No satisfactory theory was found to account for the variations of C_S^* and R_S^* with the ionic strength.

Introduction

Contemporary research on a-c electrolytic cells has been directed largely toward the goal of describing the polarization process in terms of an "equivalent circuit" which will represent adequately the known electrical properties of the cell. Although certain complexities sometimes occur which seem to demand additional circuit elements, there seems to be general agreement at the present time on what might be called a basic equivalent circuit which is adequate in the absence of these complexities. This basic circuit is, in the authors' opinion, best represented by Grahame's (1) diagram, although it differs only in symbolism from those used by Rozental and Ershler (2), Randles (3), and Gerischer (4). Grahame's circuit is the same as that shown in Fig. 1 except that R_L has been added. In this figure, C_d is the double layer capacitance at a single electrode; θ is a pure resistance related to the activation energy of ionic discharge; W is the "Warburg impedance" brought into being by concentration polarization; R_T is the electrolytic resistance of the entire cell; i_T is the total current through the cell; i_C is the charging current; and i_F is the faradaic current.

Some additional related symbols which are used in this paper are as follows. R_S and C_S are, respectively, the equivalent series values of the resistance and capacitance of the whole cell. R_S^* and C_S^* are the corresponding values for the faradaic branch of the half-cell. It is customary to use the equation

$$R_S = R_T + \Delta R \qquad [1]$$

to indicate that R_S may be broken down into two series components, one (R_T) independent of the frequency, the other (ΔR) dependent on it. It appears that ΔR increases as the electrolytic concentration decreases (2, 8–10). An exception to this generalization was found by Jones and Christian (8) who observed that ΔR decreased with decrease in concentration when platinum electrodes were used in potassium chloride solution. Grahame (11), using mercury electrodes in various salt solutions, found that ΔR is zero when no faradaic current flows.

The same investigators mentioned above in relation to the equivalent circuit [*see* (5)] have also succeeded in developing from basic principles a mathematical theory which extends the earlier theory as developed by Warburg (6) and Krüger (7). It explains the origin and describes the properties of the circuit elements, most of which are not the conventional circuit elements of physics.

[1] Manuscript received August 6, 1954. This paper was prepared for delivery before the Chicago Meeting, May 2 to 6, 1954.

Certain phases of the mathematical theory of the faradaic admittance have been tested experimentally. The theory demands that plots of R_s^* and X_s^* ($= 1/C_s^*\omega$) against $1/\sqrt{\omega}$ (where ω is the frequency in radians per second) be linear and parallel. Such linear relations have been found by Rozental and Ershler (2) using a mercury electrode in a solution of mercurous nitrate containing a large excess of perchloric acid, by Gerischer (12) using a mercury electrode in mercurous perchlorate containing a large excess of perchloric acid, by Randles (13) using both mercury and platinum electrodes with various redox systems including the ferrocyanide-ferricyanide system, and by Vetter (14) who used platinum electrodes with the iodide-iodine system in 1*N* sulfuric acid solution.

The mathematical theory also expresses R_s^* and C_s^* as functions of the concentration(s) of the depolarizer(s) (i.e., of the "potential-determining substances"). No one except Vetter (14) appears to have checked this phase of the theory experimentally. He found that the "complex diffusion resistance" (i.e., the "Warburg impedance" of Grahame) multiplied by $\sqrt{\omega}$ is a linear function of the reciprocal of the concentration of one component of his redox system when the concentration of the other is held constant. This relationship is required by the theory. He also demonstrated that the redox system in question gave the required relationship between concentration and exchange current. However, despite these demonstrations of accord between theory and experiment, diffusion constants calculated from the variation of the "complex diffusion resistance" with the concentration did not accord well with values given in the literature.

The effect of concentration on the double layer capacity has been formulated in terms of the thermodynamic theory of electrocapillarity by Grahame (15).

Much evidence is to be found in the chemical literature that poorly conducting layers are formed on solid electrodes during electrolysis by either direct or alternating currents and give rise to "resistance polarization" (19). Vetter (14) has remarked that an electrode-layer resistance should theoretically be accompanied by a capacitance, but that in practice this capacitance is found to be negligible. He argued that the electrode-layer resistance, when it occurs, must be added to the electrolytic resistance. In line with this suggestion the authors have added an electrode-layer resistance, R_L, to the basic equivalent circuit to give the circuit shown in Fig. 1.

It is hoped that this research will be of value in furnishing a test of the theoretically predicted relation between concentration and the faradaic admittance by using a different redox system from that used by Vetter and carefully controlling conditions so that the two "components" of the concentration effect, viz., ionic strength and concentration of the depolarizer as such, can be studied separately. This has been done using conditions of especial interest to the authors' plans for future research, viz., solid electrodes (platinum), a reversible redox system (ferrocyanide plus ferricyanide), and alternating current without superimposed direct current. As far as they are aware, the authors' test of the theory in relation to the concentration of the depolarizer is the first one made at constant redox ratio (i.e., the ratio of the concentration of oxidant to that of reductant). A further objective is to determine whether or not an additional resistance occupying a place in the equivalent circuit indicated by R_L in Fig. 1 is present under the chosen experimental conditions and to study its dependence on ionic strength and depolarizer concentration in case it is found to exist.

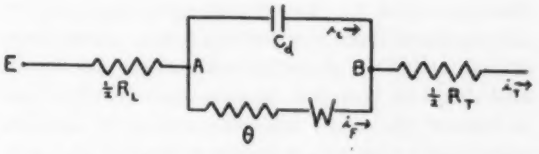

FIG. 1. Equivalent circuit for half-cell. Platinum electrode is placed at *E*.

EXPERIMENTAL METHOD

Measurements of the resistance and capacitance of the electrolytic cells were made by means of an impedance bridge constructed in the same general manner and using the same circuit elements as the bridge described by Shaw and Remick (16) except that: (*a*) shielded wire was used much more judiciously than before in order to improve frequency-independence, (*b*) both the source of alternating current and the oscillograph used as a null point detector were isolated from the bridge by shielded transformers (General Radio Co.'s type 578-B), (*c*) a Ballentine model 300 electronic voltmeter was used as a voltage amplifier in the detector circuit, (*d*) the power amplifier was shielded, and (*e*) a somewhat different type of electrolytic cell was used. As before, the cell was immersed in a constant temperature bath kept at 30° ± 0.1°, purified nitrogen was bubbled through it, and the platinum electrodes employed were made by sealing platinum disks in glass tubing so that the platinum surfaces were flush with the ends of the tubes. The new features of the cell were: (*a*) electrodes were mounted one above the other and the upper electrode was mounted in a threaded brass sleeve so that the interelectrode

distance could be varied and measured with a cathetometer, and (*b*) a piece of glass tubing, open at both ends, was slipped over the electrodes. Its inside diameter was just large enough to allow free motion of the upper electrode within it, and its upper end projected above the surface of the solution. Its purpose was to provide a conducting path of fixed diameter so that the interelectrode distance would be the only geometrical variable.

Resistances of the connecting wires and the mercury columns within the electrode tubes were measured and found to be utterly negligible.

R_T and ΔR were determined by a method introduced by Miller (17) and used effectively by Jones and Christian (8). This method is based on the equation

$$R_s = \frac{l}{a\kappa} + \Delta R \qquad [2]$$

where l is the interelectrode distance in centimeters, κ is the specific conductance of the electrolyte, and a is the electrode area in square centimeters. It is evident from equation [2] that a plot of R_s against l will give a straight line with an R_s intercept equal to ΔR. Equation [1] can then be used to calculate R_T.

The potassium sulfate, potassium ferrocyanide, and potassium ferricyanide used were Baker's analyzed reagents. Sodium benzene sulfonate was prepared from a "practical" grade of benzene sulfonic acid and twice recrystallized.

Reproducibility of Electrodes

The difficulty of getting reproducible measurements with metallic electrodes under nonequilibrium conditions is well known. The most reproducible results were obtained by immersing the electrodes in the alkaline cyanide solution recommended by Shaw and Remick (16) and cleaning them anodically for 2 min and cathodically for 4 min using 3 v with an electrode separation of about 1.8 cm. This cycle of operations was performed three times. The electrode was very quickly washed with distilled water, then with a portion of the cell solution, and immediately immersed in the cell. Electrodes so prepared gave steady readings after approximately 30 min and never changed after that by more than 2% on standing for 24 hr. In order to establish the reproducibility of electrodes prepared by this method, the electrodes were immersed in the solution of ionic strength 0.2314 shown in Table I, and allowed to stand 20–40 min; bridge measurements were made at a frequency of 800 cps. The electrodes were then removed and cleaned again. This complete cycle was carried out nine times. The mean deviation was 1.5 μF cm^{-2} (0.78%) for C_s and 0.2 ohm (0.31%) for R_s. The corresponding maximum deviations from the mean were 4 μF cm^{-2} (2.1%) and 0.5 ohm (0.77%). As a further check on reproducibility, a completely independent check run was made on the dispersion of C_s and R_s at ionic strength 0.2314 (Table I). Resistance measurements checked to within a few tenths of an ohm and the capacitance measurements within 2 μF

TABLE I. *Q-dispersion as a function of ionic strength*

Ferrocyanide = 0.005M; ferricyanide = 0.005M; supporting electrolyte = K_2SO_4; half-wave area = 0.685 microcoulomb/cm^2 interelectrode distance = 1.80 cm; electrode area = 0.253 cm^2; capacitance given in microfarads/cm^2, resistance in ohms/cm

Freq. (cps)	Ionic strength							
	0.2314		0.3821		0.5300		0.6805	
	C_S	R_S	C_S	R_S	C_S	R_S	C_S	R_S
200	343.5	52.37	359.2	33.33	369.9	24.31	397.6	19.73
400	252.1	51.61	258.1	31.65	267.5	23.58	278.1	19.18
600	200.9	51.31	202.5	31.52	215.2	23.28	215.1	18.95
800	174.8	51.15	176.3	31.37	185.3	23.12	192.2	18.80
1000	156.1	51.03	158.8	31.30	168.6	23.00	173.7	18.67
1500	122.8	50.85	127.1	31.09	134.6	22.82	138.8	18.47
2000	100.3	50.75	103.6	30.97	112.5	22.69	118.2	18.38
2500	86.9	50.73	88.6	30.92	97.7	22.64	101.4	18.34
3000	77.1	50.62	88.0	30.84	90.5	22.62	92.6	18.29
3500	69.9	50.57	73.4	30.79	82.8	22.52	84.9	18.24
4000	63.5	50.55	67.6	30.74	77.9	22.47	78.6	18.19
5000	53.4	50.45	57.9	30.64	67.8	22.44	69.9	18.14
	R_T = 33.39 R_L = 16.64		R_T = 19.76 R_L = 10.35*		R_T = 14.92 R_L = 7.03		R_T = 11.81 R_L = 5.99	

* Plot of R_S against $1/\sqrt{\omega}$ was slightly curved.

cm^{-2} except at 400 cps where the deviation was 4.4, and at 200 cps where it was 18 (or 5.2%).

A related difficulty occurs when electrodes are subjected to high current densities. When the current density gets high enough, a sort of "hysteresis" sets in. Bridge readings become unstable, drifting with time, and, if the current density is lowered, the resistance and capacitance show reluctance to return all the way to their former values. A similar hysteresis was observed by Slygin and Frumkin (18) in making direct-current charging curves for platinum in aqueous sulfuric acid.

Results of Measurements

Most of the dispersion studies reported earlier (16) were made at constant current density, this fact being emphasized by designating them as "*I*-dispersion" studies. Dispersion measurements reported in this paper are of the "*Q*-dispersion" type (i.e., the number of coulombs per half-cycle—the "half-wave area"—being kept constant). All measurements reported in the present paper were made at low current densities corresponding to a half-wave area of 0.685 microcoulomb/cm^2. In all cases the electrodes were cleaned by the authors' improved technique. No distortion of the voltage or current waves was ever observed.

Electrode Layer Resistance

Q-dispersion plots of R_s against $1/\sqrt{\omega}$ were all linear, with the one exception noted in Table I. Extrapolated values of R_s at infinite frequency were higher than R_T as determined by extrapolation to zero interelectrode distance. Inasmuch as the latter method gave the same values of R_T as determined by the Kohlrausch method (i.e., using platinized electrodes), it was deemed reliable, and the higher values obtained by the frequency extrapolation interpreted to mean that there must be at the electrode surface a frequency-independent component of R_s. Reasons are given later for suspecting that this resistive component is not the resistance associated with surmounting an activation energy hump in the electron transfer step, symbolized as θ by Grahame (1), but rather a resistance associated with a poorly conducting layer on or at the electrode surface. Tentatively it will be called the "electrode layer resistance" (R_L) and put into the equivalent circuit as shown in Fig. 1. This means that ΔR has two components, one depending and one not depending on the frequency, and that equation [1] may be rewritten as follows:

$$R_s = R_T + R_L + R_\Delta \qquad [3]$$

where R_Δ is the frequency-dependent component of ΔR.

In a series of preliminary experiments R_L varied from 2.3 to 10.3 ohms/cm^2 in a solution having the composition of the second one in Table I when the electrodes were cleaned by different methods. It is interesting to note that the improved method of cleaning electrodes makes a constant contribution to R_L as shown by a check run on the solution of ionic strength 0.2314 (Table I). The value of R_L obtained in this run was 16.37 ohms cm^{-2} which compares favorably with the value of 16.64 given in the table.

Effect of Concentration

Tables I to IV give data on the effects of ionic strength, supporting electrolyte, and concentration of depolarizer on C_s, R_s, R_Δ and their dispersions. Values of R_T and R_L are also given. Ionic strength

TABLE II. *Q-dispersion of C_S for supporting electrolyte*

Supporting electrolyte = K_2SO_4; half-wave area = 0.685 microcoulomb/cm^2; interelectrode distance = 1.80 cm; electrode area = 0.253 cm^2; capacitance given in microfarads/cm^2.

Freq.	Ionic strength			
	0.2314 C_S	0.3821 C_S	0.5300 C_S	0.6805 C_S
200	8.94	9.12	9.11	9.10
400	8.78	8.82	8.88	8.93
600	8.63	8.66	8.82	8.85
800	8.48	8.55	8.73	8.78
1000	8.37	8.44	8.67	8.74
1500	8.08	8.23	8.53	8.64
2000	7.88	8.08	8.41	8.56
2500	7.70	7.93	8.31	8.45
3000	7.53	7.82	8.18	8.36
3500	7.32	7.71	8.10	8.29
4000	7.17	7.60	8.01	8.21
5000	6.96	7.34	7.84	8.08

TABLE III. *Q-dispersion in sodium benzenesulfonate solution*

Ferrocyanide = 0.005M; ferricyanide = 0.005M; supporting electrolyte = sodium benzene sulfonate; ionic strength = 0.2314; half-wave area = 0.685 microcoulomb/cm^2; interelectrode distance = 1.80 cm; electrode area = 0.253 cm^2; R_T = 35.93 ohms/cm^2; R_L = 17.03 ohms/cm^2.

Freq.	C_S	R_S
200	350.7	54.87
400	249.6	54.16
600	203.3	53.79
800	172.5	53.69
1000	156.9	53.61
1500	125.2	53.43
2000	105.9	53.36
2500	91.2	53.28
3000	83.2	53.23
3500	75.2	53.18
4000	67.8	53.13
5000	60.5	53.05

TABLE IV. *Q-dispersion as a function of concentration of depolarizer*

Depolarizer = ferrocyanide and ferricyanide; redox ratio = unity; supporting electrolyte = K_2SO_4; half-wave area = 0.685 microcoulomb/cm²; ionic strength = 0.6805.

Freq.	m. of *OX.* and *Red.*							
	0.005M		0.010M		0.015M		0.0425M*	
	C_S	R_S	C_S	R_S	C_S	R_S	C_S	R_S
200	397.6	19.73	736.9	19.91	1096	20.49	2693	25.58
400	278.1	19.18	534.1	19.51	763.7	20.24	1998	25.53
600	215.1	18.95	430.7	19.45	638.4	20.16	1611	25.50
800	192.2	18.80	380.5	19.38	569.1	20.11	1466	25.48
1000	173.7	18.67	342.3	19.33	517.0	20.06	1311	25.45
1500	138.8	18.47	282.9	19.23	427.2	20.01	1137	25.43
2000	118.2	18.37	237.7	19.18	351.4	19.96	1069	25.40
2500	101.4	18.34	210.3	19.15	312.7	19.94	932	25.40
3000	92.6	18.29	194.5	19.13	294.3	19.93	785	25.37
3500	84.9	18.24	175.3	19.10	265.5	19.91	699	25.37
4000	78.6	18.19	162.7	19.08	245.8	19.88	681	25.35
5000	69.9	18.14	145.0	19.03	226.9	19.86	646	25.32
	$R_T = 11.81$ $R_L = 5.99$		$R_T = 12.27$ $R_L = 6.55$		$R_T = 12.82$ $R_L = 6.93$		$R_T = 16.95$ $R_L = 8.35$	

* Ferrocyanide and ferricyanide only (no supporting electrolyte).

values were calculated on a molarity basis. From this data, the following conclusions can be drawn.

1. At constant concentration of depolarizer, R_L decreases as the ionic strength increases. At constant ionic strength, R_L increases rather rapidly as the depolarizer concentration increases. The relative magnitudes of this decrease and increase were judged from the numerical values of the slopes of the respective curves.

2. At constant concentration of depolarizer, C_S increases moderately as the ionic strength increases. At constant ionic strength, C_S increases markedly as the depolarizer concentration increases. Fig. 2 shows clearly that in the presence of sufficient supporting electrolyte (i.e., all points except the one at 0.0425M) C_S is a linear function of the depolarizer concentration and that the rate of change of C_S with the concentration is greater at lower frequencies, the half-wave area being constant.

3. In view of the method used for the calculation of R_Δ, values cannot be expected to show good precision. The figures indicate that R_Δ is almost independent of ionic strength and decreases with an increase in depolarizer concentration.

It remains to be shown whether the above conclusions involve the ionic strength as such. In order to answer this question, sodium benzene sulfonate was used in place of potassium sulfate as supporting electrolyte at a total ionic strength of 0.2314 (Table III). Comparison of this data with the corresponding data of Table I shows that: (*a*) R_L is the same, within the limits of precision with which R_L can be reproduced by successive cleaning operations, in supporting electrolytes of two different charge types, at the same total ionic strength and the same depolarizer concentration; (*b*) when C_S is plotted against $1/\sqrt{\omega}$, all points fall on the same straight line regardless of which supporting electrolyte was used; and (*c*) values of ΔR are rather accurately the same for the two experiments, but values of R_Δ range from 0.9 to 1.7 ohms less (or an average of 1.3 ohms less) for sodium benzene-sulfonate than for potassium sulfate. The discrepancy in the two sets of R_Δ values is clearly the result of the difficulty of reproducing

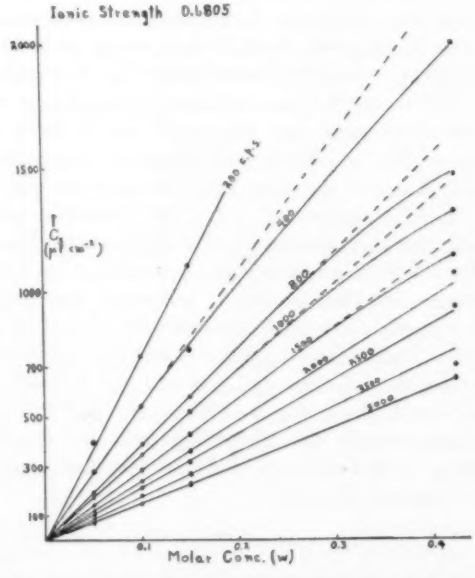

FIG. 2. Polarization capacitance (C_S) as a function of depolarizer concentration (data from Table IV).

exactly the same electrode surface each time, as shown by the fact that the difference in the two values of R_L is 1.5 ohms in the opposite direction (cf., equation [3]). Apparently, then, alteration of the kind of supporting electrolyte does not affect R_Δ.

In Fig. 2 all points correspond to the same ionic strength, but no supporting electrolyte was used in the most concentrated solution. The fact that, at each frequency, only the point corresponding to the most concentrated solution fails to be on a straight line going through the origin shows that part of the effect of the supporting electrolyte is something other than an ionic strength effect. It is presumably the elimination of electrical migration of the depolarizer ions.

Although it clearly would be desirable to have more data bearing on the subject, one can tentatively conclude from the above discussion plus the observations (*a*), (*b*), and (*c*) that conclusions 1, 2, and 3 are correctly stated in relation to "ionic strength."

Determination of the Double Layer Capacity

A satisfactory theoretical analysis of the data demands an accurate value for the double layer capacity. The method involving an extrapolation of C_S to a zero value of $1/\sqrt{\omega}$ is not to be recommended for Q-dispersion data when alternating current alone is used because the double layer capacity, C_d, is a function of E_{AB} (the potential drop from A to B of Fig. 1) and E_{AB} changes with the frequency because the Warburg impedance is frequency-dependent.

Therefore, C_d was determined by measurements on the supporting electrolyte alone as is commonly done in polarography. Results are given in Table II. Ionic strengths listed in Table II are not actual values but those which would obtain if enough depolarizer were added to each potassium sulfate solution to make the solution 0.005M in both ferrocyanide and ferricyanide. Thus, each value of C_S in Table II may be taken to be one-half of the C_d value corresponding to the same ionic strength and the same frequency in Table I (note that C_S refers to the whole cell and C_d to one electrode).

The slight dispersion observed in the capacitance values given in Table II probably is to be ascribed to a slight participation of some extraneous faradaic process. Assuming that this extraneous process persists in the presence of a ferrocyanide-ferricyanide mixture, the authors' method of correcting for the effect of the double layer capacity would correct incidentally for the extraneous impedance. In any event, the correction is a small one.

Theoretical Interpretations

In seeking a theoretical interpretation of the authors' observations, first turn to Grahame's theory of the faradaic admittance (1). All of his equations are developed for the faradaic branch of the equivalent circuit. This means that C_S and R_S must be related mathematically to the corresponding quantities C_S^* and R_S^* for the faradaic branch alone. Proceeding by the conventional method of a-c circuit analysis up to the point where the horizontal and vertical components are separated, and introducing R_Δ from equation [3],

$$\frac{2R_\Delta}{R_\Delta^2 + X_S^2} = \frac{R_S^*}{(R_S^*)^2 + (X_S^*)^2} \qquad [4]$$

$$\frac{2X_S}{R_\Delta^2 + X_S^2} - C_d\omega = \frac{X_S^*}{(R_S^*)^2 + (X_S^*)^2} \qquad [5]$$

where X_S and X_S^* are the reactances corresponding respectively to C_S and C_S^*. These two equations may now be solved simultaneously to get:

$$R_S^* = \frac{M}{M^2 + N^2} \qquad [6]$$

and

$$C_S^* = \frac{M^2 + N^2}{N\omega} \qquad [7]$$

where

$$M = \frac{2R_\Delta}{R_\Delta^2 + X_S^2} \qquad [8]$$

and

$$N = \frac{2X_S}{R_\Delta^2 + X_S^2} - C_d\omega \qquad [9]$$

Grahame's theory leads to his equations [38] and [39]. Using the authors' symbols, they become

$$R_S^* = \theta + \eta/\sqrt{\omega} \qquad [10]$$

$$C_S^* = 1/\eta\sqrt{\omega} \qquad [11]$$

θ is expected to be zero for reversible systems and η is defined by the equation

$$\eta \equiv \sum_i \beta_i \nu_i/\sqrt{2\epsilon_i} \qquad [12]$$

where

$$\beta_i \equiv \partial E/\partial w_i \qquad [13]$$

Here w_i is the concentration, expressed in coulombs per cubic centimeter, of the ith kind of substance at a distance from the electrode "just exceeding that at which the effect of the double layer begins to be appreciable." When diffusion occurs in the aqueous phase and a supporting electrolyte is pres-

TABLE V. *Calculated values of pseudocapacitance (C_S^*) and pseudoresistance (R_S^*)*
(Resistance is in ohm/cm², capacitance in microfarad/cm²)

Ionic strength. Conc. of *OX.* & *Red.*	0.6805 0.005M		0.6805 0.010M		0.6805 0.015M		0.6805 0.0425M		0.5300 0.005M		0.3821 0.005M		0.2314 0.005M	
Freq. (cps)	R_S^*	C_S^*	R_S^*	C_S^*	R_S^*	C_S^*	R_S^*	C_S^*	R_S^*	C_S^*	R_S^*	C_S^*	R_S^*	C_S^*
200	1.00	794	0.56	1457	0.37	2192	0.14	5927	1.23	744	1.17	719	1.23	687
400	0.73	556	0.35	1066	0.24	1525	0.12	4004	0.86	540	0.82	518	0.84	505
600	0.62	429	0.33	863	0.21	1276	0.10	3230	0.71	435	0.77	410	0.69	402
800	0.54	384	0.29	765	0.18	1138	0.09	2946	0.64	376	0.69	359	0.61	350
1000	0.48	347	0.27	689	0.15	1080	0.08	2632	0.58	343	0.66	328	0.49	309
1500	0.37	275	0.22	570	0.13	855	0.07	2289	0.49	276	0.56	265	0.46	245
2000	0.32	233	0.19	478	0.10	699	0.05	2154	0.42	229	0.50	216	0.42	199
2500	0.31	200	0.18	425	0.09	622	0.05	1884	0.40	201	0.48	187	0.41	174
3000	0.29	182	0.16	395	0.09	590	0.04	1570	0.39	191	0.43	190	0.35	152
3500	0.26	166	0.15	355	0.08	528	0.04	1402	0.34	170	0.42	156	0.33	137
4000	0.23	152	0.14	328	0.07	486	0.02	1358	0.31	160	0.41	146	0.32	124
5000	0.21	134	0.12	290	0.05	447	0.01	1280	0.30	141	0.34	119	0.26	100

ent in a sufficiently high concentration to reduce the transference numbers of the depolarizer ions to zero, ν_i is the number of equivalents of an ion produced by chemical action when one faraday of electricity crosses the phase interface. According to Grahame's conventions, ν_i has a value of -1 for ferricyanide ions and $+1$ for ferrocyanide ions. Finally, ϵ_i is the diffusion coefficient of the substance W_i, and E is the potential across the entire double layer corrected for the IR drop.

Equations [10] and [11] give a simple method of comparing experiment and theory. They require that plots of both R_S^* and C_S^* against $1/\sqrt{\omega}$ be linear and that the same value of η be obtained from the slope of either curve. Both curves should pass through the origin (if θ is zero). Randles' approximate equations [16] and [17] also demand these same linear relations.

The necessary data for making these tests have been computed from the data given in Tables I, II, and IV and are assembled in Table V. C_S^* is Grahame's "pseudocapacitance" and R_S^* may reasonably be called "pseudoresistance" when θ is zero. They were calculated by use of equations [7] and [6], respectively. All plots of R_S^* against $1/\sqrt{\omega}$ are linear except the one at 0.0425M and, with the same exception, all curves at ionic strength 0.6805 pass through the origin within ±0.02 ohm. (It should be recalled that the 0.0425M solution contained no supporting electrolyte.) With the same exception, the plots of C_S^* against $1/\sqrt{\omega}$ are linear for the solutions of ionic strength 0.6805, although for the 0.010M solution the points at 200 and 400 cps lie off the line just sufficiently to suggest slight curvature. These lines very nearly pass through the origin. With solutions of lower ionic strength, the lines are all curved at their low frequency ends, the curvature decreasing as the ionic strength increases, until at 0.5300 the line is almost linear and at 0.6805 completely linear.

The next phase of the test is to show that the values of η calculated respectively from the dispersion curves of R_S^* and C_S^* are the same. This may be done by eliminating η from equations [10] and [11] to get Grahame's equation [41], viz., $R_S^* C_S^* \omega = 1$ when $\theta = 0$. Values of this product are readily calculated from the data in Table V and are given in Table VI for the solutions of highest ionic strength. Agreement with theory is very good up to 2500 cps for the solution in which the excess of supporting electrolyte is the greatest.

The above tests furnish reasonably good verification for the equations developed by Grahame and by Randles insofar as they are concerned with the dispersion of C_S^* and R_S^*. This leads to examination of the concordance between theory and experiment achieved with relation to variations of the concentration of the depolarizer in the bulk of the solution, the ionic strength being maintained constant.

TABLE VI. *Values of $R_S^* C_S^* \omega$ for solutions of ionic strength 0.6805*

Freq.	Depolarizer conc.		
	0.005	0.010	0.015
200	1.00	1.02	1.02
400	1.02	0.94	0.92
600	1.00	1.07	1.01
800	1.05	1.11	1.03
1000	1.04	1.17	1.00
1500	0.97	1.18	1.05
2000	0.95	1.14	0.92
2500	0.98	1.20	0.93
3000	0.80	1.21	1.06
3500	0.95	1.20	0.79
4000	0.09	1.13	0.84
5000	0.88	1.07	0.76

Experimentally, plots of the bulk concentration of oxidant (or reductant) against the values of C_S^* at ionic strength 0.6805 (Table V) look like Fig. 2, i.e., the lines are linear up to 0.015M and nearly pass through the origin. It is not surprising that the points at 0.0425M fail to fall on the straight lines since no supporting electrolyte was used in this solution. Corresponding plots of R_S^* against the reciprocal of the depolarizer concentration are straight lines passing through the origin. No point lies more than 0.02 ohm off the line even though the points for the 0.0425M solution are included. Below 1000 cps the points lie on the lines within 0.01 ohm (the precision measure of R_S).

Evidence that these linear relationships are in accord with theory is supplied by the fact that they are demanded by Randles' equations [16] and [17]. However, if these equations are to be used for ferrocyanide-ferricyanide solutions, they involve the assumption that the diffusion coefficients of ferrocyanide and ferricyanide are the same. This assumption is not completely justified since Kolthoff and Lingane (20) give 0.74×10^{-5} and 0.89×10^{-5} cm^2 sec^{-1}, respectively, for the diffusion coefficients at infinite dilution.

Grahame's equations express concentrations in terms of w_i, not in terms of concentrations in the bulk of the solution, and are therefore difficult to apply rigorously to the authors' experimental data. An approximate solution of the problem may be achieved, however, on the basis of two reasonable assumptions: (*a*) equilibrium in the electron transfer reaction is continuously established between the electrode and the adjacent layer of electrolyte, and (*b*) using time-average values, $w_{ox} = C_{ox}$ and $w_{Red} = C_{Red}$, where C symbolizes molar concentrations in the bulk of the solution. The first assumption is surely justified at sufficiently low frequencies, the determination of the maximum valid frequency being an experimental matter. In regard to the second assumption, it must be recognized that bridge measurements give only average values of R_S and C_S and these are related to average values of w_{ox} and w_{Red}. In the steady state (or, better, in the cyclic state), which is presumably achieved in the electrolytic cell when alternating current alone is used, it would seem that w_{ox} would vary cyclically above and below C_{ox} so that on the average the two would be equal for small currents. A similar statement applies to w_{Red} and C_{Red}.

The Nernst equation in terms of concentrations rather than activities is given by

$$E = E_o - (RT/n\mathbf{F}) \ln (w_{ox}/w_{Red}) \qquad [14]$$

Partial differentiation of this equation with respect to concentration and combination with equation [13] gives:

$$\beta_{ox} = \partial E/\partial w_{ox} = -RT/n\mathbf{F}w_{ox} \qquad [15]$$

$$\beta_{Red} = \partial E/\partial w_{Red} = RT/n\mathbf{F}w_{Red} \qquad [16]$$

Combination of equations [12], [15], and [16], introduction of the numerical values for ν, and recognition that in the poised solutions $C_{ox} = C_{Red} = w_{ox} = w_{Red} = C$, yields the equation:

$$\eta = \frac{RT}{n\mathbf{F}C}\left(\frac{\sqrt{2\epsilon_{Red}} + \sqrt{2\epsilon_{ox}}}{2\sqrt{\epsilon_{ox}\epsilon_{Red}}}\right) \qquad [17]$$

Combination of equations [11] and [17] gives:

$$C_S^* = \frac{2n\mathbf{F}C}{RT\sqrt{\omega}}\left(\frac{\sqrt{\epsilon_{ox}\epsilon_{Red}}}{\sqrt{2\epsilon_{Red}} + \sqrt{2\epsilon_{ox}}}\right) \qquad [18]$$

If the temperature and frequency are held constant and assuming, as a first approximation, that in the presence of an appreciable excess of supporting electrolyte and at constant ionic strength the diffusion coefficients are independent of C, equation [18] becomes:

$$C_S^* = kC \qquad [19]$$

where k is a constant. Similarly, equations [10] and [17] give:

$$R_S^* = \frac{k'}{C} + \theta \qquad [20]$$

Remembering that $\theta = 0$ for reversible reactions, it is obvious that equations [19] and [20] are the desired equations showing that C_S^* and R_S^* are linear functions of C and $1/C$, respectively, and that both curves pass through the origin, as observed experimentally in the presence of a fairly large excess of supporting electrolyte. This same dependence of C_S^* and R_S^* on the concentration is demanded by equation [4] of Rozental and Ershler (2) although their constants are not the same as the authors' —indeed their equations were developed for a metal-metallic ion type of electrode.

The relationship between the constants in equations [19] and [20] is:

$$k = 1/k'\omega \qquad [21]$$

This equation can be tested by determining the two constants, respectively, from the slopes of the plots

TABLE VII. *Test of equation [21]*

f	k	$1/k'\omega$	f	k	$1/k'\omega$
200	0.0378	0.0382	2000	0.0119	0.0130
400	0.0273	0.0286	2500	0.0105	0.0109
600	0.0216	0.0215	3000	0.0098	0.0098
800	0.0194	0.0183	3500	0.0089	0.0097
1000	0.0175	0.0175	4000	0.0081	0.0097
1500	0.0133	0.0141	5000	0.0073	0.0087

of C_s^* against C and of R_s^* against $1/C$. Table VII gives the calculated values of k and $1/k'\omega$. The comparison is very satisfactory, especially in view of the difficulty of getting precise values for R_s^*. It is apparent, incidentally, that the assumptions which went into equation [21] are good approximations to the truth at frequencies below 1000 cps.

Critical Consideration of Electrode-Layer Resistance

The accord between theory and the experimental data was achieved on the basis of two debatable assumptions, viz.: (*a*) there is a resistance R_L, tentatively described as an electrode-layer resistance, entering the equivalent circuit as shown in Fig. 1; and (*b*) the resistance θ is essentially zero for the ferrocyanide-ferricyanide system under present experimental conditions.

These two assumptions are closely related and may be considered critically. Accepting the equivalent circuit of Fig. 1 with neither R_L nor θ equal to zero and using equation [11] and the definition of reactance, the reactance of the faradaic branch is given by:

$$X_s^* = 1/C_s^*\omega = \eta/\sqrt{\omega} \qquad [22]$$

Combination of equations [4], [10], and [22] gives:

$$\frac{2R_\Delta}{R_\Delta^2 + X_s^2} = \frac{\theta + \eta/\sqrt{\omega}}{\theta^2 + 2\theta\eta/\sqrt{\omega} + 2\eta^2/\omega} \qquad [23]$$

At infinite frequency this reduces to

$$(R_\Delta)_{\omega=\infty} = 2\theta \qquad [24]$$

and substitution of 2θ for R_Δ in equation [3] gives

$$(R_s)_{\omega=\infty} = 2\theta + R_L + R_T \qquad [25]$$

as the limiting value of R_s at $\omega = \infty$.

If neither θ nor R_L is zero, the extrapolation method used to get R_L gives, instead, $R_L + 2\theta$. From these data there appears no way in which R_L and θ can be evaluated separately, so the expedient of ascertaining whether the assumption of a zero value for θ or for R_L is in better accord with the experimental facts is used.

When θ is zero, theory demands that $R_s^*C_s^*\omega = 1$. The data were shown to be in rather good accord with this equation when R_L was taken into account. When θ is not zero, this relationship becomes

$$(R_s^* - \theta)C_s^*\omega = 1 \qquad [26]$$

When R_L is taken as zero, θ being evaluated from equation [25] and R_s^* and C_s^* calculated from equations [6] and [7] using $R_\Delta = R_s - R_T$ for the evaluation of M and N, one finds that equation [26] is not at all in accord with the best data in Table I. Therefore, the assumption of a zero value for θ is in much better accord with the data than the assumption of a zero value for R_L.

It is desirable to examine critically several paradoxical questions which arise in relation to this conclusion.

Experimentally, R_s is a linear function of $1/\sqrt{\omega}$. However, it is clear from Fig. 1 and equation [10] that this could not possibly be true unless C_d were negligible and hence considered as absent from the circuit. If this were true, $1/2\ R_L$ and θ would appear as two series resistances in a purely series circuit and would be indistinguishable. Yet when the validity of equation [26] was compared with that of equation $R_s^*C_s^*\omega = 1$, it was found that it made a great deal of difference whether θ or R_L was assigned a value of zero. This could only be true if C_d had a very appreciable influence.

The answer to this paradox emerges clearly from the following considerations. It can readily be shown that the following equation comes from Grahame's equations, equations [10] and [11], and the authors' equivalent circuit:

$$R_\Delta = \frac{2(\theta + \eta/\sqrt{\omega})}{1 + \eta C_d\sqrt{\omega} + C_d^2\omega^2\left(\theta^2 + \frac{\theta\eta}{\sqrt{\omega}} + \frac{2\eta}{\omega}\right)} \qquad [27]$$

The third term in the denominator is negligible so that, if C_d is to be negligible in the determination of R_Δ, it is necessary that

$$\eta C_d\sqrt{\omega} \ll 1 \qquad [28]$$

Similarly, it may be shown that if C_d is to be negligible in the determination of the quantity $C_s^*R_s^*\omega$, it is necessary that

$$\eta C_d\sqrt{\omega} \ll \frac{X}{\theta^2\omega + \eta^2 + X} \qquad [29]$$

where $X = \theta\eta\sqrt{\omega} + \eta^2$. Over the frequency range employed, the term on the right hand side of the inequality [29] is much smaller than unity and, therefore, condition [29] is much more difficult to satisfy than condition [28]. This fact explains the paradox and emphasizes that the required relation, $R_s^*C_s^*\omega = 1$, should give a sensitive test by which to distinguish between resistances occupying, respectively, the positions of θ and R_L in Fig. 1.

Another question which deserves brief consideration is this: if R_L results from a poorly conducting surface layer, why is it not shunted by a capacitance in Fig. 1? Considering that Vetter (14), like the authors, found no evidence that such a capacitance is appreciable, it may be concluded tentatively that such may well be the case. This is not unreasonable since one may readily calculate from the equation for a parallel plate condenser that, if the dielectric

constant of the electrode layer is about 15, then the minimum thickness of the layer required to render its capacitance negligible within limits of error and within the range of R_L values would be from 15 to 80 Å at 200 cps and proportionately larger at higher frequencies. Such layers could easily escape visual detection on electrodes like those used whose surfaces are dull, not shiny.

It has been pointed out that the data in Table IV compel one to conclude that an increase in the depolarizer concentration at constant ionic strength and constant redox ratio results in an increase of R_L. This is the reverse of the effect to be expected for θ, as is clear from Grahame's equation [24]:

$$\frac{\partial i}{\partial E} = \frac{1}{\theta} = (w_1 k_1 \alpha n^2 \mathbf{F}^2/RT) \exp(\alpha n \mathbf{F} E/RT)$$

$$+ [w_2 k_2 (1 - \alpha) n^2 \mathbf{F}^2/RT] \exp[-(1 - \alpha) n \mathbf{F} E/RT]$$

This is an additional reason for concluding that the extrapolated value $(R_s)_{\omega=\infty}$ is not 2θ.

Evidence unequivocally establishing the nature of R_L has not been presented, but it has been established that R_L: (*a*) is a resistance which is frequency-independent over the range 200 to 5000 cps, (*b*) has its seat at the electrode surface, (*c*) is of a magnitude dependent on the method employed in cleaning the electrodes, (*d*) increases with increase in depolarizer concentration at constant ionic strength and constant redox ratio, (*e*) decreases with increasing ionic strength at constant depolarizer concentration and constant redox ratio, and (*f*) fits best into the equivalent circuit as pictured in Fig. 1.

Points (*a*), (*b*), and (*f*) are in accord with the findings of Falk and Lange (19) in their studies on the resistance of thin electrode layers and with the experience of Vetter (14). Point (*c*) also suggests that R_L is an electrode layer resistance. Points (*d*) and (*e*) make it clear that part of the electrode layer is built up after the electrode is immersed in the solution and indeed this accords with observations that the impedance bridge readings became constant only after the electrodes had been immersed for about a half hour. Point (*d*) suggests that either the ferrocyanide or ferricyanide ions, or both, are adsorbed on the electrode and that the thicker or more complete layer which would form at higher concentrations impedes the electron transfer. Finally, point (*e*) might conceivably mean that the adsorbed layer is permeable to the supporting electrolyte. Beyond these suggestions the authors do not wish to venture at the present time.

Effect of Ionic Strength

Table V shows that an increase in ionic strength at constant depolarizer concentration and constant frequency results in an increase of C_s^*, while R_s^* usually rises slightly to a maximum and then falls comparatively rapidly. The maximum may not be real.

There is no theory which is even in semiquantitative accord with these experimental results. One theory, based on the diminution of coulombic interactions between the electrode and the depolarizer ions caused by an increase in ionic strength, this diminution being reflected in a decrease in the rate constant (13), is not acceptable. This is so because the electron transfer is not rate controlling. The possibility that ionic strength affects the activity coefficients of the depolarizer ions, thereby resulting in a thermodynamic effect, has also been considered. To test this possibility, the Debye-Hückel limiting law was used in connection with equations [11] and [17] and showed that the change of C_s^* with the ionic strength thus predicted occurred in a direction opposite to that observed experimentally. Of course the limiting law would not be expected to hold accurately at the concentrations used, but it is probably safe to conclude that the observed effect of ionic strength on C_s^* is not to be ascribed primarily to this thermodynamic influence.

There remains the possibility that alterations in ionic strength affect C_s^* because electrical migration of the depolarizer ions is not completely eliminated in any of the solutions of Table I except the one of highest ionic strength. This possibility could be investigated, at least in principle, by using Grahame's theory of the faradaic admittance (1) and developing the equations which would follow from that theory if electrical migration were not assumed to be absent. If it could be done and combined with the "thermodynamic effect" to give equations in accord with experimental observations, it would give a means of determining the charge type of the participating species in electro-redox reactions. Such information would be very valuable to those engaged in the study of redox mechanisms.

Acknowledgment

The authors wish to acknowledge with gratitude the generous financial support given to this research project by The Office of Naval Research.

Any discussion of this paper will appear in a Discussion Section to be published in the June 1956 Journal.

References

1. D. C. Grahame, *This Journal*, **99**, 370*C* (1952).
2. K. Rozental and B. Ershler, *Zhur. Fiz. Khim.*, **22**, 1344 (1948).
3. J. E. B. Randles, *Disc. Faraday Soc.*, **1**, 11 (1947).
4. H. Gerischer, *Z. physik. Chem.*, **198**, 286 (1951).
5. B. V. Ershler, *Zhur. Fiz. Khim.*, **22**, 683 (1948).
6. E. Warburg, *Ann. Physik. u. Chem.*, **67**, 493 (1899).

7. F. Krüger, *Z. physik. Chem.*, **45**, 1 (1903).
8. G. Jones and S. M. Christian, *J. Am. Chem. Soc.*, **57**, 272 (1935).
9. M. Wien, *Ann. Physik. u. Chem.*, **58**, 37 (1896).
10. S. Barnartt, *This Journal*, **97**, 235 (1950).
11. D. C. Grahame, *J. Am. Chem. Soc.*, **68**, 301 (1946).
12. H. Gerischer, *Z. Elektrochem.*, **55**, 98 (1951).
13. J. E. B. Randles, *Trans. Faraday Soc.*, **48**, 828, 937 (1952).
14. K. J. Vetter, *Z. phys. Chem.*, **199**, 285 (1952).
15. D. C. Grahame, *Chem. Revs.*, **41**, 441 (1947).
16. M. Shaw and A. E. Remick, *This Journal*, **97**, 324 (1950).
17. C. W. Miller, *Phys. Rev.*, [2], **22**, 622 (1923).
18. A. Slygin and A. Frumkin, *Acta Physicochim. U.R.S.S.*, **3**, 791 (1935).
19. G. Falk and E. Lange, *Z. Naturforsch.*, **1**, 388 (1946); *Z. Elektrochem.*, **54**, 132 (1950).
20. I. M. Kolthoff and J. J. Lingane, "Polarography," p. 52, Interscience Publishers, Inc., New York (1952).

Potentiometric Titrations in Liquid Ammonia

VIII. Mercury-Saturated Mercury(II) Chloride Working Reference Electrode[1,2]

GEORGE W. WATT AND DONALD M. SOWARDS

Department of Chemistry, The University of Texas, Austin, Texas

ABSTRACT

The results of an investigation of the mercury-mercury(II) halide electrode in liquid ammonia are reported. Variation of electrode potential with mercury(II) ion concentration was determined by measurement in concentration cells. These data have been interpreted and the activity coefficients of mercury(II) iodide, alone and in potassium iodide solutions, are estimated. Harned's rule was found to be obeyed in the mixed-electrolyte solutions.

It is shown that the mercury-saturated mercury(II) chloride electrode is a reversible electrode that rapidly establishes and maintains the same potential within limits which permit its use as a working reference electrode in liquid ammonia. The potential of this electrode with respect to the standard mercury-mercury(II) iodide electrode was found to be -0.068 ± 0.004 v.

A direct derivation of Harned's rule in functional form is illustrated and discussed. Variation of the coefficient α_{12} in dilute solutions is verified by experimental results, which also suggest that these coefficients are independent of solvent and dielectric constant, and are a function of temperature at higher concentrations.

INTRODUCTION

Previous work (1) shows that the difference indicator electrode is a satisfactory reference electrode for potentiometric titrations in liquid ammonia. However, the potential of this electrode was not found to be reproducible, which prohibits an accurate comparison of titration curves based on its potential. The low emf-sensitivity of measurements made with this electrode does not permit its use in cases where small changes in potential must be measured.

Concurrent with the characterization of the difference indicator electrode, equipment and procedures suitable for the study of simple electrodes in liquid ammonia were developed. It was also shown that the physical parameters of the cell, at least within the present limits, do not effect the results obtained.

Cady and Groening (2) found that, in iodide, chloride, and nitrate solutions, the mercury-mercury(II) ion electrode has a low metal-deposition overvoltage. Laitinen and Shoemaker (3) conducted a polarographic investigation of this electrode (the mercury pool anode) and found that the current-voltage relationship indicates a reversible two-electron electrode process[3] at $-36°C$. They also report that the electrode potential is a function of the mercury(II) ion concentration and is not influenced by nitrate, chloride, iodide, and ammonium ions. They confirm reported values (4, 5) for the potential of this electrode with respect to the lead-lead(II) nitrate electrode. An accurate calculation of the relative potentials in an electrochemical series in liquid ammonia is not possible, in most cases, because the activity coefficients are not known. The activity coefficient of mercury(II) iodide in a $0.1N$ solution has been estimated (5) to be 0.05.

This paper reports the results of measurements with various mercury-mercury(II) halide electrodes, and especially the mercury-saturated mercury(II) chloride electrode which is shown to be a reversible electrode with a rapidly attained, constant, known potential.

EXPERIMENTAL

The essential features of the cell and electrodes are shown in Fig. 1. Potentials were measured by the null method using equipment described elsewhere (1). The potential-measuring current was about 10 millimicroamp. The surface area of the metallic electrode elements in the reference electrodes was about 3 cm^2; that of the mercury pool, *c*, about 10 cm^2.

Reagent grade chemicals and triple-distilled mercury were used in this work. Ammonia and nitrogen were purified by scrubbing them through a solution of potassium in ammonia (1). All ammonia used in the cell was taken from cylinders where it was stored over sodium amide.

[1] Manuscript received December 15, 1954.

[2] For previous papers in this series, see reference (1).

[3] The mercury(I) ion is unstable in liquid or gaseous ammonia; reference (3) gives many references pertaining to this subject.

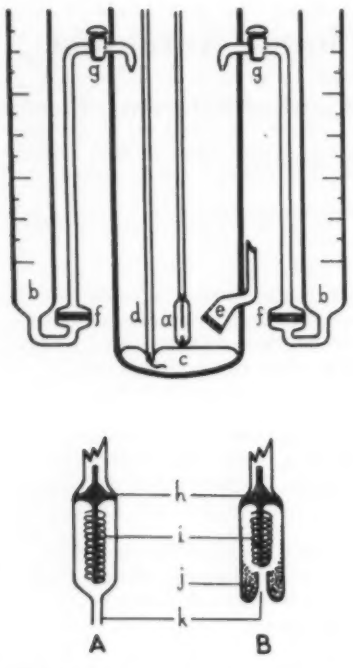

FIG. 1. Cell and electrodes. (*a*) Reference electrode assembly, *A* or *B* below; (*b*) burets; (*c*) mercury-pool electrode; (*d*) electrode lead; (*e*) fritted glass bubbler (stirrer); (*f*) fritted glass filter; (*g*) microstopcocks; (*h*) platinum lead sealed in Pyrex glass; (*i*) mercury electrode element supported on gold wire; (*j*) mercury(II) chloride; (*k*) capillary tube of about 0.6 mm OD.

The gas-scrubbing unit, burets, and cell were cleaned with aqua regia, rinsed with several portions of distilled water, rinsed with absolute ethanol, and dried. Potassium was placed in the scrubber, weighed quantities of electrolyte were put into the burets, mercury was put in the cell (at *c*), and the units were assembled. The entire system was evacuated to a pressure of 0.001 mm for several hours and then filled with gaseous ammonia at a reduced pressure. After ammoniation of the electrolyte was complete, the system was re-evacuated and filled with nitrogen. The nitrogen in the burets was replaced with a dilute solution of ammonia in nitrogen. Ammonia was next condensed in the gas-scrubbing unit until a 6–8 in. head of potassium solution obtained.

Standard solutions were prepared by condensing a measured volume of ammonia in the burets; the remaining gaseous ammonia was replaced with nitrogen. The transfer of solution from a buret to the cell was accomplished by regulating the nitrogen pressure above the solution in the buret. The pressure in the cell remained at about 5 mm above atmospheric pressure.

The temperature was −36.5°C, except where noted otherwise. It was determined with a toluene thermometer which had been checked at room temperature, the freezing point of water, and the normal boiling point of ammonia. The error in temperature measurement was probably less than 0.2°C and the variation of temperature during a series of measurements was usually less than 0.5°C.

Uncertainties in concentration are considered to be the major source of experimental error, which is estimated to be about 1%. The error is probably greater in solutions more dilute than 4 mM.

Mercury(II) halides may ammonolyze or ammoniate depending on conditions of exposure to ammonia; thus, some precautions are necessary in preparing solutions of these salts in liquid ammonia. Mercury(II) chloride was used in the working reference electrode because it reacts with ammonia to produce a single, electrochemically active mercury(II) ion species which has a desirable solubility. Further, traces of mercury(I) ion[4] react with ammonia to produce ultimately either this same mercury(II) ion species, $HgCl_2 \cdot 2NH_3$, or another, $HgNH_2Cl$, of considerably lower solubility (6).

Ammoniates of mercury(II) chloride and bromide are not sufficiently soluble to permit preparation of concentrated solutions of these salts. On the other hand, more care must be exercised with mercury(II) iodide if ammonolysis is to be prevented. When an evacuated system containing mercury(II) iodide is suddenly filled with gaseous ammonia at atmospheric pressure, the salt ammonolyzes irreversibly to produce a fused red material of relatively low solubility in liquid ammonia. Solutions of this compound undergo a gradual decomposition which is evident because of the simultaneous precipitation of a rust colored solid, probably Hg_2NI (7). Even though these solutions are stabilized by dilute ammonium iodide, they are not satisfactory for the type of work described below.

When mercury(II) iodide is exposed to ammonia either diluted with nitrogen or at a reduced pressure, the familiar $HgI_2 \cdot 2NH_3$ is produced slowly. It has a rather high decomposition pressure (7) and may be decomposed simply by reducing the pressure. At −35°C, this ammoniate, in the presence of gaseous ammonia, changes to a colorless solid which is probably $HgI_2 \cdot 4NH_3$ (7). Repeated ammoniation and deammoniation did not appear to influence the electrochemical activity of the species occurring in solutions of the ammoniated salt; thus, it was considered suitable for use in the present study.

Solutions of mercury(II) acetate produce a much smaller change in potential with changing concen-

[4] Mercury(II) ion reacts with the mercury at the electrode to produce mercury(I) ion unless the electrode is filled with ammonia. Therefore, it is desirable to store the electrode in an ammonia atmosphere.

tration than solutions of mercury(II) halides. Further, as potassium bromide or iodide solution is added to mercury(II) acetate solution, the change in potential indicates an initial increase in activity followed by a decrease as more halide solution is added. Also, it was observed that mercury(II) halide solutions containing traces of water were less active than anhydrous solutions, which is contrary to a previous report (3). It is evident that there is extensive and specific interaction of mercury(II) ion with the various species present in these solutions.

Solutions of dipotassium tetraiodomercurate(II) 2-hydrate were found to be similar in electrochemical activity to solutions of ammoniated mercury(II) iodide containing traces of water. Both of these, as well as solutions of di-(tetra-*n*-butylammonium) tetraiodomercurate, decomposed to produce ammoniated mercury(II) iodide and the other iodides when the liquid ammonia evaporated. The latter anhydrous compound is quite stable, while the corresponding potassium salt usually decomposes on dehydration. These observations, as well as the results of electrical measurements in the mixed-iodide solutions, suggest that the triiodomercurate and tetraiodomercurate ions are not present in solution.

The results in this work were obtained using three types of concentration cells with homoionic liquid junctions:

$$\mathrm{Hg} \mid \mathrm{HgI_2}\ (C_T) \parallel \mathrm{HgI_2}\ (C_R) \mid \mathrm{Hg} \qquad (p)$$

$$\mathrm{Hg} \mid \mathrm{HgI_2}\ (C_{1T}),\ \mathrm{KI}\ (C_{2T}) \parallel \mathrm{HgI_2}\ (C_{1R}),\ \mathrm{KI}\ (C_{2R}) \mid \mathrm{Hg} \qquad (q)$$

$$\mathrm{Hg} \mid \mathrm{HgX_2}\ (C_{1T}),\ MX'\ (C_{2T}) \parallel \mathrm{HgX_2}\ (C_s),\ MX'\ (C_{2R}) \mid \mathrm{Hg} \qquad (r)$$

where M is Na or K ion, X and X' are halide ions which are not necessarily the same, C is molar concentration, subscripts T and R distinguish between the electrodes at c and a, respectively (Fig. 1), and 1 and 2 indicate the electrolyte in mixed-electrolyte solutions. Cells (p) and (q) involve the use of electrode A of Fig. 1, while cell (r) utilizes electrode B with C_s as the saturation concentration.

In a typical series of measurements, solution of composition C_R (or $C_{1R} - C_{2R}$) was prepared in the cell by appropriate additions from the burets. The reference electrode, which had previously been evacuated and filled with gaseous ammonia, was inserted in the solution. Gaseous ammonia condensed, thereby completely filling the electrode compartment with solution. Additions were then made to the cell to give a series of solutions of composition C_T ($C_{1T} - C_{2T}$). The solution was stirred with nitrogen at e in Fig. 1.

Interpretation of Data and Results

Because the experimental error is relatively large, experimental data are not tabulated here; rather, the method of interpretation and the results of its application are given.

Mercury-saturated mercury(II) chloride electrode.— The reproducibility of the potential of this electrode (Fig. 1*A*) was determined by measuring its potential with respect to a series of Hg-HgX_2 (C_{1T}) electrodes, where C_{1T} had a sufficient number of values between 0.2 and 5.0 mmolar for the construction of the log C_{1T} vs. potential curve. These measurements were made at random times, with electrodes in general use, and under conditions of present use of reference electrodes in this laboratory, i.e., varying the supporting electrolyte and its concentration, and with minor variations in temperature. Since mixed mercury(II) halides are present in the electrode whenever it is reused, results are reported for both newly prepared (New) and previously used (Reused) electrodes. (In general, the reuse of this kind of electrode is not recommended; it is quite easy to clean and recharge.) The mercury(II) halide used at electrode T was also varied to determine whether any significant deviation dependent upon halide ion occurred.

The log C_{1T} vs. potential curves show a slight curvature, but they are sufficiently linear to permit a short range interpolation. Thus, the potential of the Hg-$HgCl_2$ (sat'd) electrode vs. a Hg-Hg^{2+} (0.001 m) electrode was found for a number of conditions. Results are shown in Table I. The slope of the curves from which these data were taken shows no unaccounted for deviation from the theoretical slope calculated for a two-electron electrode process; average deviation is 0.0005, maximum deviation is 0.0015. The emf-sensitivity of the measurements

TABLE I. *Reproducibility of the potential of the* Hg-$HgCl_2$ *working reference electrode*

Reference electrode No.	MX'	C_{1T} mM	Reference potential vs. Hg-HgX_2 (1 mM) electrode (v)	X	Temp °C
1 New	KBr	93	0.012	Br	−38
1 Reused	KI	94	0.020	I	−36
2 New	KCl	16[a] (sat'd)	0.016	$C_2H_3O_2$	−37
2 Reused	NaCl	98	0.013	I	−36
2 Reused	KBr	37	0.019	Br	−34
3 New	KBr	13	0.017	Br	−36
4 New	KBr	18	0.019	Br	−38
4 Reused	KI	79	0.014	I	−41

Avg: 0.016 ± 0.004 v.

[a] See reference (12).

was about 0.05 mv and the potential was observed to remain constant to within 0.1 mv for 1-hr periods.

The concentration of a saturated solution of mercury(II) chloride was determined by potentiometric titration of a measured volume of saturated solution with standard potassium solution in liquid ammonia. The average of three determinations based on the reaction

$$HgCl_2 + 2K \rightarrow Hg + 2KCl$$

was $C_s = 0.019 \pm 0.004$ moles/l at $-37°C$. Using the activity coefficient below (from Fig. 3), the potential of the mercury-saturated mercury(II) chloride electrode vs. the standard mercury-mercury(II) iodide electrode is -0.070 ± 0.001 v. This compares quite favorably with the value of -0.067 ± 0.004 v calculated from the data of Table I.

An electrode similar to that in Fig. 1*B* was constructed with a cadmium electrode element, *i*, and containing cadmium(II) chloride at *j*. This was used as the reference electrode for the determination of the log C_{1T} vs. potential curve for mercury(II) iodide in a cell of type (*p*) with no supporting electrolyte present. The solubility of $CdCl_2$ at 25°C is 0.001 moles/l (8) and is probably about one-tenth of this at −36°C. Using the limiting law activity coefficients (see below) for these concentrations, the potential of the standard Cd-$CdCl_2$ electrode with respect to the standard Hg-HgI_2 electrode is calculated to be −0.93 v. This compares favorably with the reported value (5) of −0.933 v at −50°C.

In the course of measurements with the Hg-sat'd $HgCl_2$ electrode, potentials with respect to the (Pt)H_2-NH_4Br, Pb-$PbCl_2$, and (Pt)K-KBr electrodes at −37°C were found to agree with the reported values (5) at −50°C. However, data for these comparisons were obtained in the course of other work and values within 0.05 v were considered to be in agreement.

The Hg-$HgCl_2$(sat'd) electrode attains a constant potential within 30 min after it is filled. The electrode recovered from the effects of short-circuiting and the application of 1 v for 15 sec within 1 min. For these and reasons mentioned below, this is considered to be a reversible electrode in so far as its use as a working reference electrode is concerned.

Activity of mercury(II) iodide in liquid ammonia solutions.—The relationship of potential E and electrolyte activity a for a concentration cell is

$$E = 2.303 \frac{RT}{n\mathbf{F}} \log (a_T/a_R) \equiv 1/K \log (a_T/a_R) \quad (I)$$

where R is the gas constant, T is the absolute temperature, n is the electron change in the electrode process, $\mathbf{F}$ is the faraday, the subscripts T and R distinguish between the electrodes in the cell, and K is as shown.

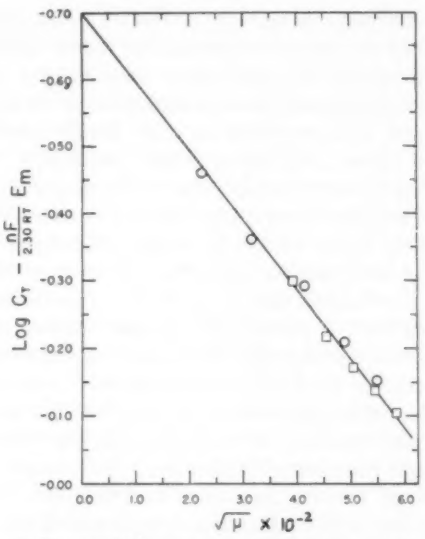

FIG. 2. Extrapolation curve according to equation (II). —— extrapolation used, slope −9.70. □ scale reading −3.284; ○ scale reading −5.290.

If the potential measured, E_m, differs by a constant factor, E_e, from the cell potential, E [with the usual assumptions concerning single ion activities and the distinction of the potentials in cells with transference (9*a*)] equation (I) gives

$$-\log f_T + (\log a_R - KE_e) = \log C_T - KE_m \equiv Y \quad (II)$$

where f is the mean molar activity coefficient, C is the molar concentration, and Y is as shown.

The results of measurements in cell (*p*) are expressed as Y and shown as a function of the square root of the ionic strength, $\sqrt{\mu}$, in Fig. 2. The parenthetical term on the left side of equation (II) was evaluated by extrapolation in Fig. 2 and substituted with Y into equation (II) to find values of the activity coefficients. The activity coefficients were applied to the reference electrode solution and E_e was found. It is a function of the concentration of the electrolyte in the electrode compartment: C_R, mmolar, 0.16, 0.31, 0.36, 1.35; E_e, mvolts, 24.5, 7.5, 4.5, 2.5. This is the result which is expected if the major part of E_e is attributed to a resistance in the cell solution. It should be noted that in the present cell over nine-tenths of the electrolyte between the electrodes does not change during a series of measurements because it is confined to the electrode compartment and connecting tube. The tip of this tube was always within 1 mm of the surface of electrode *c* (Fig. 1); thus the connecting-solution resistance remains essentially constant. No account has been

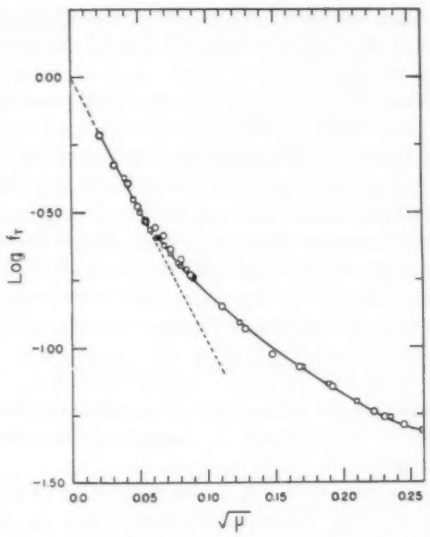

FIG. 3. Logarithm of the activity coefficient of mercury (II) iodide as a function of the square root of the ionic strength.

taken for the effects of the junction potential, except for its possible inclusion in E_e.

For measurements at higher concentrations, it is desirable to increase C_R in order to increase the electrical conductivity of the connecting solution, minimize the effects of large concentration gradients, and further lessen the chances of concentration polarization during measurement. Results at higher concentrations cannot be dealt with by means of the extrapolation procedure discussed above. In this case, the cell has been such that C_R is in the concentration range of Fig. 2. Thus, with $C_R = C_T$, the initial point in a series of measurements at high concentrations has been adjusted to data for dilute solutions. The parenthetical term on the left side of equation (II) was thus calculated and applied to the remaining data. The results of measurements over both concentration ranges are illustrated in Fig. 3. The adjusted values are represented by the solid points. The experimental curve continues in the suggested direction to $\sqrt{\mu} = 0.35$, the highest concentration measured. It is noted that $f_T = 0.05_5$ for $0.1N$ HgI_2 which is in almost exact agreement with Pleskov's (5) estimated value, 0.05.

Activity of mercury(II) iodide in potassium iodide solutions.—Previous work (1) as well as the results above indicate that for C_R greater than about 10 mM, $E_e \approx 0$. In this case equation (II) may be rearranged to give

$$\log C_{1R} - Y = \log f_{1T}/f_{1R} \qquad \text{(III)}$$

The results of measurements in cell (q) and at constant ionic strength, $\mu = \mu_{1T} + \mu_{2T}$, are seen in Fig. 4 to obey Harned's rule (10*a*)

$$\log f_{1T} = \log f_{(0)1} + \alpha_{12}\mu_{1T} = \log f_{1(0)} - \alpha_{12}\mu_{2T} \qquad \text{(IV)}$$

where $f_{(0)1}$ is the activity coefficient of mercury(II) iodide at infinite dilution in a solution of potassium iodide of ionic strength μ, $f_{1(0)}$ is the activity coefficient of mercury(II) iodide in a solution of ionic strength μ, α_{12} is a constant which is discussed below, μ_{1T} is the contribution of the mercury(II) iodide to the ionic strength of the solution, μ_{2T} is the contribution of the potassium iodide to the ionic strength of the solution, and f_{1T} is the activity coefficient of the mercury(II) iodide (in the mixed electrolyte solution).

It was found that a variation greater than 1% in the total ionic strength resulted in excessive distortion of the linear relationship shown in Fig. 4. The value of α_{12} may be found without specific knowledge of the activity coefficients on the basis of equation (III). This permits a calculation of the ratio of the limiting activity coefficients; thus, with the value of $f_{1(0)}$ or f_{1R}, all of the terms in equation (IV) may be evaluated.

Reversibility of the mercury-mercury(II) iodide electrode.—In all measurements with electrode A, there has been only one indication that the electrode was not behaving reversibly (9*b*); in most instances there was a potential of from 0.1 to 1 mv when identical solutions were at each electrode. This potential appeared to be reproducible and a function of the electrolyte concentration at concentrations less than about 5 mM. With total electrolyte concentrations above 0.1 m, the potential was zero for this condition. In the intermediate concentration range, the potential was small and unpredictable.

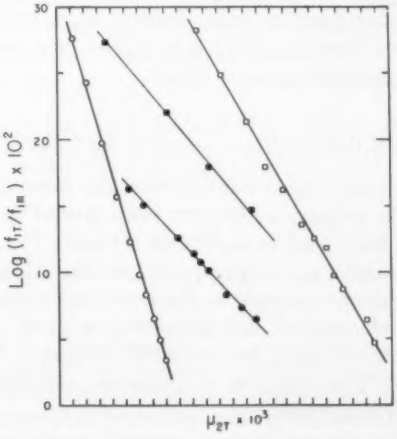

FIG. 4. Logarithm of the activity coefficient of mercury (II) iodide in solution with potassium iodide at constant total ionic strength as a function of the ionic strength of the mercury(II) iodide. Total ionic strength; ○, 15.5 mmolar; ●, 50.6 mmolar; ■, 121 mmolar; □, 322 mmolar.

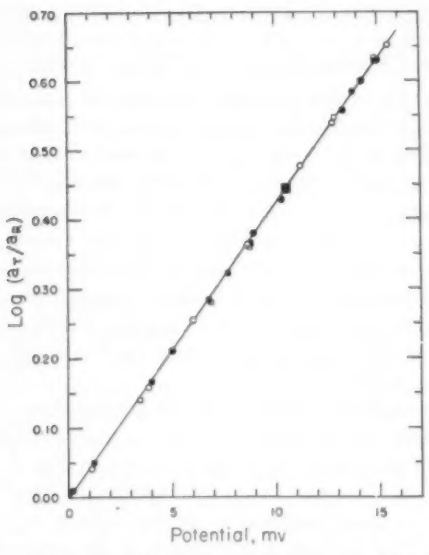

FIG. 5. The potential of the mercury-mercury(II) iodide electrode as a function of the logarithm of the activity of mercury(II) iodide. ●, No co-solute; with potassium iodide at a constant ionic strength of 15.5 mmolar ○, 50.6 mmolar ■, 322 mmolar □.

It is thought that the major part of the potential is attributable to the solution resistance, especially in the dilute solutions.

On the other hand there are many indications that the electrode was behaving reversibly. As with the previous electrode, within 20 min after the electrode was filled, the potential was constant; when the electrodes were short-circuited, they recovered within a few minutes. Vigorous stirring or stagnant conditions had no apparent effect on the measured potential. The equilibrium potential was attained within 2 or 3 min after the solution composition was changed. Equation (IV) substituted into equation (III), on rearrangement, gives

$$E_m = E = 1/K\,(\log f_{1(0)}/f_{1R} - \alpha_{12}\mu_{2T} + \log C_{1T}/C_{1R}) \quad \text{(V)}$$

which is the Nernst relation with the present notation. The activity coefficients taken from Fig. 3 and 4 have been used in equations (I) and (V); results are adjusted to a common scale by the addition of the required constants to the equations in order to show the results on a single plot (Fig. 5). It is seen that this criterion for reversible behavior is also satisfied. The electrode is, therefore, considered to be behaving reversibly.

DISCUSSION

While the purpose of this paper is to demonstrate the utility of the Hg-$HgCl_2$ (sat'd) working reference electrode and report its potential, several observations have been made during the course of this study that are of sufficient general interest to warrant further comment.

In spite of the relatively large experimental error and the possible oversimplification in interpretation of the data, the linear relationship shown in Fig. 2 strongly suggests that the Debye-Hückle limiting law is applicable to solutions of this electrolyte with concentrations as high as 1 mM. For a dielectric constant of 22 (11) and a temperature of −36.5°C, the limiting law for an electrolyte with cations of valence z_c and anions of valence $-z_a$ is

$$-\log f = 4.85\, z_c\, z_a \sqrt{\mu} \quad \text{(VI)}$$

which results in a slope in exact agreement with that in Fig. 2. This degree of agreement is probably fortuitous.[5]

Results shown in Fig. 3 are suggestive of a high degree of ionic interaction which is not an unexpected result for solutions of electrolytes that produce small ionic species in media of low dielectric constant. The curve is not amenable to expression over any appreciable concentration range by the usual one or two parameter equations. Because of results obtained in solutions which also contained relatively high concentrations of potassium iodide, results in Fig. 3 are attributed to extensive interaction of mercury(II) ion with the solvent. This conclusion has been suggested for both silver(I) and mercury(II) ions in ammonia and was an important factor for the previous low estimate of the activity coefficient of mercury(II) iodide (5). However, as is shown below, there is specific interaction between ammoniated mercury(II) and iodide ions in these solutions.

Previous discussion (10*b*) of the thermodynamic theory of mixed electrolyte solutions is based on the assumed validity of Harned's rule. There appears to be little mention in the literature of the possible direct derivation of this rule and its connection with the thermodynamic theory of single electrolyte solutions, except for the implications of its application. Thus, it has been shown (10*c*) that α_{13} and α_{23} in

$$\log f_{13} = \log f_{(0)1} + \alpha_{13}\mu_{13} = \log f_{1(0)} - \alpha_{13}\mu_{23} \quad \text{(VII)}$$

$$\log f_{23} = \log f_{(0)2} + \alpha_{23}\mu_{23} = \log f_{2(0)} - \alpha_{23}\mu_{13} \quad \text{(VIII)}$$

are thermodynamically connected through the activity coefficients or osmotic coefficients of single electrolyte solutions. Here the notation is as in equation (IV) except for the subscripts 13 and 23 which

[5] Sedlet and DeVries [*J. Am. Chem. Soc.*, **73**, 5808 (1951)] report a value of 23.8 for the dielectric constant of ammonia at −36°C, which results in a limiting law constant of 4.31. However, the specific electrical conductivity of the ammonia used in those measurements suggests that the solvent was contaminated [cf. reference (12)].

refer to the electrolyte in question on the basis of its being composed of cation 1 or 2 and anion 3 (which is common to both salts). It has also been shown *a posteriori* that the α's are coefficients of ionic strength rather than concentration terms (13) and that they are essentially independent of concentration in the range between 0.5 and 5M (14). From studies in aqueous methanol it was suggested that the α's are independent of the dielectric constant of the medium and dependent on the temperature (15).

Guggenheim (16) developed Brönsted's principle of specific interaction (17) to produce an expression that accounts for the individual characteristics of electrolytes and reduces naturally to the limiting law at high dilutions; thus for 1:1 electrolytes, for example, there results

$$\log f = \frac{A\sqrt{C}}{1 + \beta\sqrt{C}} + \beta_n C \qquad \text{(IX)}$$

Here, the first term on the right is the familiar Debye second approximation and β_n is a constant "interaction coefficient" which may take any value depending on the nature of the electrolyte and the value of β chosen. For the sake of simplicity, Guggenheim arbitrarily gave β the value 1 and made all of the specific properties of electrolytes appear in the β_n term. Equation (IX), when applied in this way, yields accurate activity coefficients for concentrations as high as 0.1M; further, this equation is applicable to mixed electrolyte solutions. Objections to this expression (10*d*) have been directed to the choice of standard electrolyte, i.e., setting β equal to unity. However, such a choice is not a necessity and β may be considered to be either an experimental or theoretical parameter with limited adjustibility.

The working equation arrived at by Guggenheim (16*b*) considers only the interaction of cations R and anions X, and may be expressed as

$$G^{el} = G^{sta} + (kT/V)\,\Sigma_{R,X} N_R N_X \nu_{R,X} \qquad \text{(X)}$$

where G^{el} is the contribution of interionic potential to the (Gibbs') free energy of the electrolyte; G^{sta} is the contribution of the perfect Debye-Hückle electrolyte chosen as standard electrolyte to G^{el} and has the property

$$(1/2.303\ kT)\,\frac{\partial G^{sta}}{\partial N_i} = \frac{A\sqrt{\mu}}{1 + \beta\sqrt{\mu}} \equiv \log f^{sta} \qquad \text{(XI)}$$

with k, the Boltzman constant; T, the absolute temperature; V, the volume in liters; N_i, any ion; and $\nu_{R,X}$ is a coefficient based on the attractive forces between anions and cations, and which depends only on the temperature and the solvent. The original discussion of this equation should be consulted for further details.

An expression for the activity coefficients of the electrolytes in the mixed electrolyte solutions involved in the present studies may be found by taking the partial derivative of G^{el} with respect to N_i in equation (X). In this case $2N_1 + N_2 = N_3$ and for the condition of constant ionic strength $3N_1 + N_2 = I$ = a constant which is a function of the ionic strength. Using the previous (16*b*) definition of the interaction coefficient: $\beta_{RX} = 1/2N\ 10^{-3}\ \nu_{R,X}$, where N is the Avogadro constant, there results at constant temperature[6]

$$\log f_{13} = \log f_{13}^{sta} + B(\beta_{13} - 4\beta_{23})\mu + 2B\left(\beta_{23} - \frac{\beta 13}{3}\,\mu_{13}\right) \qquad \text{(XIIa)}$$

$$= \log f_{13}^{sta} + B\left(\frac{\beta 13}{3} - 2\beta_{23}\right)\mu - 2B\left(\beta_{23} - \frac{\beta 13}{3}\right)\mu_{23} \qquad \text{(XIIb)}$$

$$\log f_{23} = \log f_{23}^{sta} + B\left(\frac{4}{3}\beta_{23} - \frac{\beta 13}{3}\right)\mu - 2B\left(\frac{\beta 23}{3} - \frac{\beta 13}{9}\right)\mu_{13} \qquad \text{(XIIIa)}$$

$$= \log f_{23}^{sta} + B\left(\frac{2}{3}\beta_{23} - \frac{\beta 13}{9}\right)\mu + 2B\left(\frac{\beta 23}{3} - \frac{\beta 13}{9}\right)\mu_{23} \qquad \text{(XIIIb)}$$

where $B = 2/2.303$. The other terms are defined above.

Comparison of equations (VII) and (VIII) with (XII) and (XIII) shows that they are identical in the functional relationship between $\log f_{13}$ and $\log f_{23}$, and μ_{13} and μ_{23}. According to equations (XII) and (XIII), the terms of equations (VII) and (VIII) are functions of the interaction coefficients, thus

$$\log f_{(0)1} = \log f_{13}^{sta} + 2/2.303\ (\beta_{13} - 4\beta_{23})\mu \qquad \text{(XIVa)}$$

$$\log f_{1(0)} = \log f_{13}^{sta} + 2/2.303\left(\frac{\beta 13}{3} - 2\beta_{23}\right)\mu \qquad \text{(XIVb)}$$

[6] The present derived functional relationship results, in general, for mixed electrolyte solutions containing a single anion (cation) species and cations (anions) of different valence. For similar results with mixed electrolytes of the same valence, it is necessary to include in equation (X) terms accounting for solvent-ion, cation-cation, or anion-anion interaction. Harned [ref. (10), p. 466] has pointed out the implications inherent in neglecting the solvent-ion interaction term. Its importance has long been recognized. It first appeared in Hückle's [*Physik. Z.*, **26**, 93 (1925)] extension of the limiting law and has recently been discussed by Scatchard and Breckenridge [*J. Phys. Chem.*, **58**, 596 (1954)].

$$\log f_{(0)2} = \log f_{23}^{\text{sta}} + 2/2.303 \left(\frac{2}{3}\beta_{23} - \frac{\beta 13}{9}\right)\mu \quad \text{(XV}a\text{)}$$

$$\log f_{2(0)} = \log f_{23}^{\text{sta}} + 2/2.303 \left(\frac{4}{3}\beta_{23} - \frac{\beta 13}{3}\right)\mu \quad \text{(XV}b\text{)}$$

$$\alpha_{13} = 4/2.303 \left(\beta_{23} - \frac{\beta 13}{3}\right) \quad \text{(XIV}c\text{)}$$

$$\alpha_{23} = 4/2.303 \left(\frac{\beta 23}{3} - \frac{\beta 13}{9}\right) \quad \text{(XV}c\text{)}$$

Of course such term by term correspondence is no more than a necessary condition for the interpretation of Harned's rule in terms of interaction. The comparison may be carried further. Thus, Harned's recent generalization (18) is complied with

$$z_{c(1)}\ \alpha_{23} + \alpha_{13} = \text{constant} \neq \text{function of } \mu \quad \text{(XVI)}$$

The α's are explicitly coefficients of ionic strength rather than general concentration terms, if consistent values of α are to be calculable from (a) and (b) in equations (XII) and (XIII). The α's also have no obvious dependence on ionic strength or concentration. While the cross-differentiation relations at constant molalities (19) cannot be found without further generalization or actual experimental values, the relationship

$$(\partial \log f_{13}/\partial N_2)_\mu = (\partial \log f_{23}/\partial N_1)_\mu$$

is satisfied, thus indicating that equations (XII) and (XIII) are self-consistent.

There is an explicit difference between $f_{(0)R}$ and $f_{R(0)}$ according to equations (XIV) and (XV), even if the f^{sta}'s are all considered to be the same. Also, the relationships

$$\log (f_{1(0)}/f_{(0)1}) = \alpha_{12}\mu \quad \text{(XVII}a\text{)}$$

$$\log (f_{2(0)}/f_{(0)2}) = \alpha_{23}\mu \quad \text{(XVII}b\text{)}$$

result from the accumulation of terms in either (a) and (b) of (XII) and (XIII), or (a), (b), and (c) of (XIV) and (XV), respectively.

On the basis of the above interpretation, the results in Fig. 4 suggest that there is specific cation-anion interaction in these solutions; this is not an unexpected result. The previous suggestion (10e) that the α's vary at low total ionic strength is conclusively established for these solutions. In fact, from (XVIIa), the plot of log α_{12} vs. log μ should be a straight line with a slope of -1 if the term on the left side of the equation is constant. This is seen in Fig. 6 to be the result obtained using the data from

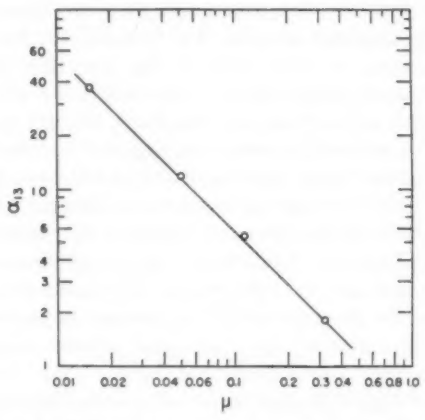

FIG. 6. Logarithm of α_{13} as a function of the logarithm of the total ionic strength in mixed-electrolyte solutions.

Fig. 4. This variation of α_{12} with ionic strength is in agreement with the conclusions of McKay and Perring (20), although, their complete expression is different from the above. Also, Glueckauf (21) suggests that Guggenheim's approach may be applied with the assumption that β_n of equation (IX) is a function of the concentration, the β_n's being eliminated from the working equation derived. The ultimate expression is found to be applicable over a large concentration range for the cases used as illustrations.

A limited comparison of the present results with those general to aqueous solutions is possible. Harned (18) reports that $\alpha_{13} = 0.085$ for aqueous $SrCl_2$-HCl solutions, $\mu = 3$ to 5. Using the temperature coefficient of α from results in the HCl-NaCl-aqueous methanol system (15), α_{13} in the present case should be about 0.12. Extrapolation of the curve in Fig. 6 yields a value of 0.15 for this μ range in the HgI_2-KI-ammonia system. This is quite good agreement considering the nature of the comparison; it indicates that α_{12} is independent of the solvent as well as the dielectric constant of the medium. This conclusion was not entirely evident in previous work (15) since the aquated ions were present in all of the solutions.

Further application of the equations above is not possible at this time because of the limited amount of data; the present result is certainly sufficient in general applicability to conclude that Harned's rule is obeyed in these liquid ammonia solutions. The present interpretation of theory to obtain the parameters of this rule in terms of interaction coefficients is consistent with previous usage (10) and does not restrict the present applications of the rule. The conclusions offer a direction of attack and point out further the necessity for considering the interaction coefficients as variable parameters in dilute solutions, at least.

ACKNOWLEDGMENTS

This work was supported in part by the Atomic Energy Commission, Contract AT-(40-1)-1639. The liquid ammonia employed in these studies was generously supplied by the Polychemicals Department, E. I. du Pont de Nemours and Company, Wilmington, Delaware.

Any discussion of this paper will appear in a Discussion Section to be published in the June 1956 JOURNAL.

REFERENCES

1. G. W. WATT AND D. M. SOWARDS, *This Journal*, **102**, 46 (1955).
2. H. P. CADY AND A. A. GROENING, *J. Phys. Chem.*, **30**, 1597 (1926).
3. H. A. LAITINEN AND C. E. SHOEMAKER, *J. Am. Chem. Soc.*, **72**, 663 (1950).
4. F. M. G. JOHNSON AND N. T. M. WILSMORE, *Trans. Faraday Soc.*, **3**, 77 (1907).
5. V. A. PLESKOV AND A. M. MONOSSOHN, *Acta Physicochim. U.R.S.S.*, **1**, 871 (1935).
6. S. D. ARORA, W. N. LIPSCOMB, AND M. C. SNEED, *J. Am. Chem. Soc.*, **73**, 1017 (1951).
7. E. C. FRANKLIN, *ibid.*, **29**, 35 (1907).
8. C. S. GARNER, E. W. GREEN, AND D. M. YOST, *ibid.*, **57**, 2055 (1935).
9. G. KORTÜM AND J. O'M. BOCKRIS, "Textbook of Electrochemistry," Elsevier Publishing Co., New York (1951), (*a*) p. 269, (*b*) p. 581.
10. H. S. HARNED AND B. B. OWEN, "The Physical Chemistry of Electrolytic Solutions," Reinhold Publishing Corp., New York (1943), (*a*) p. 459, (*b*) p. 461, (*c*) p. 462 ff, (*d*) p. 387, (*e*) p. 468.
11. C. P. SMYTH, "Dielectric Constant and Molecular Structure," Chemical Catalog Co., New York (1931).
12. C. A. KRAUS AND V. F. HNIZDA, *J. Am. Chem. Soc.*, **71**, 1565 (1949).
13. H. S. HARNED AND C. M. MASON, *ibid.*, **53**, 3377 (1931).
14. G. AKERLOF AND H. C. THOMAS, *ibid.*, **56**, 593 (1934).
15. G. AKERLOF, J. TEARE, AND H. TURCK, *ibid.*, **59**, 1916 (1937).
16. (*a*) E. A. GUGGENHEIM, *Phil. Mag.*, **19**, 588 (1935); (*b*) E. A. GUGGENHEIM AND R. H. FOWLER, "Statistical Thermodynamics," p. 416 ff, Cambridge University Press, New York (1952).
17. J. N. BRÖNSTED, *J. Am. Chem. Soc.*, **44**, 877 (1922).
18. H. S. HARNED, *J. Phys. Chem.*, **58**, 683 (1954).
19. E. GLUECKAUF, H. A. C. MCKAY, AND A. MATHIESON, *J. Chem. Soc.*, **1949**, S 299.
20. H. A. C. MCKAY AND J. K. PERRING, *Trans. Faraday Soc.*, **49**, 163 (1953).
21. E. GLUECKAUF, *Nature*, **163**, 414 (1949).

Technical Note

The Electrodeposition of Lead from Lead Phenol Sulfonate Solutions[1]

HARRY C. GATOS[2] AND FRANK C. MATHERS

Indiana University, Bloomington, Indiana

INTRODUCTION

Organic lead sulfonates are suitable for lead electroplating because they are stable, easily prepared, sufficiently soluble in water, and their aqueous solutions exhibit satisfactory electrical conductivity. This suitability for electroplating was recognized long ago (1), but further investigation has been limited. This could be attributed to the fact that the quality of lead electrodeposits obtained from aqueous solutions of lead sulfonates in the absence of suitable addition agents is unsatisfactory (2). Successful results have been reported with aqueous solutions of lead ethylbenzenesulfonate (3) and lead toluolsulfonate (4) by employing various addition agents. Sulfonate baths have the distinct advantage of being far less hazardous in handling than the commonly used fluoborate or fluosilicate baths.

LEAD PHENOL SULFONATE BATHS AND EXPERIMENTAL TECHNIQUES

Solutions of lead phenol sulfonate were prepared by neutralizing phenol sulfuric acid with lead carbonate. Insoluble lead sulfate formed by the free sulfuric acid present in the phenol sulfuric acid was filtered, and the solution was diluted with water. From this solution the final electroplating bath was prepared containing 40 g/l of lead and 70 g/l of free sulfonic acid. About 100 ml of the solution was used in each experiment.

Lead anodes (5 x 3.5 x 1 cm) were cast in a graphite mold. The cathodes were 6.3 cm^2 sheets of mild steel. They were pickled with dilute hydrochloric acid, washed thoroughly with tap and distilled water, and dried before using. The anode and cathode were suspended by thin copper wire and were approximately 3 cm apart.

During electrolysis the baths were gently stirred. Slime formed from the anodes remained at the bottom of the beakers and was not disturbed by the stirring. All experiments were performed at room temperature and 2.8 amp/dm^2 (26 amp/ft^2).

About 150 combinations of 40 different addition agents and 30 single addition agents were employed.

Addition agents were used in quantities sufficient to obtain maximum beneficial action. Usually this was accomplished with 0.1–0.2 g of solid and 1–5 ml of liquid addition agents per 100 ml of electrolyte. In some cases as much as 10 g/100 ml were employed, but to no considerable advantage. Relatively insoluble addition agents were added in sufficient quantities to insure saturation.

The time of continuous electrolysis was varied. If the electrodeposits appeared treelike, very crystalline, or nonadherent, electrolysis was interrupted within the first 24 hr, whereas in the case of adherent deposits it was carried on usually for 7–8 days.

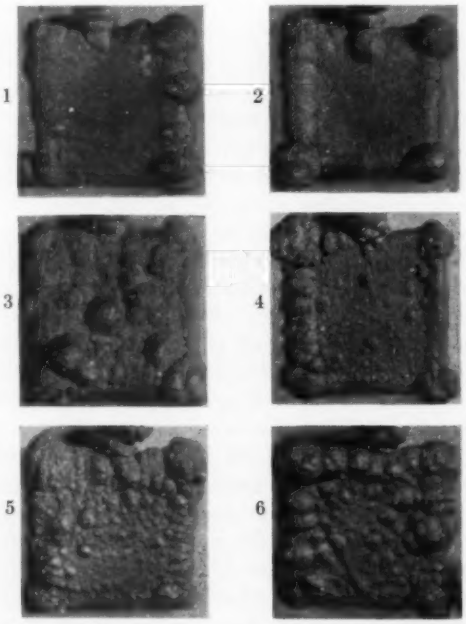

FIG. 1. Lead electrodeposits obtained from 100 ml lead phenol sulfonate electrolyte[3] at 26 amp/ft^2 (2.8 amp/dm^2) in the presence of the following addition agents: 1—0.1 g aloes residue, 0.2 g furfural polymer, and 0.2 g goulac; 2—0.1 g aloes residue and 0.2 g furfural polymer; 3—0.1 g aloin residue, 2 cc *p*-cresol, and 0.2 g goulac; 4—0.2 g goulac and 2 cc eugenol; 5—5 cc *p*-cresol; 6—0.1 g aloes residue and 0.2 g pyrogallol.

[1] Manuscript received October 26, 1954. This paper was prepared for delivery before the Boston Meeting, October 3 to 7, 1954.

[2] Present address: Engineering Research Laboratory, Engineering Department, E. I. du Pont de Nemours and Co., Inc., Wilmington, Delaware.

TABLE I. *Effect of combinations of addition agents on lead electrodeposits*

No.	Addition agents	Type of electrodeposit
1	0.1 g aloes residue 2 cc *p*-cresol 0.2 g goulac	Smooth and adherent
2	0.1 g aloes residue 2 cc eugenol	Not very smooth surface
3	0.1 g aloes residue 0.2 g furfural polymer	*
4	0.1 g aloes residue 0.2 g furfural polymer 0.2 g goulac	*
5	0.1 g aloes residue 0.2 g goulac 0.1 g phenol	Similar to 1
6	0.1 g aloes residue 0.2 g pyrogallol	Not very smooth*
7	0.1 g aloes residue 0.2 g resorcinol	*
8	0.1 g aloes residue 0.2 g thymol	Similar to 1
9	0.1 g aloin residue 2 cc *p*-cresol	Rough surface
10	0.1 g aloin residue 2 cc *p*-cresol 1 cc furfural	*
11	0.1 g aloin residue 2 cc *p*-cresol 0.2 g goulac	*
12	0.1 g aloin residue 1 cc furfural 5 cc glycerol	Heavy corners
13	0.1 g aloin residue 1 cc furfural 0.2 g goulac	Knobby*
14	0.1 g aloin residue 1 cc furfural 0.1 g thymol	Similar to 1
15	0.1 g aloin residue 0.2 g furfural polymer†	Striated
16	0.1 g aloin residue 0.05 g glue 0.2 g goulac	Similar to 1
17	0.1 g aloin residue 0.2 g goulac 0.1 g phenol	Heavy corners
18	1 cc furfural 0.2 g goulac 0.2 g tannic acid	Similar to 1
19	1 cc furfural 0.2 g tannic acid	Rough surface
20	0.05 g glue 0.1 g β-naphthol	Similar to 1
21	0.2 g goulac 2 cc eugenol	*
22	0.2 g goulac 5 cc salicylaldehyde	Similar to 1

* These electrodeposits were the best obtained during this investigation. They were very adherent and dense even when approximately ½ in. thick. They had metallic appearance and were considerably smooth. The rest of the deposits listed were also satisfactory, but to a somewhat lesser extent.

† This solid polymer was formed from common furfural after standing for about three years.

Results

Electrodeposits obtained from the phenol sulfonate bath containing no addition agents were entirely unsatisfactory, having a spongelike texture. Individual addition agents improved the quality of the electrodeposits. In general, however, a single addition agent improved only one of the desirable characteristics of the electrodeposits, i.e., denseness, adherence, crystallinity, or smoothness. Among the addition agents employed individually, *p*-cresol yielded solid, adherent, and fairly smooth electrodeposits (Fig. 1, part 5). Deposits somewhat inferior to the latter, but fairly satisfactory, were obtained with glycerol, goulac, β-napthol, phenol, resorcinol, and diphenyl sulfone.

In combining the various addition agents, an effort was made to intermix members which, when employed individually, exhibited beneficial effect on different properties of the electrodeposits. Thus, members which improved the denseness of the deposits, but did not repress the treelike formation (like pyrogallol), were combined with members which repressed the treelike formation, but not the density (like aloes residue). This approach led to very effective combinations in a number of cases. Thus, a combination of the individual addition agents mentioned above (aloes residue and pyrogallol) gave very good deposits (Fig. 1, part 6). In many cases, however, the effect of combinations of addition agents did not correspond to the sum of the individual effects.

The combinations of addition agents which gave satisfactory results are listed in Table I with a qualitative description of the nature of the electrodeposits. Some of the electrodeposits are shown in Fig. 1.

Discussion

Addition agents, alone or in combinations, which favored the formation of adherent, dense, and smooth lead electrodeposits from the lead phenol sulfonate bath contained, with few exceptions, hydroxyl or carbonyl groups. These compounds have a marked tendency to form covalent, complex ions with metal cations. Upon formation of such complex ions, concentration of the free metal cations is controlled by the dissociation equilibrium of the complex ions and is at all times maintained quite small at the cathode-electrolyte interface. This is usually a desirable condition for electrodeposition (5). To maintain equilibrium, the electrodeposited cations are replenished by dissociation of the complex. The addition agents themselves are not usually completely consumed and continue to serve as complexing agents so that relatively small amounts of addition agents may suffice for the electroposition of large amounts of metal.

High molecular weight colloidal substances like glue and goulac are effective addition agents very likely by adsorbing at the cathode and "interfering" with the crystal growth, allowing the formation of small crystallites, which in turn favor the formation of dense and adherent deposits (6).

Among the single addition agents tested, *p*-cresol proved the most efficient in electrodeposition of lead from the phenol sulfonate electrolyte. Rather simple combinations of furfural gave very satisfactory deposits. The various polymeric forms of furfural should perhaps be studied further as addition agents in sulfonate baths.

The best combination of rather easily available addition agents found for a current density of about 26 amp/ft^2 (2.8 amp/dm^2) was 2 ml *p*-cresol, 0.2 g goulac, and 0.1 g aloin residue per 100 ml of electrolyte.

Any discussion of this paper will appear in a Discussion Section to be published in the June 1956 JOURNAL.

REFERENCES

1. W. BORCHERS, *Z. angew. Chem.*, **4**, 596 (1891).
2. A. G. BETTS, "Lead Refining by Electrolysis," p. 23, John Wiley & Sons, Inc., New York (1908).
3. F. C. MATHERS AND J. F. SUTTLE, *J. (and Trans.) Electrochem. Soc.*, **93**, 47 (1948).
4. F. C. MATHERS AND J. C. GRIESS, JR., *This Journal*, **94**, 46*N* (1948).
5. W. BLUM AND G. B. HOGABOOM, "Principles of Electroplating and Electroforming," 3rd ed., p. 70, McGraw-Hill Book Co., New York (1949); G. FUSEYA AND K. MURATA, *Trans. Electrochem. Soc.*, **50**, 235 (1926); G. FUSEYA AND M. NAGANO, *ibid.*, **52**, 249 (1927); F. C. MATHERS, *Proc. Am. Electroplaters' Soc.*, **27**, 134 (1939).
6. R. TAFT AND H. E. MESSMORE, *J. Phys. Chem.*, **35**, 2585 (1931); J. A. HENDRICKS, *Metal Finishing*, **41**, 134 (1943).

er 1955

scussion

' p. 23,

Electro-

Journal,

Electro-
IcGraw-
AND K.
(1926);
(1927);
loc., 27,

35, 2585
41, 134